University of Southampton

Faculty of Medicine

Human Development & Health

Role of Environmental Oxygen in Regulating the Proteome and Fatty Acid Composition of Human Embryonic Stem Cells

by

Ada Antypiuk

Thesis for the degree of Doctor of Philosophy

June 2020

Supervisory Team:

Dr Franchesca Houghton, Prof. Philip Calder, Prof. Chao Wan

University of Southampton

Abstract

Faculty of Medicine

Human Development & Health

Thesis for the degree of Doctor of Philosophy

Role of Environmental Oxygen in Regulating the Proteome and Fatty Acid Composition of Human Embryonic Stem Cells

by

Ada Antypiuk

Human embryonic stem cells (hESCs) are pluripotent, self-renewing cells capable of giving rise to derivatives of all three germ layers. However, hESCs have a propensity for spontaneous differentiation. Compared to a standard culture in normoxia (20% oxygen), hESCs maintained under hypoxic conditions (5% oxygen) exhibit a lower rate of spontaneous differentiation and upregulation of key genes regulating pluripotency. Little is known about the effect of low oxygen level on global protein expression and fatty acid content and synthesis in hESCs and mechanisms regulating its beneficial effect. This study aimed to determine the proteome of hESCs cultured at 5% or 20% oxygen and investigate changes in fatty acid composition and metabolism.

Using mass spectrometry, 129 out of the 2674 detected proteins were differentially expressed in hESCs maintained at 5% oxygen compared to those cultured at 20% oxygen; 38 were upregulated (Log_2FoldChange > 0.5) and 31 were downregulated (Log_2FoldChange < -0.5) in cells maintained in hypoxia. Proteins involved in the cellular response to oxygen and autophagy were upregulated in hESCs cultured in hypoxic conditions. Pathway analysis revealed a strong association with functions such as cell death and survival. PARP-1 and caveolin-1, proteins regulating DNA repair mechanisms and cell membrane functions respectively, were significantly increased in hESCs cultured at 5% oxygen compared to 20% oxygen. Hypoxia was found to significantly alter the composition of fatty acids in hESCs compared to 20% oxygen. In particular, the concentration of eicosapentaenoic acid (EPA) was significantly increased in hESCs cultured at 5% oxygen. The expression of Δ5-desaturase (D5D), the enzyme mediating EPA synthesis, was also significantly higher in hESCs cultured in hypoxia. The expression of D5D in hypoxic conditions was found to be directly regulated by HIF2α which binds to a predicted hypoxia-response element within the *FADS1* (gene encoding D5D) proximal promoter. HIF2α binding was significantly enriched in hESCs cultured at 5% oxygen. EPA was supplemented to the hESC culture to investigate whether EPA might be beneficial for cells maintained at 20% oxygen. Supplementation of EPA to the medium had no effect on the self-renewal, proliferation, reactive oxygen species generation or glucose metabolism but, was found to regulate the expression of D5D and caveolin-1.

These data suggest that environmental oxygen regulates the phenotype of hESCs through changes in global protein expression. The regulation of D5D by HIF2α and increased EPA content suggests that fatty acid biosynthesis may have an important role in the maintenance of hESCs under hypoxic conditions. The better understanding of changes in hESCs maintained under hypoxic conditions could improve cell culture for future use in regenerative medicine and cell therapies.

Table of Contents

Table of Tables

Table of Figures

Table of Figures

Research Thesis: Declaration of Authorship

Print name: Ada Antypiuk

Title of thesis: Role of Environmental Oxygen in Regulating the Proteome and Fatty Acid Composition of Human Embryonic Stem Cells

I declare that this thesis and the work presented in it are my own and has been generated by me as the result of my own original research.

I confirm that:

1. This work was done wholly or mainly while in candidature for a research degree at this University;
2. Where any part of this thesis has previously been submitted for a degree or any other qualification at this University or any other institution, this has been clearly stated;
3. Where I have consulted the published work of others, this is always clearly attributed;
4. Where I have quoted from the work of others, the source is always given. With the exception of such quotations, this thesis is entirely my own work;
5. I have acknowledged all main sources of help;
6. Where the thesis is based on work done by myself jointly with others, I have made clear exactly what was done by others and what I have contributed myself;
7. None of this work has been published before submission.

Signature: ..... Date: 08/06/2020

Acknowledgements

I would like to thank the University of Southampton for the opportunity to do this research project and funders of my PhD studentship- the Centre for Human Development, Stem Cells and Regeneration and the Chinese University of Hong Kong. I would like to thank my supervisors, Dr Franchesca Houghton, Professor Philip Calder and Professor Chao Wan, who were always ready to help me, shared their knowledge and good advice. I am not able to describe how grateful I am for all the support I received.

I would also like to thank Dr Paul Skipp, who helped with mass spectrometry experiment and analysis, to Mr Chris Gelauf for technical support with gas chromatography experiments and to Dr Caroline Childs for help with flow cytometry.

I would like to acknowledge the Research Mobility Programme, which supported my visit to the Chinese University of Hong Kong.

I would like to thank my research group, Sophie Arthur, Lauren Griffith and especially Kate Parry for help and comforting me when nothing is working. I am grateful to all my family and friends, who believed in me and supported me, especially my parents, Ania and Enrico. Thank you.

Definitions and Abbreviations

AA	arachidonic acid (20:4n-6)
ALA	α-linolenic acid (18:3n-3)
Alexa488	type of green-fluorescent dye
ATP	adenosine triphosphate
BSA	bovine serum albumin
carboxy-H_2DCFDA	5-(and-6)-carboxy-2',7'-dichlorodihydrofluorescein diacetate
ChIP	chromatin immunoprecipitation
CM	iMEF-conditioned medium
D5D	Δ5-desaturase
D6D	Δ6-desaturase
DAPI	4’,6-diamidino-2-phenylindole
DGLA	di-homo-γ-linolenic acid (20:3n-6)
DHA	docosahexaenoic acid (22:6n-3)
DMEM	Dulbecco's Modified Eagle Medium
DMSO	dimethyl sulfoxide
DNase	deoxyribonuclease
DTT	dithiothreitol
EDA	eicosadienoic acid (20:2n-6)
EDTA	ethylenediaminetetraacetic acid
eNOS	endothelial nitric oxide synthase
EPA	eicosapentaenoic acid (20:5n-3)
EPAS1	gene encoding HIF2α
EPPS	3-[4-(2-Hydroxyethyl)piperazin-1-yl]propane-1-sulfonic acid
ESCs	embryonic stem cells
EV	extracellular vesicles
FAD	flavin adenine dinucleotide
$FADH_2$	reduced form of FAD
FADS1	gene encoding Δ5-desaturase
FADS2	gene encoding Δ6-desaturase
FAME	fatty acid methyl ester
FASN	fatty acid synthase
FBS	fetal bovine serum
FC	fold change
FITC	fluorescein isothiocyanate
FSC	forward-scattered light
G6PDH	glucose-6-phosphate dehydrogenase
GC	gas chromatography
GLUT1	glucose transporter type 1
GLUT3	glucose transporter type 3
GO	gene ontology
H_2O_2	hydrogen peroxide
HBSS	Hank’s balanced salt solution

hECCs	human embryonal carcinoma cells
HepG2	hepatocellular carcinoma cells
hESCs	human embryonic stem cells
HIF	hypoxia inducible factor
HRE	hypoxia-response element
ICM	inner cell mass
iMEF	irradiated mouse embryonic fibroblast
IPA	Ingenuity Pathway Analysis
iPSCs	induced pluripotent stem cells
KLF4	Krüppel-like factor 4
KO DMEM	KnockOut Dulbecco's Modified Eagle Medium
LA	linoleic acid (18:2n-6)
LDH	lactate dehydrogenase
LTB_4	leukotriene B_4
MEF	mouse embryonic fibroblast
mEpiSCs	mouse epiblast stem cells
mESCs	mouse embryonic stem cells
$MgSO_4$	magnesium sulfate
MS	mass spectrometry
MSCs	mesenchymal stem cells
NAD	nicotinamide adenine dinucleotide
NADH	reduced form of NAD
NADP	nicotinamide adenine dinucleotide phosphate
NADPH	reduced form of NADP
NANOG	homeobox protein NANOG
NaOH	sodium hydroxide
NF-κB	nuclear factor kappa-light-chain-enhancer of activated B cells
NT2	human embryonal carcinoma cell line
OCT4	POU domain, class 5, transcription factor 1
PARP-1	poly [ADP-ribose] polymerase 1
PBS	phosphate buffered saline
PCA	principal component analysis
PCNA	proliferating cell nuclear antigen
PCR	polymerase chain reaction
PGE_2	prostaglandin E_2
PHD	prolyl hydroxylase
PUFA	polyunsaturated fatty acid
RIPA buffer	radioimmunoprecipitation assay buffer
Rnase	ribonuclease
ROS	reactive oxygen species
RPA1	replication protein A 70 kDa DNA-binding subunit
RT-qPCR	real-time quantitative PCR
SDS	sodium dodecyl sulfate
SEM	standard error of the mean
shRNA	short hairpin RNA
siRNA	small interfering RNA
SOX2	transcription factor SOX-2

SREBP-1	sterol-regulatory element-binding protein-1
SSC	side-scattered light
SSEA-3	stage-specific embryonic antigen-3
SSEA-4	stage-specific embryonic antigen-4
TAG	triacylglycerol
TBHP	tert-butyl hydroperoxide
TBS	Tris-buffered saline
TCA cycle	tricarboxylic acid cycle / Krebs cycle
Tris	Tris(hydroxymethyl)aminomethane
TSS	transcription start site
WB	Western blot

Chapter 1 Introduction

1.1 Stem cells

Stem cells are unspecialised cells that have the potential to differentiate into various progenitor and mature cell types. They have unique self-renewal abilities, which means that they can indefinitely divide while maintaining the stem cell population (Zakrzewski *et al.*, 2019). The division can be symmetrical or asymmetrical. In the symmetric model, one stem cell produces either two differentiating cells or two stem cells. In the asymmetric model, one stem cell divides into one differentiated cell and one stem cell (He *et al.*, 2009; Shahriyari and Komarova, 2013). Stem cells can be found at different developmental stages, from embryo to adult. However, depending on their origin and localisation, stem cells can exhibit different properties and fulfil diverse roles. During development, self-renewal is essential to expand the number of stem cells, while for an adult organism, stem cells divide to maintain the population and restore the number after injury/healing (Bongso and Lee, 2005; Zakrzewski *et al.*, 2019). The origin of the stem cell also has an impact on the differentiation potential. As a consequence of their unique characteristics, stem cells represent a florid ground for both fundamental biology and therapeutic research.

1.2 Types of potency

Potency can be defined as the potential of a cell to differentiate into other cell types. There are five types of potency: totipotency, pluripotency, multipotency, oligopotency and unipotency.

1.2.1 Totipotency

Totipotency describes the potential of cells to become any cell type, embryonic or extraembryonic; thus each cell can give rise to a fully functional organism. A fertilised egg is an example of a totipotent cell, which is able to give rise to fertile adult (Mitalipov and Wolf, 2009). As embryos develop, cells lose their totipotency and the role of cells begins to be more directed once the blastocyst stage is reached (Condic, 2014).

1.2.2 Pluripotency

Cells of the inner cell mass (ICM) of a blastocyst are pluripotent and have the potential to give rise to cells of all three germ layers, ectoderm, mesoderm and endoderm, which are formed by the end of gastrulation. The germ layers give rise to different types of derivatives (Pansky, 1982a):

- The ectoderm
    - Nervous tissue
        - Neural tube: central nervous system, retina, posterior pituitary, pineal gland,
        - Neural crest: pigment cells, adrenal medulla, cranial and sensory nerves, cranial and sensory ganglia.
    - Epidermis
        - Hair, nails, mammary glands, cutaneous glands, anterior pituitary, teeth enamel, inner ear, eye lens.

- The mesoderm
    - Skeleton, muscle, connective tissue, circulatory system (cardiovascular and lymphatic), urinary system, spleen, adrenal cortex, genital system, dermis, dentine of teeth.
- Endoderm
    - Epithelium of gastrointestinal tract, liver, pancreas, urachus, bladder, pharynx, thyroid, trachea, bronchi, lungs, tympanic cavity, pharyngotympanic tube, tonsils, parathyroid glands.

Human embryonic stem cells (hESCs), which are pluripotent, express specific markers, such as octamer-binding transcription factor 4 (OCT4), SRY (sex-determining region Y)-box transcription factor 2 (SOX2), homeobox protein NANOG (NANOG) and stage-specific embryonic antigens (SSEA)-3 and SSEA-4 (Zhao *et al.*, 2012). These markers are downregulated when a cell undergoes differentiation. Under specific culture conditions, hESCs proliferate, self-renew, and thus maintain an undifferentiated state. However, the gold standard for testing pluripotency is teratoma formation. Upon injection into immunocompromised mice, truly pluripotent cells will form teratomas consisting of cells of all three germ layers (Thomson *et al.*, 1998; Brivanlou *et al.*, 2003).

1.2.3 Multipotency

Multipotent cells have the potential to differentiate into a subset of cell types; therefore, they are more lineage-restricted compared to pluripotent or totipotent cells. Multipotent cells are found in

many adult human tissues, for example, mesenchymal stem cells in the bone marrow which can differentiate into osteoblasts, myocytes, chondrocytes or adipocytes (Frese *et al.*, 2016). They have application in cell therapies, as they do not form teratoma and usage is free from ethical concerns. However, the isolation of multipotent stem cells from bone marrow is invasive. One emerging problem is the lack of global regulations ensuring the quality of cells and safety controls (Wei *et al.*, 2013).

1.2.4 Oligopotency

Oligopotent cells can differentiate into only a few, restricted cell types, for example, progenitor cells. Progenitor cells have limited self-renewal abilities and can differentiate into cells of one lineage. An example of an oligopotent cell is a lymphoid progenitor from bone marrow that gives rise to the T cells, B cells and Natural Killer cells (Kondo *et al.*, 1997).

1.2.5 Unipotency

Unipotent cells are the most limited type of stem cells and they have the ability to differentiate into only one cell type, for example, spermatogonial stem cells. They can self-renew to maintain the spermatogonial stem cell population or differentiate only into spermatocytes (Aponte, 2015; de Rooij, 2017).

1.3 Human embryonic stem cells

hESCs were isolated for the first time in 1998 (Thomson *et al.*, 1998). They are derived from the ICM of a blastocyst, the final stage of preimplantation embryo development. hESCs have a large nuclear to cytoplasm ratio, a small number of immature mitochondria and grow in flattened colonies. They are undifferentiated cells with a normal karyotype (Thomson *et al.*, 1998). hESCs show a higher level of telomerase activity compared to diploid somatic cells, preventing chromosomes from shortening, therefore increasing stem cell life span (Thomson *et al.*, 1998). They are known for their remarkable properties, such as self-renewal and being pluripotent they have the ability to give rise to cells of all three germ layers: ectoderm, endoderm and mesoderm (Thomson *et al.*, 1998). Hence, they have great potential for cell therapy treatments, regenerative medicine applications and the study of developmental mechanisms.

hESCs are difficult to maintain in culture and have a tendency to spontaneously differentiate and thus require special conditions to maintain pluripotency and the undifferentiated state (Chen *et al.*, 2007a; Park *et al.*, 2008). hESC culture may be on a feeder cell layer or feeder-free. Standard feeder cell culture involves co-culture of hESCs on mitotically inactivated mouse embryonic

fibroblasts (iMEFs). A commonly used method for feeder-free hESC culture is growth on the extracellular matrix, Matrigel (a mouse Engelbreth-Holm-Swarm (EHS) sarcoma tumour extract) that is an attachment substrate. hESCs cultured on Matrigel-coated plates may be incubated with medium conditioned by iMEFs (Yao *et al.*, 2006). However, a limitation of using this method is the risk of zoonotic infections originating from the iMEFs and Matrigel (Yusuf *et al.*, 2013). Thus, many human-derived feeder layers are now used such as human foreskin fibroblasts (Amit *et al.*, 2003) or human fetal muscle fibroblasts (Richards *et al.*, 2002) that support an undifferentiated pluripotent state of hESCs in a xeno-free environment. There are also feeder-free systems for culturing hESCs, which include commercially available defined, feeder-independent media, such as mTeSR and use of extracellular matrix such as Matrigel, laminin-521/E-cadherin or vitronectin (Ludwig and Thomson, 2007; Rodin *et al.*, 2014). These methods hold promise for utilising hESCs in cell therapies without risk of infection with animal pathogens. However, there are other aspects of hESCs which could potentially limit therapeutic usage, such as immunological responses to transplanted cells or risk of spontaneous differentiation after cell injection, leading to tumour development (Swijnenburg *et al.*, 2008; Ozolek and Castro, 2011; Pearl *et al.*, 2012). However, some oppose this view and claim that hESCs are immune privileged and therefore transplantation of cells or cell-derivatives would not trigger host immune rejection (Li *et al.*, 2004; van der Torren *et al.*, 2017). Despite the opposite views, hESCs are classified as less immunogenic than somatic cells (Drukker *et al.*, 2006). Nonetheless, there are cell therapy trials based on hESCs, such as treatment of macular degeneration with hESC-derived retinal pigment epithelial cells (Schwartz *et al.*, 2015; Liu *et al.*, 2018; Mehat *et al.*, 2018). Another example is the therapy treating spinal cord injury with hESCs, accepted for clinical trials on humans by the US Food and Drug Administration (Shroff, 2016).

1.4 Derivation of hESCs

In a fertilised human egg, called a zygote, the first cleavage begins around one day after fertilisation. The embryo continues to divide to form the 2-cell, 4-cell and then an 8-cell structure. The next mitotic division forms the 16-cell morula that by cavitation becomes a blastocyst. A blastocyst consists of an outer layer of cells called the trophectoderm, which surrounds the blastocoel cavity, and ICM. The trophectoderm gives rise to extraembryonic lineages and the ICM to the embryo proper (Pansky, 1982b; Gilbert, 2000). hESCs are derived from the inner cell mass of a blastocyst (Figure 1.1).

Embryos used for derivation of hESCs cells are obtained following informed consent from patients undergoing in vitro fertilisation and embryo transfer. hESCs are isolated by either immunosurgery, blastocyst outgrowth (Figure 1.1) or laser dissection (Turksen and Troy, 2006).

Immunosurgery enables isolation of ICM by disruption and elimination of trophectoderm cells in a two-step procedure (Kim *et al.*, 2005; Chen and Melton, 2007). First, the zona pellucida surrounding the embryo is removed using acid tyrodes. The blastocyst is incubated in antiserum that binds to the trophectoderm, followed by complement lysis that causes the destruction of the trophectoderm. The outer layer of blastocyst cells is impermeable to the antibody ensuring the inner cell mass stays intact. The impermeability is due to tight junctions and the presence of desmosomes between trophectoderm cells that make it impermeable for macromolecules, such as immunoglobulins, therefore shielding the ICM. Mechanical removal of trophectoderm cells is used to isolate ICM. This method was first developed for murine blastocysts (Solter and Knowles, 1975) and later adapted for human blastocysts (Thompson, 1998), which includes using rabbit serum to BeWO cells (trophoblastic endocrine cell type) and guinea pig complement. Immunosurgery enables the isolation of the inner cell mass in a relatively short time. However, the use of animal-derived products carries a risk of pathogen transfer and this method is not suitable for the use on poor quality embryos, with a small inner cell mass (Vazin and Freed, 2010). The blastocyst outgrowth method relies on the blastocyst to hatch from the zona pellucida; ICM cells are able to survive while trophectoderm cells undergo senescence and deteriorate. This technique does not require the use of antibodies or removing trophectoderm cells (Lee *et al.*, 2010a; Lee and Lee, 2011).

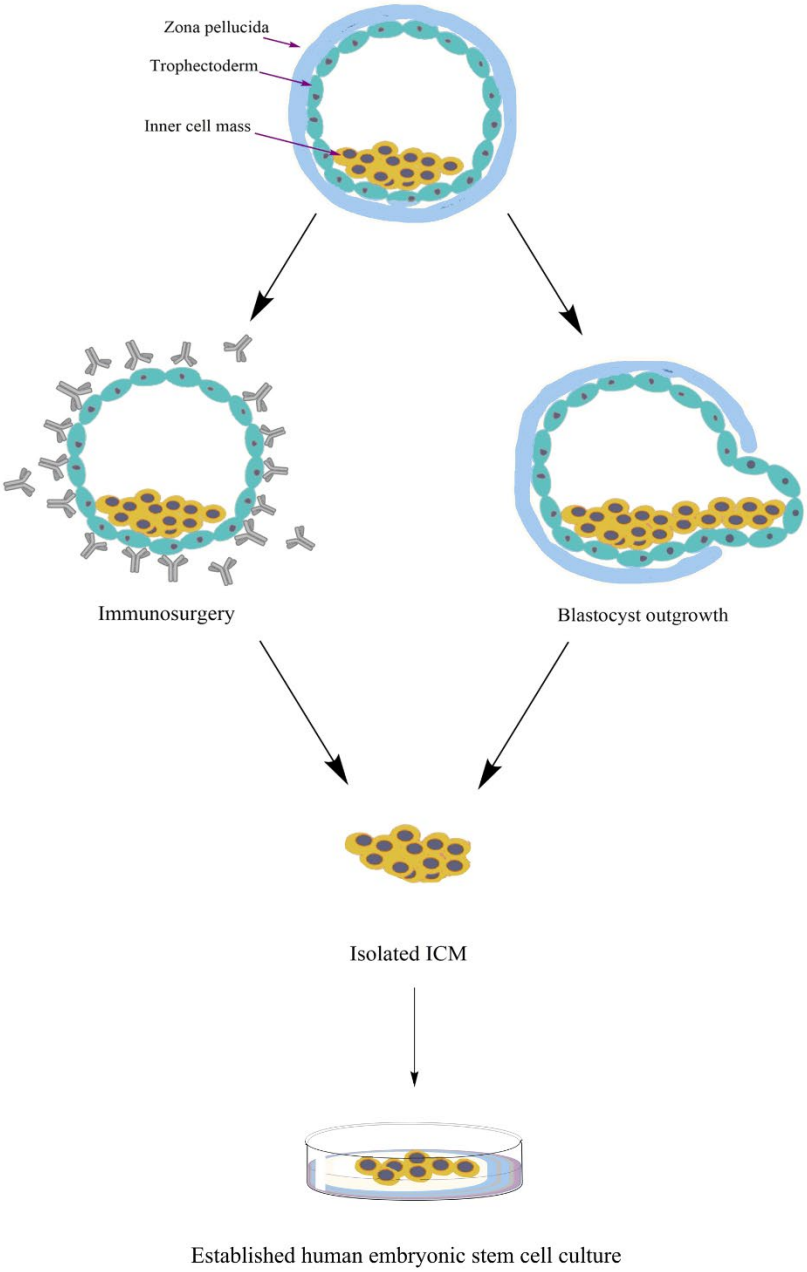

Figure 1.1 **Schematic representation of the principles of derivation and establishment of hESCs.**

Immunosurgery (on the left) or blastocyst outgrowth (on the right) method can be used for derivation of hESCs. Immunosurgery consist of removal of zona pellucida and incubation of an embryo with antibodies that bind to the trophectoderm, followed by complement lysis. ICM remains intact due to cell-cell connections of the trophectoderm. The trophectoderm is removed and isolated ICM can be cultured. The blastocyst outgrowth method relies on the ability of the blastocyst to hatch from the zona pellucida; trophectoderm cells undergo senescence and ICM can be isolated and cultured.

Another animal-free derivation method is laser-assisted dissection of the ICM from the human blastocyst (Turetsky et al., 2008). This technique requires micromanipulation through infrared laser pulses that allow separation of the ICM from the rest of a blastocyst. The laser should be directed from an appropriate distance from the ICM to prevent damage and heating. This method, similar to mechanical isolation, requires technical competence and precision (Turetsky *et al.*, 2008).

Successful implementation of immunosurgery methods on human blastocysts was one of the aspects that enabled the Thompson group to establish the first hESC line (Thompson, 1998). This started a new era in stem cell research, which progressed studies on human development and explored the potential of hESCs in regenerative medicine.

1.5 Naïve and primed pluripotency state

During embryo development, the ICM of a blastocyst generates another cell layer - the hypoblast - and remaining ICM cells eventually become the epiblast. The epiblast can give rise to all three germ layers and can develop into a fetus. Murine epiblast cells can also be isolated and derived from a post-implantation mouse embryo and are termed mouse epiblast stem cells (mEpiSCs). Such cells are pluripotent but have different properties than mouse embryonic stem cells (mESCs); thus two pluripotency states are distinguished: naïve and primed. mESCs represent the naïve state and mouse mEpiSCs the primed (Nichols and Smith, 2009). Interestingly, hESCs resemble mEpiSCs and they are classified as primed (Tesar *et al.*, 2007). Naïve mESCs can form chimaeras, which means that pluripotent cells injected back into a mouse blastocyst will give rise to all somatic lineages, including the germline. In contrast, mEpiSCs do not have the ability to form chimaeras. In female cells, X chromosome status is a good marker of pluripotency state. In naïve state cells both X chromosomes are active but in primed cells only one X chromosome is (Heard, 2004). Naïve cells prefer glycolysis as the pathway for energy generation, while primed cells rely on both glycolysis and oxidative phosphorylation (Teslaa and Teitell, 2015). Cells of both pluripotency states express key pluripotency markers such as Oct4, Sox2, Nanog, however, mESCs express also Klf4 (Nichols and Smith; Kumari, 2016). The introduction of Klf4 appeared to be essential to enable the switch of primed mEpiSCs to the naïve state (Guo *et al.*, 2009).

hESCs are considered to be primed, as they exhibit several properties associated with this pluripotency state, such as lack of global DNA hypomethylation or dependence on MEK–ERK signalling to maintain pluripotency (Li *et al.*, 2007a; Gafni *et al.*, 2013; Smith *et al.*, 2014). However primed hESCs can be induced to the naïve state, which is believed to have increased developmental capacity. The naïve state in hESCs is manifested by increased expression of naïve

pluripotency markers, such as transcription factor CP2-like protein 1 (TFCP2L1) and KLF4, or DNA hypomethylation (Takashima *et al.*, 2014). The naïve state can be induced by reprogramming with, for example, kinases or histone deacetylase inhibitors (Messmer *et al.*, 2019). The naïve state in mice is tested by the ability to form chimaeras, however, in humans it cannot be tested with pluripotent stem cells due to ethical concerns. Therefore several markers can be used to confirm the naïve state such as the formation of cross-species chimaeric mouse embryos upon injecting human naïve pluripotent stem cells into mouse morula or ability to maintain pluripotency upon inhibition of the MEK-ERK signalling cascade (Gafni *et al.*, 2013; Weinberger *et al.*, 2016).

1.6 Induced pluripotent stem cells

The reprogramming of somatic cells into a pluripotent state produces induced pluripotent stem cells (iPSCs). In 2006, the innovative research led by Shinya Yamanaka proved that somatic cells can be reprogrammed by introducing factors such as Oct4, Sox2, c-Myc, or Klf4 (Takahashi and Yamanaka, 2006). Oct4 and Sox2 are pluripotency markers, while c-Myc is responsible for proliferation and histone acetylation that enables pluripotency marker binding (Araki *et al.*, 2011). KLF4 directly binds to the promoter of *NANOG* to regulate expression of this pluripotency marker (Chan *et al.*, 2009). iPSCs have self-renewal abilities, express pluripotency markers and can form teratoma when injected into an immunocompromised mouse (Takahashi and Yamanaka, 2006). iPSCs form teratomas more efficiently (100%) and significantly faster regardless of the site of injection when compared to hESCs. The efficiency of teratoma formation by hESCs was 81% when injected subcutaneously and 94% for intratesticularly. Different efficiency and time for teratoma formation are suggested to be the result of genetic differences between hESCs and iPSCs (Gutierrez-Aranda *et al.*, 2010). iPSCs are considered not controversial and are not restricted, in comparison to hESCs; however, derivation of iPSCs is a relatively long and inefficient process. The quality of cells obtained depends on the somatic cell type used, species and delivery method (Gonzalez *et al.*, 2011). The first hiPSCs were reprogrammed using a viral delivery method (Takahashi and Yamanaka, 2006). However, this technique limits the usage of iPSCs in cell therapy due to a risk associated with virus utilisation, such as the potential hazard of oncogene expression. Other methods include cell transfection of linear DNA, use of liposomes or electroporation, protein or transient episomal delivery or use of synthetic mRNA; the efficiency of these processes depends from the method (Warren *et al.*, 2010; Gonzalez *et al.*, 2011). One of the most efficient methods to date is reprogramming of hematopoietic stem cells into iPSCs using Sendai viruses encoding Oct4, KLF4, Myc and Sox2. Efficiency is reported to reach almost 50% using this method (Wang *et al.*, 2019). Despite the similarities between iPSCs and hESCs, such as

pluripotent state and expression of self-renewal markers, iPSCs were found to exhibit some differences when compared to hESCs, for example retaining "epigenetic memory", inherited from parental cells (Vaskova *et al.*, 2013). Chromatin of hESCs was shown to stay in rather open, decompacted state, compared to that of somatic cells which is more condensed (Bibikova *et al.*, 2006). The open configuration of hESC chromatin can support the dynamic posttranslational remodelling of histones and DNA methylation/demethylation upon differentiation (Bartova *et al.*, 2008). iPSCs were found to have retained epigenetic characteristics, such as residual DNA methylation signatures, of the somatic cells of origin. This affects the differentiation of iPSCs where differentiation towards lineages related to somatic cells of origin is preferred (Kim *et al.*, 2010; Vaskova *et al.*, 2013; Noguchi *et al.*, 2018). A study showed that iPSCs derived from pancreatic islet beta cells retained the epigenetic signature of beta cells but also had enhanced ability to differentiate into insulin-producing cells, compared to iPSCs that were not derived from beta cells (Bar-Nur *et al.*, 2011). Thus, epigenetic memory can influence the effectiveness of directed differentiation in iPSCs, while hESCs do not possess that feature (Tompkins *et al.*, 2012). However, Kyttälä *et al.* (2016) reported that source (donor) is a more important factor for differentiation efficiency than the type of somatic cell used; genetic background can impact transcription profile and differentiation capacity.

1.7 NT2 cells

Human embryonal carcinoma cells (hECCs) are malignant counterparts of hESCs and originate from a testicular germ cell tumour (Stevens, 1967). NT2 (also known as NTera2) is an isolated and characterised ECC line. The NT2 cells are large, flat and strongly adherent with a high nuclear to cytoplasmic ratio. NT2 cells are able to maintain pluripotency, an undifferentiated state and express pluripotency markers, OCT4, SOX2, NANOG, as well as stage-specific embryonic antigens SSEA3 and SSEA4 (Drakulic *et al.*, 2015). NT2 cells can differentiate into neurons when treated with, for example, retinoic acid or 2R-hydroxycholesterol (Abolpour Mofrad *et al.*, 2016) but they can also spontaneously differentiate if the cell density in culture is too low.

hECCs cultured under hypoxia display enhanced stemness and an increased rate of proliferation compared to cells maintained at 20% oxygen (Silvan *et al.*, 2009). However, as well as being more proliferative at reduced oxygen tension, the cells also participate in neovascularisation processes and support the expression of cell migration factors, leading towards tumour invasion and development (Silvan *et al.*, 2009). Low oxygen tension (5%) increases the effectiveness of NT2 neuronal differentiation, which is mediated by upregulation of Hypoxia Inducible Factor 1α (HIF1α) (Wu *et al.*, 2008).

NT2 cells are used for pluripotency and differentiation studies and therefore may be used as a surrogate for hESCs (Mojsin *et al.*, 2015).

1.8 Pluripotency markers

OCT4, SOX2 and NANOG are key pluripotency markers. They are expressed in hESCs and help to maintain pluripotency by regulating target genes involved in differentiation and embryo development (Chambers *et al.*, 2003; Hay *et al.*, 2004; Boyer *et al.*, 2005; Masui *et al.*, 2007).

1.8.1 OCT4

OCT4 encoded by the *POU5F1* gene is a member of the POU family of DNA binding proteins and is a regulatory factor in early embryogenesis. It can recognise and bind to the DNA octamer motif ATGCAAAT in the promoter or enhancer region of the target gene to regulate expression (Schöler *et al.*, 1989). OCT4 is known to play an important role during human embryogenesis (Fogarty *et al.*, 2017). A study on human zygotes with the depleted expression of OCT4 showed that the ICM was not properly formed, which eventually led to embryo degeneration, highlighting the importance of OCT4 for development (Fogarty *et al.*, 2017). OCT4 is found in blastomeres of human embryos, until the morula stage, and in the blastocyst where cells of the ICM express *OCT4* mRNA at a much higher level than cells of the trophoblast (Hansis *et al.*, 2000). On the protein level, OCT4 is uniformly expressed in both ICM and trophoblast in the early human blastocyst (5 days post-fertilization; 33-128 cells). However, by the day 6 post-fertilization (129–256 cells), OCT4 expression is restricted to the ICM cells of the blastocyst (Niakan and Eggan, 2013). In vitro, OCT4 is expressed in high levels by embryonic stem cells, embryonic carcinoma cells and embryonic germ cells. The level of OCT4 expression is crucial for stem cell fate by either maintaining pluripotency of stem cells or driving cells toward lineage-specific differentiation. Babaie *et al.* (2007) found that when the expression of OCT4 in hESCs was silenced with siRNA, there was a significant decrease in expression of self-renewal genes such as *SOX2*, *NANOG* as well as markers of undifferentiated stem cells, *LEFTY1*, *LEFTY2*, *DPPA4* and *THY1*. OCT4 was shown to repress the expression of HCGβ (human chorionic gonadotropin), which is known as a placental marker, therefore preventing differentiation of hESCs (Zafarana *et al.*, 2009; Zeineddine *et al.*, 2014). The knockdown of OCT4 expression in hESCs and NT2 cells resulted in differentiation, proving the crucial role of OCT4 in pluripotency maintenance (Matin *et al.*, 2004). However, too high expression of Oct4 (at least 3-fold increase) can cause cell differentiation into primitive endoderm and mesoderm in mESCs while too low expression leads toward trophectoderm (Niwa *et al.*, 2000). OCT4 has the ability to form complexes with proteins that belong to the SOX family (Kondoh and Kamachi, 2010; Merino *et al.*, 2014). The SOX2/OCT4 complex regulates expression

of genes involved in pluripotency maintenance. However, if OCT4 is highly upregulated, or SOX2 is downregulated, OCT4 binds to SOX17, rather than SOX2, which is known as a gene involved in cardiogenesis (Stefanovic *et al.*, 2009). OCT4 not only interacts with SOX2 but also with NANOG; it was shown that they co-occupy at least 353 genes in hESCs (Boyer *et al.*, 2005). Thus together, they regulate a large number of target genes involved in differentiation and development to maintain pluripotency (Boyer *et al.*, 2005). OCT4 is also a crucial factor in the induced reprogramming of somatic cells to pluripotent stem cells (Takahashi and Yamanaka, 2006).

1.8.2 SOX2

SOX2 is a transcription factor that belongs to the SOX (SRY-related HMG-box) family. Members of the SOX family are characterised by the presence of a highly conserved DNA binding domain - HMG (high-mobility group), which is 80 amino acids long. The binding of SOX2 to the ATTGTT DNA sequence through the HMG domain plays a gene regulatory role (Kamachi and Kondoh, 2013). SOX2 is involved in the early embryogenesis and pluripotency maintenance of undifferentiated embryonic stem cells. Sox2 is expressed in the ICM and trophectoderm in murine blastocysts. It has been shown that Sox2 null murine embryos arrest at the morula stage, therefore not forming a blastocyst (Avilion *et al.*, 2003; Keramari *et al.*, 2010) as Sox2 is one of the earliest markers of inner cells, which later form the ICM (Guo *et al.*, 2010). Sox2 is also known to be expressed in the embryonic nervous system and neuronal progenitor cells (Pevny and Nicolis, 2010). Thus, SOX2 serves as a pluripotency marker as well as a neuronal differentiation marker and the role depends mainly on environmental conditions. It has been shown that hESCs overexpressing SOX2, which were maintained in conditioned medium supporting undifferentiated culture, had a lower rate of spontaneous differentiation and increased mRNA levels of *OCT4* and *NANOG*. However, when the cells were maintained in basic unconditioned medium, hESCs showed signs of neural differentiation (Zhang *et al.*, 2019). However, in mESCs and mECCs overexpression of Sox2 was shown to inhibit the expression of Oct4/Sox2 target genes, for example, *Nanog* or fibroblast growth factor 4 *(Fgf4)* (Boer *et al.*, 2007). Silencing of Sox2 expression led to the differentiation of mESCs and downregulation of, for example, Oct4 or Sox2 (Chew *et al.*, 2005); suggesting that Sox2 is responsible for maintaining an appropriate level of Oct4 expression (Masui *et al.*, 2007).

SOX2 forms a protein complex with OCT4 that together with NANOG co-occupies enhancers/promoter regions of target genes and regulate protein expression. This complex can activate expression of genes responsible for pluripotency, like *NANOG*, *SOX2* or *OCT4*, as well as inhibit expression of genes responsible for cell differentiation and development, such as *PAX6* or *MEIS1* (Boyer *et al.*, 2005). Another proof of the importance of SOX2 in maintaining stem cell pluripotency is the fact that SOX2 was used as one of four factors necessary to reprogram somatic

cells into iPSCs (Takahashi and Yamanaka, 2006). In conclusion, SOX2, together with OCT4 and NANOG, is one of the main transcription factors that maintain the undifferentiated state by regulating the expression of genes involved in pluripotency.

1.8.3 NANOG

NANOG (named from 'Tir Na Nog,' the mythological Celtic land of the forever young) is a member of the homeobox family of DNA binding transcription factors and one of the key pluripotency markers. NANOG is expressed in embryonic stem cells and embryonal carcinoma cells and is downregulated in somatic cells (Hart *et al.*, 2004). During embryogenesis, Nanog is expressed mainly in the ICM of the murine blastocyst and downregulated during embryo implantation to be expressed again by the post-implantation egg-cylinder stage (Chambers *et al.*, 2007; Komatsu and Fujimori, 2015). In human embryos, NANOG was detected in the morula stage and ICM cells of the blastocyst (Hambiliki *et al.*, 2012). In vivo, Nanog-deficient cells of the murine ICM differentiate toward primitive endoderm. Thus, Nanog is crucial for inhibition of the endoderm lineage differentiation process (Mitsui *et al.*, 2003). However, it was shown that *in vitro* Nanog-deficient mESCs could remain as a pluripotent population, but the proliferation rate is lower compared to control cultures. Moreover, spontaneous differentiation was observed more often compared to the control mESCs (Chambers *et al.*, 2007). In hESCs, NANOG was found to repress ectoderm differentiation (Wang *et al.*, 2012c). Another study showed that when the expression of NANOG in hESCs was silenced using siRNA, there was a significant upregulation of trophectoderm-associated genes, such as *CDX2*, *GATA2* or *hCGβ* as well as extraembryonic endoderm-associated genes *GATA4* or *GATA6* (Hyslop *et al.*, 2005). This highlights the role of NANOG in preventing differentiation in hESCs.

NANOG as a transcription factor binds to promoters which can be either transcriptionally active or inactive and most of them are also co-occupied by both OCT4 and SOX2 (Boyer *et al.*, 2005). Transcription activity can be regulated by the interaction of NANOG with coactivators within C-terminal domains or on the contrary, by interaction with corepressors within N-terminal (Chang *et al.*, 2009).

1.8.4 Interaction of OCT4, SOX2 and NANOG

OCT4, SOX2 and NANOG are transcription factors that are responsible for maintaining the pluripotent state of cells by activating or repressing gene expression. It is predicted that OCT4, SOX2 and NANOG might target and interact with more than 4000 genes in hESCs (Li *et al.*, 2016). It is known that they co-occupy at least 353 genes in hESCs (Boyer *et al.*, 2005) while a study on in

mESCs identified more than 400 genes (Rafiee *et al.*, 2016). However, the binding sites of OCT4 and NANOG were found not to be conserved across species. Only 2% of the regions occupied by OCT4 and 1.9% by NANOG in humans were also occupied in mice, suggesting transcriptional circuitry is species-specific (Kunarso *et al.*, 2010). OCT4, SOX2 and NANOG are responsible for regulating cell fate; they co-occupy transcriptionally active genes, such as *DKK1* and *FRAT2* (Boyer *et al.*, 2005), which are involved in the Wnt signalling pathway, known to play a role in pluripotency maintenance (Sato *et al.*, 2004). OCT4, SOX2 and NANOG can also inhibit the expression of genes that are responsible for cell differentiation and are known to promote development, e.g. *PAX6* or *MEIS1* (Boyer *et al.*, 2005). Each of these key pluripotency markers was found to be responsible for repressing differentiation; NANOG prevented differentiation towards ectoderm while SOX2 towards mesendoderm, which can give rise to both mesoderm and endoderm (Wang *et al.*, 2012c). The study by Wang *et al.* (2012c) also found that OCT4 is connected to the expression of bone morphogenetic protein 4 (BMP4), known to have a role in hESC differentiation towards trophoblast (Xu *et al.*, 2002). OCT4 repressed BMP4 to maintain self-renewal; however knock-down of OCT4 or induction of BMP4 expression led to differentiation towards mesendoderm, ectoderm or extraembryonic lineages (Wang *et al.*, 2012c). When expression of OCT4, SOX2 and NANOG is downregulated due to differentiation, genes that were originally repressed in hESCs were found to be upregulated leading to, eventually, loss of pluripotency (Boyer *et al.*, 2005). OCT4, SOX2 and NANOG also autoregulate themselves, which can have importance in maintaining the stability of gene expression and rapid response to environmental changes (Figure 1.2) (Boyer *et al.*, 2005).

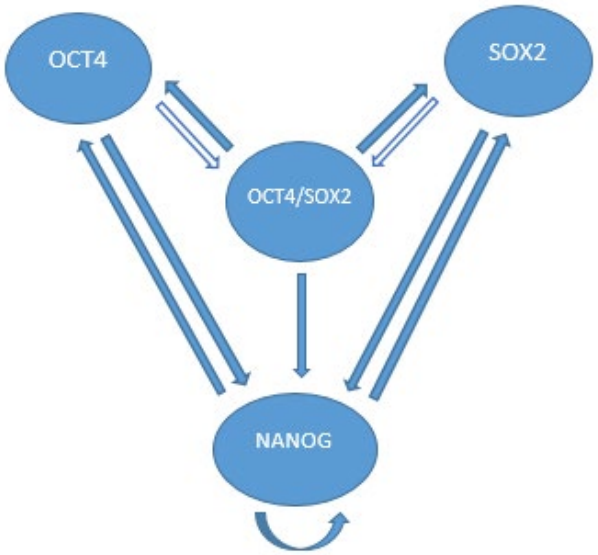

Figure 1.2 **Schematic representation of the autoregulatory loop of key pluripotency markers, OCT4, SOX2 and NANOG.**

OCT4, SOX2 and NANOG autoregulate themselves. OCT4 can form a protein complex with SOX2 (white arrows) and the OCT4/SOX2 complex regulates the gene expression of OCT4, SOX2 and NANOG (blue arrows). NANOG is also responsible for regulating the gene levels of OCT4, SOX2 as well as its own expression (blue arrows). Adapted from Boyer *et al.* (2005).

The expression level of OCT4 is regulated by the protein complex OCT4/SOX2 that is formed by the direct interaction of OCT4 POU domain and the high mobility group domain of SOX2. The complex can bind to the target enhancer or promoter region and control gene activity (Okumura-Nakanishi *et al.*, 2005). Oct4/Sox2 was identified as a nonreciprocal interaction, with Oct4 guiding Sox2 to the target site and stabilizing the binding (Li *et al.*, 2019). Expression of OCT4 protein is also regulated by NANOG, which activates transcription; thus a deficiency of NANOG results in OCT4 downregulation (Loh *et al.*, 2006).

In the same manner, NANOG autoregulates its own transcription (Loh *et al.*, 2006). *NANOG* gene is also regulated by OCT4/SOX2 complex that binds to the *NANOG* promoter. It was shown that SOX2 could bind to the *NANOG* promoter on its own, in the absence of OCT4; however binding with OCT4 is preferred. Thus, the protein complex OCT4/SOX2 has a high affinity to the *NANOG* promoter region (Rodda *et al.*, 2005). It was shown that binding to the *NANOG* promoter by the protein complex is favoured over binding to other genes, such as *FGF4* (Yuan *et al.*, 1995).

SOX2 transcription is regulated by an OCT4/SOX2 protein complex. *SOX2* contains regulatory regions that are recognised by the complex that can bind to it and activate *SOX2* expression

(Tomioka *et al.*, 2002). NANOG is also responsible for regulating *SOX2* expression level. The absence of NANOG results in downregulation of SOX2 (Loh *et al.*, 2006).

1.8.5 Other pluripotency markers

Antibodies for TRA-1-60 and TRA-1-81 are widely used to detect the expression of those antigens on the cell adhesion protein podocalyxin, which is located on the cell surface (Schopperle and DeWolf, 2007; Wright and Andrews, 2009). They are good embryonic stem cell markers because when cells undergo differentiation, the expression of TRA-1-60 and TRA-1-81 significantly decreases, enabling monitoring of the pluripotency state (Schopperle and DeWolf, 2007; Zhao *et al.*, 2012; Bharathan *et al.*, 2017). Other commonly used markers of embryonic stem cells are SSEA3 and SSEA4 (stage-specific embryonic antigen-3 and stage-specific embryonic antigen-4). SSEA3 and SSEA4 are sphingolipids that are expressed on the membrane surface in undifferentiated hESCs. Loss of pluripotency due to differentiation is characterised by rapid down-regulation of SSEA3 and SSEA4. SSEA3 and SSEA4 are markers specific for hESCs but not mESCs (Henderson *et al.*, 2002; Zhao *et al.*, 2012; Bharathan *et al.*, 2017). However, some of the mentioned pluripotency markers are not specific for hESCs (Table 1.1).

Table 1.1 **Expression of stem cell markers.**

Green colour indicates the type of cell where the expression occurs; OCT4, SOX2 and NANOG are expressed in hESCs, ECC and mESCs. TRA-1-60, TRA-1-81, SSEA-3 and SSEA-4 are expressed in hESCs and ECC. SSEA-1 is a marker specific for mESCs. Adapted from (Zhao *et al.*, 2012).

	Stem cell marker	Stem cell type		
		hESC	ECC	mESC
Transcription factors	OCT4			
	SOX2			
	NANOG			
Surface markers	TRA-1-60			
	TRA-1-81			
	SSEA-3			
	SSEA-4			
	SSEA-1			

1.9 Fatty acids: characteristics, biosynthesis and functions

Fatty acids serve as fuels for energy generation, are vital components of cell membrane lipids, and act as substrates for the synthesis of bioactive mediators (Calder, 2016). Fatty acids are monocarboxylic acids with a hydrocarbon chain and a methyl group terminating the non-carboxyl end of the chain. Fatty acids can be classified according to structural features (Figure 1.3). For example, they can be divided into:

- saturated fatty acids, which have only single bonds between carbon atoms,
- unsaturated fatty acids, which have double bonds between some carbon atoms and can be further classified into:
    - monounsaturated: that contain only one double bond between carbon atoms,
    - polyunsaturated (PUFA): that contain two or more double bonds between carbon atoms.

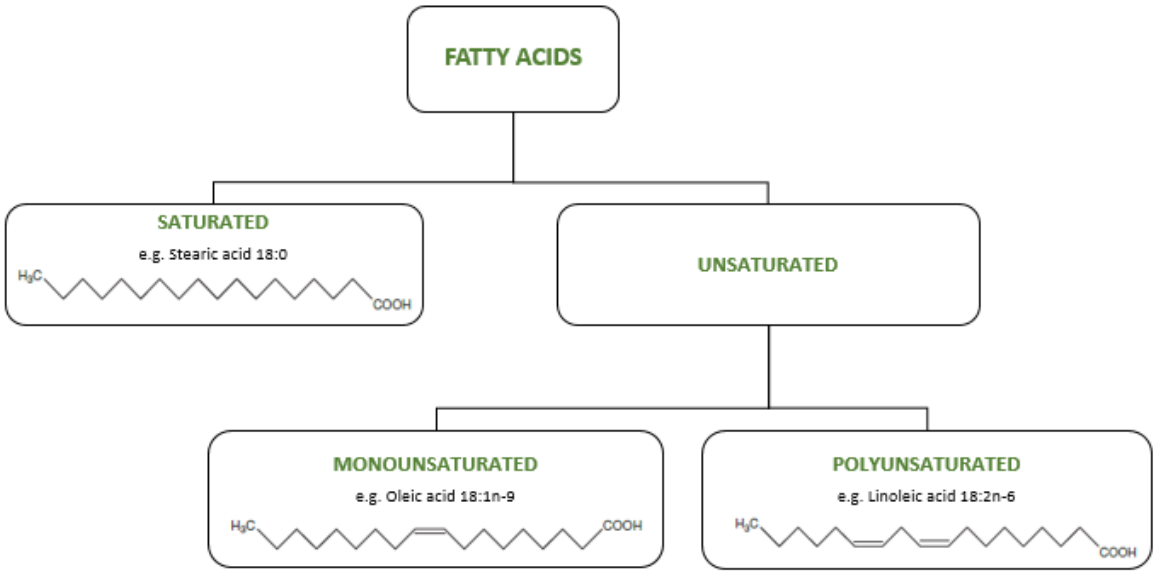

Figure 1.3 **Classification of fatty acids according to the degree of saturation and unsaturation.**

Fatty acids can be classified into saturated and unsaturated. Saturated fatty acids have only single bonds between carbon atoms, while unsaturated have double bond(s) between carbon atoms. Monounsaturated fatty acids have only one double bond between carbon atoms, while polyunsaturated contain two or more double bonds.

Unsaturated fatty acids can be cis or trans isomers, meaning that the dimensional position of atoms adjacent to the double bond differs between cis and trans configurations (Figure 1.4). This changes the structure of the fatty acid where the cis structure has a kink and trans is straight. The configuration has an impact on properties such as the melting point (cis fatty acids have a lower melting point than trans) and the structure of the cell membrane (Calder, 2016).

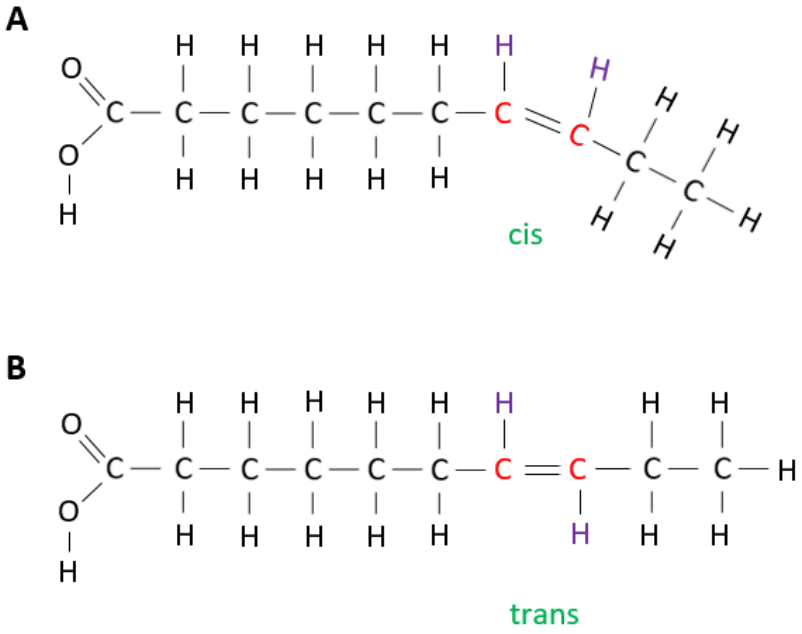

Figure 1.4 **The difference in the structure of cis and trans fatty acids.**

Example of cis (A) and trans (B) fatty acid structure. In cis configuration, hydrogen atoms adjacent to the double bond are on the same side, while in trans isomers hydrogen atoms are on opposite sides of the double bond.

PUFAs can be further divided into families according to the position of the double bond closest to the methyl terminus of the hydrocarbon chain. Most interest is in the omega-6 (n-6) and omega-3 (n-3) PUFA families. Linoleic acid (LA, 18:2n-6) and α-linolenic acid (ALA, 18:3n-3) are the simplest members of these families. They are both essential fatty acids, which means that they cannot be synthesised *de novo* in mammals, and therefore, need to be obtained from the diet. Both LA and ALA can be metabolised to more unsaturated and longer chain derivatives; the products of conversion of LA belong to n-6 PUFA and those of ALA conversion to the n-3 PUFA. The series of conversion is catalysed by enzymes, desaturases and elongases, or during the β-oxidation process (Figure 1.5) (Calder, 2016).

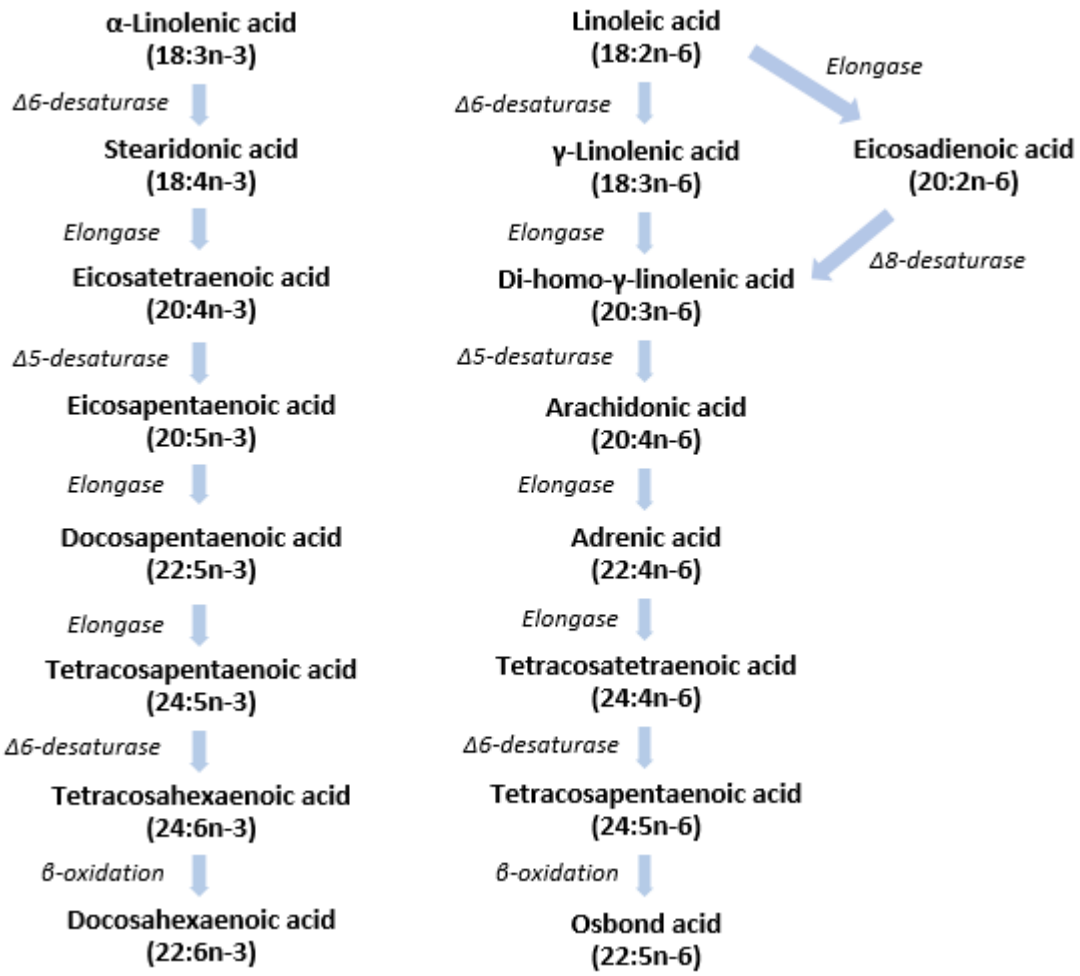

Figure 1.5 **The pathways of synthesis of n-3 and n-6 PUFAs.**

Linoleic acid (LA, 18:2n-6) and α-linolenic acid (18:3n-3) are essential fatty acids that need to be obtained from the diet. Both LA and ALA can be metabolised to more unsaturated and longer chain derivatives. The series of conversion is catalysed by desaturases and elongases, or during the β-oxidation process. Adapted from Calder (2016).

The first step during n-3 or n-6 PUFA biosynthesis pathway is the conversion of α-linolenic acid (18:3n-3) into stearidonic acid (18:4n-3), or linoleic acid (18:2n-6) into γ-linolenic acid (18:3n-6) by a desaturation process. This is mediated by Δ6-desaturase, encoded by the *FADS2* gene, the activity of which is regulated by sterol-regulatory element-binding protein-1c (SREBP-1c). Δ6-desaturase requires oxygen as the electron acceptor and NADH for enzymatic activity (Lee *et al.*, 2016). It catalyses the desaturation - removal of two hydrogens and insertion of the double bond at the 6th carbon from carboxyl group end of the fatty acid (Cook and McMaster, 2002; Lee et al., 2016). Since n-3 and n-6 PUFAs are metabolised by the same enzyme, there is a substrate

competition between the families although Δ6-desaturase prefers n-3 PUFA over n-6 PUFA (Calder, 2016).

Stearidonic acid (18:4n-3) can be further converted into eicosatetraenoic acid (20:4n-3) or γ-linolenic acid (18:3n-6) into di-homo-γ-linolenic acid (20:3n-6) by elongation - the process that consists of incorporation of two more carbons into the fatty acid chain, therefore, increasing the length. Elongation is catalysed by elongases and to date, there are seven known subtypes of elongases, encoded by *ELOVL1* to *ELOVL7* genes. Each subtype has a different preference for reaction substrate, which in general is determined from the level of unsaturation (Jump, 2009). The activity of elongases was also found to be dependent upon the developmental stage. mRNA levels of *Elovl* genes, *Elovl3* and *Elovl6,* were found to be decreased in mESCs compared to the expression level measured in embryoid bodies (Park *et al.*, 2010). This resulted in a change of composition and proportion of subspecies of ceramides within cells. This is interesting, since ceramides are known to be involved in the induction of apoptosis, but also in cell signalling (Bieberich, 2008; Park et al., 2010). Chain elongation can occur in mitochondria or the endoplasmic reticulum and the latter is predominant. During this process, two carbons are donated by 3-carbon malonyl-CoA and incorporated by 3-keto acyl-CoA synthase (elongase) (Cook and McMaster, 2002; Jump, 2009).

The next step in the biosynthesis pathway is desaturation of eicosatetraenoic acid (20:4n-3) or di-homo-γ-linolenic acid (20:3n-6) to eicosapentaenoic acid (20:5n-3) or arachidonic acid (20:4n-6), respectively, by Δ5-desaturase (D5D), encoded by the *FADS1* gene. D5D catalyses the insertion of a double bond at the 5th carbon from the carboxyl group end of the fatty acid. Similar to Δ6-desaturase, it requires oxygen and NADH for enzymatic activity and D5D prefers n-3 PUFA over n-6 PUFA as a reaction substrate. Desaturase activity is also regulated by sterol-regulatory element binding protein-1c (SREBP-1c) (Cook and McMaster, 2002).

Eicosapentaenoic acid (20:5n-3) is further converted into docosapentaenoic acid (22:5n-3) and arachidonic acid (20:4n-6) into adrenic acid (22:4n-6) in an elongation process. The next step in the pathway involves incorporation of 2 carbons by elongase, producing tetracosapentaenoic acid (24:5n-3) out of docosapentaenoic acid (22:5n-3) and tetracosatetraenoic acid (24:4n-6) out of adrenic acid (22:4n-6). Tetracosapentaenoic acid (24:5n-3) or tetracosatetraenoic acid (24:4n-6) can be then desaturated by Δ6-desaturase that converts it into tetracosahexaenoic acid (24:6n-3) or tetracosapentaenoic acid (24:5n-6), respectively. The last step in the PUFA biosynthesis consists of β-oxidation of tetracosahexaenoic acid (24:6n-3) into docosahexaenoic acid ((22:6n-3) and of tetracosapentaenoic acid (24:5n-6) into osbond acid (22:5n-6) (Calder, 2016). β-oxidation is a process that takes place in mitochondria (in eukaryotic cells) during which long-chain fatty acids

are broken down by enzymatic reactions that release acetyl-CoA, $FADH_2$ and NADH. The acetyl-CoA produced by β-oxidation is then used during Krebs cycle (Houten and Wanders, 2010).

1.9.1 FADS1

Fatty acid desaturase 1 (*FADS1*) is a gene encoding the enzyme Δ5-desaturase (D5D) that desaturates fatty acids by introducing a cis double bond at carbon 5 from the carboxyl group end of the fatty acid (Leonard *et al.*, 2000). *FADS1* is found on chromosome 11 where it forms a cluster, together with the *FADS2* gene (see below). D5D consists of a hydrophilic N-terminal heme-binding domain and a C-terminal desaturase domain, with three histidine-rich regions being responsible for non-heme iron binding necessary for enzymatic activity (Marquardt et al., 2000). D5D is also indirectly a regulator of the inflammatory response because it is a rate-limiting enzyme for the biosynthesis of 20:4n-6 (AA) from 20:3n-6 (DGLA), both precursors of eicosanoids, involved in the inflammatory response. However, AA-derived eicosanoids are mainly pro-inflammatory whilst DGLA-derived are anti-inflammatory. Interestingly, inhibition of D5D activity with oral intake of *compound-326*, led to decreased atherosclerosis in mice due to decreased levels of AA and increased levels of DGLA (Takagahara *et al.*, 2019). In breast cancer cells D5D was found to be involved in cancer invasion. The study found that breast cancer cells expressed high levels of cyclooxygenase-2 (COX-2), which metabolises AA and DGLA to produce eicosanoids. However, when the expression of D5D was silenced, and therefore biosynthesis of AA was reduced, COX-2 was found to metabolise the available DGLA into 8-hydroxyoctanoic acid (8-HOA), which can inhibit cancer growth and migration (Yang *et al.*, 2016; Xu *et al.*, 2018). Nonetheless, AA is necessary for a healthy organism. The study by Fan *et al.* (2012) reported that *Fads1* knockout mice (therefore AA or/and EPA deficient) died prematurely and had a number of pathologies, such as decreased proliferation rate of colonic cells and lower number of mononuclear and $CD3^+$ T-cells. The same study found that supplementation of the diet with AA helped to prolong lifespan that was then comparable to that of the wild type mice (Fan *et al.*, 2012). This suggests that D5D regulates the balance of fatty acids, which in turn is important for survival. D5D activity is also dependent on the type of diet. D5D activity was increased in animals fed with an essential fatty acid-deficient diet, and analogously when the diet was high in n-3 and n-6 PUFAs, enzyme activity was decreased (Cho et al., 1999). Interestingly, there is an alternative transcript of *FADS1*, FADS1AT that has no desaturase activity; however, it promotes the activity of Δ6-desaturase as the production of 18:3n-6 via this enzyme is enhanced, which also results in increased formation of eicosanoid precursors (Park et al., 2012). *FADS1* was found to be highly up-regulated in the hatched blastocyst, which suggests an important role of this gene during embryonic development (Rekik et al., 2011). In mESCs, inhibition of the activity of D5D and Δ6-desaturase by curcumin and

sesamin, respectively, was found to promote the pluripotent state through the upregulation of Oct4 and Nanog whilst neuronal differentiation was reduced (Yanes et al., 2010). To date, little is known about the role of D5D in pluripotency maintenance in hESCs.

1.9.2 FADS2

Δ6-desaturase, encoded by *FADS2*, contains the same domains as D5D (Marquardt et al., 2000). It introduces a cis double bond in PUFAs at carbon 6 from the carboxyl group end of the fatty acid. It can also mediate a bioconversion of palmitic acid (16:0) to sapienic acid (16:1n-10), an abundant fatty acid found in human sebum (Ge *et al.*, 2003). Other factors that have an impact on Δ6-desaturase activity includes the presence of cofactors (pyridoxine, zinc, nicotinic acid, magnesium), age (the activity of the enzyme decrease with age) and the type of diet. Total fasting and a glucose-rich diet reduce enzymatic activity, whereas partial caloric restriction increases desaturase activity (Das, 2007).

1.9.3 The biological significance of fatty acids

Fatty acids play an important role within an organism, for example in metabolism as an energy source and as a component of phospholipids. Phospholipids are vital constituents of all cell membranes and consist of a hydrophilic head (phosphate group) connected to two hydrophobic fatty acid tails by glycerol (Figure 1.6).

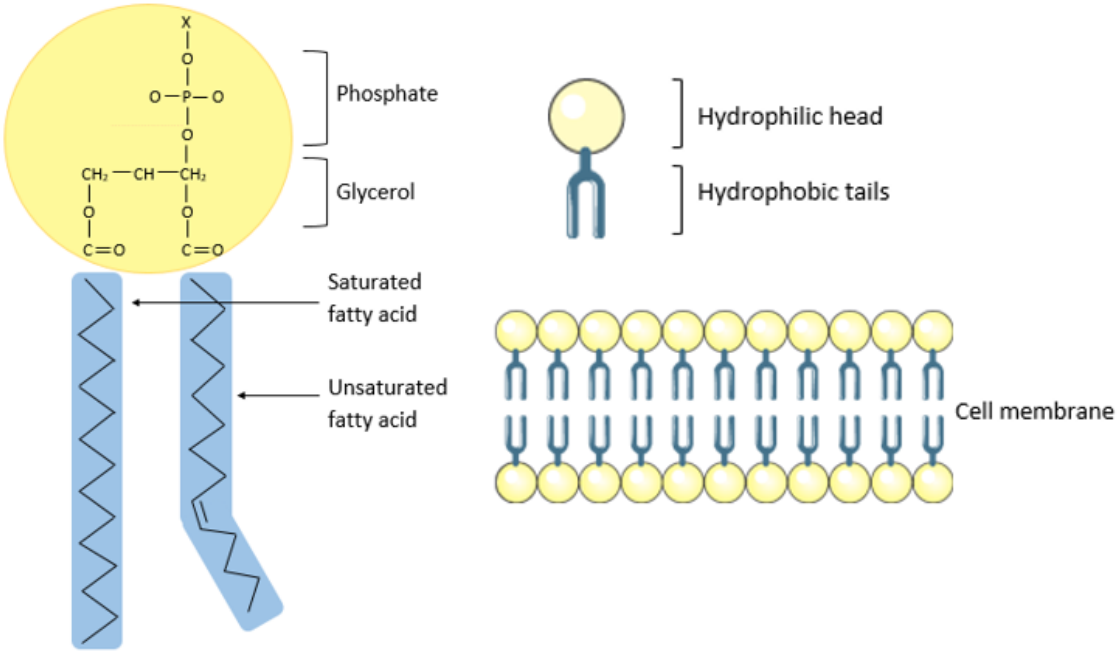

Figure 1.6 **Cell membrane consists of phospholipids.**

Phospholipids consist of two fatty acid chains connected to a phosphate group through glycerol. The phosphate group can be modified by attachment of, for example, choline or serine (marked as X). Phospholipids are the main component of the cell membrane.

Properties of membranes depend upon the type of fatty acids present, such as the presence of unsaturated fatty acids increasing the fluidity of the membrane (Calder, 2016). This is believed to be important in the regulation of many membrane proteins that act as receptors, transporters, channels and enzymes (Calder, 2016; Chatgilialoglu et al., 2017). Also, a membrane consisting of shorter chain fatty acids is more flexible due to weaker interactions compared to those between long-chain fatty acids (Cooper, 2000).

N-3 and n-6 fatty acids are known to be biologically active. They are involved in various processes, such as regulation of cellular responses through their conversion to eicosanoids and other lipid mediators (Weylandt *et al.*, 2012; Jarc and Petan, 2020). Arachidonic acid (AA, 20:4n-6) is a precursor for the synthesis of proinflammatory lipid mediators, such as n-6 eicosanoids like prostaglandin E_2 (PGE_2) and leukotriene B_4 (LTB_4). However, the n-3 PUFA eicosapentaenoic acid (EPA, 20:5n-3) is an antagonist to AA and can inhibit the synthesis of these mediators (Caughey et al., 1996). Furthermore, n-3 PUFAs are substrates for the synthesis of resolvins and protectins, lipid mediators that are involved in the termination of inflammation and maintenance of cell homeostasis (Ariel and Serhan, 2007). Interestingly, in mESCs, PGE_2 inhibits apoptosis, but the presence of 15-deoxy-delta-12,14-prostaglandin J_2 (15d-PGJ_2), also produced from AA, decreases

proliferation and self-renewal through inhibition of the JAK-STAT pathway (Niwa *et al.*, 1998; Rajasingh and Bright, 2006; Liou *et al.*, 2007; Kang *et al.*, 2014). This evidence highlights the diverse role of fatty acid metabolites in stem cell self-renewal maintenance and proliferation but also presents the importance of PUFA for cellular growth. In a study on human fetal membrane mesenchymal stromal cells (hFM-MSCs) it was presented that the PUFA content of the cells *in vitro* decreases with each cell passage and is lower compared to freshly isolated cells. However, supplementation of the cell culture medium with fatty acids decreased the loss of PUFA, especially n-6 PUFA, and resulted in an increased rate of cell proliferation (Chatgilialoglu *et al.*, 2017). Restored levels of PUFA was also shown to affect inflammation response, through increased levels of lipid mediators, such as lipoxin A_4, known to be responsible for resolving an inflammation (Cianci *et al.*, 2016; Chatgilialoglu *et al.*, 2017).

It was shown that n-3 PUFAs could alter cell signalling and functions through changes in lipid raft organisation (Hashimoto *et al.*, 2005; Schley *et al.*, 2007; Kim *et al.*, 2008; Hou *et al.*, 2016). Lipid rafts are small cell membrane domains, enriched with cholesterol, sterol- and sphingolipids. They are involved in cellular processes, such as signalling, by concentrating and anchoring membrane lipids and proteins (Pike, 2006). A higher level of n-3 PUFAs in a cell membrane can cause clustering of lipid rafts and formation of larger domains that result in weaker lipid raft activity. The composition of lipid rafts was found to be altered by an environment enriched with n-3 PUFAs, leading to changes in cell signalling events (Turk and Chapkin, 2013). Such changes were found to modulate the activity of transcription factors, such as NF-κB, which is involved in regulating the proinflammatory response. It was shown that supplementation of T-cells with n-3 PUFA altered the lipid raft composition, leading to inhibited transcriptional activity of NF-κB (Fan *et al.*, 2004). This presents the important bioregulatory role of PUFA and shows how changes in the microenvironment of lipid raft can affect cell signalling.

Caveolae are a subtype of lipid rafts with the flask- or U-shape structure formed within the cell membrane. Caveolae are composed of tightly bound sphingolipids and cholesterol, enriched with proteins from the caveolin family, especially caveolin-1, and cannot be easily disintegrated by exposure to high salts or detergents (Rothberg *et al.*, 1992; Sohn *et al.*, 2016). Caveolae are known to be involved in regulating various signalling pathways. This is due to the structure of caveolin-1, which contains scaffolding domains that can bind molecules, such as kinases or proteins from the Ras family, and in consequence either inhibit or activate the signalling cascade (Martinez-Outschoorn *et al.*, 2015). The mechanism of this regulation is still too be fully elucidated; however, so far the best-characterised is binding of endothelial nitric oxide synthase (eNOS) to caveolin-1. Through this interaction, caveolin-1 can inhibit eNOS functions, leading to decreased nitric oxide generation (García-Cardeña *et al.*, 1996; Harvey and Calaghan, 2012;

Martinez-Outschoorn *et al.*, 2015). Caveolae are also involved in fatty acid trafficking, mechanisms dependent on caveolin-1 expression and cholesterol level (Meshulam *et al.*, 2006). Thus, adipocytes have increased number of caveolae and increased expression of caveolin-1 compared to other types of cells (Pilch *et al.*, 2007). It was shown that hepatocytes of caveolin-1 deficient mice had decreased ability for lipid accumulation and proliferation leading to worse liver regeneration after injury (Fernández *et al.*, 2006). Caveolae are also responsible for cellular sensing and response to external stimuli. Disrupting caveolae led to swelling of rat ventricular myocytes in a hypotonic environment presenting a role of this subtype of lipid raft in regulating membrane tension in response to stimuli (Kozera *et al.*, 2009). In mESCs, destruction of caveolae or silencing of caveolin-1 led to decreased proliferation rate as well as downregulation of Oct4 and Sox2 expression (Lee et al., 2010). Therefore, caveolae are important cell membrane structures shown to be involved in proliferation, cell signalling but also in the maintenance of embryonic stem cell self-renewal.

1.10 Hypoxia Inducible Factors

A change of oxygen tension within a cell triggers responses to maintain homeostasis, such as altered regulation of gene expression. The response to a low oxygen concentration is mediated by Hypoxia Inducible Factors (HIFs): HIF1α, HIF2α (also known as EPAS-1), HIF3α, and HIF1β.

HIF1α is known to be the predominant regulator of the hypoxic response. It can directly regulate a number of genes involved in various processes such as angiogenesis (Tsuzuki *et al.*, 2000; Kelly *et al.*, 2003; Nikitenko *et al.*, 2003), differentiation (Gustafsson *et al.*, 2005; Zhang *et al.*, 2008; Takubo *et al.*, 2010) or metabolism (Hayashi *et al.*, 2004; Obach *et al.*, 2004; Papandreou *et al.*, 2006). Regulation of carbohydrate metabolism by HIF1α is especially well-known and established. In hypoxic conditions, HIF1α was found to positively regulate expression of glucose transporters, GLUT1 and GLUT3, therefore increasing the rate of glucose uptake (Mobasheri *et al.*, 2005). A switch in metabolism from oxidative phosphorylation to glycolysis is also recognised by upregulation of glycolytic enzymes, such as phosphoglycerate kinase 1 (PGK1) and pyruvate kinase (PKM2), as well as lactate dehydrogenase (LDH) (Iyer *et al.*, 1998; Semenza, 2013). Increased expression of pyruvate dehydrogenase kinase (PDK1) by HIF1α causes decreased flow of pyruvate into mitochondria leading to a higher level of lactate produced by LDH (Kim *et al.*, 2006; Papandreou *et al.*, 2006).

HIF2α was found to regulate gene expression connected to embryonic development, for example, maturation of the vascular network (Duan *et al.*, 2014) or tubular system of lungs (Huang *et al.*,

2012). HIF3α has 7 alternative isoforms identified so far, which contain DNA binding motifs that were not identified in HIF1α and HIF2α (Maynard *et al.*, 2003; Pasanen *et al.*, 2010). HIF3α is believed to have a mainly negative regulatory role, for example by decreasing hypoxia-induced expression of VEGF and enolase 2 (Augstein *et al.*, 2011). HIF3α is a target gene for HIF1α but interestingly it can also regulate HIF1α and HIF2α activity (Maynard *et al.*, 2005; Tanaka *et al.*, 2009; Pasanen *et al.*, 2010).

All HIF α-subunits contain similar domains (Figure 1.7) (Wang *et al.*, 1995; Ortmann *et al.*, 2014; Duan, 2016).

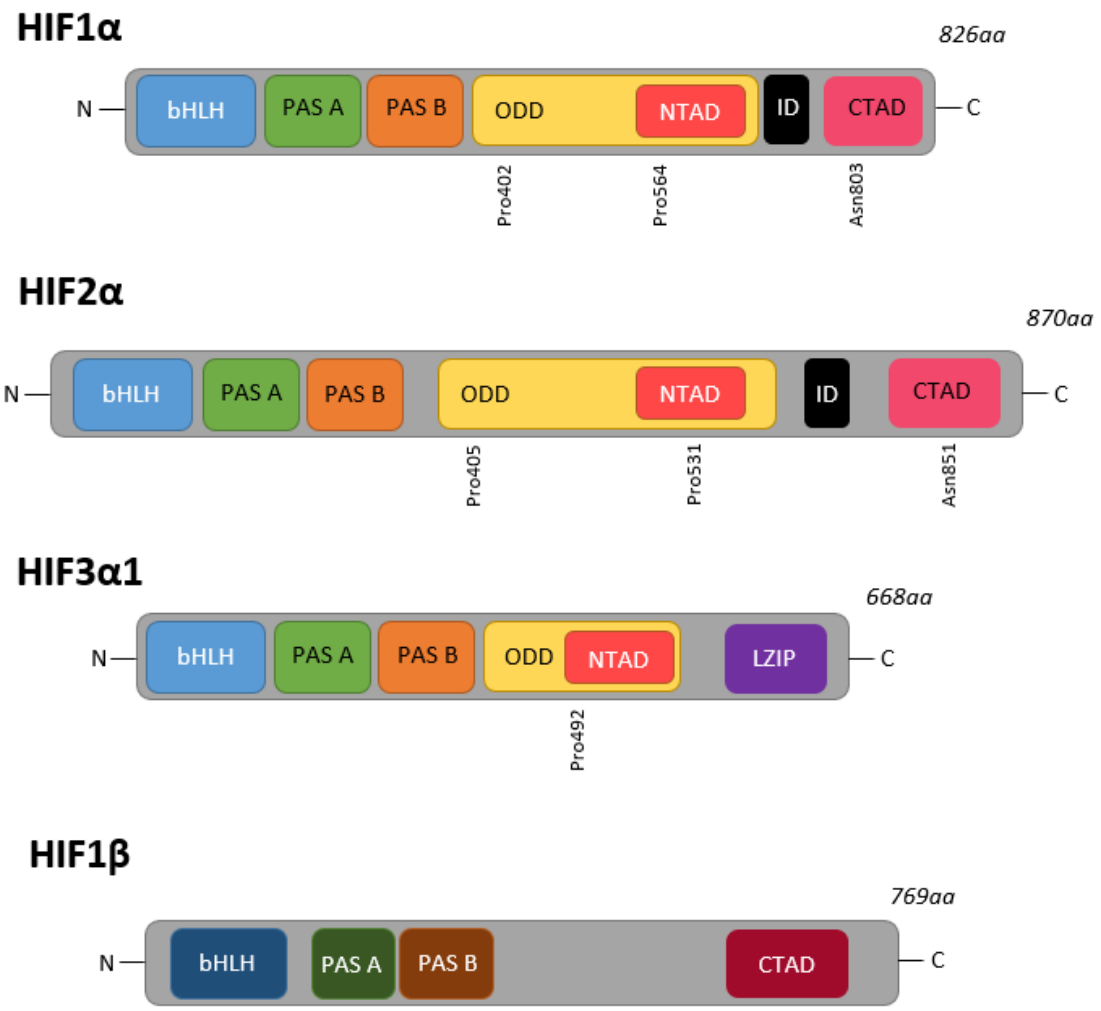

Figure 1.7 **Structural domains of the HIF member proteins.**

Schematic overview of domains within HIF1α, HIF2α, HIF3α isoform 1 (HIF3α1) and HIF1β. bHLH (basic helix-loop-helix) and PAS (Per-Arnt-Sim) domains are responsible for DNA binding and dimerization. The oxygen-dependent degradation (ODD) domain contains conserved proline(s) (Pro), which can be hydroxylated in normoxic conditions leading to HIFα degradation. The N-terminal transactivation domain (NTAD), present in all HIFα subunits, and the C-terminal transactivation domain (CTAD), absent in HIF3α, are the interaction sites for coactivators regulating the transcriptional activity of the protein. In normoxia, an asparagine residue (Asn) within CTAD can be hydroxylated by Factor Inhibiting HIF (FIH), impeding the interaction of HIFα with coactivators. The inhibitory domain (ID) is responsible for inhibiting the activity of HIFα in normoxic conditions. Leucine zipper (LZIP) is a unique domain found in HIF3α1 and is involved in DNA binding and protein-protein interactions. Protein length is shown for each subunit. Adapted from Fernandez-Torres *et al.* (2017).

Each subunit contains a bHLH (basic helix-loop-helix) domain, followed by the PAS (Per-Arnt-Sim), responsible for DNA binding and dimerization (Semenza, 2012). More specifically, the PAS domain can be divided into PAS A and PAS B (Yang *et al.*, 2005). Both domains are necessary for heterodimerization with the β subunit that result in a transcriptionally active complex. The PAS B domain of HIF2α contains a cavity that was found to be the binding site for small molecules (ligands) (Scheuermann *et al.*, 2009). Importantly, the bHLH-PAS domain was shown to be responsible for recognition and binding to the sequence 5'-(A/G) CGTG-3', known as hypoxia-response element (HRE) located within the proximal promoter or enhancer of hypoxia-responsive genes (Semenza and Wang, 1992; Wu *et al.*, 2015; Wu and Rastinejad, 2017). ODD (oxygen-dependent degradation) domain is involved in protein degradation dependent on oxygen tension through prolyl hydroxylases (PHDs) activity (Huang *et al.*, 1998). N-terminal transactivation domain (NTAD) is located within ODD and is the interaction site of HIFα coactivators, such as p300/CBP, steroid receptor coactivator-1 (SRC1) and transcription intermediary factor 2 (TIF2) (Arany *et al.*, 1996; Carrero *et al.*, 2000; Ruas *et al.*, 2010). The deletion of ODD containing NTAD led to significant reduction in transcriptional activity of HIFα, highlighting the importance of this domain for driving gene expression (Klinger *et al.*, 2011). C-terminal transactivation domain (CTAD) has a similar role as NTAD and interacts with coactivators p300/CBP, SRC1 and TIF2 (Carrero *et al.*, 2000; Lisy and Peet, 2008; Ruas *et al.*, 2010). However, it was shown that CTAD and NTAD are responsible for regulating expression of different sets of genes (Dayan *et al.*, 2006; Yan *et al.*, 2007). Interestingly, when activity of NTAD was inhibited, there was a significant increase in expression of genes, such as DNA-damage-inducible transcript 4 *(DDIT4)* or plasminogen activator, urokinase receptor *(PLAUR)*. When only NTAD was active, expression of BCL2 Interacting Protein 3 *(BNIP3)* or phosphofructokinase, liver type *(PFKL)* was induced (Dayan *et al.*, 2006). This presents that each transactivation domain has distinctive function in transcriptional activity of HIFα. However, only NTAD was identified as a domain necessary for HIFα target gene specificity (Hu *et al.*, 2007). The inhibitory domain (ID) is located between NTAD and CTAD and was found to negatively regulate transcriptional activity of these transactivation domains. The inhibition was shown to be attenuated upon exposure to hypoxia or when the ID sequence was removed (Jiang *et al.*, 1997). HIF3α does not possess CTAD, however it contains a leucine zipper (LZIP) domain, which is responsible for DNA binding and protein-protein interactions (Maynard *et al.*, 2003).

HIF1β is constitutively expressed whereas HIF1α is synthesised but in normoxia (atmospheric oxygen concentration) is hydroxylated on a conserved proline residue within ODD domain by PHDs: PHD1, PHD2 and PHD3 (Ivan *et al.*, 2001; Jaakkola *et al.*, 2001; Maynard *et al.*, 2003). PHDs require molecular oxygen and thus activity is sensitive to oxygen changes. All three PHDs are

involved in HIFα regulation; however, they differ from each other according to the level of affinity to HIFs. PHD1 and PHD3 have a higher affinity for HIF2α than HIF1α and PHD2 prefers to hydroxylate HIF1α (Berra *et al.*, 2003; Appelhoff *et al.*, 2004). Hydroxylation of HIFα enables binding of pVHL (von Hippel-Lindau tumour suppressor protein) to HIF that can be recognised by ubiquitin ligase complex, which leads to proteasomal degradation (Figure 1.8 A) (Cockman *et al.*, 2000; Ohh *et al.*, 2000). Another mechanism is hydroxylation of a conserved asparagine residue of HIFα within the C-terminal transactivation domain by Factor Inhibiting HIF (FIH) (Lando *et al.*, 2002). That results in no interaction between HIFs and coactivators of HIF, such as p300/CBP, which are involved in the transcriptional activity of HIF complex on hypoxia-responsive genes (Figure 1.8 B) (Arany *et al.*, 1996; Lando *et al.*, 2002).

In hypoxia, catalytic activity of PHDs is inhibited due to low oxygen level and, therefore, HIFα is not degraded. HIFα subunits translocate to the nucleus where they form a heterodimeric complex composed of HIFα and a constitutively expressed HIFβ subunit (Semenza, 2012). Moreover, the hypoxic condition enables the binding of the C-terminal transactivation domain of HIFα with p300/CBP coactivators. This results in the activation of HIF complex transcriptional activity and binding to HRE of target genes (Semenza and Wang, 1992; Arany *et al.*, 1996). Through this binding, the HIF complex regulates the expression level of a broad range of target genes (Figure 1.8 C) (Semenza *et al.*, 1996).

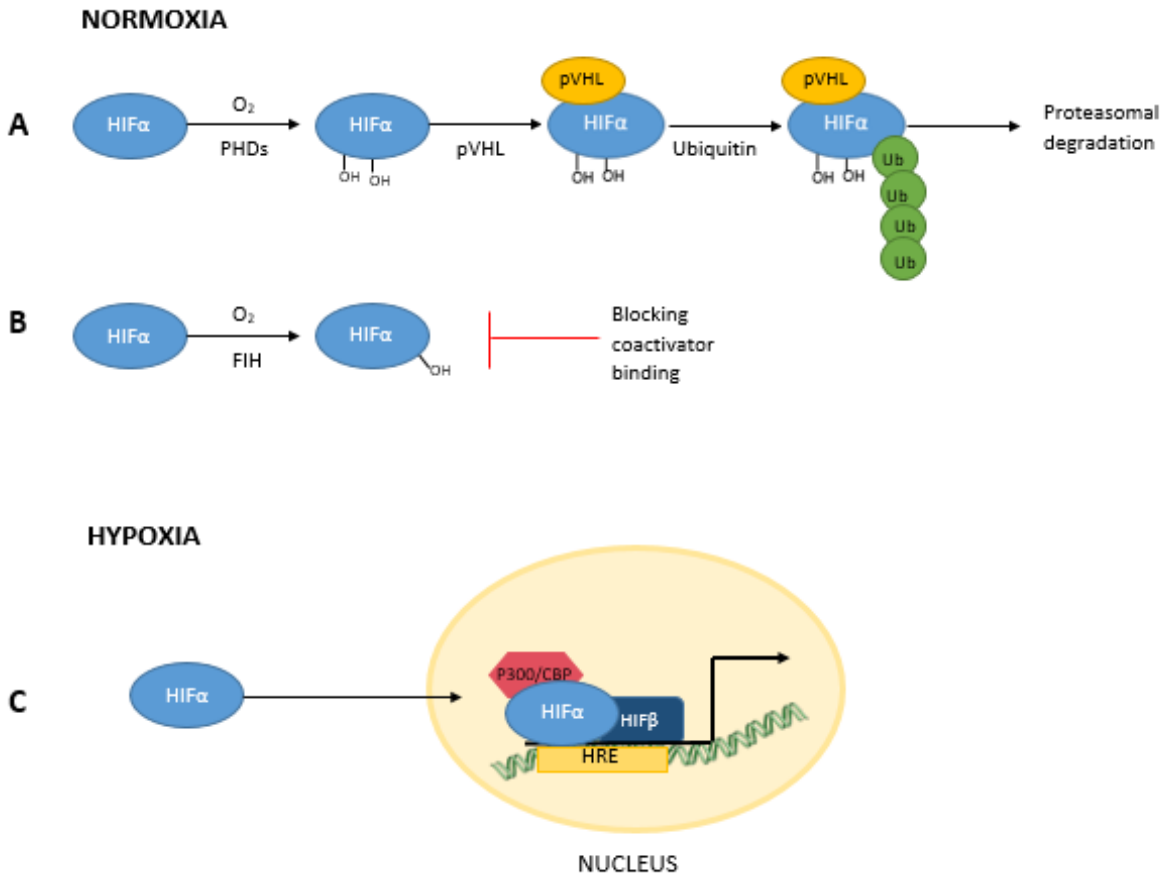

Figure 1.8 **HIFα activity is regulated by oxygen tension.**

Schematic representation of HIFα regulation in normoxia (A, B) and hypoxia (C). In normoxia, HIFα is hydroxylated by PHDs, then bounded by pVHL and targeted by ubiquitin ligase, which leads to proteasomal degradation. Another mechanism present in normoxia involves hydroxylation of HIFα by FIH that prevents binding of HIF coactivators. In hypoxia, the activity of PHDs and FIH is inhibited and HIFα is not degraded. HIFα can translocate to the nucleus where it dimerises with β subunit and bind to the HRE of target genes, therefore regulating their expression.
PHD- prolyl hydroxylase, pVHL- von Hippel-Lindau tumour suppressor protein, FIH- Factor Inhibiting HIF, Ub- ubiquitin, HRE- hypoxia response element. Adapted from Taabazuing *et al.* (2014) and Cerychova and Pavlinkova (2018).

HIFs are known to be involved in the regulation of fatty acid/lipid metabolism. In hypoxic conditions, β-oxidation, a process through which fatty acids are oxidized to yield acetyl CoA, the substrate for the TCA cycle, is reduced (Huang *et al.*, 2014a). This is a consequence of the low oxygen level, which is known to induce a switch in metabolism - cells rely more on glycolysis than mitochondrial respiration to produce energy. Fatty acid degradation is also reduced in hypoxic condition through HIF1α and HIF2α downregulation of enzymes involved in β-oxidation, such as

carnitine palmitoyltransferase 1 (CPT-1) (Mylonis *et al.*, 2019) or proliferator-activated receptor-γ coactivator-1α (PGC-1α), rate-limiting enzymes of fatty acid oxidation (Liu *et al.*, 2014). HIF1α was found to be responsible for mediating the response to low oxygen by regulating peroxisome proliferator-activated receptor gamma (PPARγ) expression (Krishnan *et al.*, 2009). PPARγ is a transcription factor that can regulate the expression of genes involved in, for example, fatty acid metabolism, such as acyl-CoA oxidase (Lehrke and Lazar, 2005). PPARγ activity in hypoxia was found to lead to increased exogenous fatty acid uptake and synthesis of neutral triacylglycerols (TAGs) that can be stored in the form of non-toxic lipid droplets (Krishnan *et al.*, 2009). Extracellular fatty acid uptake and lipid droplet formation is also enhanced by Fatty Acid Binding Protein 3 (FABP3), Fatty Acid Binding Protein 4 (FABP4) and Fatty Acid Binding Protein 7 (FABP7), all of them being regulated by HIF1α in low oxygen conditions (Bensaad *et al.*, 2014; Hu *et al.*, 2015). HIF1α is also known to play a role in *de novo* fatty acid synthesis through activating enzymes, for example isocitrate dehydrogenase (NADP(+)) 1 (IDH1), involved in glutamine metabolism (Wise *et al.*, 2011; Gameiro *et al.*, 2013; Huang *et al.*, 2014a) (Figure 1.9). Glutamine can be converted to glutamate, which can be then utilised for TCA cycle to produce energy but can also serve as a substrate for fatty acid and lipid synthesis (Huang *et al.*, 2014a).

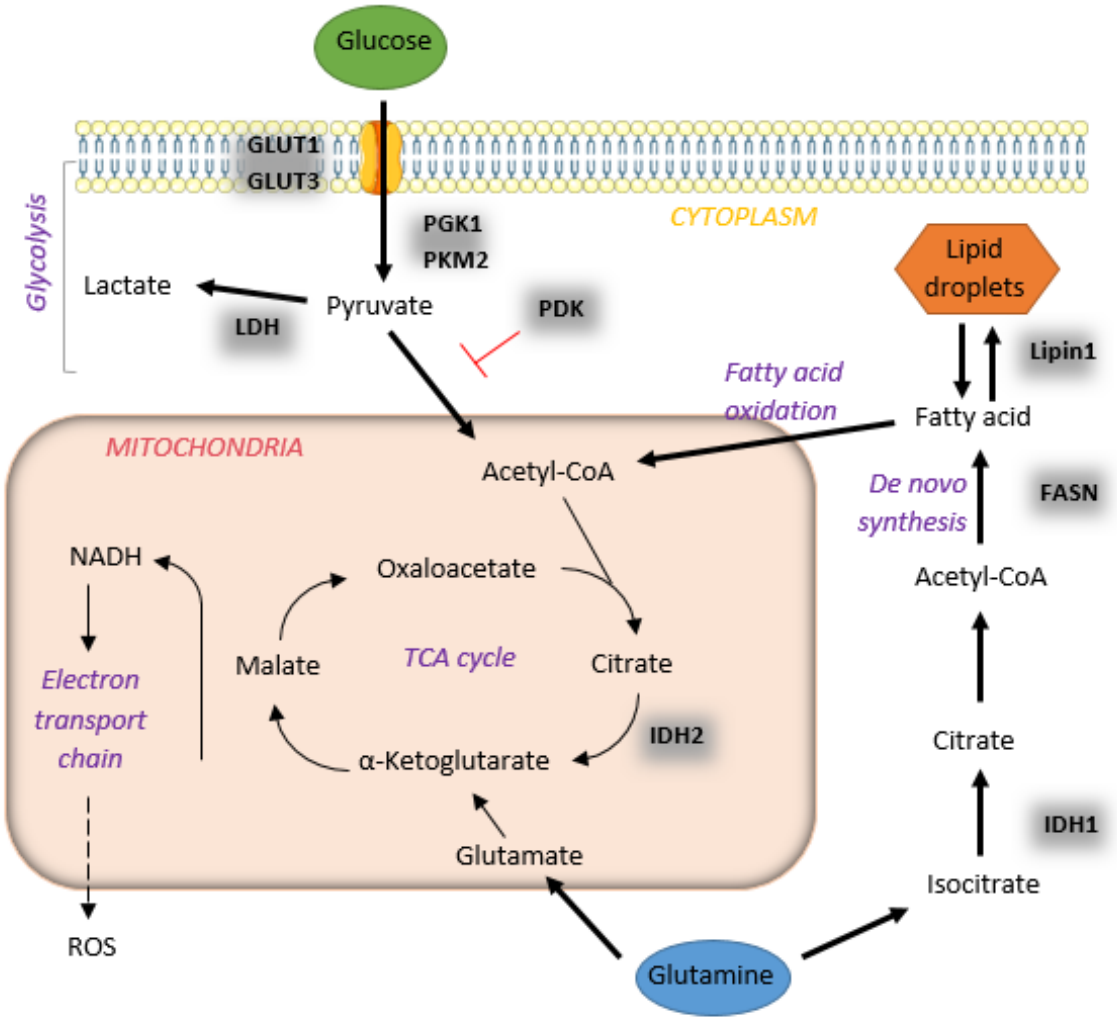

Figure 1.9 **HIFα regulates glutamine metabolism to enhance fatty acid *de novo* synthesis.**

Proteins highlighted with grey box were found to be regulated by HIFs. HIF-regulated proteins are involved in glucose transport, glycolysis, glutamine metabolism as well as fatty acid synthesis. Increased expression of these proteins in hypoxia promotes fatty acid synthesis and accumulation while inhibiting β-oxidation through the activity of HIFs. IDH1/2- isocitrate dehydrogenase 1/2, FASN- fatty acid synthase, Lipin1- Phosphatidate phosphatase LPIN1, ROS- reactive oxygen species. Adapted from Huang *et al.* (2014a).

Fatty acid synthase (FASN) is an important enzyme that catalyses the synthesis of long-chain fatty acids from acetyl-CoA, malonyl-CoA and NADPH. The expression of FASN was found to be upregulated in hypoxia (Furuta *et al.*, 2008; Sun *et al.*, 2017; Ezzeddini *et al.*, 2019). There is a direct binding of sterol regulatory element-binding protein 1 (SREBP1) to the *FASN* promoter, which regulates its expression. SREBP1 is known to be a transcription factor responsible for maintaining lipid homeostasis and is one of the target genes of HIF1α (Furuta *et al.*, 2008). However, the enhanced fatty acid synthesis might lead to the accumulation of too high a level of

free fatty acids within a cell. To prevent lipotoxicity, fatty acids need to be stored in the form of neutral lipid droplets. Phosphatidate phosphatase LPIN1 (Lipin1) is an enzyme catalysing the synthesis of TAGs that can form lipid droplets and HIF1α directly binds to the promoter of Lipin1 to regulate the expression (Mylonis *et al.*, 2012). In human clear cell renal cell carcinoma, HIF2α, but not HIF1α, is responsible for upregulating perilipin-2 (PLIN-2), the coat protein of lipid droplets, leading to enhanced lipid accumulation in a neutral form (Qiu *et al.*, 2015). Lipid droplets serve as storage so fatty acids can be later utilized when needed, for example for the production of phospholipids that are necessary for cell membrane production of proliferating cells (Petan *et al.*, 2018). In conclusion, hypoxia promotes fatty acid synthesis and accumulation while inhibiting β-oxidation through the activity of HIFs.

In hESCs, HIF1α is present in the nucleus for approximately 48 hours following the first introduction of cells to low oxygen tension (Forristal *et al.*, 2010) and thus it is believed that HIF1α is responsible for an initial hypoxic response. In contrast, HIF2α and HIF3α are present in the cytoplasm but translocate to the nucleus after long-term hypoxic culture to play a role in transcriptional regulation (Forristal *et al.*, 2010). In hESCs, HIF2α seems to be the major response regulator. HIF2α binds to the HRE sites in the proximal promoters of key pluripotency markers, *OCT4, SOX2* and *NANOG* to promote expression under hypoxia (Petruzzelli *et al.*, 2014). HIF2α also interacts with *NANOG* after reoxygenation, as a consequence of changes in the oxygen levels, leading to increased *NANOG* gene expression to possibly maintain homeostasis of cells due to oxidative stress (Petruzzelli *et al.*, 2014). HIF2α was found to regulate Myc proto-oncogene protein (MYC), which is necessary for maintaining pluripotency in hESCs by repressing differentiation genes such as *PAX3* or *PAX7* (Varlakhanova et al., 2011; Närvä et al., 2013). When HIF2α was silenced, expression of MYC was significantly decreased. It is another example that presents the role of HIF2α in self-renewal maintenance in hESCs (Närvä *et al.*, 2013). HIF3α was found to be involved in the regulation of HIF1α and HIF2α levels in hESCs (Forristal et al., 2010). However, little is known about the hypoxic regulation of lipid metabolism in hESCs and whether HIF2α, as main hypoxia regulator, might play a role.

1.11 DNA damage and ROS impact in hESCs

hESCs have immature mitochondria and metabolically rely more on glycolysis than on oxidative phosphorylation, especially if they are cultured in hypoxic condition (Forristal *et al.*, 2013). It was shown that reduced mitochondrial activity is beneficial for the stemness of hESCs (Zhou *et al.*, 2012). It can also lead to upregulation of NANOG while maintaining OCT4 expression level within limits, as too high upregulation of OCT4 causes cells to differentiate (Varum et al., 2009). Aerobic metabolism also produces toxic by-products, reactive oxygen species (ROS), such as superoxide

anion (O_2^-), hydrogen peroxide (H_2O_2), and the hydroxyl radical (OH^-) (Ray *et al.*, 2012). ROS can be produced during the electron transport chain in mitochondria: electrons are passed from electron donors to electron acceptors to create a proton gradient that is necessary for ATP production. The final electron acceptor is oxygen, which is reduced to water. However, in some cases, electrons 'leak' and oxygen is reduced to superoxide radical instead (Li *et al.*, 2013). Environmental oxygen was identified as one of the factors that can affect ROS generation but the effect is suggested to be cell type-specific (Tafani *et al.*, 2016; Lee *et al.*, 2018). In cancer cells, hypoxia induces ROS generation that can lead to tumour progression (Chandel *et al.*, 1998; Tafani *et al.*, 2016; Azimi *et al.*, 2017). However, in hematopoietic stem cells cultured in low oxygen, HIF2α was identified to be responsible for decreasing levels of ROS and protection from apoptosis (Rouault-Pierre *et al.*, 2013).

ROS are involved in various processes, for example, activation of expression of the transcription factor NF-κB (Schreck *et al.*, 1991). NF-κB is known to be involved in maintaining the undifferentiated state of hESCs; when the IκB kinase/NF-κB signalling pathway was inhibited, pluripotency markers were shown to be downregulated and hESC differentiation toward mesenchymal stromal cells was enhanced (Deng *et al.*, 2016). However, too high level of ROS is known to induce DNA damage. Hydrogen peroxide was identified as a product responsible for increasing the rate of telomere shortening in human fibroblasts (Petersen *et al.*, 1998; von Zglinicki, 2000). Telomeres are protective sequences at the end of chromosomes; however, they undergo a shortening process with each cell division. When telomere length reaches its limit, a cell is fated for apoptosis (Shammas, 2011). hESCs show a higher level of telomerase activity compared to diploid somatic cells, preventing chromosomes from shortening, therefore increasing stem cell life span (Thomson *et al.*, 1998). Also, elevated levels of ROS result in stem cell differentiation, with hESCs losing pluripotency and differentiating into mesendodermal lineage (Ji *et al.*, 2010). It has been shown that antioxidant enzymes, like Superoxide Dismutase 2 (SOD2) and Glutathione Peroxidase 2 (GPX2) are downregulated during differentiation of hESCs, leading to an increased level of ROS in a cell (Saretzki *et al.*, 2008). In mESCs, Sod1 expression was found to be downregulated upon silencing of Oct4, Sox2 and Nanog, showing the connection between self-renewal and redox homeostasis (Solari *et al.*, 2018).

hESCs have enhanced DNA repair systems, minimising the chance of proliferation of cells containing damaged DNA. Maynard *et al.* (2008) found that the expression level of repair genes, such as *BER*, *NER*, *DSBR* and *ICL*, is higher in hESCs compared to differentiated cells. *In vitro* mutations can be caused by a variety of factors, such as acidification and accumulation of lactic acid in the culture medium as a result of high-density culture (Jacobs *et al.*, 2016). Cells containing mutations or damaged DNA should not be part of a stem cell population, and thus they are fated

to differentiate or must undergo apoptosis. However, despite the repair systems, hESCs are known to have a tendency for mutations (Keller *et al.*, 2018). One of the proteins involved in DNA repair and the apoptotic response in a cell is poly (ADP-ribose) polymerase 1 (PARP-1). PARP-1 is localised in the nucleus and has the ability to post-translationally modify proteins through PARylation - attachment of poly(ADP-ribose). PARP-1 can PARylate itself to activate the DNA repair response on single-strand breaks (SSBs) and double-strand breaks (DSBs) (Lindahl *et al.*, 1995). PARP-1 was found to have three main domains in its structure (Kameshita *et al.*, 1984; Petrucco and Percudani, 2008; Ali *et al.*, 2012; Langelier *et al.*, 2012):

- amino-terminal DNA-binding domain (DBD) - contains zinc-finger motifs that can bind to single- or double-strand DNA breaks; the site for DNA binding,
- BRCT domain - automodification domain for accepting poly(ADP-ribose),
- carboxy-terminal catalytic domain - site for binding of a substrate (NAD^+).

PARP-1 can recognise DNA damage and bind to those sites while attaching numerous ADP-ribose polymers to itself (Figure 1.10 A). Proteins involved in DNA repair and metabolism can then bind to chains of poly(ADP-ribose) on PARP-1 if they contain in their structure ADP-ribose-binding consensus motifs (Krietsch *et al.*, 2013). This way they are recruited to the site of damage where through the non-covalent binding to poly(ADP-ribose) repair functions are activated (Ray Chaudhuri and Nussenzweig, 2017). An example of such interaction can be p53 protein, which repair activity was found to be connected to the presence of poly(ADP-ribose) (Malanga *et al.*, 1998). PARP-1 is necessary for an efficient DNA repair system, as depletion of PARP-1 in adenocarcinomic human alveolar basal epithelial cells caused an increased rate of single-strand breaks (Fisher *et al.*, 2007). Interestingly, one of the studies showed that centenarians (people older than 100 years) have significantly increased activity of PARP-1 compared to the control group (people aged 20-70 years), suggesting that this enzyme might be one of the factors essential for long life (Muiras *et al.*, 1998).

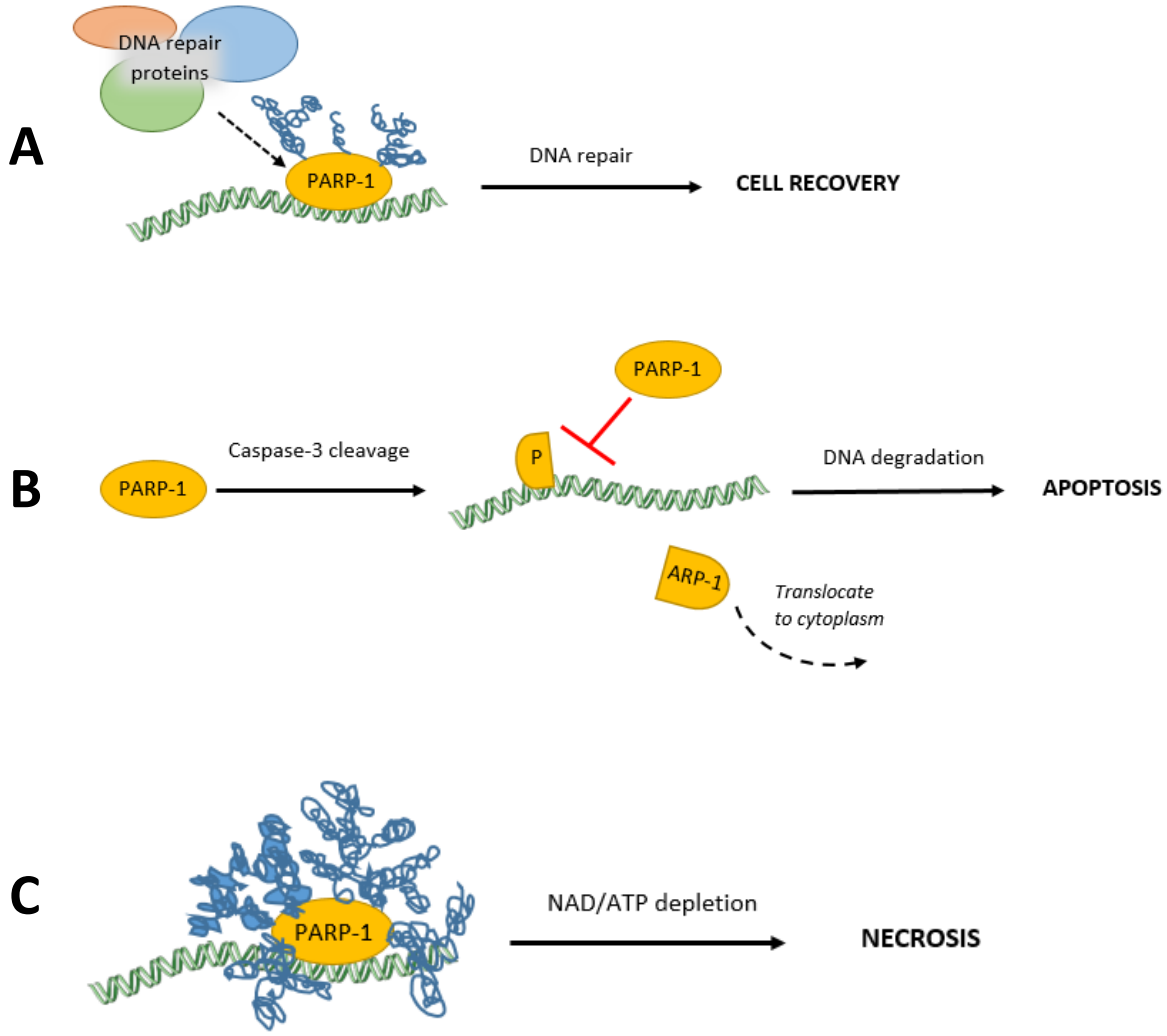

Figure 1.10 **PARP-1 in DNA repair, apoptosis and necrosis.**

Schematic mechanism of PARP-1 function in DNA repair (A), apoptosis (B) and necrosis (C). (A) PARP-1 can bind to damaged DNA and attach poly(ADP-ribose) to itself. Proteins involved in DNA repair can then non-covalently bind to poly(ADP-ribose) to activate their repair functions. (B) PARP-1 can be cleaved by Caspase-3 into two fragments; smaller part remains in the nucleus where it binds to the DNA, preventing binding of uncleaved PARP-1. The bigger part translocate from the nucleus and has no activity. No PARP-1 activity leads to apoptosis. (C) Overactivated PARP-1 attach numerous poly(ADP-ribose) groups to itself leading to NAD depletion and therefore necrosis. Blue curly lines around PARP-1 represent poly(ADP-ribose). Adapted from Swindall *et al.* (2013).

If the cell is fated for apoptosis, PARP-1 is cleaved by caspase-3, resulting in two fragments, an 89 kDa part containing BRCT and catalytic domain, and a 24 kDa part that consists of DBD. The 89 kDa fragment is translocated from the nucleus into the cytoplasm and has no catalytic ability. However, the DBD part remains in the nucleus where it binds to DNA, preventing uncleaved PARP-1 to bind thus no DNA repair can be initiated (Figure 1.10 B) (D'Amours *et al.*, 2001; Soldani *et al.*, 2001).

When DNA is extremely damaged, PARP-1 can be overactivated leading to high rate of PARylation (Figure 1.10 C). Caspase can stop this process by inhibiting PARP-1 through cleavage; however during cell death processes caspase activity might not be sufficient (Herceg and Wang, 1999). Overactivation of PARP-1 leads to depletion of NAD (and therefore ATP) resulting in cell necrosis (Los et al., 2002; Chaitanya et al., 2010).

1.12 Conclusions

hESCs have remarkable properties, thus they hold a great promise for use in medicine. It has been 22 years since hESCs were first isolated and successfully cultured (Thomson *et al.*, 1998) and certainly it can be said that research progress has been made. Clinical trials using hESCs are being developed, such as therapy for age-related macular degeneration utilising retinal pigment epithelium patch derived from hESCs or spinal cord injury treated through oligodendrocytes derived from hESCs (Keirstead *et al.*, 2005; da Cruz *et al.*, 2018). However, there is still a lot to learn about hESCs, such as more in-depth knowledge about mechanisms regulating pluripotency, differentiation or optimal culture conditions. It has been shown that environmental oxygen has an impact on hESC properties and hypoxic conditions are more beneficial for cells than atmospheric oxygen tension (Forristal *et al.*, 2010; Forristal *et al.*, 2013; Petruzzelli *et al.*, 2014; Christensen *et al.*, 2015). Hypoxia is also known to alter the expression of various proteins involved in, for example, pluripotency maintenance (Forristal *et al.*, 2013) and metabolism (Christensen *et al.*, 2015). However global proteome changes have not been explored. It is also known that hESCs cultured at 5% oxygen rely more on glycolysis than oxidative phosphorylation, compared to cells maintained at 20% oxygen (Forristal *et al.*, 2013). However little is known about the role of environmental oxygen tension in regulating the fatty acid metabolism or content of hESCs.

1.13 Project aims and objectives

Hypothesis: Environmental oxygen alters global protein expression, fatty acid composition and biosynthesis to regulate the self-renewal of hESCs.

The key objective of this thesis is to examine the effect of environmental oxygen on fatty acid metabolism in hESCs and to identify the role of fatty acids in the regulation of hESC pluripotency as well as investigating the role of oxygen tension on proteins expressed by hESCs.

The aims of this thesis are:

1. To investigate the effect of environmental oxygen on the global protein expression profile of hESCs and characterise differences in the proteome using bioinformatic tools.
2. To investigate the role of fatty acids in the hypoxic regulation of hESCs and the effect of hypoxia on fatty acid composition and synthesis.
3. To investigate the role of EPA on cellular properties, self-renewal and metabolism of hESCs.

Chapter 2 Materials and methods

2.1 Culture of hESCs

2.1.1 Derivation of mouse embryonic fibroblasts (MEFs)

12.5-day pregnant MF-1 or CF-1 mice were euthanised by cervical dislocation. The abdomen was cut through the skin and peritoneum to expose the uterine horns that were removed and placed in a petri dish containing sterile PBS without Ca^{2+} and Mg^{2+}. Embryos were removed from the embryonic sac; placenta and membranes were dissected and discarded. Embryos were decapitated, eviscerated and transferred to a 50 ml tube (9 embryos per tube) and washed twice with 30 ml of PBS. Washed tissue was transferred to a clean dish and shredded finely with a razor blade. The tissue was transferred to a 50 ml tube, in 15 ml of Trypsin-EDTA (0.05%) (Gibco), mixed and incubated for 5 minutes at 37ºC, mixed two more times before 200 µl of DNase (10 mg/ml stock in water) and 15 ml of MEF medium (High glucose DMEM (Gibco) containing 1% Penicillin-Streptomycin, 10% fetal bovine serum (FBS) and 1% Glutamax (Gibco)) was added. This mixture was incubated at 37ºC until it appeared liquid throughout (around 5 minutes). The volume was then made up to 50 ml with MEF medium and centrifuged at 200 x *g* for 5 minutes. The supernatant was removed and the pellet resuspended in 15 ml of MEF medium. The cell suspension was transferred to flasks (5 ml of cell suspension per T175 flask), with approximately three embryos per flask and incubated at 37ºC, in a humidified atmosphere of 20% O_2, 5% CO_2. The medium was changed on the next day and cells were cultured until confluent (usually after 2 days). Cells in each flask were then washed with 6 ml of PBS before adding 6 ml of Trypsin-EDTA (0.05%) and incubated for 5 minutes at 37ºC, 20% O_2 and 5% CO_2. 6 ml of MEF medium was added to each flask, 1 ml was removed for mycoplasma testing and the rest of the mixture was transferred into a falcon tube and centrifuged at 450 x *g* for 4 minutes. The supernatant was removed and the cell pellet resuspended in freezing medium (90% FBS and 10% DMSO (Dimethyl sulfoxide)). Cell suspension in the freezing medium was aliquoted (1 ml/cryovial) and cryovials were placed at -80ºC in a Mr Frosty containing isopropanol, which gradually reduces the temperature. The next day cryovials were transferred to liquid nitrogen for long-term storage.

2.1.2 Mycoplasma testing

E-Myco PCR detection kit (Chembio) was used to test for mycoplasma in MEFs. 1 ml of the MEF cells collected in the previous step was centrifuged at 450 x *g* for 5 minutes and the supernatant discarded. The cell pellet was resuspended in 1 ml of PBS and then centrifuged again at 10000 x *g*

for 10 seconds. The supernatant was removed and cells resuspended in 1 ml of PBS. The cell suspension was centrifuged at 10000 x *g* for 10 seconds and the supernatant removed. The cell pellet was resuspended in 100 µl of PBS. The sample was heated at 95°C for 10 minutes and then vortexed for 10 seconds. The sample was centrifuged at 16000 x *g* for 2 minutes at room temperature and the supernatant was transferred to a clean 1.5 ml tube to be used as the template in the PCR. 10 µl of the template was added to a reaction tube and mixed with 10 µl of DNase/RNase-free Distilled Water for 20 µl PCR reaction volume. 1 µl of positive control DNA (Recombinant DNA with included partial 16S sequence of *M. hyorhinis*) was added to a reaction tube and resuspended in 19 µl of DNase/RNase-free Distilled Water. The negative control consisted of 20 µl DNase/RNase-free Distilled Water. PCR was performed and the following parameters were used for amplification: initial denaturation: 94°C for 1 minute; 35 cycles; denaturation: 94°C for 30 seconds; annealing: 60°C for 20 seconds; extension: 72°C for 1 minute; PCR reaction finished with a final extension at 72°C for 5 minutes.
Samples were then loaded on 1.5% agarose gel and run at 100 V for approximately 40 minutes. Mycoplasma contamination was determined based on the gel image (Figure 2.1). The positive control contained, as expected, the band at approximately 260 bp indicating mycoplasma contamination. The results of gel image showed that tested sample of MEF was not contaminated with mycoplasma as indicated by the lack of band at approximately 260bp (Figure 2.1).

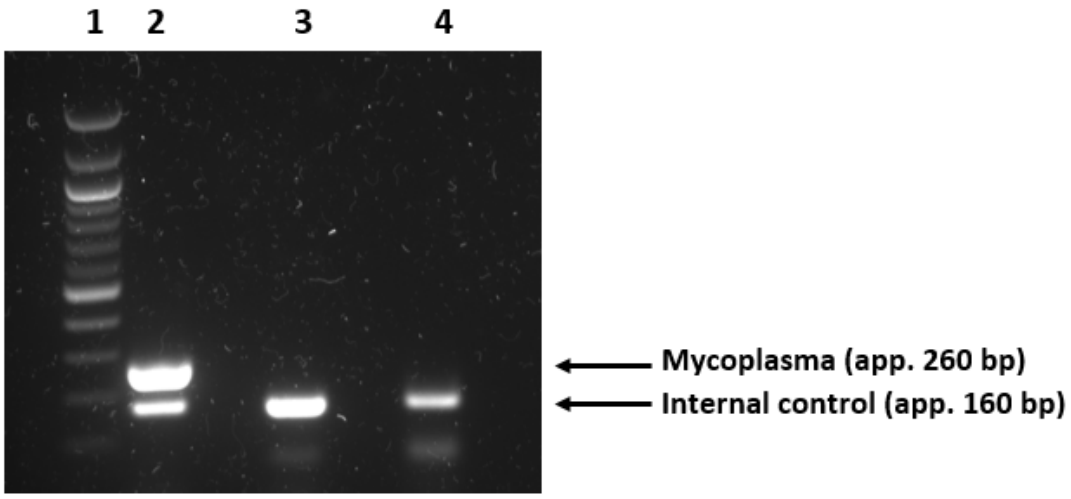

Figure 2.1 **Agarose gel image showing the results of a mycoplasma detection PCR.**

Genomic DNA was isolated from MEFs and tested for mycoplasma contamination. The internal control band (approximately 160 bp) confirms that PCR reaction was performed properly. Lane 1: 100 bp ladder, lane 2: positive control DNA, lane 3: negative control, lane 4: MEF genomic DNA.

2.1.3 Culturing and irradiating MEFs

1 vial of unirradiated MEFs was slowly thawed at 4°C and then added to 10 ml of MEF medium. The cell suspension was centrifuged at 450 x *g* for 4 minutes, the supernatant removed and the cell pellet resuspended in 3 ml of MEF medium. 1 ml of the cell suspension was added to each T175 flask containing 20 ml of MEF medium, giving in total 3 flasks. Cells were incubated at 37°C in a humidified incubator with 5% CO_2. After 2-3 days, when the cells were 90% confluent, the medium was removed and cells were washed with 6 ml of PBS. 6 ml of Trypsin-EDTA (0.05%) was added to each flask and incubated for 5 minutes at 37°C. Once the cells detached, 6 ml of MEF medium was added to inactivate Trypsin-EDTA. The cell suspension from all 3 flasks was transferred to a 50 ml tube and centrifuged for 4 minutes at 450 x *g*. The supernatant was removed and the cell pellet was resuspended in 9 ml of MEF medium. 1 ml of the cell suspension was added to each T175 flask that contained 19 ml of MEF medium. Cells were incubated for 2-3 days until they reached 90% confluency and the passaging process was repeated but this time after centrifugation, the cell pellet was resuspended in 20 ml of MEF medium and 1 ml of cell suspension was added to each flask (20 flasks in total). Flasks were returned to the incubator and again incubated for 2-3 days until they were 90% confluent to passage them again. However, after the centrifugation step, the supernatant was removed and all cell pellets were resuspended in a total of 10 ml of MEF medium and transferred to a 50 ml falcon tube. The volume of cell suspension was made up to 40 ml with MEF medium and irradiated in the X-ray irradiator at 50 Gy by an authorised gamma irradiator user to mitotically inactivate the MEFs. After irradiating, cells were centrifuged at 450 x *g* for 4 minutes before resuspending the pellet in 20 ml of freezing medium (10% DMSO in FBS) and divided between 20 cryovials. The cryovials were placed at -80°C in a Mr Frosty containing isopropanol, which gradually reduces the temperature. The next day irradiated MEFs (iMEFs) were transferred to liquid nitrogen for long-term storage.

2.1.4 The culture of Hues7 hESCs on feeder layers

One vial of iMEFs was thawed and resuspended in 15 ml MEF medium before centrifugation at 450 x *g* for 4 minutes. The supernatant was removed and the cell pellet was resuspended in 12 ml MEF medium. Each well of a 6-well plate was coated with gelatin (0.1% gelatin in water) and was allowed to set for at least 30 minutes. Gelatin was removed, 1 ml of MEF medium was added to each well followed by 1 ml of iMEF suspension. Plates were incubated at 37°C, in a humidified atmosphere of 20% O_2, 5% CO_2 for 24 hours. After the incubation time, the medium was replaced with 2 ml of hESC medium (Table 2.1) and incubated for 24 hours to be used for MEF-conditioned medium (CM) or as a feeder layer for culturing hESCs.

Table 2.1 **Composition of hESC culture medium.**

Component	Final concentration	Volume
KnockOut DMEM (KO DMEM) (Gibco)		410 ml
Knockout Serum Replacement (Gibco)	15%	75 ml
Non-Essential Amino Acids 100x (Gibco)	1%	5 ml
Penicillin-Streptomycin 100x (Gibco)	1%	5 ml
L- Glutamax 100x (Gibco)	1%	5 ml
50 mM β-Mercaptoethanol (Sigma)	55 µM	500 µl
0.1 µg/µl bFGF (Basic Fibroblast Growth Factor) (PeproTech)	10 ng/µl	50 µl

Hues 7 hESCs (obtained from Harvard University; Boston; USA) were cultured on a layer of iMEFs in the presence of hESC medium (Table 2.1). The cells were maintained at 37ºC, in a humidified atmosphere of 5% CO_2, and at either 20% or 5% oxygen. Before cells cultured at 5% oxygen were used in any experiments, they were maintained under hypoxic conditions for at least 3 passages. To passage cells, 1 ml per well of Collagenase IV (1 mg/ml in KO DMEM; Gibco) was added and cells were incubated at 37ºC for 4 minutes. Then the medium containing Collagenase was removed and hESC medium added, 2ml for 1:2 passage ratio or 3 ml for 1:3. The cells were gently scraped, pipetted once up and down and 1 ml/well of the hESC suspension was added to 6-well plate containing a layer of iMEFs and hESC medium (1 ml/well). The cells were passaged every 3-4 days and the passage ratio was usually 1:2 or 1:3, dependent on confluency of the cells. The medium was replaced every 24 hours with fresh hESC medium.

2.1.5 The culture of Hues7 hESCs on Matrigel-coated plates

To prepare Matrigel-coated plates for feeder-free culture of hESCs, Matrigel (BD Biosciences) was diluted using ice-cold KO DMEM medium to the concentration of 6 mg/ml and 400 µl aliquots were stored at -20ºC. To coat plates, Matrigel aliquots were thawed (1 aliquot per one 6-well plate) and 5.6 ml of cold KO DMEM was added. 1 ml of Matrigel solution was added to each well and Matrigel-coated plates were ready to use after overnight incubation at 4ºC.

Hues 7 hESCs were passaged as described in section 2.1.4 onto Matrigel coated 6-well plates in the presence of CM. CM was obtained by addition of hESC medium (Table 2.1) to plates coated

with iMEFs, as described in section 2.1.4, and incubation of plates at 37°C, 20% O_2, 5% CO_2 for 24 hours before collecting CM. Cells were maintained at 37°C, 5% CO_2, and at either 20% or 5% oxygen and normally passaged every third day using Collagenase type IV (1 mg/ml in KO DMEM). Cells required at least 3 passages before being ready to use for experiments to eliminate MEFs and were maintained at 5% oxygen for a minimum of 3 passages before use.

2.2 NT2 cells culture

A cryovial containing NT2 cells (human embryonal carcinoma cell line; ATCC®CRL-1973™) was thawed on ice. The cell suspension was mixed with 5 ml of NT2 medium (high glucose DMEM medium, 10% FBS, 1% penicillin/streptomycin) and centrifuged at 450 x *g* for 4 minutes. The supernatant was removed, the cell pellet was resuspended in 15 ml of NT2 medium and added to a T75 flask. Cells were incubated at 37°C, 5% CO_2 and at either 5% or 20% oxygen. Cells were passaged when they reached around 90% confluency (usually 3-4 days) by removing medium, washing cells with 6 ml of PBS and adding 6 ml of Trypsin-EDTA (0.05%). NT2 cells were then incubated for 5 minutes at 37°C and then 5 ml of medium were added to neutralise the Trypsin. The cell suspension was collected into a 15 ml tube and centrifuged at 450 x *g* for 4 minutes. The supernatant was removed and the pellet was resuspended in 3 ml of NT medium for 1:3 split ratio. 1 ml of cell suspension was added to a T75 flask containing 12 ml of NT2 medium and incubated at 37°C, 5% CO_2 and at either 5% or 20% oxygen. At least 3 passages at 5% oxygen were required to before cells were used in experiments.

2.3 RNA interference

Silencing of gene expression using small interfering RNA (siRNA) was carried out on hESCs cultured on Matrigel in hypoxic conditions for at least three passages. For protein isolation, at least 3 wells out of 6-well plate were transfected with siRNA and 3 wells with negative control siRNA. The transfection solution was prepared for 3 wells of cells by using either 50 nM siRNA silencing *FADS1* (sense strand: 5' CCAUAUUCCCAUGCACAUUtt 3'), *PARP-1* (sense strand: 5' GGCCAGGAUGGAAUUGGUAtt 3') (both siRNA by Ambion), *EPAS1* (sense strand: 5' CGGAUAGACUUAUUGCCAATT 3') (siRNA by Qiagen), or negative control mixed in 600 µl KO-DMEM by vortexing for 5 seconds. 30 µl of transfection reagent (INTERFERin, Polyplus for PARP-1 siRNA or HiPerFect, Qiagen for FADS1 and EPAS1 siRNA) was then added to the mixture and vortexed again. The mix was incubated for 10 minutes at room temperature. On the 1st day post-passage medium was replaced from hESCs and 1.3 ml of CM per well was added. Transfection solution was added dropwise and incubated for 24 hours at 37°C, 5% O_2, 5% CO_2. After the

incubation time, fresh medium was added to cell culture and incubated for another 24 hours. 48 hours post-transfection cell lysate was collected into RIPA buffer (25 mM Tris-HCl pH 7.6, 150 mM NaCl, 1% NP-40, 1% sodium deoxycholate, 0.1% SDS (sodium dodecyl sulfate) containing 4 µl of commercially available protease inhibitor cocktail (cOmplete™, EDTA-free Protease Inhibitor Cocktail, Roche)). Negative control used was AllStars (Qiagen) siRNA that has no homology to any known mammalian gene.

2.4 Immunocytochemistry

Hues 7 hESCs were plated onto either iMEF-containing 4-well Chamber slides or Matrigel coated 12-well plates and cultured at either 5% or 20% oxygen. When colonies were an appropriate size (usually 1 day post-passage for Chamber slides and 3 days post-passage for 12-well plates), cells were washed twice with PBS and fixed with 4% paraformaldehyde in PBS for 15 minutes at room temperature before being washed twice with PBS. If cells were cultured on the slides, chambers were removed and each well sealed around the edge with an ImmEdge pen (Vector Laboratories). Cells were incubated with 100 mM glycine in PBS for 10 minutes at room temperature before permeabilizing with 0.2% Triton X-100 in PBS (for intracellular markers) or incubated with PBS (for surface markers) for 10 minutes. The cells were washed with PBS for 10 minutes and blocked with 10% fetal calf serum in PBS for 30 minutes. Cells were incubated with diluted primary antibody (Table 2.2) in 0.6% bovine serum albumin (BSA) in PBS for 90 minutes at room temperature in a humidified container in the dark. The slides were washed twice with PBS and incubated with the appropriate diluted FITC/Alexa 488 conjugated secondary antibody (Table 2.2) in 0.6% BSA in PBS for 60 minutes at room temperature in a humidified container in the dark. Cells were washed twice with PBS, once with water and Vectashield antifade mounting medium containing DAPI was added (Vector Laboratories). Slides or plates were stored overnight in a dark chamber at 4°C before microscopic evaluation. Expression was imaged using a Zeiss fluorescence microscope and AxioVision imaging software (Zeiss).

Table 2.2 **Primary and secondary antibodies used for immunocytochemistry.**

	Primary antibody	**Secondary antibody**
Intracellular markers	anti-NANOG rabbit monoclonal; Abcam, ab109250 dilution 1:100	goat anti-rabbit, Alexa 488 Molecular Probes, A-11008 dilution 1:700
	anti-SOX2 rabbit monoclonal; Cell Signaling, (D6D9) XP dilution 1:200	
	anti-OCT4 mouse monoclonal IgG_{2b}; Santa Cruz, sc-5279 dilution 1:100	goat anti-mouse, IgG-FITC Sigma, F2012 dilution 1:100
	anti-PARP1 mouse monoclonal $IgG_{1;}$ Santa Cruz, sc-74470 dilution 1:50	
Surface markers	anti-TRA 1-60 mouse monoclonal IgM; Santa Cruz, sc-21705 dilution 1:100	goat anti-mouse, IgM-FITC Sigma, F9259 dilution 1:200
	anti-SSEA-1 mouse monoclonal IgM; Santa Cruz, sc-21702 dilution 1:200	
	anti-Caveolin-1 rabbit polyclonal; Abcam, ab2910 dilution 1:500	goat anti-rabbit, Alexa 488 Molecular Probes, A-11008 dilution 1:700
	anti-GLUT3 rabbit polyclonal ; Abcam, ab15311 dilution 1:100	
	Anti-FADS1 rabbit monoclonal ; Abcam, ab126706 dilution 1:100	

2.5 Protein isolation and quantification using the Bradford Assay

On a 3rd day post-passage, a 6-well plate containing at least 3 wells of hESCs was placed on ice and washed twice with PBS. 100 µl of RIPA buffer was added to the first well of the culture plate, cells were scraped and transferred to the next well and this procedure was repeated for at least 3 wells. Collected cells were transferred to an Eppendorf tube and incubated on ice for 20 minutes. Proteins were extracted by sonicating (3x10 seconds) followed by centrifuging at 13,000 x *g* for 10 minutes at 4ºC. The protein supernatant was collected and quantified using the Bradford Assay. Samples were analysed in duplicate or triplicate. BSA standards were prepared at concentrations of: 20 µg/ml, 10 µg/ml, 5 µg/ml, 2.5 µg/ml, 1.25 µg/ml. The protein supernatant was diluted 1:1000. 180 µl of each standard/blank/protein sample and 20 µl of Bradford assay reagent (Bio-Rad) were added to wells of a clear, flat-bottomed 96-well plate and mixed. The plate was incubated at room temperature for 2-5 minutes and the absorbance was read at 595 nm. The protein concentration of the protein lysates was calculated from the BSA standard curve (Figure 2.2).

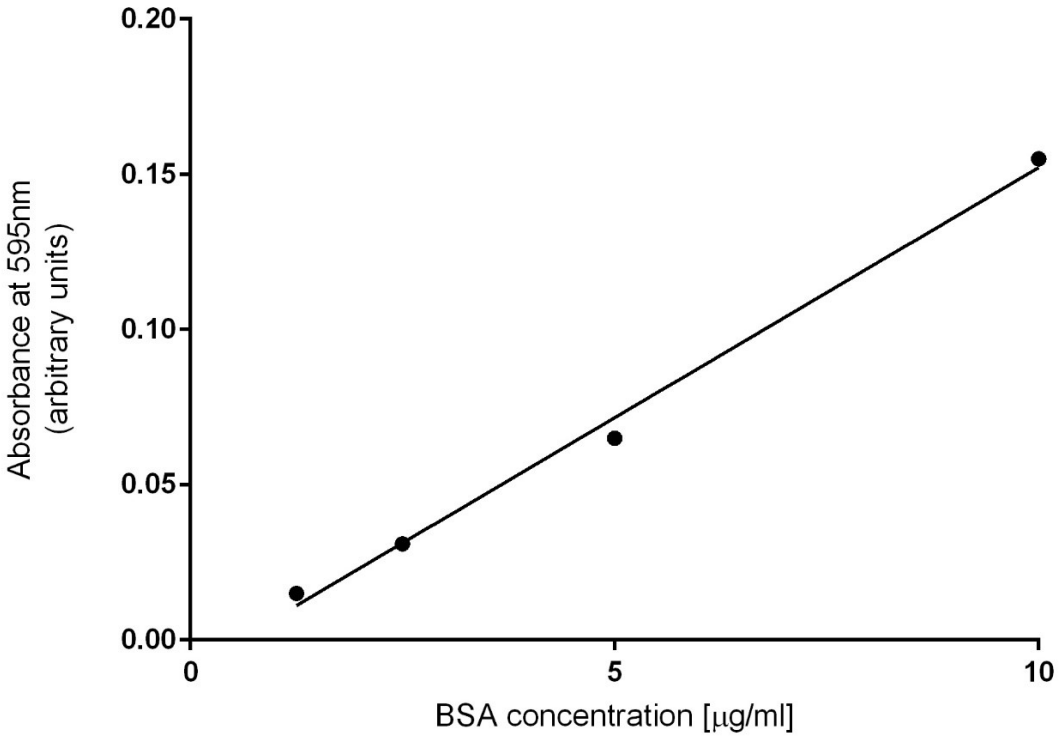

Figure 2.2 **Representative standard curve of BSA concentration determined using the Bradford assay.**

2.6 Western blotting

A 8% or 12% resolving gel (Table 2.3) was added between 0.75 mm thick glass plates in supports and covered with isopropanol on the top. Once the gel polymerised, the isopropanol was washed away with water. A 5% stacking gel (Table 2.4) was added on the top of a resolving gel and left to set with inserted 10-well combs.

Table 2.3 **Resolving gel composition.**

Component	Volume for 8% gel	Volume for 12% gel
1.5 M Tris pH 8.8	2.5 ml	2.5 ml
10% SDS	100 µl	100 µl
Acrylamide mix (Acrylamide:N,N'-Methylenebisacrylamide 29:1 solution, 40% in H_2O)	2 ml	3 ml
Distilled water	5.3 ml	5 ml
10% ammonium persulphate in H_2O	100 µl	100 µl
TEMED (N,N,N',N'-tetramethylethane-1,2-diamine)	7.5 µl	7.5 µl

Table 2.4 **5% stacking gel composition.**

Component	Volume
0.9 M Tris pH 6.8	695 µl
10% SDS	50 µl
Acrylamide mix	625 µl
Distilled water	3.63 ml
10% ammonium persulphate in H_2O	50 µl
TEMED	7.5 µl

50 µg of protein lysate was added to 7.5 µl of dithiothreitol (DTT; 1 M in H_2O), 7.5 µl of 4x Sample Buffer (NuPAGE Sample Buffer (4X) containing lithium dodecyl sulfate (LDS), Invitrogen) and made

up to 30 µl with RIPA buffer. Samples were denatured at 95°C for 5 minutes (except when detecting expression of GLUT1 and GLUT3) and stored on ice. 5 µl of a pre-stained ladder (Fisher BioReagents) and 25 µl of samples were loaded into the gels, completely covered with 1X running buffer (diluted 5X running buffer) (Table 2.5).

Table 2.5 **Composition of 5X running buffer.**

Component	Volume/amount
Tris	15.1 g
Glycine	94 g
Deionized water	900 ml
10% SDS	50 ml
Distilled water	Make up to 1 l
	pH adjusted to 8.3

Gels were run at 55 mA until bands reached the bottom of the gel (approximately 40-60 minutes). Proteins were transferred onto a nitrocellulose membrane (Amersham Protran 0.45 µm) at 250 mA for 2 hours immersed in transfer buffer (Table 2.6).

Table 2.6 **Transfer buffer composition.**

Component	Volume/amount
Glycine	2.93 g
1.5 M Tris pH 8.3	32 ml
Methanol	200 ml
Distilled water	Make up to 1 l

The membrane was blocked with 5% non-fat powdered milk in either PBS or TBS/0.1% Tween20 (Tris-buffered saline (TBS) containing 0.1% Tween 20; 20 mM Tris, 150 mM NaCl, 0.1% Tween 20 (w/v)), for one hour. HIF2α was blocked in 5% non-fat powdered milk and 1% BSA in TBS/0.1% Tween20 for 1.5 hours. After that, the membrane was incubated overnight at 4°C in appropriate

dilution of primary antibody in 5% milk or BSA (Table 2.7). The optimal antibody dilution was established by a titration experiment; it involved using series of dilutions, which helped to choose the most appropriate concentration.

Table 2.7 **Antibodies and buffers used for Western blot experiments.**

Mouse β-Actin peroxidase-conjugated anti-body (Sigma; A3854) followed the development of each protein and was diluted 1:50000 in the same buffer as used for blocking step.

Protein	**Company**	**Host**	**Dilution**	**Blocking**	**Secondary antibody [dilution]**
OCT4	Santa Cruz (sc-5279)	Mouse	1:1000	5% milk in PBS/0.1% Tween20	anti-mouse GE Healthcare (NXA931) [1:100000]
PARP-1	Santa Cruz (sc-74470)	Mouse	1:1000	5% milk in PBS/0.1% Tween20	
SOX2	Cell Signaling (D6D9) XP	Rabbit	1:3000	5% BSA in TBS/0.1% Tween20	anti-rabbit GE Healthcare (NA934) [1:50000]
NANOG	Abcam (ab109250)	Rabbit	1:500	5% milk in PBS/0.1% Tween20	
HIF2α	Novus (NB100-122)	Rabbit	1:250	5% milk and 1% BSA in TBS/0.1% Tween20	
Caveolin-1	Abcam (ab2910)	Rabbit	1:1000	5% milk in PBS/0.1% Tween20	
D5D	Abcam (ab126706)	Rabbit	1:500	5% milk in PBS/0.1% Tween20	
GLUT1	Abcam (ab652)	Rabbit	1:500	5% milk in TBS/0.1% Tween20	
GLUT3	Abcam (ab15311)	Rabbit	1:500	5% milk in TBS/0.1% Tween20	

The membrane was washed 3 times, 5 minutes each washing with PBS or TBS/0.1% Tween20 before the horseradish peroxidase-conjugated secondary antibody at appropriate dilution in 5% milk or BSA was added (Table 2.7) and incubated for 1 hour at room temperature. The membrane was washed 3 times in PBS or TBS/0.1% Tween20, each for 5 minutes. Detection was performed by adding 1 ml of chemiluminescent reagent (ECL Luminogen enhanced detector kit, Amersham) on the membrane and incubating for 5 minutes protected from light. The film was developed in a dark room for the appropriate amount of time and then washed with the developer, water, fixer and again water, respectively. Films were left to dry. The membrane was washed 3 times, 5 minutes each wash, with PBS or TBS/0.1% Tween20 before staining with β-actin-HRP (dilution 1:50000 in 5% milk) for 1 hour at room temperature. The membrane was washed 3 times with PBS or TBS/0.1% Tween20 and 1 ml of ECL western detector kit (ECL Select Luminogen detector kit, Amersham) was added. The membrane was incubated for 5 minutes protected from light and film was developed as described above. Dried, developed films were scanned and the intensity of bands was measured using Image J software.

2.7 Gas chromatography

2.7.1 Preparation of total lipid extract

NT2 cells or hESCs were cultured on 6 well-plates at either 5% or 20% oxygen and collected on the third day after passage. Cells were counted with a haemocytometer and 1 million cells were collected. Cells were then centrifuged at 450 x *g* for 4 minutes, the pellet re-suspended in 800 µl of 0.9% (w/w) NaCl and stored at -80°C. Total lipids were extracted by adding 10 µl of internal standard (Dipentadecanoyl PC 1 mg/ml), 5 ml chloroform:methanol (2:1) containing butylated hydroxytoluene (BHT) (50 mg/l) antioxidant and 1 ml of 1 M NaCl to each sample. Samples were centrifuged at 400 x *g* for 10 minutes at room temperature. The lower phase was collected and dried under nitrogen at 40°C.

2.7.2 Preparation of fatty acid methyl esters

Derivatization of lipid extract to fatty acid methyl esters (FAMEs) improves volatility of components that in consequence reduces the time required to carry out the analysis and improves separation. FAMEs were prepared by adding 0.5 ml of dry toluene to the samples containing total lipid extract and vortexing. 1 ml of methylation reagent (methanol containing 2% (v/v) H_2SO_4) was added to each sample, mixed and incubated for 2 hours at 50°C before allowing to cool. 1 ml of neutralising solution (0.25M $KHCO_3$ (25.03 g/l), 0.5M K_2CO_3 (69.10 g/l)) and 1 ml of dry hexane was added to each sample, which was then vortexed and centrifuged at 200 x *g* for 2

minutes at room temperature. The upper phase containing FAMEs was collected and dried under nitrogen at 40°C. 75 µl of dry hexane was added to each dried sample, which was vortexed, transferred to the corresponding insert of a gas chromatography (GC) autosampler vial and repeated to obtain a final volume of 150 µl of hexane within the vial. Each vial was dried under nitrogen and hexane was added to obtain a final volume of 50 µl in each. Samples were then ready for GC analysis.

2.7.3 Measurement of fatty acid composition using gas chromatography

Samples containing FAMEs were loaded into vials in an autoinjector mounted on an Agilent 6890 gas chromatograph. Standard 37FAMES (37 different FAME components) was added to a separate vial; carrier gas was helium. The following parameters were used: injection temperature: 300°C, split ratio 2:1, injection volume: 1 µl, oven temperature: 115°C to 250°C (2 minutes), column type: BPX-70, 30 m long, 220 µm of diameter, flame ionisation detector temperature: 300°C. Total run time was 37.7 minutes. The data were collected using ChemStation software. The results were visualised as shown in Figure 2.3, where each peak represents an individual fatty acid (as its methyl ester) and the peak area is related to the amount of the particular fatty acid in a sample.

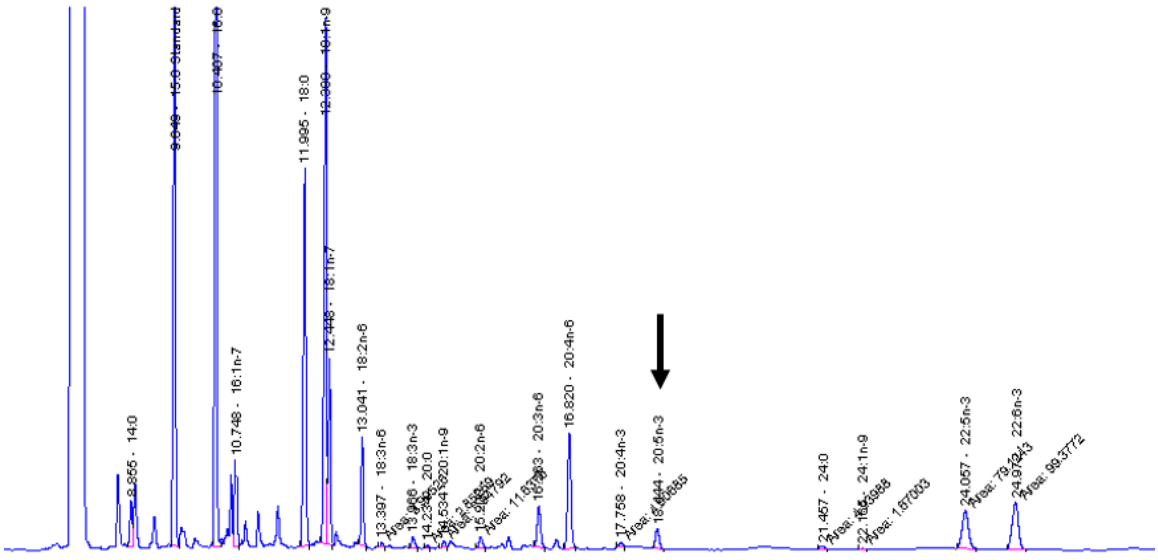

Figure 2.3 **Typical GC chromatogram of the fatty acids from a hESC sample.**

Peaks present on the chromatogram correspond to individual fatty acids; the area under the peak is equal to the amount of particular fatty acid in a sample. The black arrow shows peak that corresponds to EPA (eicosapentaenoic acid; 20:5n-3).

2.8 Statistical analysis

All data were tested using the Anderson Darling normality test to determine if they were normally distributed and whether parametric or non-parametric tests were appropriate. In all experiments statistical analysis was performed using unpaired Student t-test in GraphPad Prism 7 software, unless specified otherwise. Protein expression was normalised to β-actin and to a value of 1 for cells cultured at 5% oxygen or cells transfected with negative control siRNA. A value of $p < 0.05$ was considered as significant. All data represent at least 3 independent experiments and are presented as mean + SEM unless specified otherwise.

Chapter 3 Effect of environmental oxygen on the proteome of human embryonic stem cells

3.1 Introduction

Mass spectrometry can be used as a high throughput approach to study protein expression and to provide a wealth of information regarding protein structure, properties and interactions within the studied matrix including cells (Clark and Pazdernik, 2013). Post-translational modifications or altered protein expression have been found to be associated with various diseases; for example, hyperphosphorylation and glycosylation of microtubule-associated protein tau are connected with Alzheimer's disease (Patterson and Aebersold, 2003; Gong *et al.*, 2005). A collection of proteins expressed by a cell, tissue or organism is called a proteome. Mass spectrometry can be used to provide information about how the proteome varies, for example, during hESC neuronal differentiation compared to pluripotent culture, providing insights into potential biomarkers of neuronal differentiation (Yocum *et al.*, 2008). Mass spectrometry can also help to characterise the proteome of individual components of a cell, such as the plasma membrane (Dormeyer *et al.*, 2008), nucleus (Barthelery *et al.*, 2009) or organelles (Shekari *et al.*, 2017). The proteome of the cell can be altered by internal or external stimuli, such as availability of the nutrients or oxygen tension (Tomanek, 2011).

Previous studies demonstrated the importance of environmental oxygen in regulating hESC properties (Forristal *et al.*, 2010; Christensen *et al.*, 2015; Gu *et al.*, 2016). One of the main roles of oxygen is being the terminal electron acceptor in the mitochondrial electron transport chain that produces energy in the form of ATP during cellular respiration. However, some cells show a tendency to prefer a low oxygen environment, such as cells from preimplantation embryos of the rhesus monkey, which in vivo reside in a highly hypoxic condition (1.5% oxygen) (Fischer and Bavister, 1993). In humans, the environment of the oviduct and uterus is also characterised by hypoxic conditions and therefore there is an ongoing debate about the most optimal oxygen concentration for human preimplantation embryo culture for in vitro fertilization (IVF) and culture. An environment of 5% oxygen was found to be more beneficial for human embryos, resulting in an increased success rate of IVF (Bontekoe *et al.*, 2012). It has similarly been demonstrated that low oxygen tension is beneficial for the culture of hESCs; hESCs cultured under hypoxia display a reduction in spontaneous differentiation (Ezashi *et al.*, 2005) and a higher

expression of the key pluripotency markers OCT4, SOX2 and NANOG (Forristal *et al.*, 2010). Additionally, oxygen tension alters the metabolic profile of hESCs (Forristal *et al.*, 2013; Lees *et al.*, 2015; Gu *et al.*, 2016). Environmental oxygen regulates hESC metabolism, whereby cells cultured under hypoxic conditions exhibit a greater rate of flux through glycolysis than those maintained at 20% oxygen, which rely more on oxidative phosphorylation (Forristal *et al.*, 2013). Despite the lower ATP production through glycolysis (2 ATP per mole of glucose) compared to oxidative phosphorylation (approximately 32 ATP per mole of glucose), studies have shown hypoxia to be more beneficial for hESC culture. This might be because mitochondrial respiration generates reactive oxygen species (ROS), which have been found to be responsible for DNA damage and the induction of differentiation in mESCs and hESCs (Saretzki *et al.*, 2008; Crespo *et al.*, 2010). Thus, maintaining a low level of ROS is crucial for hESCs to remain undifferentiated. Low levels of environmental oxygen are also responsible for increasing the expression of the glucose transporter, GLUT3. When expression of GLUT3 was silenced in hESCs cultured under hypoxia, glucose uptake and lactate production were reduced as was the expression level of OCT4 (Christensen *et al.*, 2015). However, the cellular response to low oxygen conditions requires careful regulation to maintain cell homeostasis; an effect regulated by Hypoxia-Inducible Factors (HIFs). HIF1β is constitutively expressed in normoxic conditions while the HIF α subunit is degraded (Jaakkola *et al.*, 2001). In hypoxic conditions, the alpha and beta subunits of HIF complexes dimerise and bind to the hypoxia-response element (HRE) within the promoter of hypoxia-responsive genes. Through this binding, the HIF complex can upregulate target gene expression level (Semenza *et al.*, 1996). Interestingly, activity of HIF complex in hypoxic conditions was found to be positively regulated by PARP-1, protein mainly known for its role in DNA repair (Martin-Oliva *et al.*, 2006; Elser *et al.*, 2008; Gonzalez-Flores *et al.*, 2014; Ray Chaudhuri and Nussenzweig, 2017). HIF1α was thought to be the main gene regulator in hypoxic cells; however in hESCs HIF1α was found to be present for only first 48 hours of hypoxic culture and was absent in the prolonged culture at 5% oxygen (Forristal *et al.*, 2010). HIF2α plays a crucial role in maintaining stem cell pluripotency, by binding to an HRE in the proximal promoters of *OCT4, SOX2* and *NANOG* only in hESCs cultured under hypoxic conditions (Petruzzelli *et al.*, 2014). Hypoxia has an effect not only on gene expression but also on protein function, such as through post-translational modifications. For example, cyclic AMP response element-binding protein (CREB) was shown to be phosphorylated in hypoxic conditions, which is necessary for CREB-mediated transcriptional activation (Beitner-Johnson and Millhorn, 1998). Although various stimuli were tested, such as the presence of kinases mediating phosphorylation, low oxygen tension was the most efficient at inducing this post-translational modification.

Environmental oxygen has a profound effect on the regulation of hESC phenotype, but the proteins and network interactions involved have not been fully elucidated. It is known that environmental oxygen affects the expression of glycolytic enzymes and the efficiency of glucose uptake in hESCs (Christensen *et al.*, 2015; Lees *et al.*, 2015). Previous mass spectrometry studies with hESCs mostly focus on the total proteome (Zhao *et al.*, 2015a), proteins expressed during differentiation (Yocum *et al.*, 2008; Chaerkady *et al.*, 2009), profiling of low, medium, and high passage hESCs (Vaňhara *et al.*, 2018), or on comparison to the tumorigenic counterpart, embryonal carcinoma cells (Dormeyer *et al.*, 2008). The effect of hypoxia has been investigated in different stem cells; for example exposure of mesenchymal stem cells to low oxygen (1%) caused upregulation of proteins involved in glycolysis or autophagy (Wobma *et al.*, 2018). However, the effect of culture oxygen tension on the global proteome of hESCs is not well studied. An altered proteome could provide a link between oxygen tension and hESC phenotype.

3.2 Chapter aims

The aim of this chapter was to investigate the effect of environmental oxygen on the proteome of hESCs.

Specific aims were:

- To characterise Hues7 hESCs cultured at either 5% or 20% oxygen based on the presence of pluripotency markers using immunocytochemistry and quantify expression levels with Western blotting.
- To use mass spectrometry to identify proteins that are differentially expressed in hESCs cultured at either 5% or 20% oxygen and characterise the proteome using bioinformatic analyses.
- To validate the differential expression of a subset of proteins in hESCs cultured at either 20% or 5% oxygen using Western blotting and examine if the increased expression in hypoxic conditions is regulated by HIF2α.
- To investigate whether PARP-1 regulates self-renewal in hESC cultured at 5% oxygen.

3.3 Materials and methods

3.3.1 Cell lysate collection for mass spectrometry

Cell lysates of hESCs cultured at either 5% or 20% oxygen on 6-well plates per condition were collected for mass spectrometry analysis. Cells were washed with PBS before adding 1 ml of trypsin-EDTA (0.05%) per well. After cells started detaching, 1 ml per well of PBS was added. Wells were scraped and cells were harvested into a tube and centrifuged for 4 minutes at 450 x *g*. The supernatant was removed and the cell pellet was resuspended in 5 ml of PBS. 10 µl was taken and the cell number counted using a haemocytometer. The cell suspension was centrifuged again for 4 minutes at 450 x *g* and the supernatant removed before adding 5 cell-pellet volume of 100 mM ammonium bicarbonate and 0.1% SDS. A sample was sonicated on ice using a probe sonicator and centrifuged for 10 minutes at 13,000 x *g* at 4°C. The supernatant (protein lysate) was collected and stored at -80°C until required. Protein concentration was calculated using the Bradford Assay (chapter 2.4).

3.3.2 Sample clean-up and digestion

100 µg of protein lysate of each sample was transferred to a fresh tube and made up to 100 µl with 100 mM ammonium bicarbonate. 1 µl of 500 mM DTT was added to each sample, which was then vortexed and incubated at 56°C for 1 hour. The mix was quickly centrifuged before adding 3.5 µl of iodoacetamide (IAA) and incubated at room temperature in the dark for 20 minutes. After that, 4 µl of trypsin-EDTA (0.05%) was added to each sample to digest proteins; the sample was vortexed and incubated at 37°C overnight. The peptide samples were dried using a vacuum concentrator, then reconstituted in a solution of 150 µl 3% acetonitrile and 0.1% formic acid and vortexed. The pH of the samples was adjusted to <3.0 with trifluoroacetic acid (TFA) before loading them onto an Empore C18 96-well solid phase extraction plate (3M, Maplewood, MN) and washing with 20 µl of 0.5% acetic acid. Peptides were eluted from the plate using 40 µl of 80% acetonitrile and 0.5% of acetic acid. Samples were dried again using a vacuum concentrator and resuspended in 25 µl 2% acetonitrile and 0.1% formic acid containing 100 fmol/µl of the internal enolase digestion standard (Waters).

3.3.3 Label-free liquid chromatography mass spectrometry in data-independent acquisition mode (LC-MS^E) analysis

A reverse phase trap column (Symmetry C18, 5 µm, 180 µm x 20 mm, Waters Corporation, Milford, MA) was loaded with 1 µl of prepared peptide digest at a trapping rate of 5 µl/min and

washed for 10 minutes with buffer A (0.3 M borate, pH 8.6), before analytical nanoscale LC separation on a C18 reversed phase column (HSS T3, 1.8 µm, 500 mm x 75 µm, Waters). The peptides were eluted over a 120 minutes linear gradient from 1% acetonitrile and 0.1% formic acid to 60% acetonitrile and 0.1% formic acid, at a flow rate of 300 nl/min. Samples were then sprayed into a Synapt G2-Si mass spectrometer (Waters Corporation, Wilmslow, UK) using data independent High Definition Mass Spectrometry ($HDMS^E$) mode. Alternate low and high collision energy (CE) scans were used to collect data from 50 to 2000 *m/z*. Low CE was set as 5 V and high CE was elevated from 15 V to 40 V. Ion mobility was implemented before fragmentation using a wave height of 650 m/s and wave velocity of 40 V. The work undertaken in this section was carried out by Dr Paul Skipp and his group from University of Southampton, UK.

3.3.4 Database search

Raw data were processed using a custom package (Regression tester) based upon executable files from ProteinLynx Global Server 3.0 (Waters). The settings for peak detection were optimised using Threshold Inspector (Waters). The threshold for low energy was equal to 100 counts and for high energy 30 counts. Regression tester was applied to perform a database search against the UniProt human reference database (24/07/2017; 71,599 entries) with added information about the internal standard sequence (Enolase). Fixed modification for carboxyamidomethylation of cysteine and a variable modification for the oxidation of methionine was chosen and a maximum of two missed cleavages for tryptic digestion was allowed. Precursor and product ion mass tolerances were calculated automatically during data processing and the false discovery rate (FDR) was set at 4% and then filtered to 1%. Absolute quantification was calculated based on the top three method (Silva *et al.*, 2006). Python scripts were used to generate a single .csv document containing summary information for the whole analysis. The work undertaken in this section was carried out by Dr Paul Skipp and his group from University of Southampton, UK.

3.3.5 Bioinformatic analysis

Hierarchical clustering, heatmaps and principal component analysis (PCA) were performed using R v. 3.6.3 (R Development Core Team, 2020). Complete linkage and Euclidean distances were used while performing hierarchical clustering. A Volcano plot was generated using Plotly (Inc.). GOrilla (Gene Ontology Enrichment Analysis and Visualization Tool) (Eden *et al.*, 2009), REVIGO ('Reduce and Visualize Gene Ontology') (Supek *et al.*, 2011) and PANTHER (Mi *et al.*, 2018) tools were used for gene ontology analysis. Redundant GO terms were removed in REVIGO based on semantic similarity, using the *simRel* score, which is a functional similarity measure for comparing two GO terms with each other (Schlicker *et al.*, 2006). Gene ontology results were visualised in R based on

results obtained from REVIGO. Ingenuity Pathway Analysis (IPA) (QIAGEN) software was used to further characterise the proteomics results obtained and STRING was used to visualise protein relationships (Szklarczyk *et al.*, 2019).

3.4 Results

3.4.1 Characterisation of Hues7 human embryonic stem cells

3.4.1.1 Characterisation of Hues7 hESCs cultured at either 5% or 20% oxygen

hESCs were successfully cultured at both 20% and 5% oxygen. The cells grew in flattened oval colonies with defined borders as shown in phase contrast images (Figure 3.1 D, H, L, P, T). Expression of self-renewal markers in hESCs cultured at either 20% or 5% oxygen level was characterised using immunocytochemistry.

Pluripotency markers were expressed by hESCs cultured at 5% oxygen as well as by cells maintained under 20% oxygen (Figure 3.1 – Figure 3.8). The transcription factors OCT4, SOX2 and NANOG were expressed in the nucleus of the cells (Figure 3.2 and Figure 3.6) as indicated by the presence of FITC/Alexa488 labelling merged with DAPI. hESCs were also labelled with surface markers, TRA-1-60, which is pluripotency marker, and SSEA-1, known as a marker of early differentiation (Figure 3.3 and Figure 3.7). SSEA-1 was not detected in cells cultured at either hypoxia or normoxia.

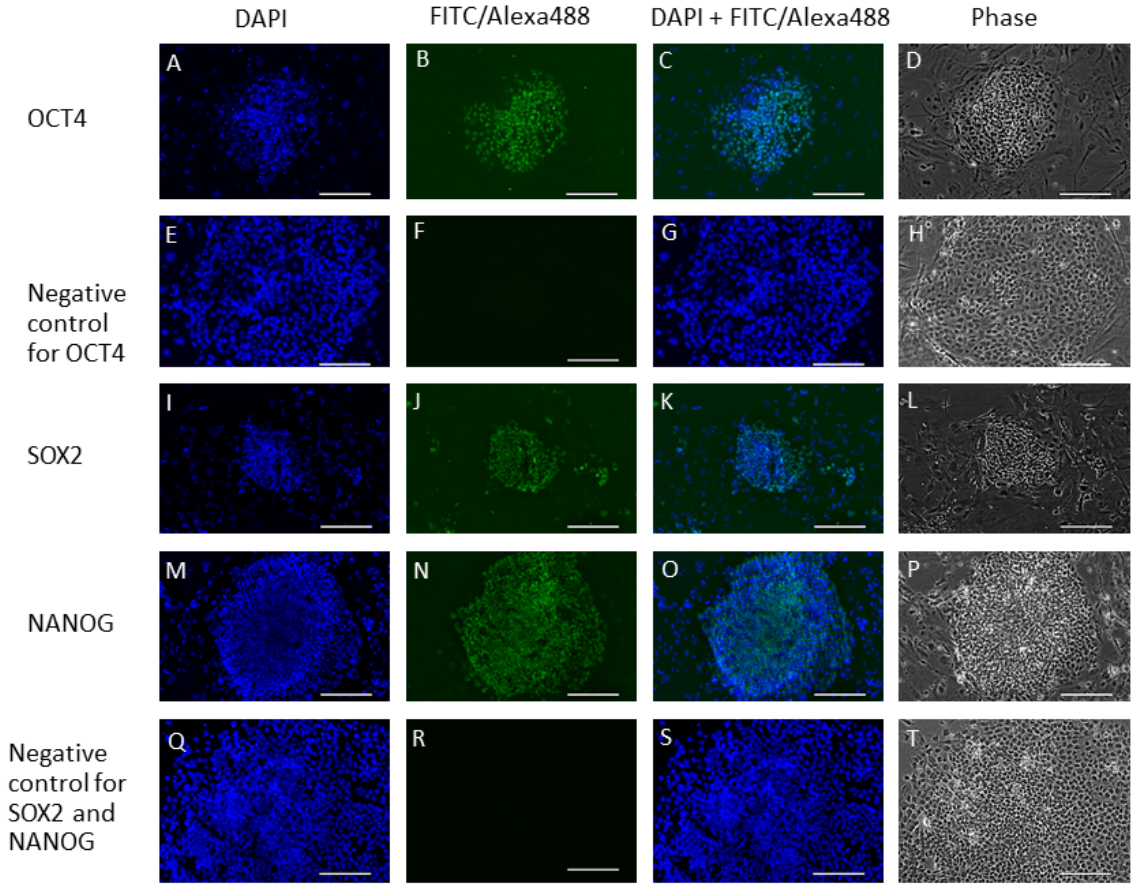

Figure 3.1 **Hues7 hESCs maintained under atmospheric oxygen express pluripotency markers.**

Representative images of protein expression of OCT4 (A-D), SOX2 (I-L) and NANOG (M-P) in Hues7 hESCs cultured on iMEF feeder layers at 20% oxygen. DAPI was used to visualise nuclei (blue; A, E, I, M, Q), FITC/Alexa488 for localisation of a protein of interest (green; B, J, N) and phase contrast (D, H, L, P, T) for colony morphology. For negative control, only FITC or Alexa Fluor 488 conjugated secondary antibodies were added (E-H and Q-T). Scale bars indicate 200 µm.

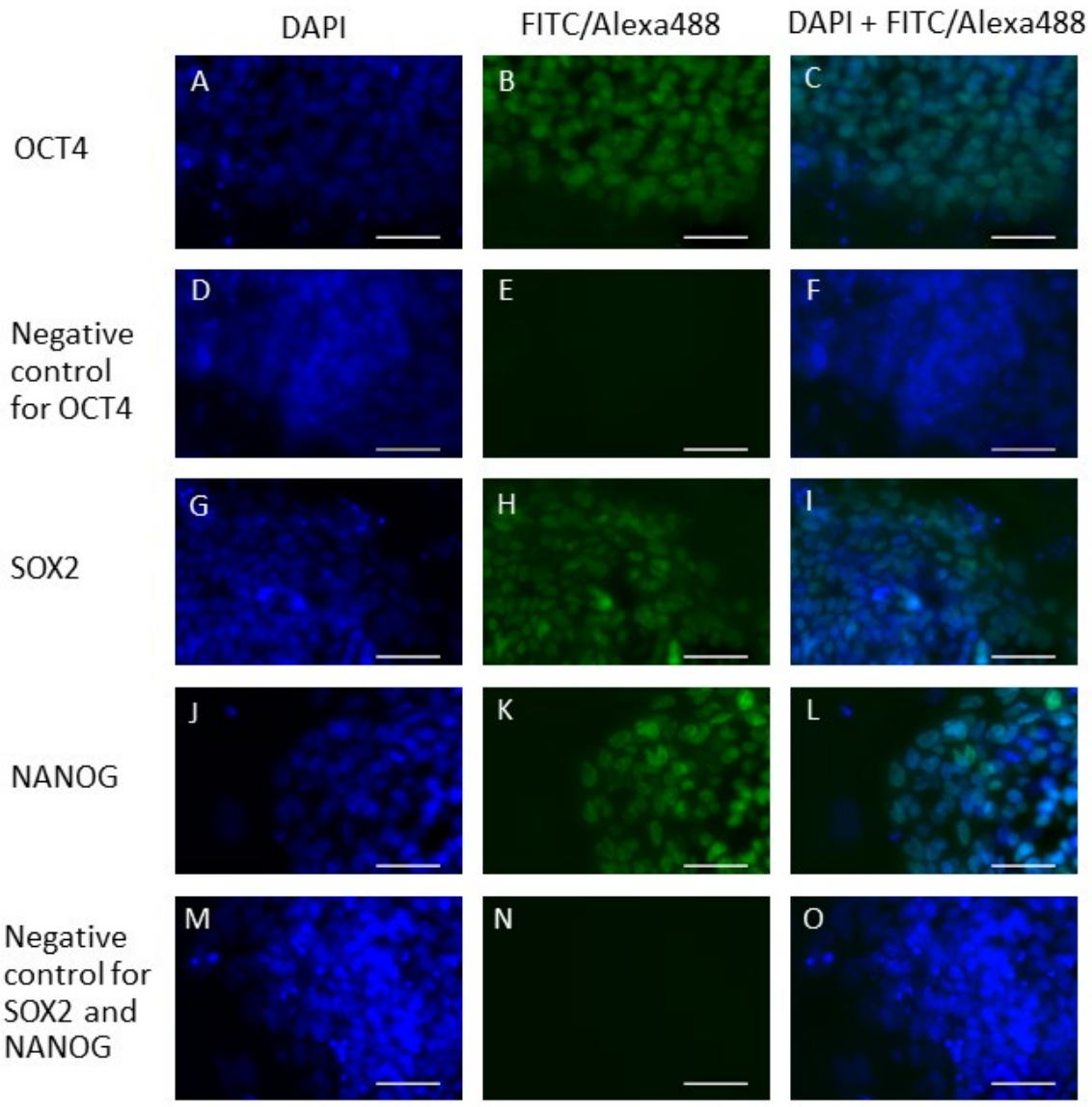

Figure 3.2 **OCT4, SOX2 and NANOG are expressed in the nucleus in Hues7 hESCs maintained under atmospheric oxygen.**

Representative images in high magnification of protein expression of OCT4 (A-C), SOX2 (G-I) and NANOG (J-L) in Hues7 hESCs cultured on iMEF feeder layers at 20% oxygen. DAPI was used to visualise nuclei (blue; A, D, G, J, M) and FITC/Alexa488 for localisation of a protein of interest (green; B, H, K). For negative control, only FITC or Alexa Fluor 488 conjugated secondary antibodies were added (D-F and M-O). Scale bars indicate 50 µm.

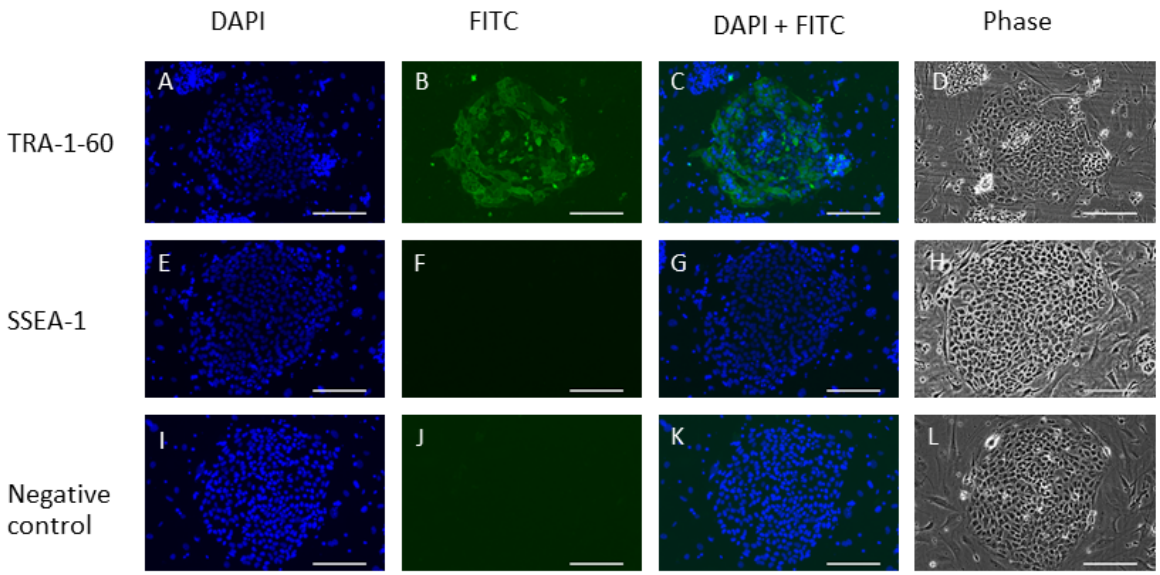

Figure 3.3 **Hues7 hESCs maintained under atmospheric oxygen express pluripotency marker TRA-1-60.**

Representative images of protein expression of TRA-1-60 (A-D) and SSEA-1 (E-H) in Hues7 hESCs cultured on iMEF feeder layers at 20% oxygen. DAPI was used to visualise nuclei (blue; A, E, I), FITC for localisation of a protein of interest (green; B, F) and phase contrast (D, H, L) for colony morphology. For negative control, only FITC conjugated secondary antibody was added (I-L). Scale bars indicate 200 µm.

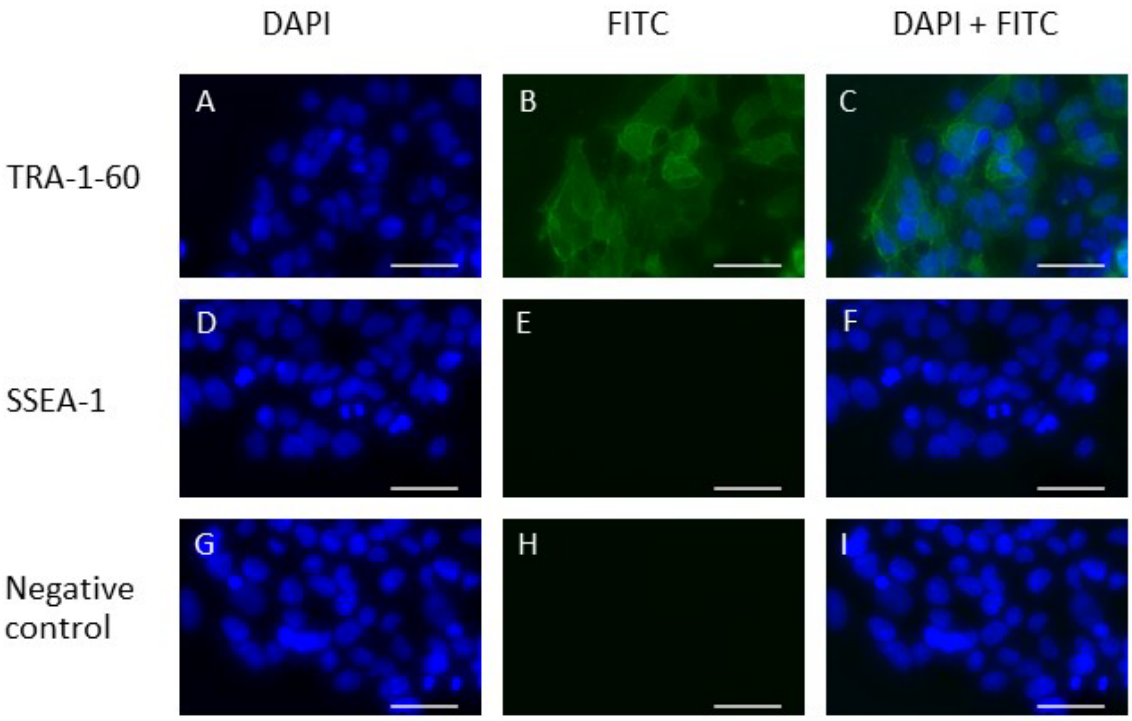

Figure 3.4 **Surface marker TRA-1-60 is expressed in Hues7 hESCs cultured at 20% oxygen.**

Representative images in high magnification of protein expression of TRA-1-60 (A-C) and SSEA-1 (D-F) in Hues7 hESCs cultured on iMEF feeder layers at 20% oxygen. DAPI was used to visualise nuclei (blue; A, D, G) and FITC for localisation of a protein of interest (green; B, E). For negative control, only FITC conjugated secondary antibodies were added (G-I). Scale bars indicate 50 µm.

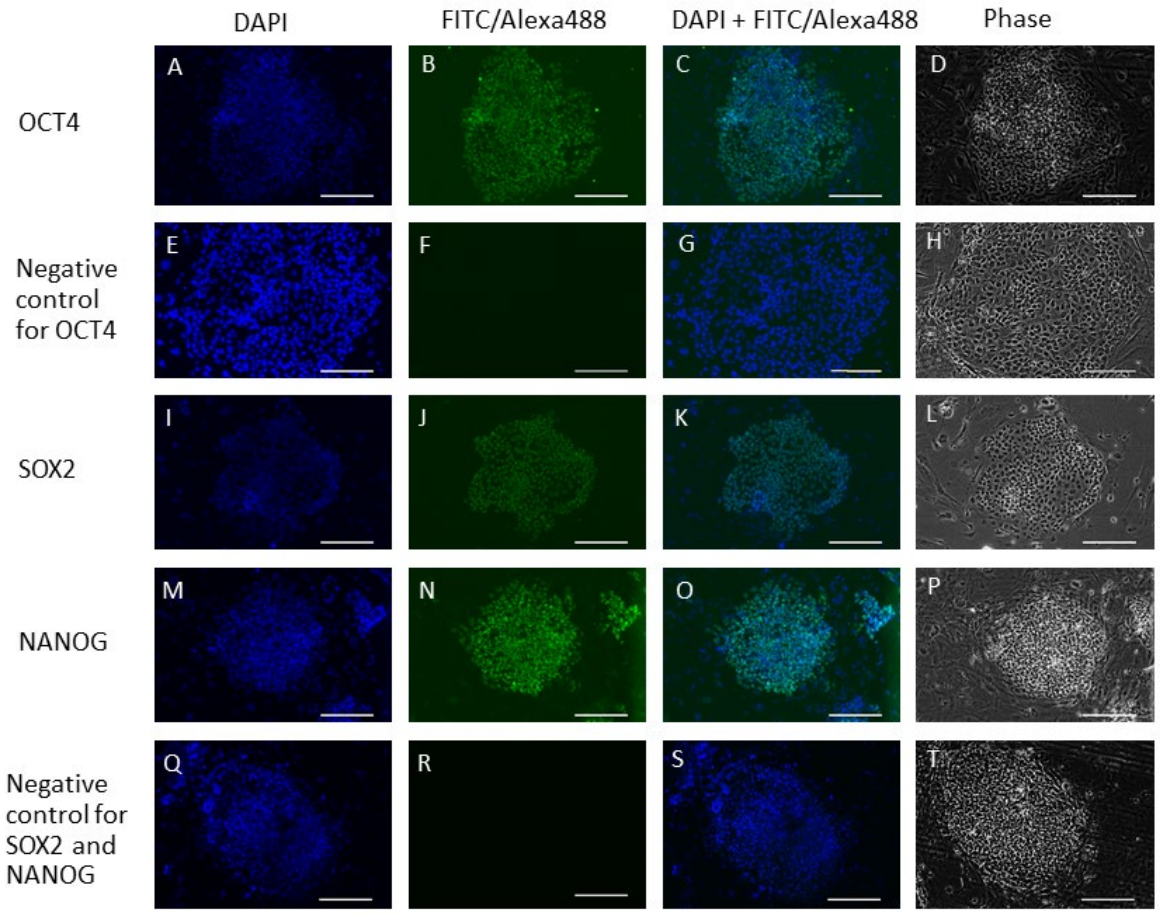

Figure 3.5 **Hues7 hESCs cultured at 5% oxygen express pluripotency markers.**

Representative images of protein expression of OCT4 (A-D), SOX2 (I-L) and NANOG (M-P) in Hues7 hESCs cultured on iMEF feeder layers under hypoxic condition. DAPI was used to visualise nuclei (blue; A, E, I, M, Q), FITC/Alexa488 for localisation of a protein of interest (green; B, J, N) and phase contrast (D, H, L, P, T) for colony morphology. For negative control, only FITC or Alexa Fluor 488 conjugated secondary antibodies were added (E-H and Q-T). Scale bars indicate 200 µm.

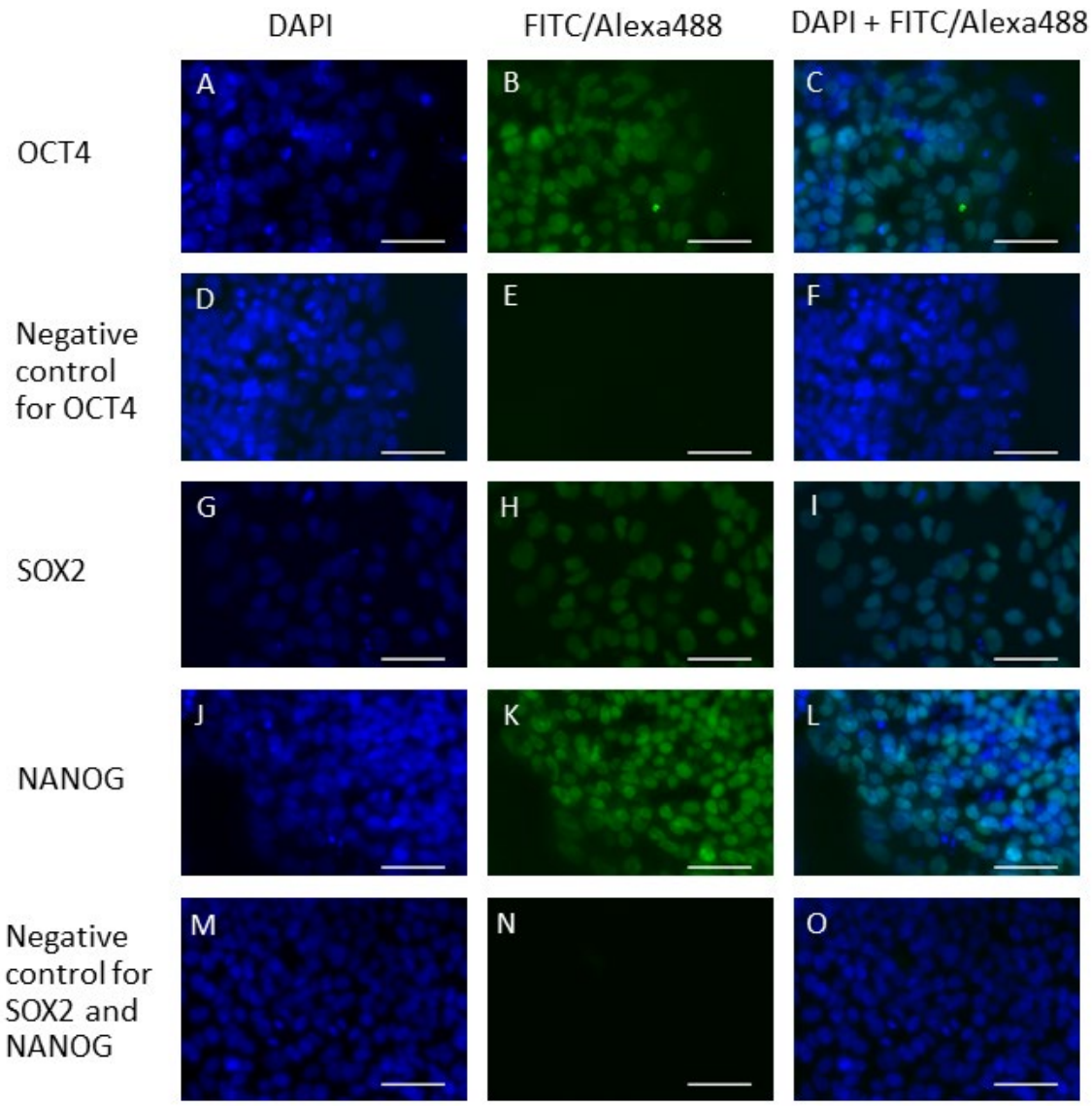

Figure 3.6 **OCT4, SOX2 and NANOG are expressed in the nucleus in Hues7 hESCs cultured at 5% oxygen.**

Representative images in high magnification of protein expression of OCT4 (A-C), SOX2 (G-I) and NANOG (J-L) in Hues7 hESCs cultured on iMEF feeder layers under hypoxic condition. DAPI was used to visualise nuclei (blue; A, D, G, J, M) and FITC/Alexa488 for localisation of a protein of interest (green; B, H, K). For negative control, only FITC or Alexa Fluor 488 conjugated secondary antibodies were added (D-F and M-O). Scale bars indicate 50 μm.

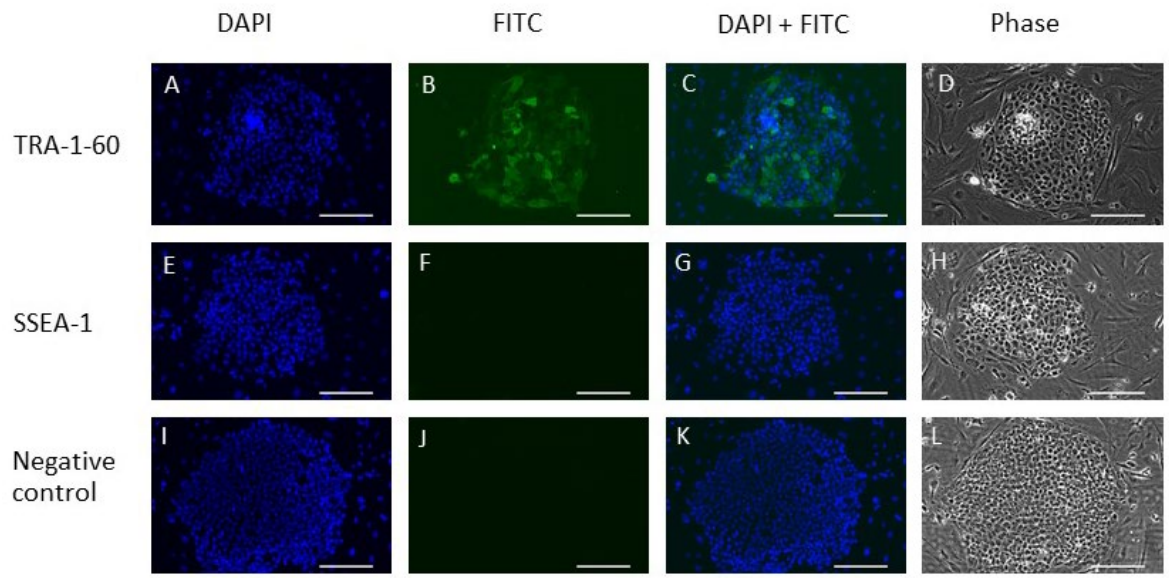

Figure 3.7 **Characterisation of surface markers in Hues7 hESCs cultured at 5% oxygen.**

Representative images of protein expression of TRA-1-60 (A-D) and SSEA-1 (E-H) in Hues7 hESCs cultured on iMEF feeder layers at 5% oxygen. DAPI was used to visualise nuclei (blue; A, E, I), FITC for localisation of a protein of interest (green; B, F) and phase contrast (D, H, L) for colony morphology. For negative control, only FITC conjugated secondary antibody was added (I-L). Scale bars indicate 200 µm.

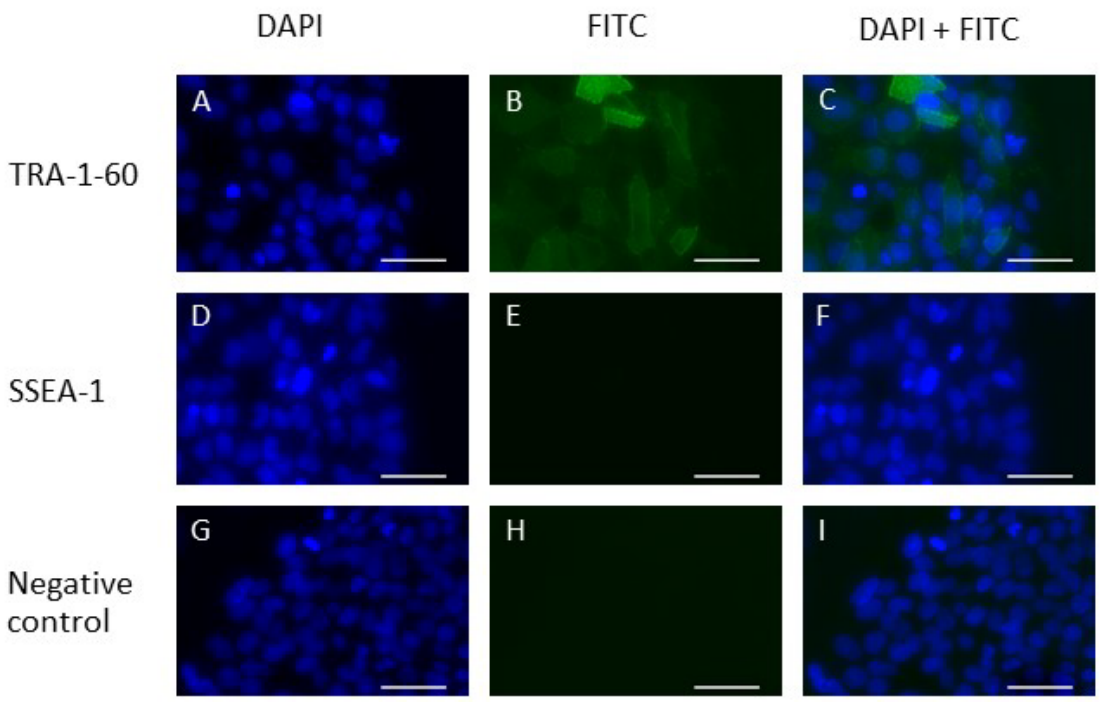

Figure 3.8 **Surface marker TRA-1-60 is expressed in Hues7 hESCs cultured at 5% oxygen.**

Representative images in high magnification of protein expression of TRA-1-60 (A-C) and SSEA-1 (D-F) in Hues7 hESCs cultured on iMEF feeder layers at 5% oxygen. DAPI was used to visualise nuclei (blue; A, D, G) and FITC for localisation of a protein of interest (green; B, E). For negative control, only FITC conjugated secondary antibodies were added (G-I). Scale bars indicate 50 µm.

3.4.1.2 Effect of oxygen tension on the expression of OCT4, SOX2 and NANOG in hESCs

Immunocytochemistry visualises the presence and localisation of proteins but does not provide quantitative data. Thus, Western blotting was used to investigate the effect of either 20% or 5% oxygen on the expression of OCT4, SOX2 and NANOG in hESCs. A single OCT4 band was identified at an approximate size of 45 kDa while β-actin used as a loading control gave a ~42 kDa band (Figure 3.9 A). Quantification of Western blot results revealed that OCT4 protein expression was significantly downregulated ($p<0.001$) in hESCs maintained under atmospheric oxygen in comparison to cells cultured under hypoxic conditions (Figure 3.9 B). SOX2 Western blot results showed a single band at the size of 35 kDa (Figure 3.9 C) and expression was significantly decreased ($p=0.018$) by 43% in hESCs maintained at 20% oxygen compared to those cultured at 5% oxygen (Figure 3.9 D). NANOG protein is approximately the same size as SOX2 (35 kDa) (Figure 3.9 E), and expression was shown to be significantly decreased, by more than 60%, in hESCs cultured at 20%, compared to 5% oxygen (Figure 3.9 F).

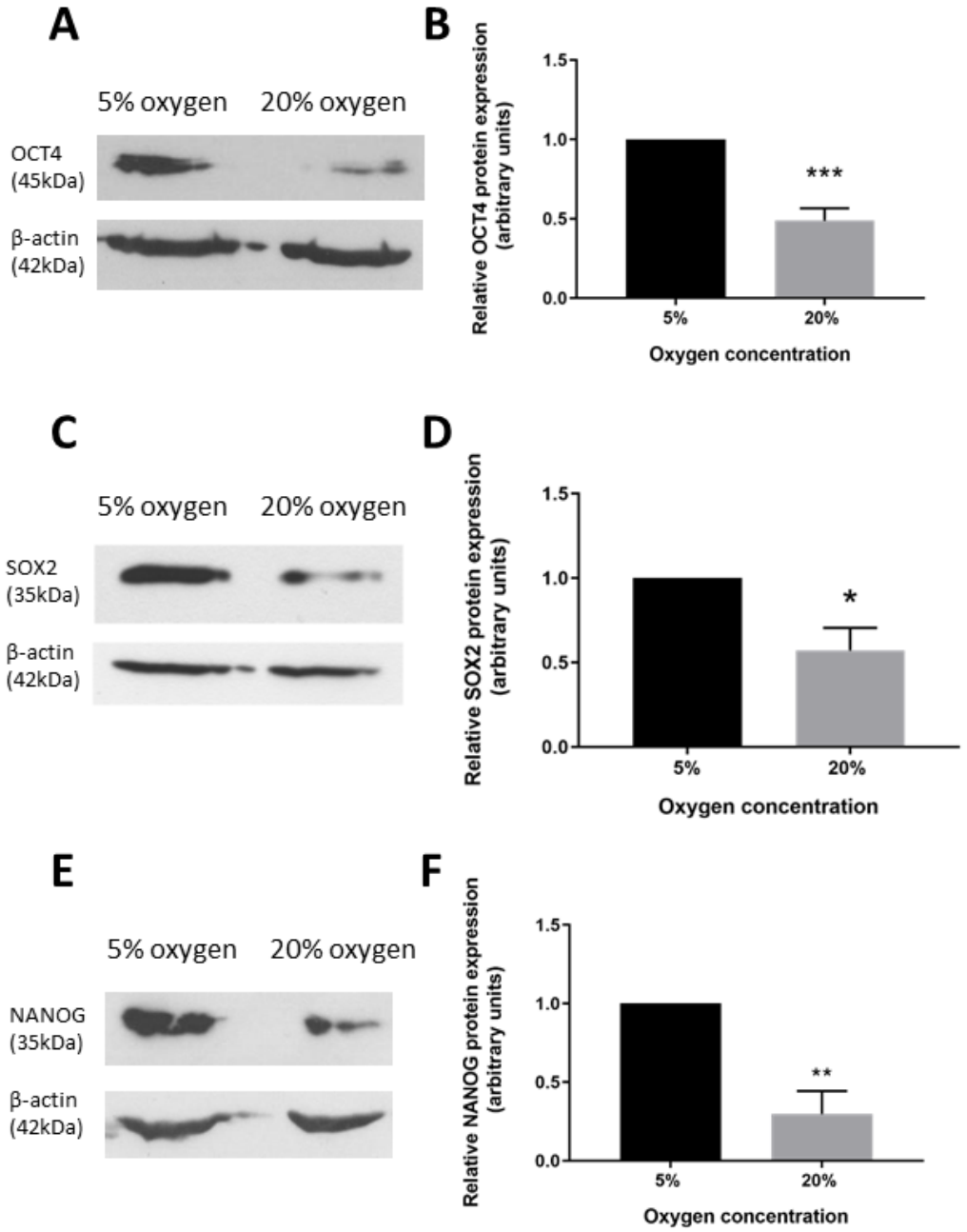

Figure 3.9 **Hypoxia promotes the expression of OCT4, SOX2 and NANOG in hESCs compared to the culture at atmospheric oxygen.**

Representative Western blot of OCT4 (A), SOX2 (C), NANOG (E) and β-actin in hESCs cultured at either 5% or 20% oxygen. Quantification of OCT4 (B), SOX2 (D) and NANOG (F) Western blot. Data were normalized to β-actin and to 1 for 5% oxygen. Bars represent mean + SEM. *p<0.05, **p<0.01, ***p<0.001 significantly different between 5% and 20% oxygen. n=4

3.4.2 Characterisation of mass spectrometry results

Three independent, biological replicates of hESCs cultured at either 5% oxygen or 20% oxygen were subject to the label-free mass spectrometry. The label-free method can provide absolute quantification of proteins within samples without the need for metabolic or chemical labelling. A total of 2674 proteins were identified in at least 1 out of the 6 samples. Reproducibility of results is presented in Figure 3.10 and should be understood as an appearance of a particular protein across replicates at a given condition. The number of identified proteins between paired samples of hESCs cultured at 5% and 20% oxygen varied (Figure 3.10). Sample pair a and d share a similar number of proteins but the difference is bigger between pair b and d, to almost twice as many proteins in sample f compared to c. However, overall, 2275 proteins were identified in hESCs cultured at 5% oxygen which was similar to the 2337 proteins identified in cells maintained under atmospheric oxygen tension (Figure 3.10 C). In total, 1938 proteins were common for samples of hESCs cultured at either 5% or 20% oxygen; 399 proteins were identified only in samples of cells maintained under atmospheric oxygen and 337 proteins were unique for hESC samples cultured in hypoxia (Figure 3.10 C).

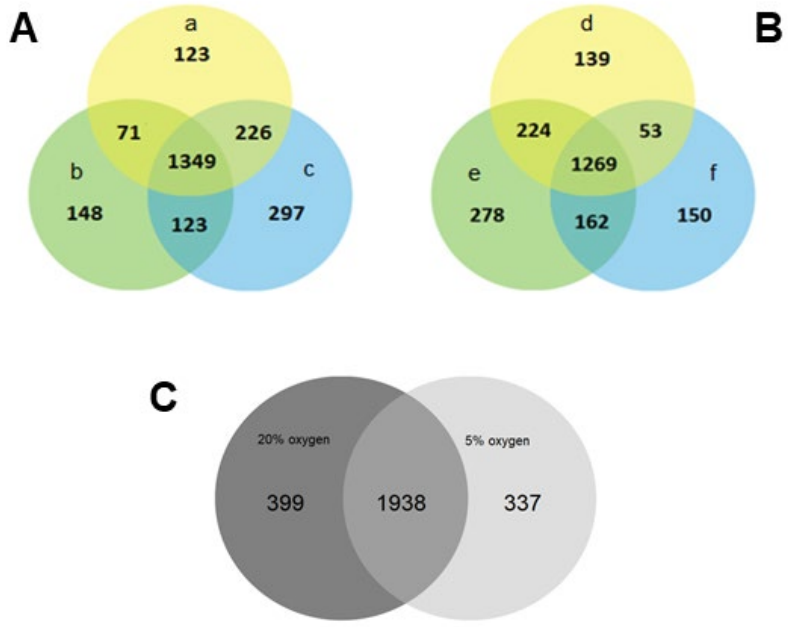

Figure 3.10 **Reproducibility of samples of hESCs cultured at either 5% or 20% oxygen.**

(A) The total number of proteins identified in each of the replicate samples of hESCs cultured at 20% oxygen (n=3) and (B) at 5% oxygen (n=3). Circles of the same colour represent paired samples (sample a with d, b with e and c with f). (C) A total number of proteins identified across all 3 replicate samples (n=3 for each condition).

The label-free technique used for mass spectrometry not only allowed proteins to be identified but also quantified. 2674 proteins were identified in total; however in some cases, expression was only found in 1 sample out of 6, and therefore it was not possible to calculate fold change. Fold change and p-value (based on Student t-test) were determined for 1498 proteins out of 2674. To characterise the expression of proteins across samples, hierarchical clustering was applied to the dataset of 1498 proteins to cluster sample data using the complete linkage method and Euclidean distance metric. Whilst the linkage defines the set of rules to agglomerate samples, the distance metric measures the similarity of samples. It revealed that, as expected, samples a and b (hESCs cultured at 20% oxygen) were clustered together by the similarity of the expression level of proteins, as well as samples d and f (hESCs cultured at 5% oxygen). Surprisingly samples c and e did not cluster with the respective group at 20% and 5% oxygen, yet exhibited greater similarity to the proteomic profile of hESCs cultured at 20% oxygen (Figure 3.11).

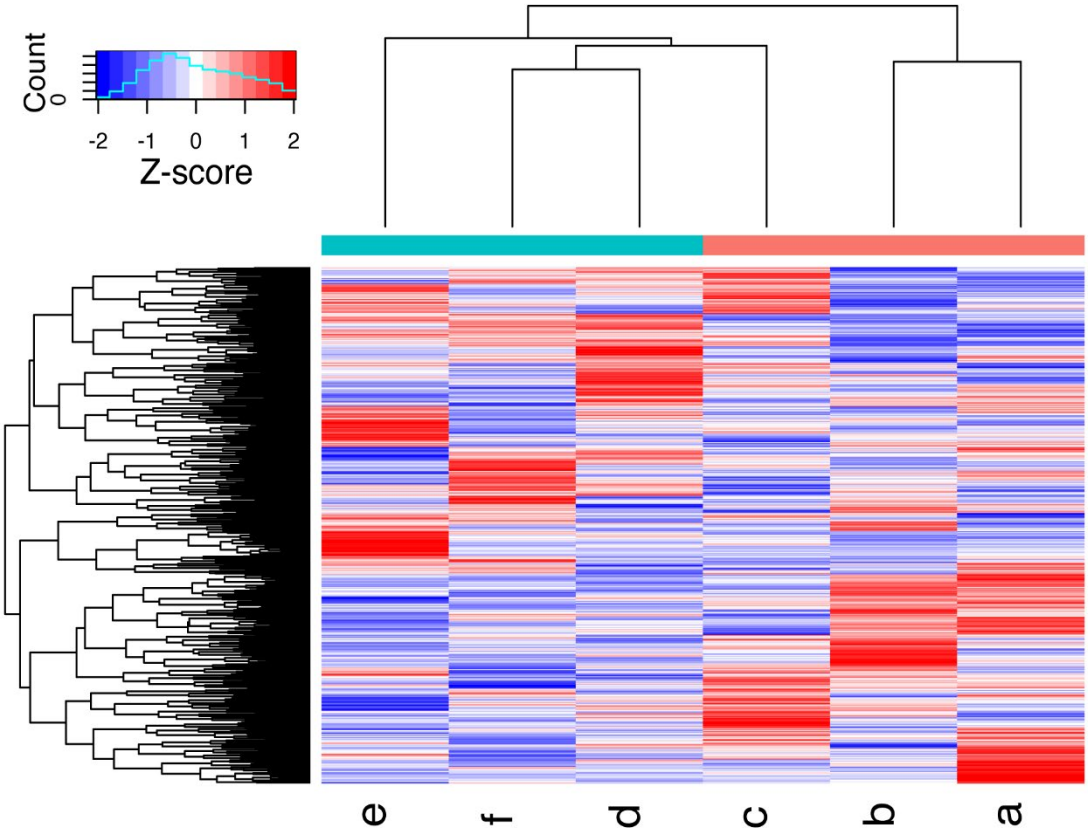

Figure 3.11 **Similarity of expressed proteins between samples of hESCs.**

Samples a, b, c- hESCs cultured at 20% oxygen; samples d, e, f- hESCs cultured at 5% oxygen. Z-score indicates scaled protein expression data.

Principal component analysis (PCA) provided insight into the variance between samples used for mass spectrometry. The first two components are representative of ~53% of the dataset variance and similarly to what was observed through hierarchical clustering, showed clustering of samples a and b and samples d and f (Figure 3.12). Samples c and e appear as outliers in the clustering, with sample c being more similar to hESCs cultured at 20% oxygen according to PC1. hESCs cultured at 5% oxygen were observed to be clustering when visualising PC1 and PC3 (Appendix 1).

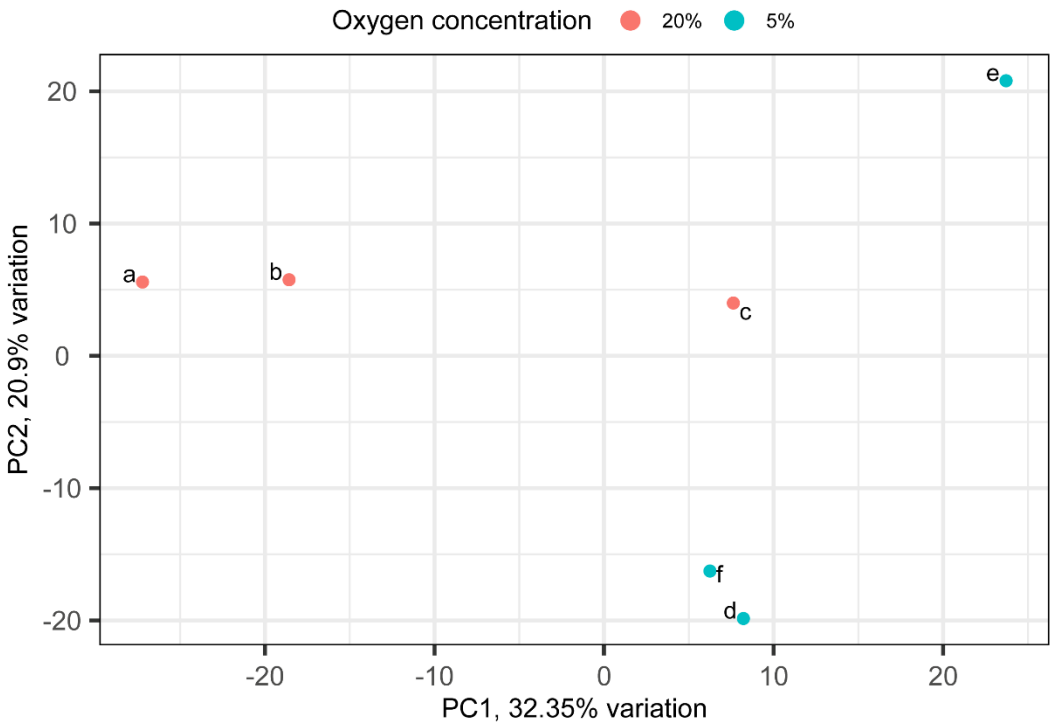

Figure 3.12 **Principal component analysis of hESC sample data.**

Samples a, b, c- hESCs cultured at 20% oxygen; samples d, e, f- hESCs cultured at 5% oxygen.

A Volcano plot was generated for 1498 proteins to visualise differences in the expression level of proteins across the dataset. The proteins that are highly significant appear on the top of the plot while increasing difference in fold change is displayed on either the right or left side. A large number of proteins have similar expression level in hESCs cultured at either 5% or 20% oxygen (Figure 3.13; the bottom central part of the plot). However some proteins are placed by the end of plot 'arms' meaning that they are significantly different between conditions and are either up- or down-regulated in hESCs cultured in hypoxia compared to normoxia (Figure 3.13).

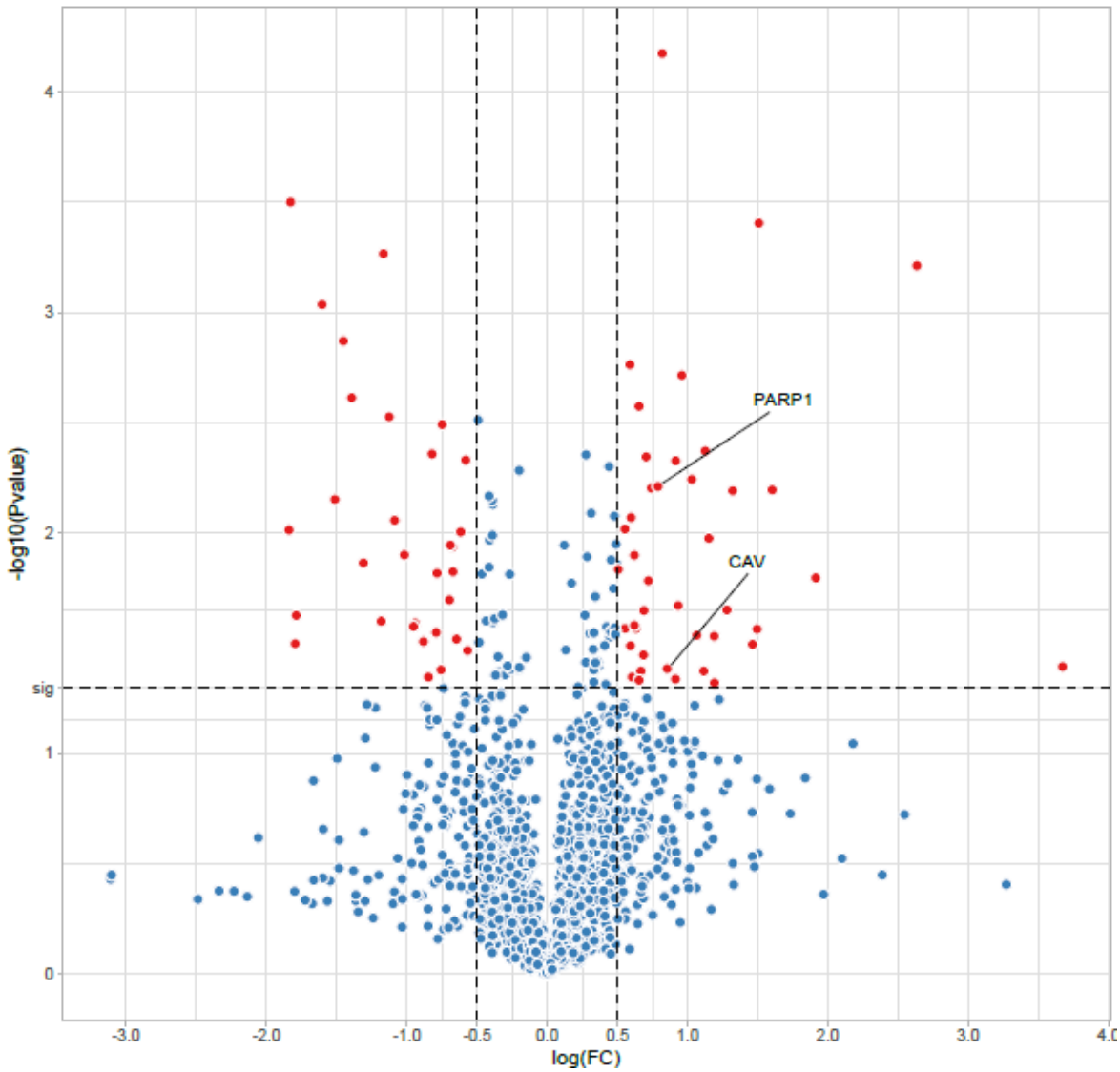

Figure 3.13 **Volcano plot of proteins expressed in hESCs.**

Analysis based on 1498 proteins for which p-value and fold change could be determined. Red dots indicate proteins that have p-value < 0.05 and Log_2(FoldChange) is either >0.5 or < -0.5. Dashed lines corresponds to mentioned p-value and FC thresholds. PARP-1 (PARP1) and caveolin-1 (CAV) are marked in the figure.

Student's t-test was applied on the entire dataset of detected and quantified proteins to identify significant differences in expression of proteins between hESCs cultured at either 5% or 20% oxygen. The threshold of significance was set as p-value <0.05. 129 proteins were found to be significantly different in expression level between the two culture conditions (Appendix 2). When the threshold (Log_2FoldChange > 0.5) was applied to determine proteins upregulated in hESCs cultured at 5% oxygen compared to those maintained at 20% oxygen, 38 proteins were found to

be upregulated. In contrast, 31 proteins were downregulated in hESCs cultured in hypoxic condition, in comparison to cells cultured in normoxia (threshold Log_2FoldChange < -0.5).

3.4.3 Gene ontology analysis

Gene ontology (GO) is a method of classification that helps to characterise genes, groups them into categories and represents relationships between these. There are three main GO aspects: cellular components, molecular functions and biological processes. GO helps to identify overrepresented elements of these aspects when provided with a list of genes or proteins of interest. GO analysis was applied to further characterise the dataset of 2674 proteins. Based on the REVIGO tool (Supek *et al.*, 2011) proteins were grouped based on cellular components (Figure 3.14). The majority of proteins were found to be localised within the cytosol (44% of all proteins), while only 7% of proteins were characterised as a 'nuclear part'. Interestingly, 800 proteins were associated with 'extracellular exosomes' GO term.

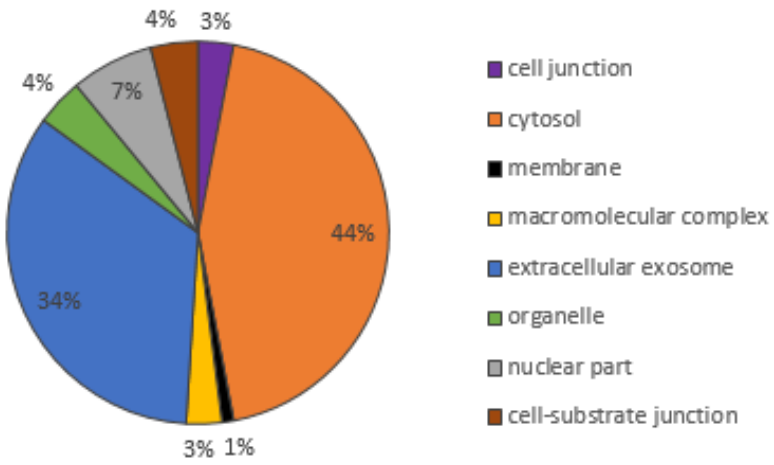

Figure 3.14 **The cellular localisation of proteins identified in hESCs cultured at either 5% or 20% oxygen.**

Analysis based on the full dataset; 2634 proteins out of 2674 were associated with GO terms and used for analysis. Percentage of each cellular component was calculated by dividing the number of proteins associated with a particular term by the total number of proteins.

The dataset was further interrogated by only including the 129 proteins that were significantly altered by oxygen concentration (Appendix 2). Cellular component enrichment analysis found that

the majority of these proteins were associated with either cytoplasm (40%) or organelles (35%). 12% of proteins were part of the nucleus whereas the rest of the proteins were linked to the actin cytoskeleton and ribonucleoprotein complex GO terms (6% and 7% respectively) (Figure 3.15).

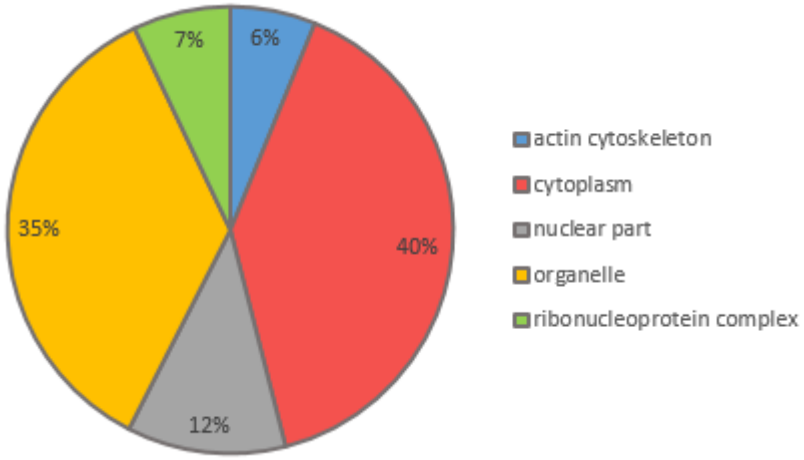

Figure 3.15 **The cellular localisation of the 129 proteins showing significant differences between hESCs cultured at either 5% or 20% oxygen.**

Analysis based on the 129 proteins with expression significantly altered by oxygen concentration. Percentage of each cellular component was calculated by dividing the proteins associated with a particular term by the total number of proteins.

The 129 proteins whose expression was significantly different in hESCs cultured at either 5% or 20% oxygen were analysed using PANTHER GO tool (Mi *et al.*, 2018) to investigate if there was any major enrichment in protein class within this particular dataset. Proteins were found to be distributed into various classes, but two major families could be distinguished, 'RNA binding protein' (12% of analysed proteins) and 'nucleic acid binding' (16% of analysed proteins) (Figure 3.16).

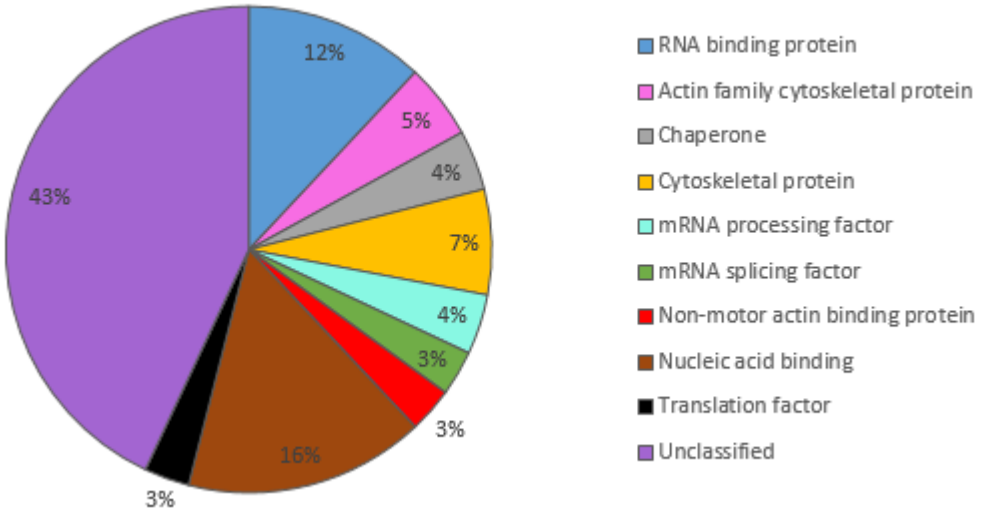

Figure 3.16 **The main protein classes of the 129 proteins showing significant differences between hESCs cultured at either 5% or 20% oxygen.**

Analysis based on the 129 proteins with expression significantly altered by oxygen concentration. Percentage of each protein class was calculated by dividing the number of proteins associated with a particular term by the total number of proteins.

GO analysis was performed to establish enriched GO processes within proteins that were either significantly upregulated (38 proteins) or downregulated (31 proteins) in hESCs cultured at 5% oxygen compared to 20% oxygen. When the cut-off point for proteins significantly upregulated was set as $\log_2FC > 0.5$, and for downregulated as $\log_2FC < -0.5$, the REVIGO tool was used to analyse subsets. The protein target set (38 or 31 proteins) was analysed compared to the background set (all identified proteins- 2674) and redundant GO terms were removed based on semantic similarity. It helped to better summarise and visualise results by removing GO terms that were too general, merging similar ones together and keeping unique clusters. The analysis showed that the most enriched processes were 'cellular response to oxygen levels' and 'regulation of autophagy', for proteins upregulated in hESCs maintained in hypoxic compared to normoxic conditions (Figure 3.17). Analysis based on downregulated proteins showed that the most enriched GO terms were 'negative regulation of apoptotic process', 'nitric oxide biosynthesis', 'protein folding' and 'reactive nitrogen species metabolism' (Figure 3.18).

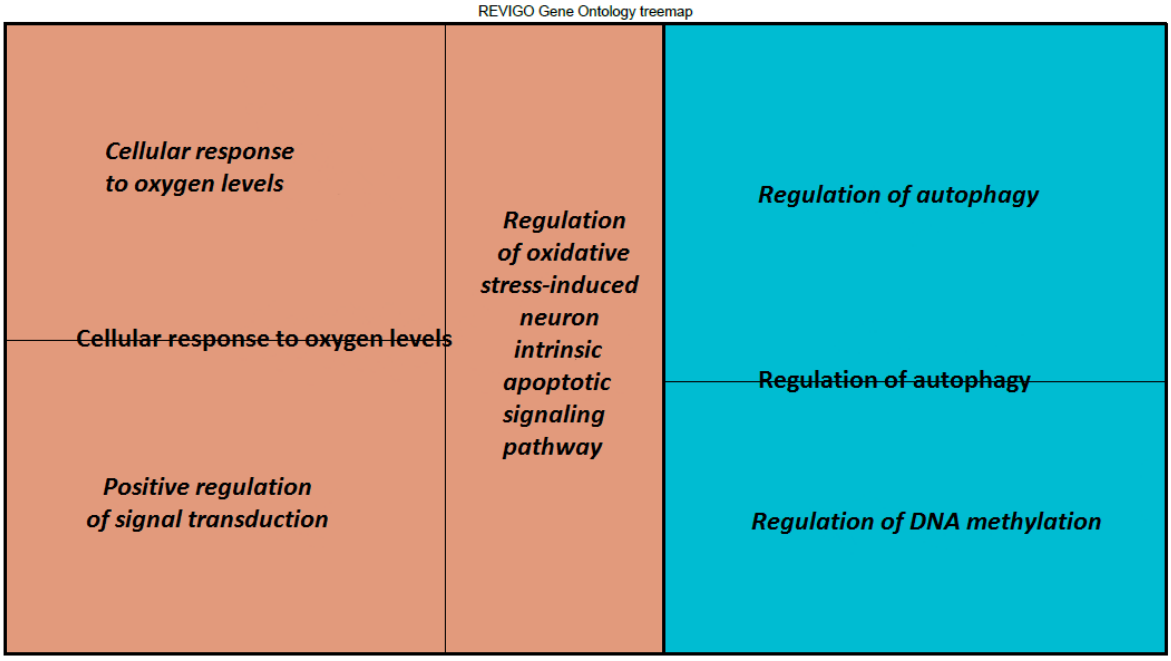

Figure 3.17 **REVIGO gene ontology treemap of enriched GO terms based on proteins that are upregulated in hESCs cultured at 5% oxygen.**

The analysis based on the target set of 38 proteins identified as significantly upregulated by hypoxia in hESCs. The box size corresponds to the value of $\log_{10}$p-value of the given GO-term enrichment i.e. the bigger the box the greater the enrichment. Boxes with the same colour are grouped by semantic similarity. Cut-off point was set as $\log_2 FC > 0.5$

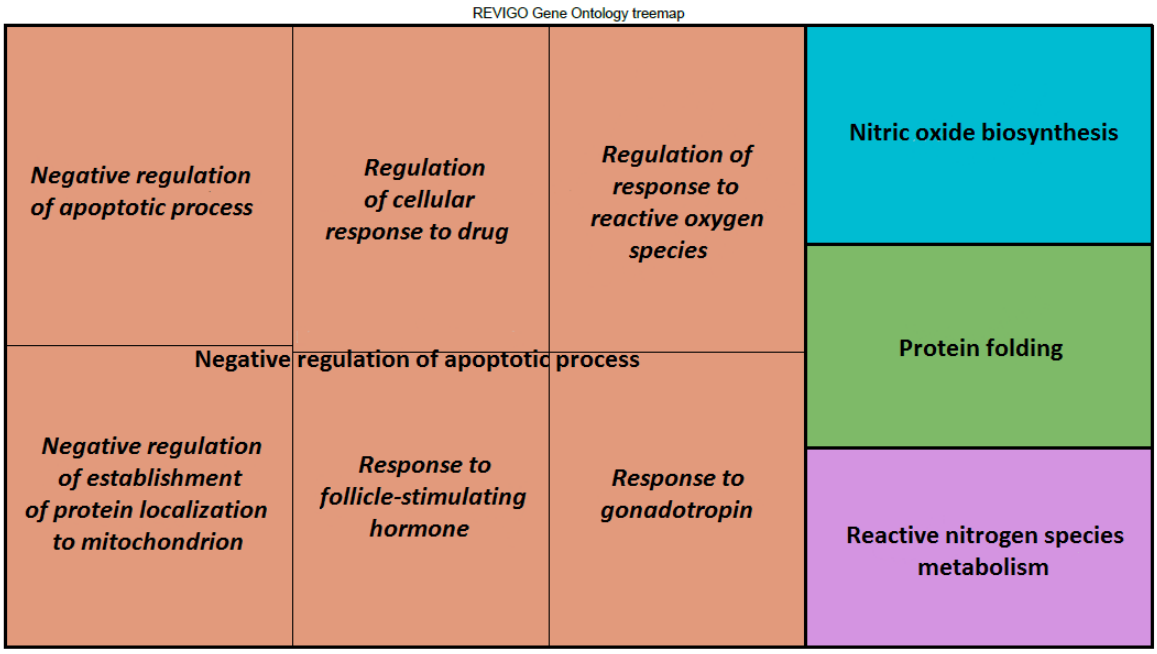

Figure 3.18 **REVIGO gene ontology treemap of enriched GO terms based on proteins that are downregulated in hESCs maintained under low oxygen tension.**

The analysis based on the target set of 31 proteins identified as significantly downregulated by hypoxia in hESCs. The box size is corresponding to the value of $\log_{10}$p-value of the given GO-term enrichment. Boxes with the same colour are grouped by semantic similarity. Cut-off point was set as $\log_2 FC < -0.5$

The list of genes associated with particular GO terms is presented in Table 3.1 for enriched GO terms based on the input of upregulated proteins, and in Table 3.2 for downregulated proteins in hESCs cultured at 5% oxygen in comparison to cells cultured at 20% oxygen.

Table 3.1 **List of genes and corresponding GO terms.**

Analysis based on proteins that were upregulated in hESCs cultured in hypoxia compared to normoxia.

GO term	**Genes**
regulation of autophagy	ATP6V1G1 - ATPase, h+ transporting, lysosomal 13kda, v1 subunit g1
	PARK7 - Parkinson protein 7
	SNRNP70 - small nuclear ribonucleoprotein 70kda (u1)
	SEC22B - sec22 vesicle trafficking protein homolog b (s. cerevisiae) (gene/pseudogene)
	LAMTOR1 - late endosomal/lysosomal adaptor, MAPK and mTOR activator 1
	GNAI3 - guanine nucleotide binding protein (g protein), alpha inhibiting activity polypeptide 3
	UBQLN4 - ubiquilin 4
regulation of macroautophagy	ATP6V1G1 - ATPase, h+ transporting, lysosomal 13kDa, v1 subunit g1
	SEC22B - sec22 vesicle trafficking protein homolog b (s. cerevisiae) (gene/pseudogene)
	LAMTOR1 - late endosomal/lysosomal adaptor, MAPK and mTOR activator 1
	GNAI3 - guanine nucleotide binding protein (g protein), alpha inhibiting activity polypeptide 3
	UBQLN4 - ubiquilin 4
cellular response to oxygen levels	ATP6V1G1 - ATPase, h+ transporting, lysosomal 13kDa, v1 subunit g1
	PGK1 - phosphoglycerate kinase 1
	GNB1 - guanine nucleotide binding protein (g protein), beta polypeptide 1
	CAV1 - caveolin 1, caveolae protein, 22kDa

GO term	**Genes**
positive regulation of signal transduction	PARP1 - poly (ADP-ribose) polymerase 1
	DDX5 - dead (asp-glu-ala-asp) box helicase 5
	EIF2A - eukaryotic translation initiation factor 2a, 65kDa
	LGALS1 - lectin, galactoside-binding, soluble, 1
	PRMT5 - protein arginine methyltransferase 5
	PARK7 - Parkinson protein 7
	UBE2O - ubiquitin-conjugating enzyme e2o
	CAV1 - caveolin 1, caveolae protein, 22kDa
	VAPA - vamp (vesicle-associated membrane protein)-associated protein a, 33kDa
	PSMD5 - proteasome (prosome, macropain) 26s subunit, non-ATPase, 5
	LAMTOR1 - late endosomal/lysosomal adaptor, MAPK and mTOR activator 1
regulation of oxidative stress-induced neuron intrinsic apoptotic signalling pathway	PARP1 - poly (ADP-ribose) polymerase 1
	PARK7 - Parkinson protein 7
regulation of DNA methylation	PARP1 - poly (ADP-ribose) polymerase 1
	PRMT5 - protein arginine methyltransferase 5

Table 3.2 **List of genes and corresponding GO terms.**

Analysis based on proteins that were downregulated in hESCs cultured at 5% oxygen compared to 20% oxygen.

GO term	**Genes**
negative regulation of apoptotic process	ASNS - asparagine synthetase (glutamine-hydrolyzing)
	PYCR1 - pyrroline-5-carboxylate reductase 1
	HSPA1B - heat shock 70kDa protein 1b
	DFFA - DNA fragmentation factor, 45kDa, alpha polypeptide
	DNAJA1 - Dnaj (HSP40) homolog, subfamily a, member 1
	DDAH2 - dimethylarginine dimethylaminohydrolase 2
	PAWR - PRKC, apoptosis, WT1, regulator
	NQO1 - NAD(P)H dehydrogenase, quinone 1
	HSPH1 - heat shock 105kDa/110kDa protein 1
	TXNDC5 - thioredoxin domain containing 5 (endoplasmic reticulum)
	ARF4 - ADP-ribosylation factor 4
regulation of hydrogen peroxide-induced cell death	PYCR1 - pyrroline-5-carboxylate reductase 1
	PAWR - PRKC, apoptosis, WT1, regulator
	HSPH1 - heat shock 105kDa/110kDa protein 1
negative regulation of establishment of protein localization to mitochondrion	DNAJA1 - Dnaj (HSP40) homolog, subfamily a, member 1
	HSPH1 - heat shock 105kDa/110kDa protein 1
regulation of cellular response to drug	PYCR1 - pyrroline-5-carboxylate reductase 1
	PAWR - PRKC, apoptosis, WT1, regulator
	HSPH1 - heat shock 105kDa/110kDa protein 1

GO term	Genes
regulation of response to reactive oxygen species	PYCR1 - pyrroline-5-carboxylate reductase 1
	PAWR - PRKC, apoptosis, WT1, regulator
	HSPH1 - heat shock 105kDa/110kDa protein 1
response to gonadotropin	ASNS - asparagine synthetase (glutamine-hydrolyzing)
	HMGCS1 - 3-hydroxy-3-methylglutaryl-coa synthase 1 (soluble)
response to follicle-stimulating hormone	ASNS - asparagine synthetase (glutamine-hydrolyzing)
	HMGCS1 - 3-hydroxy-3-methylglutaryl-coa synthase 1 (soluble)
nitric oxide biosynthetic process	DDAH2 - dimethylarginine dimethylaminohydrolase 2
	NQO1 - NAD(P)H dehydrogenase, quinone 1
protein folding	HSPA1B - heat shock 70kDa protein 1b
	DFFA - DNA fragmentation factor, 45kDa, alpha polypeptide
	DNAJA1 - Dnaj (HSP40) homolog, subfamily a, member 1
	FKBP10 - fk506 binding protein 10, 65 kDa
	FKBP4 - fk506 binding protein 4, 59kDa
	HSPH1 - heat shock 105kDa/110kDa protein 1
	TXNDC5 - thioredoxin domain containing 5 (endoplasmic reticulum)
reactive nitrogen species metabolic process	DDAH2 - dimethylarginine dimethylaminohydrolase 2
	NQO1 - NAD(P)H dehydrogenase, quinone 1
nitric oxide metabolic process	DDAH2 - dimethylarginine dimethylaminohydrolase 2
	NQO1 - NAD(P)H dehydrogenase, quinone 1

3.4.4 Clustering of differentially expressed proteins in hESCs cultured at either atmospheric or hypoxic conditions

The expression of 129 proteins identified as significantly different between hESCs cultured at either 5% or 20% oxygen was visualised using a heatmap (Figure 3.19). Complete linkage and Euclidean distances were used as the clustering method. However, no obvious tendency was recognised regarding the type of proteins within groups; they did not belong to the same family or were not necessarily involved in the same functions. The top 5 upregulated and downregulated proteins out of 129 proteins are shown in Table 3.3.

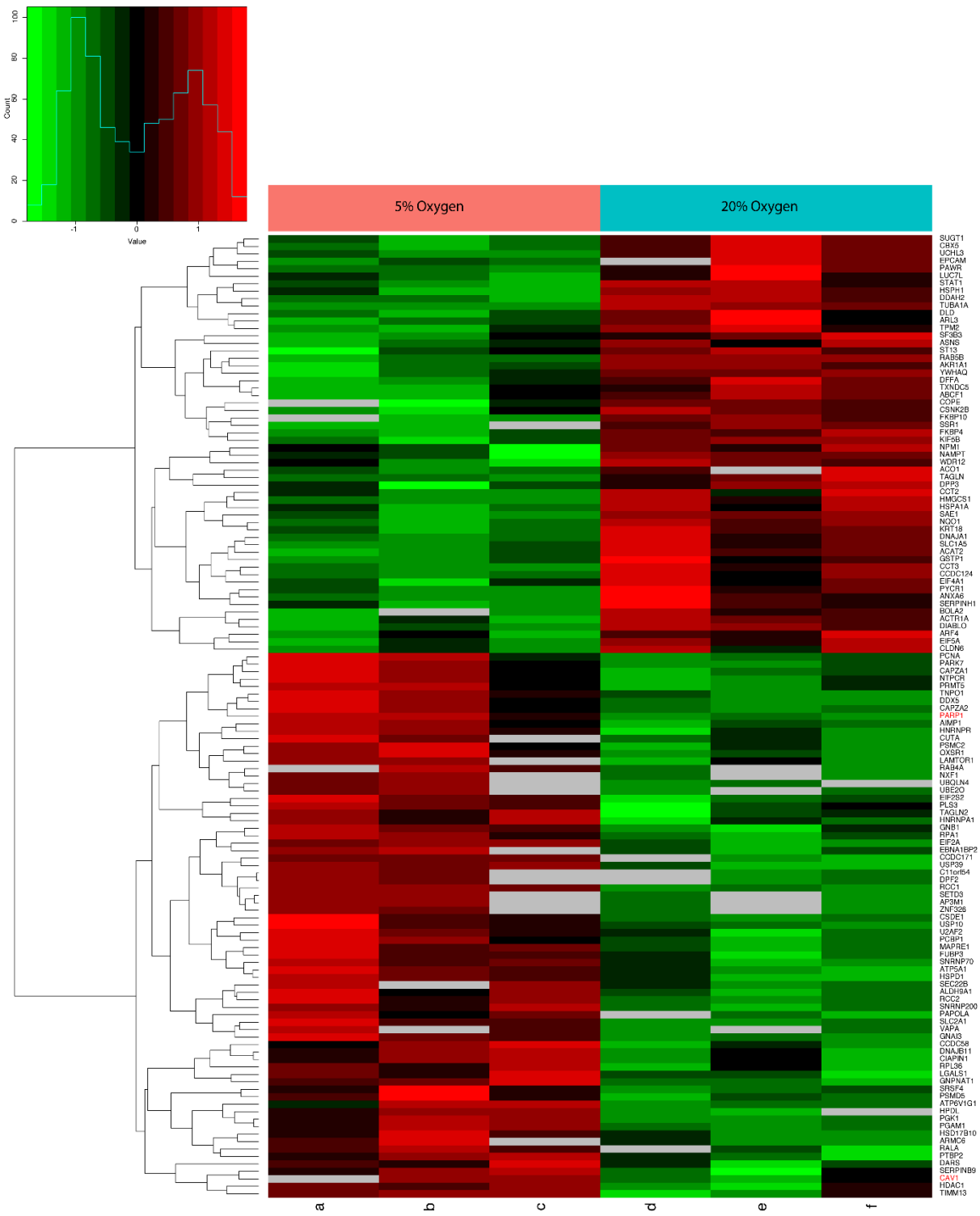

Figure 3.19 **Differential protein expression in hESCs cultured at 5% oxygen compared to those maintained at 20% oxygen.**

Heatmap presenting expression of 129 proteins identified as significantly altered by environmental oxygen in hESCs. Red colour indicates proteins upregulated in hESCs cultured at 5% oxygen; downregulated proteins are marked as green and grey means no value.

Table 3.3 **The top 5 proteins that are up- and downregulated in hESCs cultured at 5% oxygen.**

Downregulated proteins		
UniProt ID	**Protein name (gene name)**	**Log_2FC**
P43307	Translocon-associated protein subunit alpha (SSR1)	-2.03728
Q71U36	Tubulin alpha-1A chain (TUBA1A)	-1.83036
Q96CT7	Coiled-coil domain-containing protein 124 (CCDC124)	-1.79676
Q9UBE0	SUMO-activating enzyme subunit 1 (SAE1)	-1.6045
Q9BWD1	Acetyl-CoA acetyltransferase cytosolic (ACAT2)	-1.51302

Upregulated proteins		
UniProt ID	**Protein name (gene name)**	**Log_2FC**
P11233	Ras-related protein Ral-A (RALA)	2.047507
Q6TFL3	Coiled-coil domain-containing protein 171 (CCDC171)	2.092077
Q96IR7	4-hydroxyphenylpyruvate dioxygenase-like protein (HPDL)	2.498115
Q86TU7	Histone-lysine N-methyltransferase (SETD3)	2.633625
P20338	Ras-related protein Rab-4A (RAB4A)	3.670681

3.4.5 Pathway and function analysis of hESC proteome

IPA (Ingenuity Pathway Analysis) is a software used for analysis, integration, and interpretation of 'omics data based on a chosen parameter, such as p-value or fold change. The whole dataset (2674 proteins) was provided for analysis; however fold change and p-value, required by the software, were available for 1498 proteins.

3.4.5.1 Canonical Pathways

IPA analysis revealed the involvement of proteins from the dataset in Canonical Pathways. The pathway significance is indicated by a probability of association of molecules from the dataset with a particular pathway. The Canonical Pathways that appear to be most significantly affected by the proteins within the dataset are EIF2 signalling pathway, regulation of eIF4 and p70S6K

signalling, protein ubiquitination pathway or remodelling of epithelial adherens junctions (Figure 3.20). Canonical Pathways were considered as significant if p-value < 0.05 and the coverage by proteins from the dataset was not less than 10% of the total number of known proteins from the particular pathway. Based on these criteria, 178 Canonical pathways were identified as significantly enriched. Higher coverage by proteins from the dataset was obtained for pathways where the total known number of involved proteins is small. For example, results indicate that pathway coverage by proteins from the dataset for RAN signalling is around 80% (14 proteins from the dataset were associated with that pathway) but the total number of known proteins involved in that pathway is only 17. There was no clear trend in the number of proteins involved in pathways that were up-regulated or down-regulated in hESCs cultured at 5% compared to 20% oxygen. It can be observed that proteins within a pathway were changed in expression by environmental oxygen (indicated by green colour for downregulated proteins and red colour for upregulated in hypoxia) but the proportion is generally equal. Many significant pathways are related to translation and cell turnover.

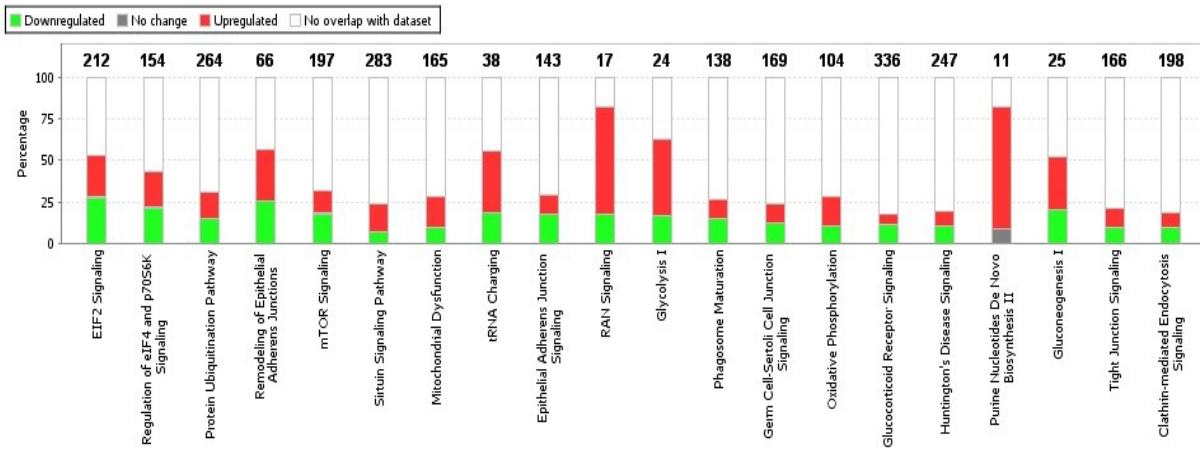

Figure 3.20 **The most significant Canonical Pathways across the dataset.**

IPA generated a long list of Canonical Pathways and due to the clarity of the figure, only first 20 the most significant Canonical Pathways affected by hypoxia in hESCs are displayed. The most significant Canonical Pathways are displayed on the left and less significant on the right. The colouring of the bar indicates if molecules associated with a pathway remain the same (grey), are downregulated (green), or upregulated (red) in hESCs cultured at 5% oxygen compared to 20% oxygen. The number above each bar represents the total number of molecules involved in that pathway. The total bar height shows an overlap of the analysis with the Canonical Pathway, i.e. percentage coverage of the pathway by proteins within the dataset. Canonical Pathways with a p-value greater than 0.05 were not included.

Some proteins from the dataset are also involved in more than one Canonical Pathway. Relationships between pathways are presented in Figure 3.21. This visualisation enables the identification of pathways that share the same molecules and therefore show connections between pathways that were assumed unrelated. An example could be a relationship between actin cytoskeleton signalling pathway, which controls the rearrangements of the filament network, and EIF2 signalling, involved in protein synthesis. These two pathways were found to have 5 common proteins: serine/threonine-protein phosphatase PP1-beta catalytic subunit, growth factor receptor-bound protein 2, actin cytoplasmic 1, ras-related protein R-Ras2 and tyrosine-protein phosphatase non-receptor type 11. However, some of the pathways, like RAN signalling, do not share any proteins with other presented pathways.

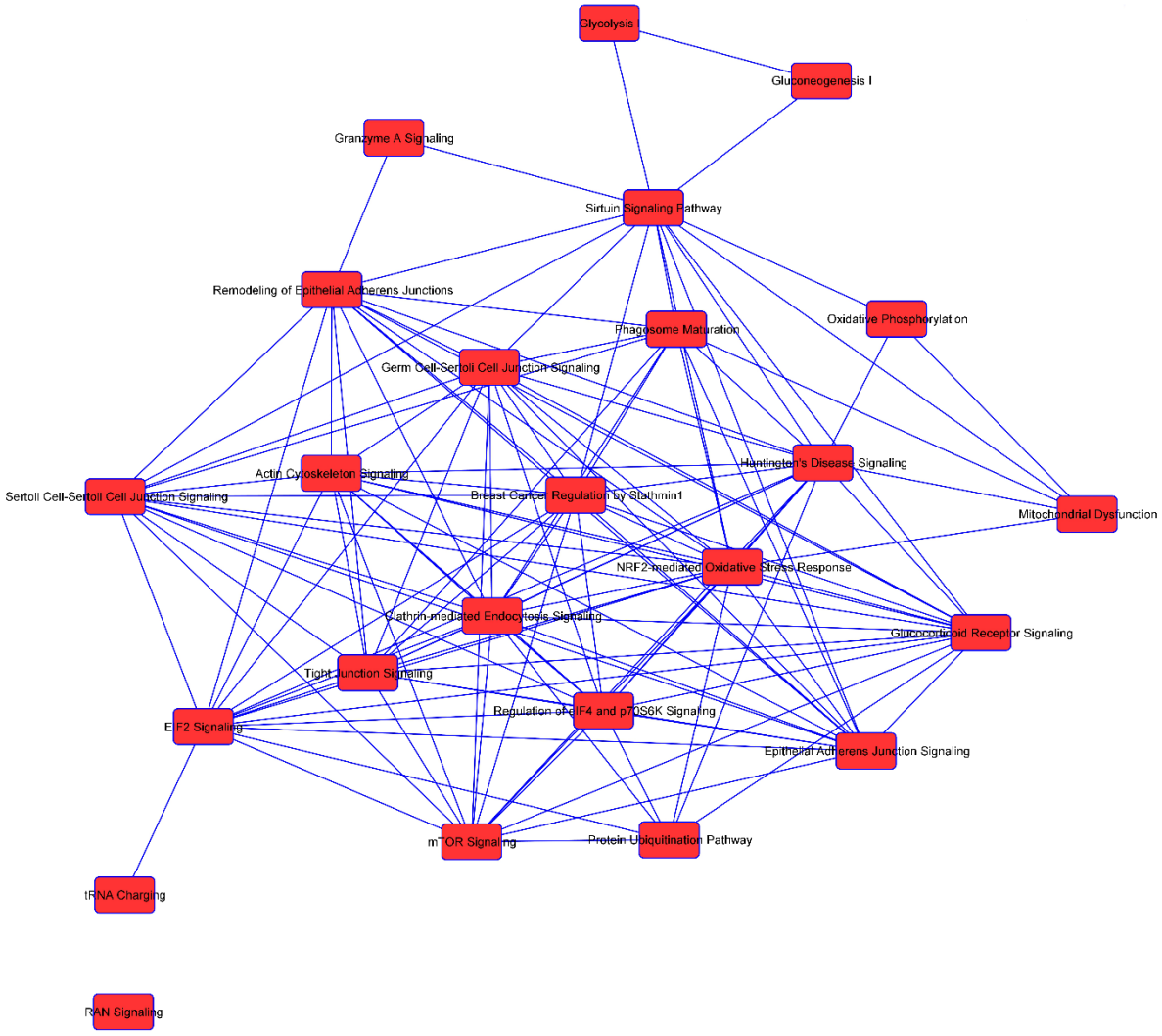

Figure 3.21 **Overlapping Canonical Pathways generated by IPA.**

Map of connections between most significant canonical pathways. The connections between canonical pathways (red boxes) are represented by blue lines, which indicate that at least one protein from the full dataset (i.e. 1498 proteins) is shared between pathways.

3.4.5.2 Functions

Proteins from the dataset were analysed in the context of functions that they are involved in. The analysis was performed to identify functions that have the strongest association with proteins from the dataset (i.e. 1498 proteins). Functions that appear to be most significantly affected by the proteins within the dataset are associated with post-transcriptional modification, cell death and survival, organismal survival, as well as functions connected to protein expression, for example, 'protein synthesis' and 'protein folding'. In general, there is a trend for functions with a low p-value to have a role in either transcription, translation or cell survival (Figure 3.22).

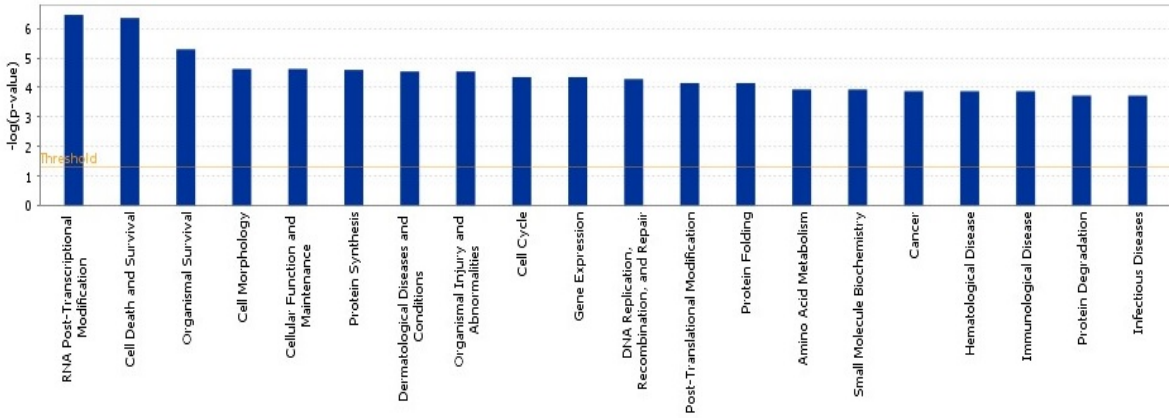

Figure 3.22 **The most significant functions associated with proteins detected in hESCs cultured at either 5% or 20% oxygen.**

Analysis based on 1498 proteins. IPA generated a long list of Functions affected by the proteins from the dataset and due to the clarity of the figure, only first 20 are displayed. The most significant functions are displayed on the left and less significant on the right. The threshold was set as p-value ≤ 0.05

Proteins from the dataset involved in 'Cell Death and Survival' were investigated further and two proteins were identified, PARP-1 (encoded by *PARP1*) and caveolin-1 (encoded by *CAV1*), that were common to each subsection of this function, such as apoptosis, cell death, necrosis, cell viability, cell survival (Table 3.4). The expression of both proteins, PARP-1 and caveolin-1, was found to be significantly increased in hESCs cultured at 5% oxygen compared to 20% oxygen, based on mass spectrometry results. Therefore, PARP-1 and caveolin-1 were further investigated as proteins of interest.

Table 3.4 **List of genes involved in 'cell death and survival' as identified by IPA.**

Genes encoding PARP-1 and caveolin-1 are highlighted with yellow.

Function	Gene names
Cell Death and Survival	ABCE1,ACO2,ADH5,ADRM1,AHSA1,AIFM1,AIMP1,AIMP2,AKAP12,AKR1B1,ANXA2,ANXA5,AP2M1,APEX1,API5,APOE,APP,ARHGDIA,ARID3B,ASNS,ATP1A1,ATP2A1,ATP2A2,ATP5A1,BAX,BCAP31,BCAS2,BCLAF1,BSG,BUB3,CALR,CAPNS1,CASP3,CAV1,CBR1,CBX5,CCAR2,CCDC6,CCT2,CCT4,CDC37,CDC42,CDK1,CDK2,CHMP5,CHTOP,CLTC,CNN2,CNPY2,COPZ1,COX5A,COX6B1,CRABP2,CS,CSE1L,CSNK2A1,CSNK2A2,CTNNA2,CTNNB1,CTNND1,CTSD,CTTN,CYB5A,CYCS,DCTN1,DDX3X,DEK,DFFA,DHX9,DIABLO,DNAJB1,DNM1L,DNM2,DNMT1,DSG2,DUT,EEF1A1,EEF2,EIF1AX,EIF2A,EIF2S1,EIF3G,EIF3M,EIF4B,EIF4E,EIF4G2,EIF5A,ELAVL1,ELOC,ENO1,EWSR1,EZR,FAU,FDFT1,FEN1,FKBP5,FKBP8,FUBP1,G6PD,GAPDH,GLO1,GLS,GNAS,GPI,GPX1,GPX4,GSTP1,H2AFX,HAT1,HDAC1,HDAC2,HK1,HK2,HMGA1,HMGCS1,HNRNPA1,HNRNPC,HNRNPH1,HNRNPK,HSP90AB1,HSPA4,HSPA5,HSPA8,HSPA9,HSPB1,HSPD1,IDE,IGF2BP1,IGF2BP2,ILF2,IMMT,ITGB1,JUP,KHDRBS1,KIF11,KPNA2,KPNB1,KRT18,LETM1,LGALS1,LMNA,LMNB1,LONP1,MAT2A,MCM7,MIF,MRPL49,MSH2,MSN,MYBBP1A,NAMPT,NAPA,NASP,NAT10,NCL,NME1,NPM1,NQO1,NUP93,OCLN,OTUB1,P4HB,PA2G4,PAK1,PAK2,PARK7,PARP1,PAWR,PCBP2,PCK2,PCNA,PDCD6IP,PDHA1,PDK1,PEA15,PEBP1,PGAM5,PGRMC1,PHB,PHB2,PHGDH,PKM,POU5F1,PPAT,PPIA,PPID,PPP1CA,PPP2CA,PPP2R1A,PPP2R2A,PPP5C,PPT1,PRDX1,PRDX2,PRMT1,PRMT5,PRPF19,PRPS1,PSIP1,PSMD14,PSMD2,PSMD7,PTMA,PTPN11,PTRH2,PUF60,RAB35,RAC1,RACK1,RAD23B,RBM17,RDX,RHOA,RPA1,RPAP3,RPL27A,RPL34,RPLP0,RPS19,RPS24,RRM1,RRM2,RRP1B,RTN4,S100A11,SAE1,SALL2,SALL4,SAR1A,SF3A1,SF3B3,SFPQ,SLC25A5,SLC25A6,SLC3A2,SMARCD1,SMARCE1,SMC1A,SND1,SOD1,SRI,SRSF1,SRSF2,SSB,SSRP1,STAT1,STAT3,STK26,STMN1,STOML2,SUMO1,TACC3,TAGLN2,TCP1,TFRC,THY1,TMED10,TMSB10/TMSB4X,TNPO2,TOP1,TOP2A,TOP2B,TP53BP1,TPD52,TPT1,TRAP1,TRIAP1,TRIM28,TUBA1A,TUBB3,TUBB6,TUFM,TXN,TXNRD1,TYMS,UBA2,UBA3,UBE2I,UBE2K,UBE2L3,UBE2S,UBE2V1,UBQLN1,UBTF,UCHL1,UCHL5,USP10,VCP,VDAC1,VDAC2,VSNL1,XPO1,XRCC5,XRCC6,YARS,YBX1,YWHAE,YWHAG,YWHAH,YWHAZ

3.4.6 Poly [ADP-ribose] polymerase 1 (PARP-1)

The relationship between PARP-1 and the other 128 proteins differentially expressed in hESCs cultured at both 20% and 5% oxygen as well as proteins that were predicted to interact with PARP-1 was investigated using IPA and STRING (Szklarczyk *et al.*, 2019), a tool that helps to detect known and predicted interaction between proteins. The analysis showed multiple interactions between PARP-1 and other proteins, including a number of proteins provided for the analysis (Figure 3.23). The analysis revealed a direct relationship between PARP-1 and OCT4, suggesting PARP-1 may be involved in the regulation of hESC self-renewal (Figure 3.23).

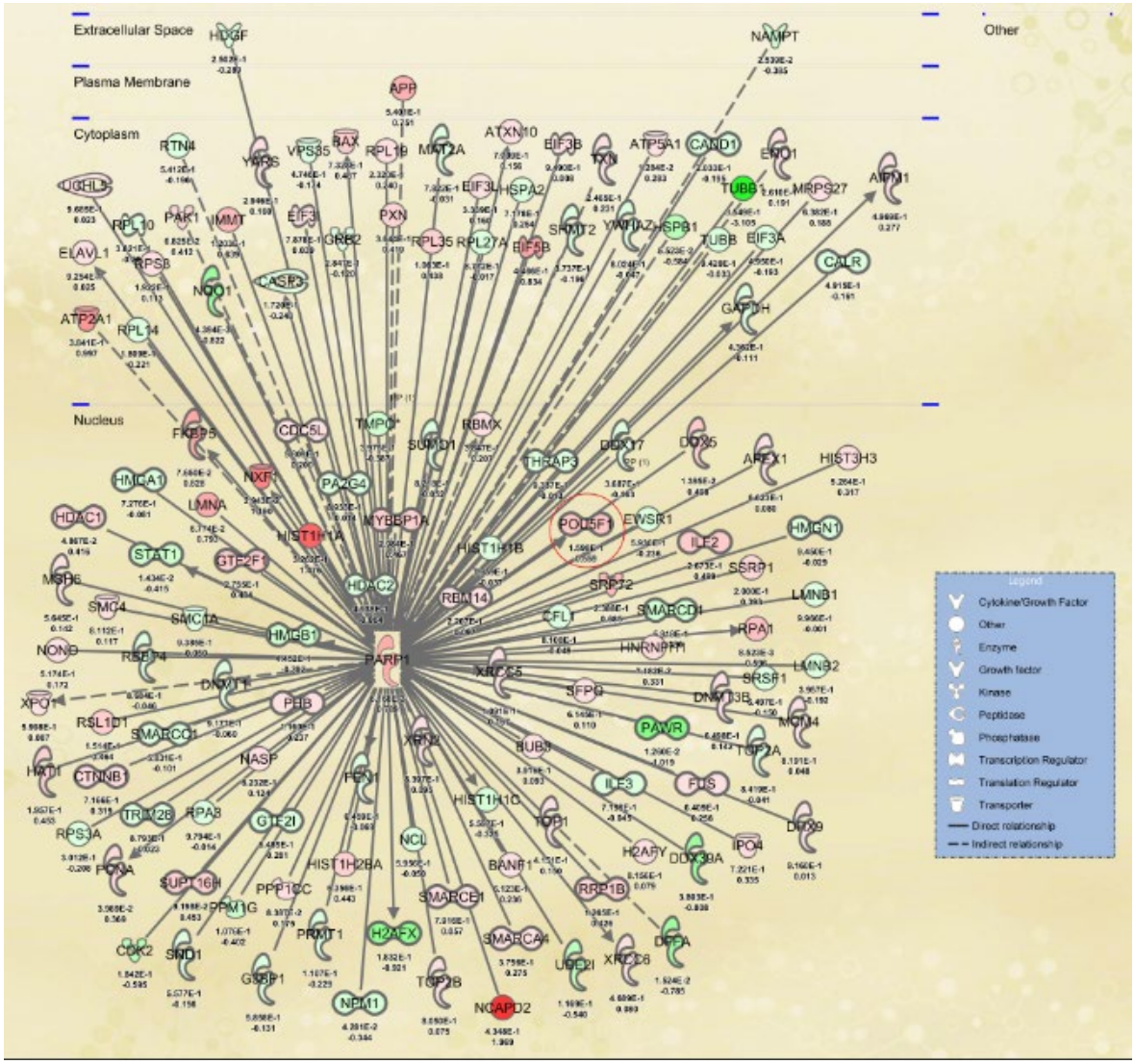

Figure 3.23 **Representation of relationships between PARP-1 and other proteins that were either differentially expressed in hESCs cultured at either 5% or 20% oxygen or are predicted to interact with PARP-1.**

IPA analysis of the relationship between PARP-1 and proteins that were found to be significantly different in expression in hESCs cultured at either 5% or 20% oxygen or are predicted to interact with PARP-1 but were not identified within provided dataset. PARP-1 is placed in the centre. Filling colour of the protein symbol corresponds to whether the protein is or is predicted to be upregulated (red) in hESCs cultured at 5% oxygen compared to those maintained at 20% oxygen, or is downregulated or predicted to be downregulated (green). The more intense the colour, the more upregulated/downregulated is the protein. OCT4 (POU5F1) is highlighted with a red circle.

STRING analysis was also used to provide information about the relationship between PARP-1 and other proteins found to be significantly altered by the environmental oxygen in hESCs. PARP-1 was found to form a group that interacts highly with each other. Proteins within that group, ubiquitin carboxyl-terminal hydrolase 10 (USP10), proliferating cell nuclear antigen (PCNA), replication protein A 70 kDa DNA-binding subunit (RPA1), are mainly associated with response to DNA damage and DNA replication, which is crucial for cell proliferation (Figure 3.24)

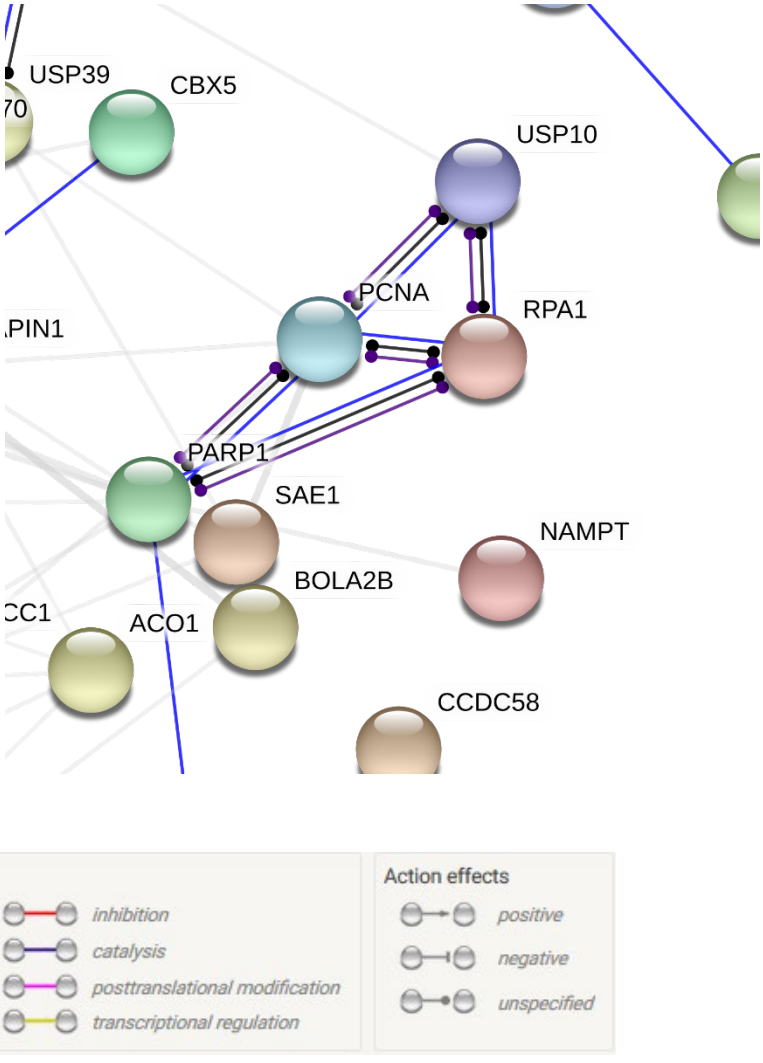

Figure 3.24 **PARP-1 interacts with other differentially expressed proteins responsible for DNA damage control and proliferation in hESCs cultured at 5% or 20% oxygen.**

Fragment of STRING analysis showing a cluster of protein interactions involving PARP-1 protein.

3.4.7 Effect of oxygen tension on the expression of PARP-1 protein in hESCs

Analysis of mass spectrometry results showed that PARP-1 was significantly upregulated (p-value= 0.006) in hESCs cultured in hypoxia compared to cells maintained under normoxic conditions. Immunocytochemistry was used to visualise the localisation of PARP-1 in hESCs cultured at either 5% or 20% oxygen. PARP-1 was expressed in the nucleus of the cells as indicated by the presence of FITC labelling merged with DAPI (Figure 3.25).

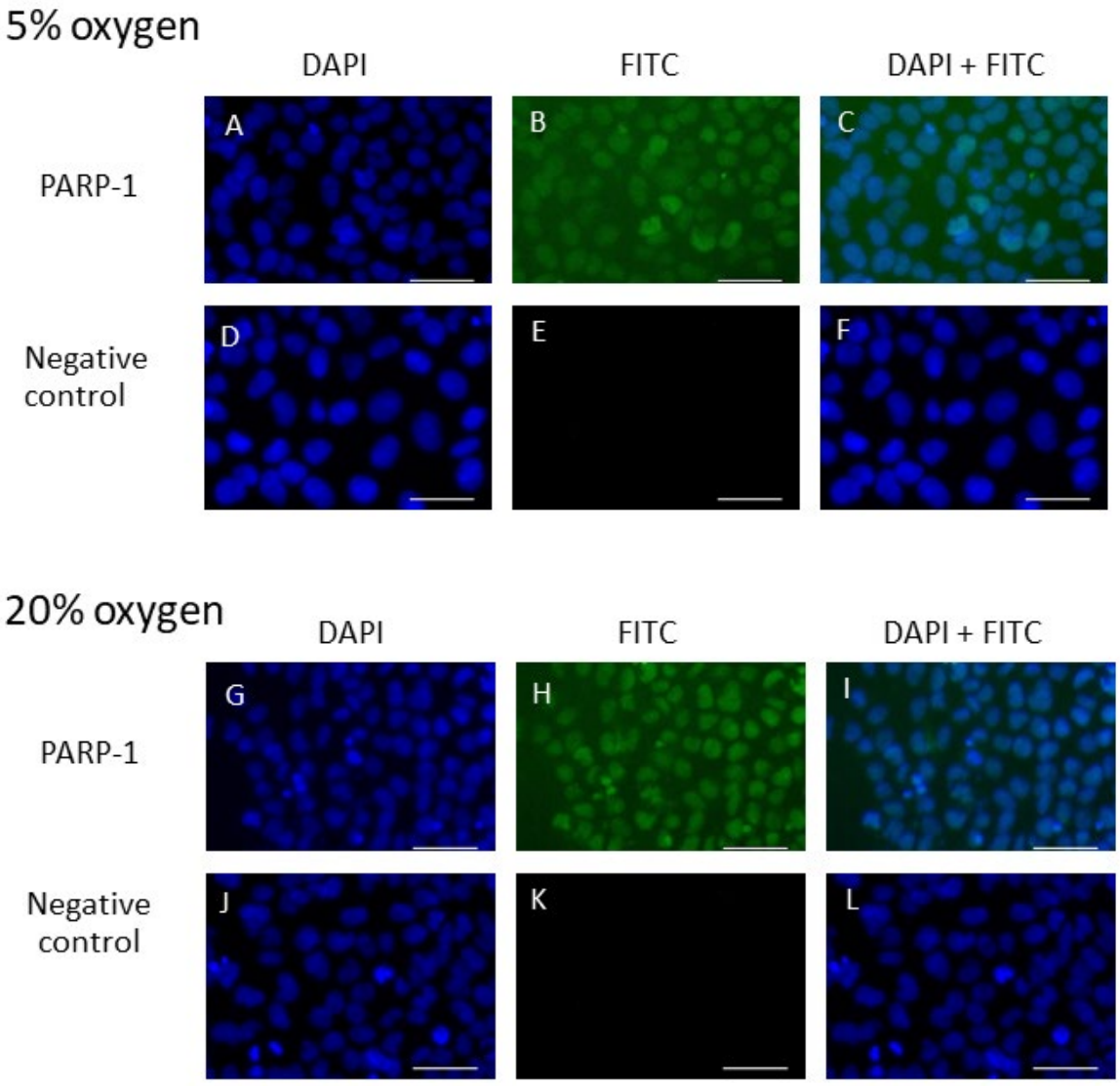

Figure 3.25 **hESCs cultured at either 5% or 20% oxygen express PARP-1 in the nucleus.**

Representative images of protein expression of PARP-1 (A-C and G-I) in hESCs cultured at either 5% or 20% oxygen. DAPI was used to visualise nuclei (blue; A, D, G, J) and FITC for localisation of the protein of interest (green; B, H). For negative control, only FITC conjugated secondary antibodies were added (D-F and J-L). Scale bars indicate 50 µm.

To validate the mass spectrometry result, Western blotting was used to quantify PARP-1 expression in hESCs cultured at either 5% or 20% oxygen. Using immunoblotting, PARP-1 was detected by the presence of a band at the size of 116 kDa. When PARP-1 was quantified relative to β-actin, there was a significant (p-value=0.024), around 40%, reduction in expression in hESCs maintained at 20% oxygen compared to those cultured at 5% oxygen (Figure 3.26).

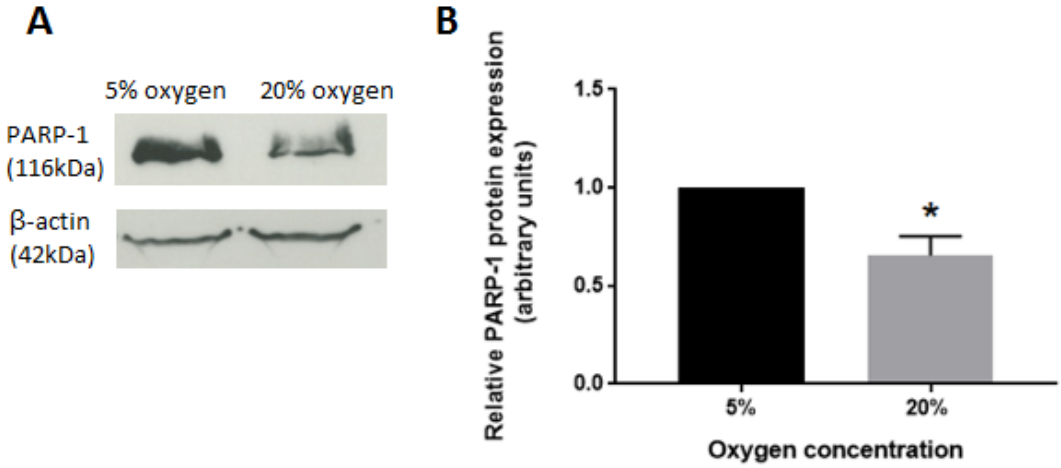

Figure 3.26 **Hypoxia promotes the protein expression of PARP-1 in hESCs.**

(A) Representative Western blot of PARP-1 and β-actin in hESCs cultured at either 5% or 20% oxygen. (B) Quantification of PARP-1 Western blot. Data were normalized to β-actin and to 1 for 5% oxygen. Bars represent mean + SEM. *p<0.05 significantly different between 5% and 20% oxygen. n=3.

3.4.8 Effect of silencing HIF2α on the expression of PARP-1 in hESCs cultured at 5% oxygen

HIF2α is a transcription factor known to regulate the expression of various genes in hypoxic conditions. To determine whether HIF2α might be responsible for the increased level of PARP-1 in hESCs cultured at 5% oxygen, siRNA was used to silence the expression of HIF2α. hESCs were cultured at 5% oxygen and transfected with HIF2α siRNA, or a negative control siRNA (AllStars) on the day after passaging. Silencing HIF2α did not affect hESC cell morphology (Figure 3.27 A). The protein lysate was collected 48 hours later and PARP-1 expression quantified using Western blotting. Expression of HIF2α was recognised by the presence of a single band at the size of approximately 118 kDa (Figure 3.27 B). When HIF2α was silenced there was an approximate 40% reduction in HIF2α expression compared to the AllStars negative control (Figure 3.27 C). However, silencing HIF2α did not affect the expression of PARP-1 compared to the AllStars negative control (Figure 3.28) in hESCs cultured at 5% oxygen.

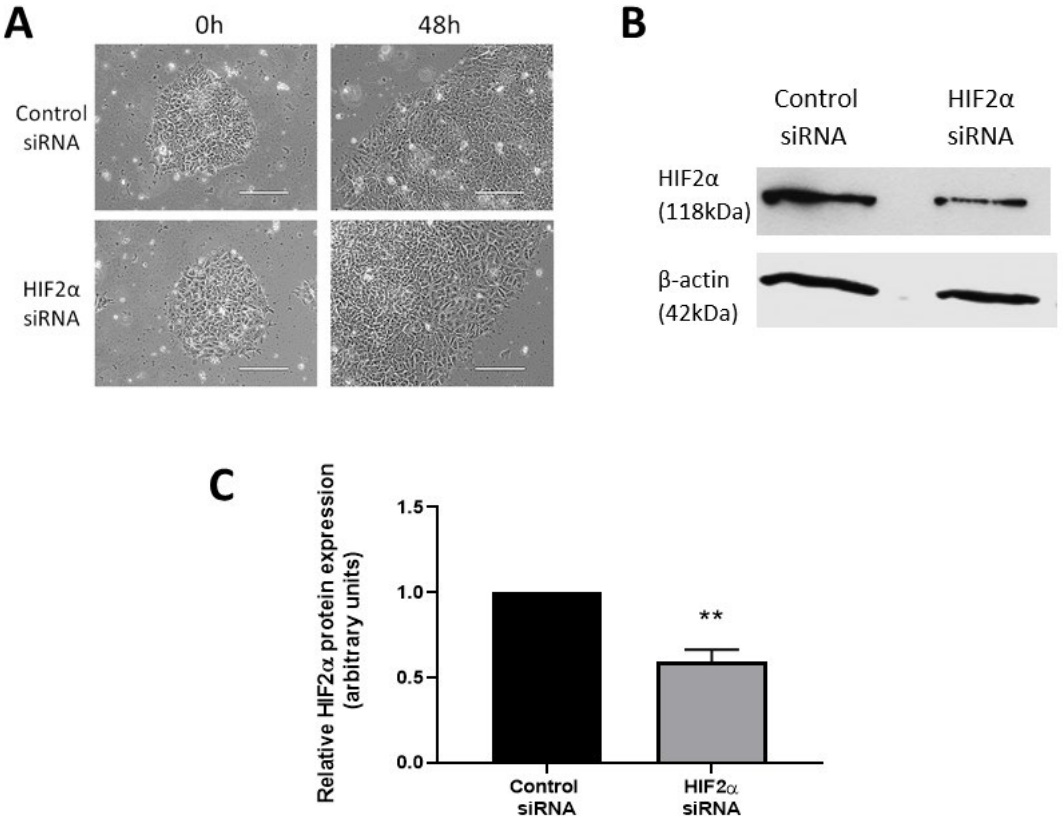

Figure 3.27 **HIF2α expression was silenced following transfection with HIF2α siRNA.**

(A) Phase contrast images of hESCs morphology cultured at 5% oxygen before and after transfection for 48 hours with either AllStars negative control siRNA or HIF2α siRNA. Scale bar indicates 200 µm. (B) Representative Western blot of HIF2α and β-actin expression in hESCs cultured at 5% oxygen and transfected with either HIF2α siRNA or AllStars negative control siRNA. (C) Quantification of HIF2α protein expression. Data were normalized to β-actin and to 1 for control siRNA. Bars represent mean + SEM. **P<0.01 significantly different between the expression level of HIF2α and AllStars negative control. n=3

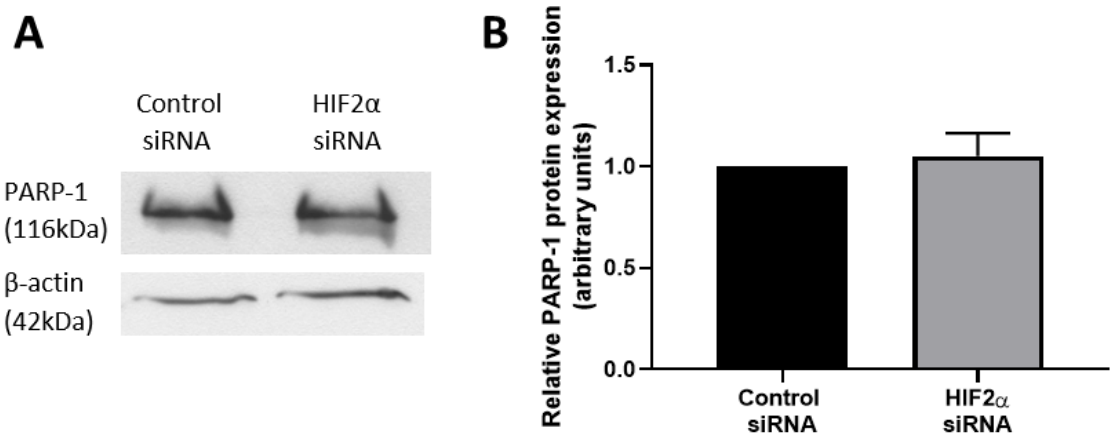

Figure 3.28 **Silencing HIF2α does not affect the expression of PARP-1 in hESCs cultured at 5% oxygen.**

(A) Representative Western blot of PARP-1 and β-actin expression in hESCs cultured at 5% oxygen and transfected with either HIF2α siRNA or AllStars siRNA negative control. (B) Quantification of PARP-1 protein expression in hESCs where HIF2α has been silenced. Data were normalized to β-actin and to 1 for control siRNA. Bars represent mean + SEM. n=3

3.4.9 Effect of silencing PARP-1 on the expression of pluripotency markers in hESCs cultured at 5% oxygen

The role of PARP-1 in regulating the expression of key pluripotency markers in hESCs cultured at 5% oxygen was investigated by transfecting cells with either PARP-1 siRNA or AllStars negative control siRNA. Silencing PARP-1 did not affect hESC cell morphology (Figure 3.29 A). The expression level of PARP-1 was quantified using Western blotting. When PARP-1 expression was silenced, there was around 50% reduction in PARP-1 protein level ($p<0.001$) compared to AllStars siRNA negative control (Figure 3.29 C).

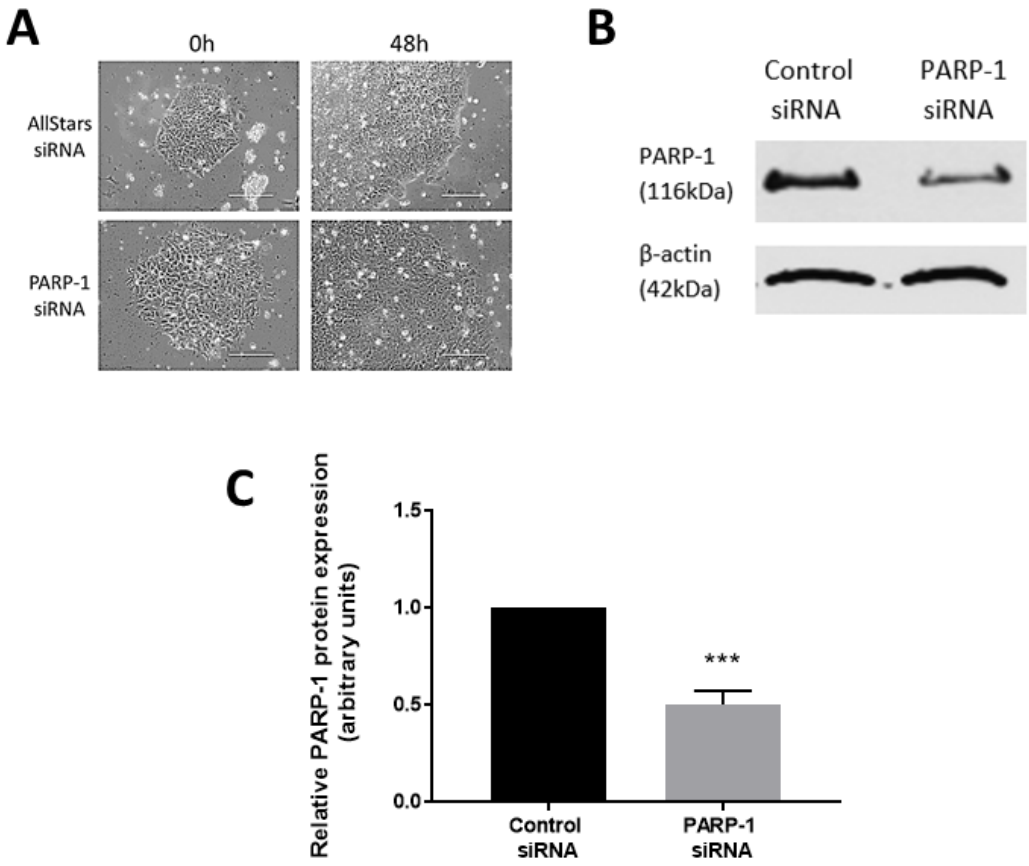

Figure 3.29 **PARP-1 expression was silenced following transfection with PARP-1 siRNA.**

(A) Phase contrast images of hESCs morphology cultured at 5% oxygen before and after transfection for 48 hours with either AllStars negative control siRNA or PARP-1 siRNA. Scale bar indicates 200 µm. (B) Representative Western blot of PARP-1 and β-actin expression in hESCs cultured at 5% oxygen transfected with either PARP-1 siRNA or AllStars negative control siRNA. (C) Quantification of PARP-1 protein expression. Data were normalized to β-actin and to 1 for control siRNA. Bars represent mean + SEM. ***P<0.001 significantly different between the expression level of PARP-1 and AllStars negative control. n=7

To determine whether PARP-1 is involved in the regulation of hESC self-renewal, the expression of OCT4, SOX2 and NANOG protein expression was quantified in hESCs where PARP-1 has been silenced. There was no significant difference in the expression of OCT4, SOX2 or NANOG in hESCs cultured at 5% oxygen and transfected with PARP-1 siRNA compared to the Allstars negative control siRNA. (Figure 3.30).

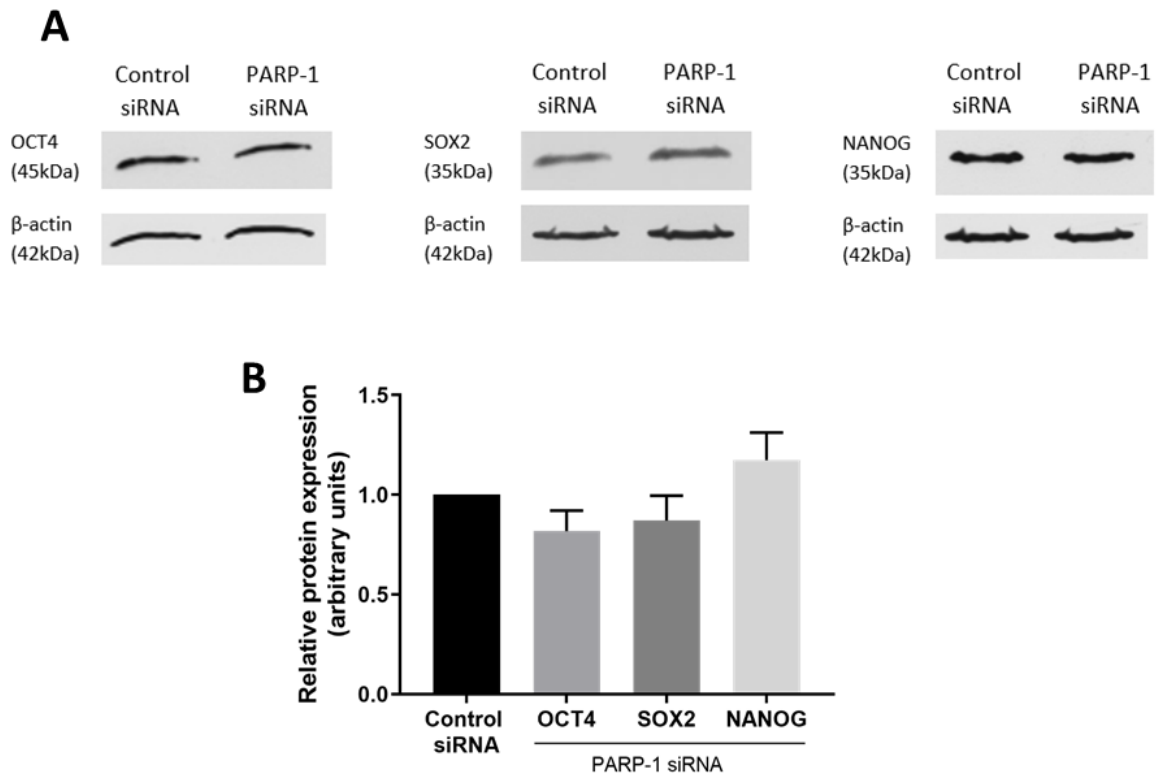

Figure 3.30 **Silencing PARP-1 does not affect OCT4, SOX2 or NANOG expression in hESCs cultured at 5% oxygen.**

(A) Representative Western blot of OCT4, NANOG, SOX2 and β-actin expression in hESCs cultured at 5% oxygen transfected with either PARP-1 siRNA or AllStars siRNA negative control. (B) Quantification of OCT4, SOX2 and NANOG protein expression in hESCs where PARP-1 has been silenced. Data were normalized to β-actin and to 1 for control siRNA. Bars represent mean + SEM. n=3-6

3.4.10 Effect of oxygen tension on the expression level of caveolin-1 in hESCs

The mass spectrometry data showed that caveolin-1 was one of the significantly upregulated proteins (p-value= 0.041) in hESCs cultured in hypoxia compared to cells maintained under normoxic conditions. Immunocytochemistry was used to visualise the localisation of caveolin-1 in hESCs cultured at either 5% or 20% oxygen. Caveolin-1 was found to be located in the plasma membrane (Figure 3.31) as also observed by Abulrob *et al.* (2004) and it was indicated by the presence of Alexa Fluor 488 labelling not merged with DAPI.

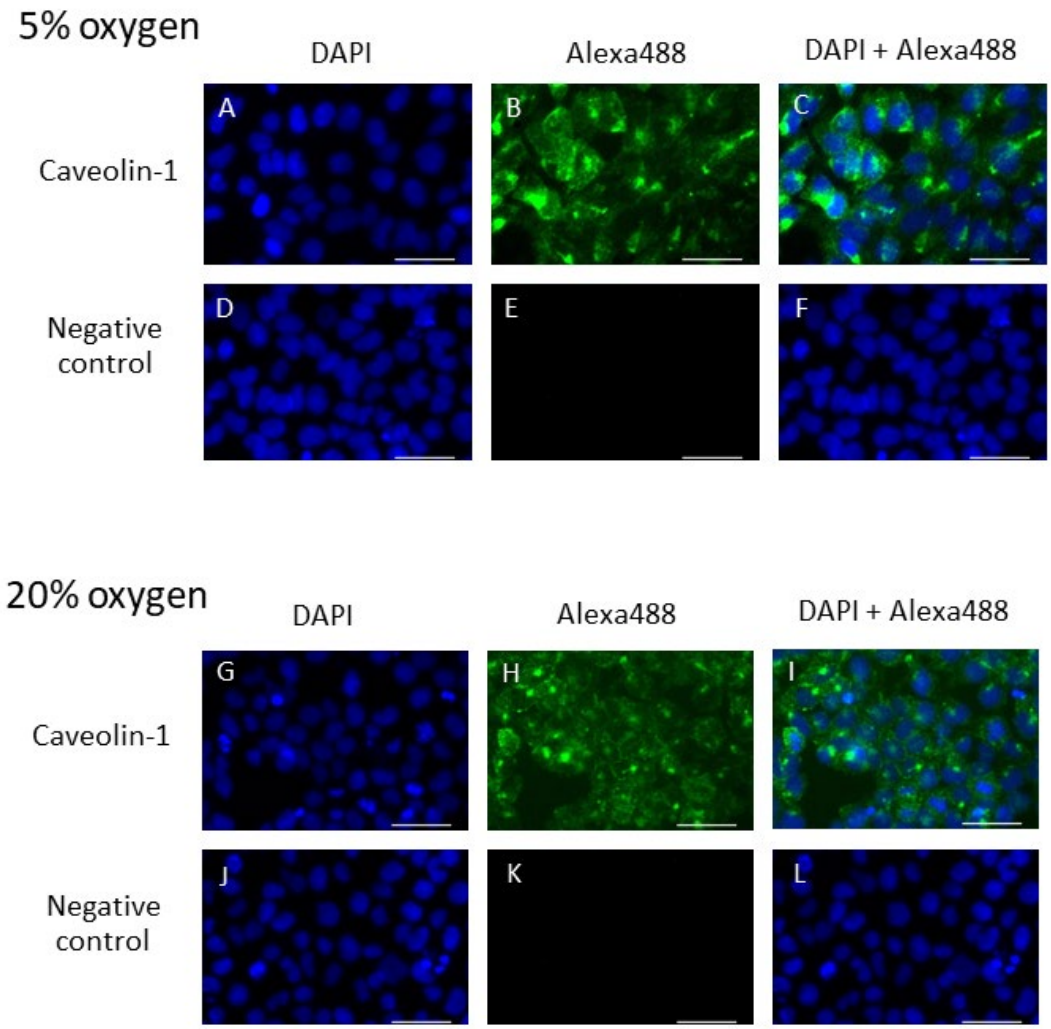

Figure 3.31 **hESCs cultured at either 5% or 20% oxygen express caveolin-1.**

Representative images of protein expression of caveolin-1 (A-C and G-I) in hESCs cultured at either 5% or 20% oxygen. DAPI was used to visualise nuclei (blue; A, D, G, J) and Alexa488 for localisation of the protein of interest (green; B, H). For negative control, only Alexa488 conjugated secondary antibodies were added (D-F and J-L). Scale bars indicate 50 µm.

To validate the mass spectrometry result, Western blotting was used to quantify caveolin-1 protein expression in hESCs cultured at either 5% or 20% oxygen. Caveolin-1 was detected by the presence of a band at an approximate size of 22kDa. When caveolin-1 was quantified relative to β-actin, there was a significant ($p= 0.012$), around 43%, reduction in expression in hESCs maintained at 20% oxygen compared to those cultured at 5% oxygen (Figure 3.32).

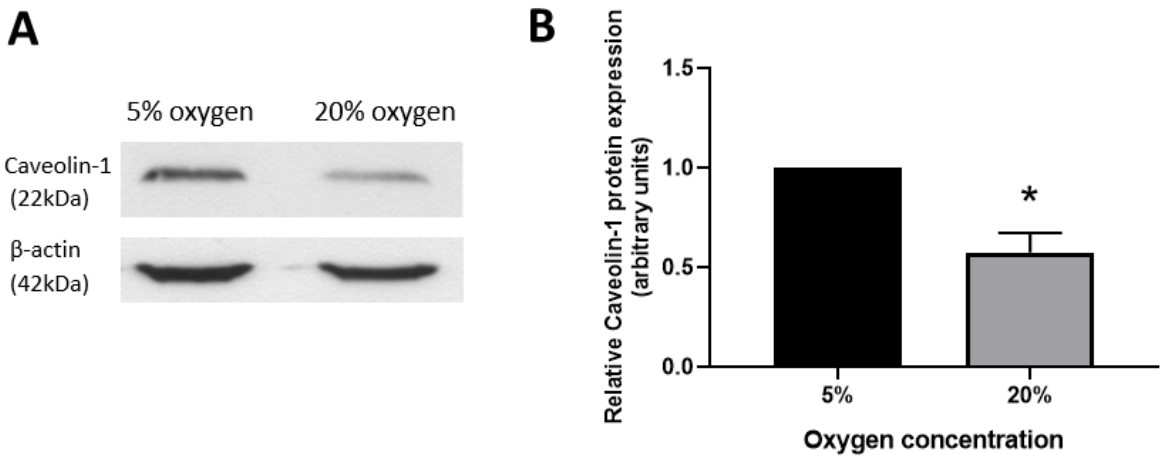

Figure 3.32 **Oxygen tension affects the expression of caveolin-1 in hESCs.**

(A) Representative Western blot of caveolin-1 and β-actin in hESCs cultured at either 5% or 20% oxygen. (B) Quantification of caveolin-1 protein expression in hESCs cultured at either 5% or 20% oxygen. Data were normalized to β-actin and to 1 for 5%. Bars represent mean + SEM. *p<0.05 significantly different between 5% and 20% oxygen. n=3

3.4.11 Effect of silencing HIF2α on the expression of caveolin-1 in hESCs cultured at 5% oxygen

Caveolin-1 expression was found to be significantly increased in hESCs cultured under hypoxic conditions compared to cells maintained under normoxia. It was investigated whether HIF2α is involved in regulating the expression of caveolin-1 in hESCs cultured at 5% oxygen. HIF2α expression was silenced in hESCs cultured in hypoxia and expression of caveolin-1 was quantified using Western blotting. The analysis revealed that when HIF2α was silenced (Figure 3.27) expression of caveolin-1 was not affected, compared to AllStars negative control siRNA (Figure 3.33).

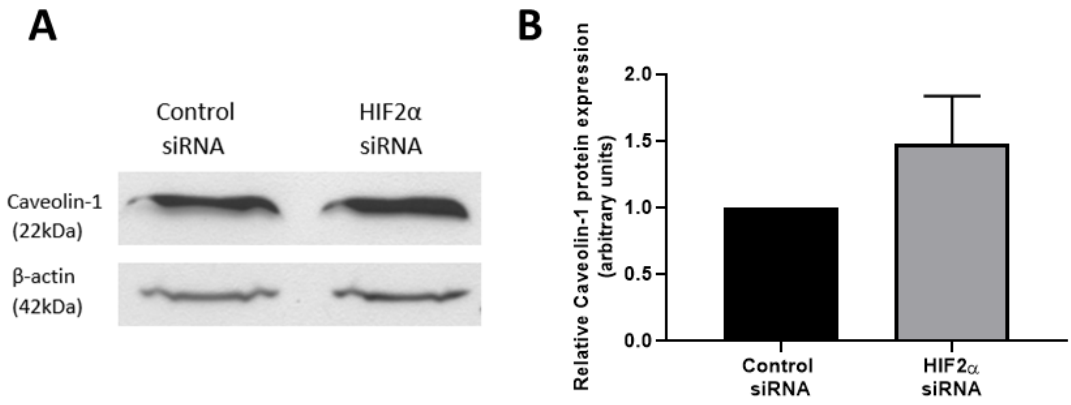

Figure 3.33 **Silencing HIF2α does not affect the expression of caveolin-1 in hESCs cultured at 5% oxygen.**

(A) Representative Western blot of caveolin-1 and β-actin expression in hESCs cultured at 5% oxygen transfected with either HIF2α siRNA or AllStars siRNA negative control. (B) Quantification of caveolin-1 protein expression in hESCs where HIF2α has been silenced. Data were normalized to β-actin and to 1 for control siRNA. Bars represent mean + SEM. n=3

3.5 Discussion

There are several hESC lines established and even though all cell lines are pluripotent and self-renew, there are differences between them, for example, genetic stability in long-term culture (Allegrucci and Young, 2007). The morphology of these cells is similar; they grow in flattened colonies, have a large nuclear to cytoplasmic ratio and a small number of immature mitochondria (Thomson *et al.*, 1998). The true pluripotent state can be only proven by injection of cells into immunocompromised mice where pluripotent cells would form teratomas that have derivatives of all three germ layers (Thomson *et al.*, 1998). Such an experiment with the use of an animal model was not performed during this project. However, self-renewal abilities of hESCs can be characterised by the expression of pluripotency markers, such as OCT4, SOX2, NANOG, TRA-1-60 or SSEA-4. In agreement with Thomson et al. (1998), Hues7 hESCs used in this project expressed OCT4, SOX2, NANOG and TRA-1-60 and did not show expression of SSEA-1, an early marker of cell differentiation, therefore confirming the undifferentiated state of the cells (Figure 3.1 - Figure 3.8). Although hypoxia has been shown to be beneficial for the culture of hESCs, in agreement with Forristal et al. (2010), no obvious difference in expression of pluripotency markers was observed using immunocytochemistry between hESCs maintained at 20% oxygen and those

cultured at 5% oxygen. However, Western blot results revealed that expression of OCT4, SOX2 and NANOG was significantly increased in hESCs cultured at 5% oxygen, compared to normoxic culture. This corroborates the findings of Forristal *et al.* (2013) of the increased expression level of OCT4, SOX2 and NANOG in hESCs cultured in hypoxic culture conditions compared to those maintained at 20% oxygen. The high expression level of OCT4 is necessary for the maintenance of pluripotency in undifferentiated cells and is involved in (co)activation of pluripotency genes, such as SOX2 (Chew *et al.*, 2005), and inhibition of genes involved in differentiation processes, for example, Caudal Type Homeobox 2 (Cdx2), which is involved in trophectoderm differentiation (Niwa *et al.*, 2005). These data demonstrate that low oxygen tension is beneficial for the culture of hESCs by improving self-renewal compared to cells maintained at 20% oxygen.

Mass spectrometry is a powerful technique that provides qualitative and quantitative analytical data. In this study, the number of proteins expressed in hESCs was identified and quantified. However, even though mass spectrometry is extremely sensitive and specific, it is not possible to detect the whole proteome of the cell due to differences in protein solubilisation, protein digest, peptide selection by mass spectrometry, protein abundance or database matching (Bell *et al.*, 2009). Thus, some proteins that are known to be expressed in hESCs, such as SOX2 or NANOG, were not detected. For the same reasons, there are missing values in the dataset, i.e. some proteins were not consistently detected in all three replicates per condition. Proteins with more than two missing values per condition were excluded from downstream analyses.

Gene ontology analysis was performed on the whole dataset (all proteins identified with mass spectrometry) to establish which cellular components, protein classes or biological processes are overrepresented across the samples. The majority of identified proteins were localised within the cytosol and only a small percentage of proteins (7%) were found to be nuclear. This is probably due to the sensitivity of mass spectrometry and the abundance of nuclear proteins (Bell *et al.*, 2009). It would be possible to identify a higher number of proteins localised in the nucleus by performing mass spectrometry on isolated nuclear fractions (Barthelery *et al.*, 2009). However, this approach would not provide information about the whole proteome which was the aim of this research. Interestingly, the second largest protein localisation GO term consisted of proteins classified as part of 'extracellular exosome'. The extracellular exosome is defined in gene ontology terms as 'a vesicle that is released into the extracellular region by fusion of the limiting endosomal membrane of a multivesicular body with the plasma membrane' (GO:0070062). Proteins associated with that term and identified by mass spectrometry in the current work were keratins (for example Keratin type I cytoskeletal 18, Keratin 2 or Keratin 19), actinins (actinin alpha 2 or actinin alpha 3) as well as proteins involved in processes such as cell-cell junction assembly (for example Fascin), or proliferation (DnaJ homolog subfamily A member 2). Extracellular vesicles (EV)

are important for a cell population, containing proteins, lipids or mRNA and are probably involved in signalling and cell to cell interactions (Valadi *et al.*, 2007). To better understand the role of EV, a study by Liu *et al.* (2019) examined the effect of EV produced by iPSCs on senescent MSCs. The results showed that delivery of EV produced by iPSCs to MSCs reduced ageing of the latter cell type, which was associated with a decrease in the level of γ-H2AX, known as a marker for cellular senescence (Liu *et al.*, 2019). ROS production was also decreased and cell growth was found to be increased (Liu *et al.*, 2019). These observations highlight the importance of EV for stem cell population; hESCs are known as highly proliferative cells with self-renewal abilities and EV might play an important role in maintaining the homogenous pluripotent population.

GO analysis revealed that proteins, which expression was significantly altered, belonged to various classes but the majority of them are involved in protein synthesis. However, there is not enough evidence to claim that protein synthesis is affected by environmental oxygen in hESCs. Moreover, there was no significant enrichment in GO terms of molecular processes connected to protein synthesis showing that this process is not affected by the proteins up- or downregulated in hESCs cultured at 5% oxygen.

Hypoxic culture of stem cell is believed to be beneficial for reducing ROS levels due to cell metabolism that relies more on glycolysis than oxidative phosphorylation (ROS is a by-product of oxidative phosphorylation) (Mohyeldin *et al.*, 2010). Upon differentiation, hESCs rely more on aerobic metabolism rather than glycolysis, which is coupled with an increase in ROS generation (Cho *et al.*, 2006). The differentiation process of hESCs was also found to be enhanced in cells with induced ROS production, as indicated by downregulation of OCT4, SOX2, NANOG and upregulation of lineage-specific markers, such as Sox17, HNF3β (endoderm) or brachyury (mesoderm) (Ji *et al.*, 2010; Nugud *et al.*, 2018). In the current work, analysis of enriched GO processes revealed that proteins downregulated in hESCs cultured under hypoxic conditions are mostly associated with ROS. This suggests that low oxygen culture of hESCs is favourable for maintaining low levels of ROS and therefore the undifferentiated state. 'Cellular response to oxygen levels' and 'regulation of autophagy' GO terms were the most enriched in proteins upregulated in hESCs cultured under hypoxia. This is in agreement with expected results, as cells need to trigger appropriate responses to low oxygen levels to maintain homeostasis, such as enhanced autophagy to remove protein aggregates or defective organelles. Decreased autophagy was shown to be a signal of the differentiation of hematopoietic stem cells (Guan *et al.*, 2013). However, hypoxia is known to induce autophagy in cancer cells as well as in mesenchymal stem cells (Lee *et al.*, 2013; Tan *et al.*, 2016; Daskalaki *et al.*, 2018; Sotthibundhu *et al.*, 2018; Wobma *et al.*, 2018). Moreover, autophagy was found to be intrinsic for hESC self-renewal as it is responsible for the degradation of OCT4, SOX2 and NANOG to maintain the appropriate protein level

necessary for undifferentiated state (Cho *et al.*, 2014). A study by Cho *et al.* (2014) also observed that inhibition of autophagy caused downregulation of stem cell surface markers TRA1–60, TRA1–81 and SSEA-4. Therefore, enhanced autophagy regulation in hESCs cultured at 5% oxygen might suggest that in hypoxic conditions there is an improved mechanism for maintaining self-renewal and eliminating differentiated cells.

It was expected that proteins involved in glycolysis would be upregulated in hESCs cultured in hypoxia, which rely more on glycolysis than on oxidative phosphorylation, in comparison to cells maintained under atmospheric oxygen level (Forristal *et al.*, 2013). Phosphoglycerate kinase 1 was identified as upregulated in hESCs cultured at 5% oxygen. However, it was surprising that the significant scores list does not include other proteins known to have increased expression in hESCs cultured in hypoxic conditions. Such an example is OCT4, which is known to have an increased expression level in hESCs cultured at 5% oxygen compared to 20% oxygen (Forristal *et al.*, 2013). A probable explanation might involve the abundance of OCT4 and the sensitivity of the mass spectrometry technique.

PARP-1 was one of the identified proteins that was differentially expressed between hESCs cultured at either 5% or 20% oxygen. Proteins from the PARP family are best known for having a role in DNA repair (Pascal, 2018). However, they are involved in other processes, such as apoptosis and transcription (Ziegler and Oei, 2001; Gupte *et al.*, 2017; Rodríguez-Vargas *et al.*, 2019). PARP-1 was previously shown to be an important protein involved in the hypoxic response (Elser *et al.*, 2008; Gonzalez-Flores *et al.*, 2014). PARP-1 can form a complex with HIF1α or HIF2α in hypoxic condition and that complex regulates expression of target genes of HIF1α or HIF2α (Elser *et al.*, 2008; Gonzalez-Flores *et al.*, 2014). PARP-1 can also directly bind to the HIF2α promoter and thus regulate its expression (Gonzalez-Flores *et al.*, 2014). However, since protein expression of PARP-1 was significantly increased in hESCs cultured at 5% oxygen, it was investigated whether it could be due to HIF2α regulation. The results of this thesis showed that when the expression of HIF2α was silenced, there was no effect on the PARP-1 protein level. HIF2α is known to regulate expression of various genes in hypoxic conditions (Petruzzelli *et al.*, 2014) but PARP-1 is not one of them. The mechanism regulating the expression of PARP-1 in response to environmental oxygen could involve specificity protein 1 (Sp1). This transcription factor is known to regulate expression of PARP-1 in MEFs (Zaniolo *et al.*, 2007) but also there is emerging evidence suggesting that Sp1 might be involved in the hypoxic response (Koizume and Miyagi, 2015). To investigate whether increased expression of PARP-1 in hESCs cultured at 5% oxygen is due to Sp1 regulation it would be necessary to perform Sp1 siRNA experiment together with chromatin immunoprecipitation (ChIP).

PARP-1 was chosen as a possible target to study its regulatory role in pluripotency of hESCs. The IPA analysis of PARP-1 relationships showed predicted interaction with OCT4. Previous studies on mESCs also presented interactions of Parp-1 with Oct4 (Pardo *et al.*, 2010) and Sox2 (Gao *et al.*, 2009; Lai *et al.*, 2012). Parp-1 deficiency or inhibition in mESCs was found to be responsible for an increased rate of spontaneous differentiation, thus highlighting the role of Parp-1 in maintaining pluripotency (Roper *et al.*, 2014). Moreover, PARP-1 is involved in activation of telomerase expression and a high level of telomerase activity is known to play a role in maintaining self-renewal of hESCs (Hsieh *et al.*, 2017). However, the work undertaken in this thesis found that when the expression of PARP-1 was silenced, expression of OCT4, SOX2 and NANOG was unaffected, indicating that PARP-1 is not directly regulating self-renewal abilities in hypoxic hESCs.

Caveolin-1 was another protein identified by mass spectrometry which was found to be significantly increased in hESCs cultured at 5% oxygen compared to those maintained under atmospheric oxygen. Western blotting confirmed the results obtained through mass spectrometry. Caveolin-1 is mainly localised in the cell membrane and is known as a scaffolding protein for caveolae, which are flask-shaped structures within the cell membrane responsible for lipid trafficking and regulating cell signalling, for example, Wnt/beta-catenin/Lef-1 signalling by recruiting and binding beta-catenin (Galbiati *et al.*, 2000). Caveolin-1 was found to be an important factor in maintaining mESC renewal; when the caveolin-1 expression was silenced using siRNA, Oct4 expression was decreased and proliferation rate was significantly lower (Lee *et al.*, 2010b). There is also evidence that caveolin-1 has an inhibitory role in neuronal differentiation (Li *et al.*, 2011a; Li *et al.*, 2011b; Wang *et al.*, 2013). The increased expression of caveolin-1 observed in hESCs cultured in hypoxia compared to atmospheric oxygen might suggest a role for caveolin-1 in maintaining self-renewal. An elevated level of caveolin-1 was already observed in different types of cancer in low oxygen conditions (Mao *et al.*, 2016; Castillo Bennett *et al.*, 2018) and caveolin-1 was reported to be regulated by HIF1α and/or HIF2α (Wang *et al.*, 2012b; Castillo Bennett *et al.*, 2018). In hESCs, HIF1α is only present in the nucleus for approximately 48 hours following the introduction of cells to low oxygen tension. After this time, HIF2α was found to regulate the hypoxic response (Forristal *et al.*, 2010). Work presented in this chapter investigated whether the increased expression of caveolin-1 observed in hESCs cultured at 5% oxygen compared to 20% oxygen was regulated by HIF2α. When HIF2α expression was silenced in hESCs, the expression of caveolin-1 was not affected, in contrast to the effect observed in human cancer cell lines (Wang *et al.*, 2012b), indicating that caveolin-1 expression in hypoxia might be regulated by different mechanisms in different cell types. Interestingly, the evidence suggests that regulation of caveolin-1 is cell-type specific; for example expression of caveolin-1 is activated by HIF1α, but not HIF2α, in hepatocellular carcinoma (Mao *et al.*, 2016) but by HIF2α in mouse colon

(Xie *et al.*, 2014). Therefore it can be speculated whether caveolin-1 regulation in hESCs might involve HIF3α. HIF3α, as well as HIF2α, is located in the nucleus of hESCs cultured at 5% oxygen (Forristal *et al.*, 2010). The role of HIF3α in gene regulation is not well understood in hESCs, however, Forristal *et al.* (2010) observed that when HIF3α was silenced, there was a decrease in expression of OCT4, SOX2 and NANOG. That suggests that HIF3α is involved in regulating gene expression and it remains to be elucidated whether caveolin-1 is one of the targets.

Caveolin-1 is an important regulator of fatty acid trafficking and membrane composition (Meshulam *et al.*, 2006; Heimerl *et al.*, 2008) and highly connected to fatty acid metabolism, for example, by forming a complex with fatty acid synthase (FASN) (Di Vizio *et al.*, 2008). In astrocytes, caveolin-1 expression was also found to be regulated by fatty acid binding protein 7 that results in control of caveolae function by modulating the level of caveolin-1 (Kagawa *et al.*, 2015) suggesting that hypoxia not only affects the proteome but might have an impact on fatty acid-enriched cell membrane properties. The effect of fatty acids on caveolin-1 expression will be further investigated in Chapter 5.

In conclusion, oxygen tension alters the proteomic profile of hESCs. Identified proteins were involved in various functions and processes but the majority of them were associated with cell death/survival, suggesting that hypoxic hESCs are more associated with those activities than cells maintained under atmospheric oxygen. PARP-1 and caveolin-1 were validated to be significantly increased in hESCs cultured at 5% oxygen, compared to those maintained under atmospheric oxygen. However, data presented in this chapter suggests that neither of them is regulated by HIF2α, pointing at other oxygen-dependent mechanisms. This chapter provides evidence that environmental oxygen regulates the proteome of hESCs and hypoxia promotes the self-renewal and undifferentiated state of cells.

Chapter 4 Hypoxic regulation of fatty acids in human embryonic stem cells

4.1 Introduction

Fatty acids are important metabolites involved in various molecular and cellular processes. Fatty acids are best known as an energy source in metabolic processes, acting as substrates for mitochondrial β-oxidation, where they are metabolised to form acetyl-CoA, $FADH_2$ and NADH. The acetyl-CoA produced by β-oxidation can then enter the Krebs cycle, providing substrates for generating ATP (Houten and Wanders, 2010). Fatty acids are also important as components of phospholipids and other complex lipids that build cell membranes (Hashimoto and Hossain, 2018). Properties of membranes depend upon the type of fatty acids present, and therefore a different composition can result in the altered membrane characteristics. For example, higher content of n-6 or n-3 fatty acids can increase cell membrane fluidity (Calder, 2016). In turn, this can affect the movement of proteins in membranes and protein interactions affecting signalling events (Hashimoto and Hossain, 2018). Lipid rafts, structures localised within the cell membrane and highly enriched with various lipids, are particularly involved in signal transduction (Pike, 2003). Fatty acid content was found to have a significant impact on lipid raft composition and functions (Fan *et al.*, 2004; Ma *et al.*, 2004; Seo *et al.*, 2006; Kim *et al.*, 2008). The increase in the level of n-3 polyunsaturated fatty acids (PUFAs) in membranes of MEFs was shown to decrease lipid raft activity that can cause, for example, alteration in H-Ras signalling, due to clustering and formation of rafts into bigger domains, which can affect signals instructing cell growth or division (Roy *et al.*, 1999; Turk and Chapkin, 2013). Destruction or inhibition of lipid rafts caused downregulation of Oct4 or Sox2 in mESCs, highlighting the importance of these domains in maintaining stem cell self-renewal properties (Lee *et al.*, 2010b).

The fatty acid composition, especially PUFA content has been implicated in the regulation of stem cell fate and proliferation (Kang *et al.*, 2014; Rashid *et al.*, 2016; Mathew and Bhonde, 2018; Chen *et al.*, 2020). Supplementation of mesenchymal stromal stem cell culture medium with a defined lipid mixture enhanced the stemness of the cells by increasing overall PUFA content. This change in fatty acid composition did not affect cell morphology or viability, however, it was shown to result in increased cell proliferation and enhanced induced angiogenic differentiation, perhaps due to increased plasticity and fluidity of the membrane (Chatgilialoglu *et al.*, 2017). The PUFA

content was also found to decrease upon differentiation in mESCs, supporting a connection between the fatty acid profile and pluripotency (Yanes *et al.*, 2010). Fatty acids and their metabolites play an important role in regulating proliferation rate in mESCs, neural stem cells and mesenchymal stromal stem cells by modulating the level of proteins involved in signalling pathways, such as PLC/PKC, PI3K/Akt, and p44/42 MAPKs (Kim *et al.*, 2009; Sakayori *et al.*, 2011; Chatgilialoglu *et al.*, 2017). Fatty acids are recognised as important bioregulators, for example as a Na^+/K^+ -ATPase activator. Increasing cis-unsaturation of the fatty acid chain causes the enhanced activity of this enzyme during suboptimal conditions, such as low ATP supply (Jack-Hays *et al.*, 1995).

Cells can produce some fatty acids by the pathway of *de novo* synthesis. This process involves several steps catalysed by fatty acid synthase enzymes that lead to building a carbon chain with the final product being palmitic acid (16:0), although shorter chain fatty acids can sometimes be synthesised as well (Calder, 2016). *De novo* synthesis of fatty acids was shown to help maintain the pluripotent state of mESCs (Wang *et al.*, 2017). Overexpression of acetyl-coenzyme A carboxylase alpha (Acc1), a rate-limiting enzyme involved in the *de novo* fatty acid synthesis, led to increased expression of key pluripotency markers, such as Oct4 or Sox2. Analogously, when fatty acid synthesis was blocked or expression of Acc1 was silenced with shRNA, the same markers were downregulated (Wang *et al.*, 2017). These observations suggest a role for the *de novo* synthesis of fatty acids in the maintenance of stem cell pluripotency.

Despite the de novo synthesis pathway, some fatty acids, such as linoleic acid (18:2n-6) and α-linolenic acid (18:3n-3) cannot be synthesised in humans so must be obtained from the diet. They are referred to as essential fatty acids and are synthesised in plants. Linoleic and α-linolenic acids can be metabolised further by desaturation and elongation processes. Elongation processes are catalysed by elongases that incorporate two carbons into a fatty acid chain, therefore, increasing the length (Jump, 2009). Desaturation is the removal of two hydrogens and insertion of a double bond into the fatty acid carbon chain. The desaturation enzymes involved in n-3 and n-6 biosynthesis pathway are Δ6-desaturase, encoded by the FADS2 gene, and Δ5-desaturase (D5D), encoded by the FADS1 gene (Marquardt *et al.*, 2000). Reactions within the pathways of metabolism of n-3 and n-6 PUFAs are catalysed by the same enzyme and there is a substrate competition between members of these two families. Nevertheless, Δ6-desaturase prefers n-3 PUFAs over n-6 PUFAs. Δ6-desaturase and D5D require oxygen as the electron acceptor and NADH for enzymatic activity (Cook and McMaster, 2002; Calder, 2016). These enzymes generate different products depending on the type of PUFA (described in chapter 1.9).

There is increasing evidence suggesting that fatty acid metabolism is regulated by oxygen tension. A study on human U87 glioblastoma cells found that during hypoxia, Fatty Acid Binding Protein 3 (FABP3) and FABP7 were upregulated due to HIF1α regulation resulting in increased cellular fatty acid uptake compared to cells cultured in normoxia (Bensaad *et al.*, 2014). Fatty Acid Synthase as well as other enzymes participating in *de novo* synthesis were also found to be up-regulated in human cancer cells maintained in low oxygen level and were regulated by HIF1α, highlighting the importance of this process in hypoxic cells (Furuta *et al.*, 2008; Valli *et al.*, 2015). Hypoxic conditions not only affect fatty acid synthesis but also metabolic processes. During hypoxia, HIF1α was found to suppress fatty acid oxidation in cancer cells that led to increased proliferation of the cells due to a reduced level of ROS and enhanced glycolysis (Huang *et al.*, 2014b). This evidence indicates that oxygen tension plays a crucial role in lipid metabolism.

To date, little is known about the role of fatty acids in regulating hESC self-renewal or how environmental oxygen might affect the composition and metabolism of fatty acids in hESCs.

4.2 Chapter aims

The aim of this chapter was to investigate the effect of environmental oxygen on the regulation of fatty acid metabolism in hESCs.

Specific aims were:

- To determine the fatty acid composition of hESCs cultured at either 5% or 20% oxygen using gas chromatography.
- To quantify the expression of D5D in hESCs cultured at either hypoxia or normoxia using Western blot analysis.
- To investigate whether HIF2α regulates D5D expression in hESCs cultured at 5% oxygen using siRNA.
- To investigate whether HIF2α binds directly to a potential HRE site in the proximal promoter of *FADS1* in hESCs cultured at 5% oxygen using ChIP assays.

4.3 Materials and methods

4.3.1 Chromatin immunoprecipitation

Chromatin Immunoprecipitation was conducted using a commercially available kit (ChIP-IT Express Enzymatic kit from Active Motif).

4.3.1.1 Cell fixation

On day 3 post-passage, 3 x 6-well plates of hESCs maintained at either 5% or 20% oxygen were fixed by adding 1.5 ml of 1% formaldehyde in KnockOut DMEM and incubated at room temperature on an orbital shaker for 10 minutes. The cells were rinsed with ice-cold PBS and 1 ml Stop-Fix solution (1:10 10 x glycine buffer, 1:10 10 x PBS and 8:10 dH_20) added and incubated on an orbital shaker at room temperature for 5 minutes. Each well was rinsed quickly with ice-cold PBS and 0.5 ml/well of Cell Scraping solution (1:10 10 x PBS, 9:10 dH_2O and phenylmethylsulfonyl fluoride (PMSF) to a final concentration of 500 µM) added and the cells were scraped from the plates and transferred to two 15 ml Falcon tubes, one for hESCs cultured at 20% oxygen and the other for hESCs cultured at 5% oxygen. The cell solution was centrifuged for 10 minutes at 1250 x *g* at 4°C, the supernatant removed and 1 µl of 100 mM of PMSF and 1 µl protease inhibitor cocktail (PIC) was added to the cell pellet which was stored at -80°C.

4.3.1.2 Preparation of enzymatically sheared chromatin

The pellet was thawed on ice and resuspended in 1 ml ice-cold lysis buffer (included with kit) supplemented with 5 µl PIC and 5 µl 100 mM PMSF, incubated on ice for 30 minutes and lysed using an ice-cold dounce homogeniser. Lysed cells were transferred to a microcentrifuge tube and centrifuged for 10 minutes at 2400 x *g* at 4°C. The pellet was resuspended in 350 µl Digestion Buffer 1 (included with kit) supplemented with 1.75 µl PIC and 1.75 µl 100 mM PMSF and incubated for 5 minutes at 37°C. Enzymatic shearing was carried out by adding 17 µl of Enzymatic Shearing Cocktail (Enzymatic Shearing Cocktail 2 x 10^4 U/ml 1:100 in 50% glycerol in dH_2O) and incubating the sample at 37°C for 15 minutes. During incubation, the sample was briefly vortexed every 2 minutes to increase shearing efficiency. The reaction was stopped with the addition of 7 µl ice-cold 0.5 M EDTA and incubated on ice for 10 minutes before the sheared chromatin samples were centrifuged for 10 minutes at 18000 x *g* at 4°C. The supernatant was transferred to another microcentrifuge tube and 50 µl was removed to assess the DNA concentration and shearing efficiency. The rest of the sample was stored at -80°C until required.

4.3.1.3 DNA clean up to assess shearing efficiency and DNA concentration

150 µl of dH_2O and 10 µl 5 M NaCl was added to a 50 µl aliquot of sheared chromatin. The sample was incubated overnight at 65°C and cooled down to room temperature before adding 1 µl RNase A and incubating for 15 minutes at 37°C. After that, 10 µl of Proteinase K was added to the sample which was then incubated at 42°C for 1.5 hours. 200 µl of phenol/chloroform/isoamyl alcohol mix (25:24:1) was added to the sample, vortexed and centrifuged for 5 minutes at 18000 x *g*; the aqueous phase was carefully transferred to a fresh microcentrifuge tube. 20 µl of 3 M Sodium Acetate pH 5.2 and 500 µl of 100% ethanol was added to the aqueous phase sample, followed by at least one hour incubation at -80°C. The sample was centrifuged for 10 minutes at 18000 x *g* at 4°C and supernatant was removed. Pellet was washed in 500 µl 70% ethanol and centrifuged for 5 minutes at 18000 x *g* at 4°C. The supernatant was removed and the pellet was left to air-dry before resuspending in 30 µl dH_2O. Nanodrop was used to assess DNA concentration (1.0 A_{260} unit = 50 µg/ml). 16 µl of the sample was mixed with 4 µl of a 6 x loading buffer (New England Biolabs) and two different quantities of the sheared sample (5 µl and 10 µl) were loaded on 1% TAE (40mM Tris(hydroxymethyl)-aminomethane, 20mM acetic acid and 1mM EDTA) agarose gel. Gel electrophoresis was run at 100 V for around an hour. The gel was imaged to assess shearing efficiency; optimal enzymatic shearing should result in a 200-1500 bp banded pattern (Figure 4.1).

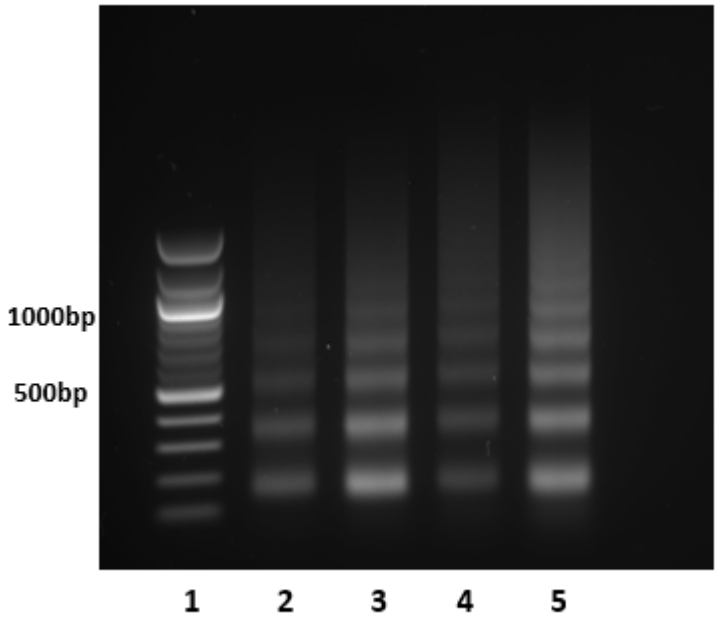

Figure 4.1 **Gel analysis of enzymatic shearing.**

Representative gel image of optimally sheared chromatin collected from hESCs cultured at either 5% or 20% oxygen. Chromatin was sheared with an enzymatic shearing cocktail for 15 minutes and the reaction stopped with cold EDTA. Lane 1: 100bp ladder, lane 2: 5 µl of sheared chromatin isolated from hESCs cultured at 5% oxygen, lane 3: 10 µl of sheared chromatin isolated from hESCs cultured at 5% oxygen, lane 4: 5 µl of sheared chromatin isolated from hESCs cultured at 20% oxygen, lane 5: 10 µl of sheared chromatin isolated from hESCs cultured at 20% oxygen.

4.3.1.4 Immunoprecipitation

Sheared chromatin from step 4.3.2.2 was thawed on ice. 10 µl was transferred to a microcentrifuge tube and stored at -20ºC until ready to process as 'Input DNA'. The immunoprecipitation reaction was set (Table 4.1). The amount of sheared chromatin was equal for all ChIP reactions (9 µg) and the required volume of sheared chromatin was calculated based on DNA concentration established with nanodrop. An antibody was added as the last component, HIF2α ChIP validated antibody (Novus Biologicals) was used for 'HIF2α' reaction sample and normal rabbit IgG antibody (Santa Cruz Biotechnology) was used for 'IgG' reaction sample.

Table 4.1 **Example of a typical ChIP reaction set up.**

DNA concentration established from nanodrop results: 63.9 ng/µl for 20% oxygen sample and 63.6 ng/µl for 5% oxygen sample.

	20% oxygen samples		5% oxygen samples	
Sample / Reagent	HIF2α	IgG	HIF2α	IgG
Protein G Magnetic Beads	25 µl	25 µl	25 µl	25 µl
ChIP buffer 1	20 µl	20 µl	20 µl	20 µl
Sheared chromatin - **9 µg**	140.8 µl	140.8 µl	141.8 µl	141.8 µl
PIC	2 µl	2 µl	2 µl	2 µl
dH_2O	9.2 µl	9.2 µl	8.2 µl	8.2 µl
Antibody	3 µl	3 µl	3 µl	3 µl
Total volume	200 µl	200 µl	200 µl	200 µl

Samples were incubated overnight on rotator at 4°C. After that, tubes were placed on a magnetic stand to pellet magnetic beads before removing the supernatant.

4.3.1.5 Magnetic beads wash

Magnetic beads were washed three times, 3 minutes each wash, with 800 µl ChIP buffer 1 (included with kit) and four times, 3 minutes each wash, with ChIP buffer 2 (included with kit). Care was taken to not let the magnetic beads dry out. After the final wash, all of the supernatant was removed.

4.3.1.6 Chromatin elution, cross-link reversal and Proteinase K treatment

Magnetic beads were resuspended in 50 µl Elution buffer AM2 1 (included with kit) and incubated at room temperature on an end-to-end rotor for 15 minutes. 50 µl of Reverse-Cross-linking buffer (included with kit) was added and mixed by pipetting. Samples were placed on a magnetic stand to allow beads to pellet on the side of the tubes. The supernatant was transferred to a fresh tube. 10 µl of sheared chromatin aliquoted before setting immunoprecipitation reaction as 'Input DNA' was processed by adding 88 µl ChIP Buffer 2 and 2 µl 5 M NaCl. ChIP reaction samples and Input DNA samples were incubated together at 95°C for 15 minutes. Samples were returned to room

temperature before adding 2 µl Proteinase K and incubation for 1 hour at 37°C. At the end of this incubation, 2 µl of Proteinase K Stop Solution was added to each sample.

4.3.1.7 DNA clean up prior to RT-qPCR

An equal amount of phenol/chloroform/isoamyl alcohol mix (25:24:1) was added to samples, which were vortexed briefly and centrifuged at 18000 x *g* for 5 minutes. The aqueous phase was collected and 0.1 volume of 3 M Sodium Acetate pH 5.2 and 3 volumes of 100% ethanol were added. Samples were left at -80°C for at least an hour before centrifuging them at 18000 x *g* for 30 minutes at 4°C. The supernatant was removed and the pellet was washed with 500 µl ice-cold 70% ethanol. Samples were centrifuged again at 18000 x *g* for 5 minutes at 4°C. The pellet was left to air-dry and later resuspended in 30 µl dH_2O.

4.3.1.8 Real-time qPCR

Primers were designed to amplify a region within the *FADS1* proximal promoter that contains a potential Hypoxia Response Element (HRE). Quality and specificity of designed primers (Table 4.2) were tested on genomic DNA.

Table 4.2 **The sequence of the primer pair used in the ChIP experiment.**

The amplicon size was 83bp.

Oligo name	**Sequence (5'-3')**
FADS1 HRE forward	GCAACTTTCAAGGGCTCTCAG
FADS1 HRE reverse	GGTTGGAAACTACTGCCTGC

The RT-qPCR reaction was set up in a 96-well plate in duplicate or triplicate for 6 samples:

- '5% HIF2α' – DNA from cells maintained at 5% oxygen; immunoprecipitation reaction was set with HIF2α antibody to test whether HIF2α binds to a potential HRE in the *FADS1* proximal promoter.
- '5% IgG' – negative control for ChIP reaction from DNA of cells cultured at 5% oxygen; immunoprecipitation reaction was set with rabbit IgG antibody.
- '20% HIF2α' - DNA from cells maintained at 20% oxygen; immunoprecipitation reaction was set with HIF2α antibody to test if HIF2α binds to a potential HRE in the *FADS1* proximal promoter.
- '20% IgG' - negative control for ChIP reaction from DNA of cells cultured at 20% oxygen.
- '5% Input DNA' – genomic DNA from cells cultured at 5% that was not immunoprecipitated.
- '20% Input DNA' – genomic DNA from cells maintained at 20% oxygen that was not immunoprecipitated.

18 µl of Master Mix (10 µl 2 x Master Mix Sybr green, 4 µl dH_2O, 2 µl forward primer, 2 µl reverse primer) was added to each well followed by addition of 2 µl of DNA sample. The RT-qPCR negative control consisted of 18 µl Master Mix and 2 µl of dH_2O. The plate was sealed with film, briefly centrifuged and loaded onto RT-qPCR machine. The following cycling parameters were used for amplification:
Holding stage: 50°C for 2 minutes; Holding stage: 95°C for 10 minutes; Cycling stage: 95°C for 15 seconds (Step 1), 60°C for 1 minute (Step 2), 40 cycles; Melt Curve Stage: 95°C for 15 seconds (Step 1), 60°C for 1 minute (Step 2), 95°C for 30 seconds (Step 3) and 60°C for 15 seconds (Step 4).

4.3.1.9 Determination of fold enrichment

Enrichment was calculated based on the equation:

ΔCt_1 = mean Ct of Input DNA - mean Ct IgG
ΔCt_2 = mean Ct of Input DNA – mean Ct ChIP

% IgG (enrichment) = $2^{\Delta Ct1}$ x 100%
% ChIP (enrichment) = $2^{\Delta Ct2}$ x 100%

Ratio of binding was calculated as %ChIP ÷ %IgG

The calculation was performed for RT-qPCR results on DNA from hESCs cultured at either 5% or 20% oxygen.

4.4 Results

4.4.1 Fatty acid composition of NT2 cells

The fatty acid content of NT2 cells (human embryonal carcinoma cell line) maintained at either hypoxic or normoxic conditions was measured using gas chromatography. NT2 cells were used to work up the gas chromatography technique to establish the number of cells required for later implementation with hESCs. Overall, the fatty acid content of NT2 cells cultured at either 5% or 20% oxygen was similar (Figure 4.2). However, environmental oxygen significantly altered the proportion of palmitoleic acid (16:1n-7) (Figure 4.2 B), eicosapentaenoic acid (20:5n-3; EPA) and docosapentaenoic acid (22:5n-3) (Figure 4.2 A). Palmitoleic and docosapentaenoic acids were significantly increased ($p= 0.003$ and $p= 0.033$, respectively) in NT2 cells cultured at 5% oxygen compared to 20% oxygen. In contrast, there was a significant, more than 1.5 fold decrease ($p= 0.008$) in the EPA content of NT2 cells cultured at 5% oxygen compared to those maintained at 20% oxygen.

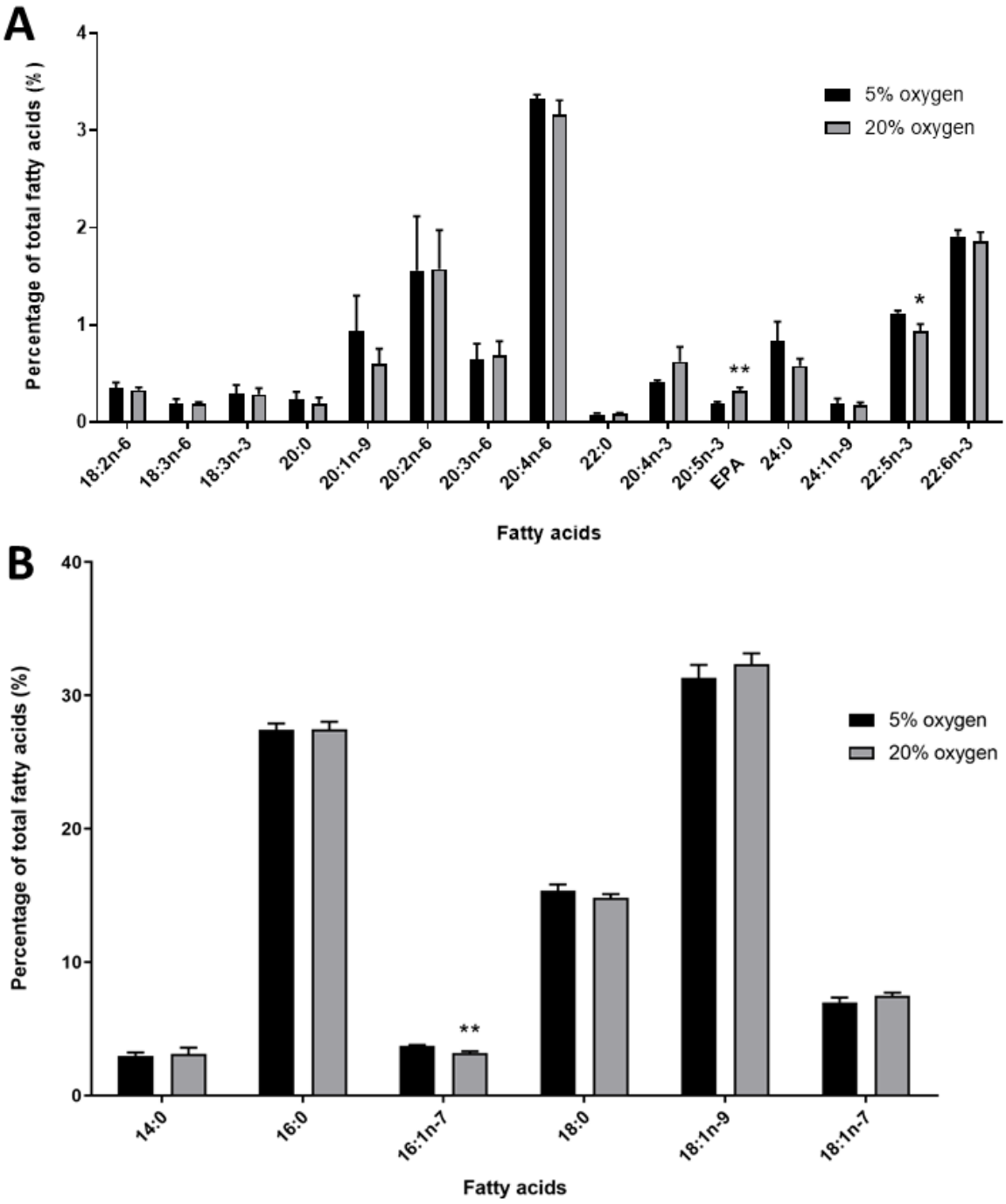

Figure 4.2 **Oxygen tension affects the fatty acid composition of NT2 cells.**

Individual fatty acids expressed as a percentage of total fatty acids that is (A) lower than 4% or (B) higher than 4%. EPA- eicosapentaenoic acid. Bars represent mean + SEM. *P<0.05, **P<0.01 significantly different between 5% and 20% oxygen. n=6.

4.4.2 The fatty acid composition of hESCs

The fatty acid content of hESCs cultured at either 5% or 20% oxygen level was measured using gas chromatography. The percentage of fatty acids were broadly similar between hESCs cultured at

5% or 20% oxygen (Figure 4.3). However, there was a significant, 1.5 fold increase ($p<0.001$), in the level of EPA in hESCs cultured at 5% oxygen compared to those maintained at 20% oxygen. In contrast, eicosadienoic acid (20:2n-6; EDA) was decreased ($p=0.014$) in hESCs cultured under hypoxic conditions compared to those maintained under atmospheric oxygen (Figure 4.3 A). Moreover, there was a near significant ($p=0.053$) increase in the percentage of linoleic acid (18:2n-6) in hESCs cultured in hypoxia compared to normoxia (Figure 4.3 A).

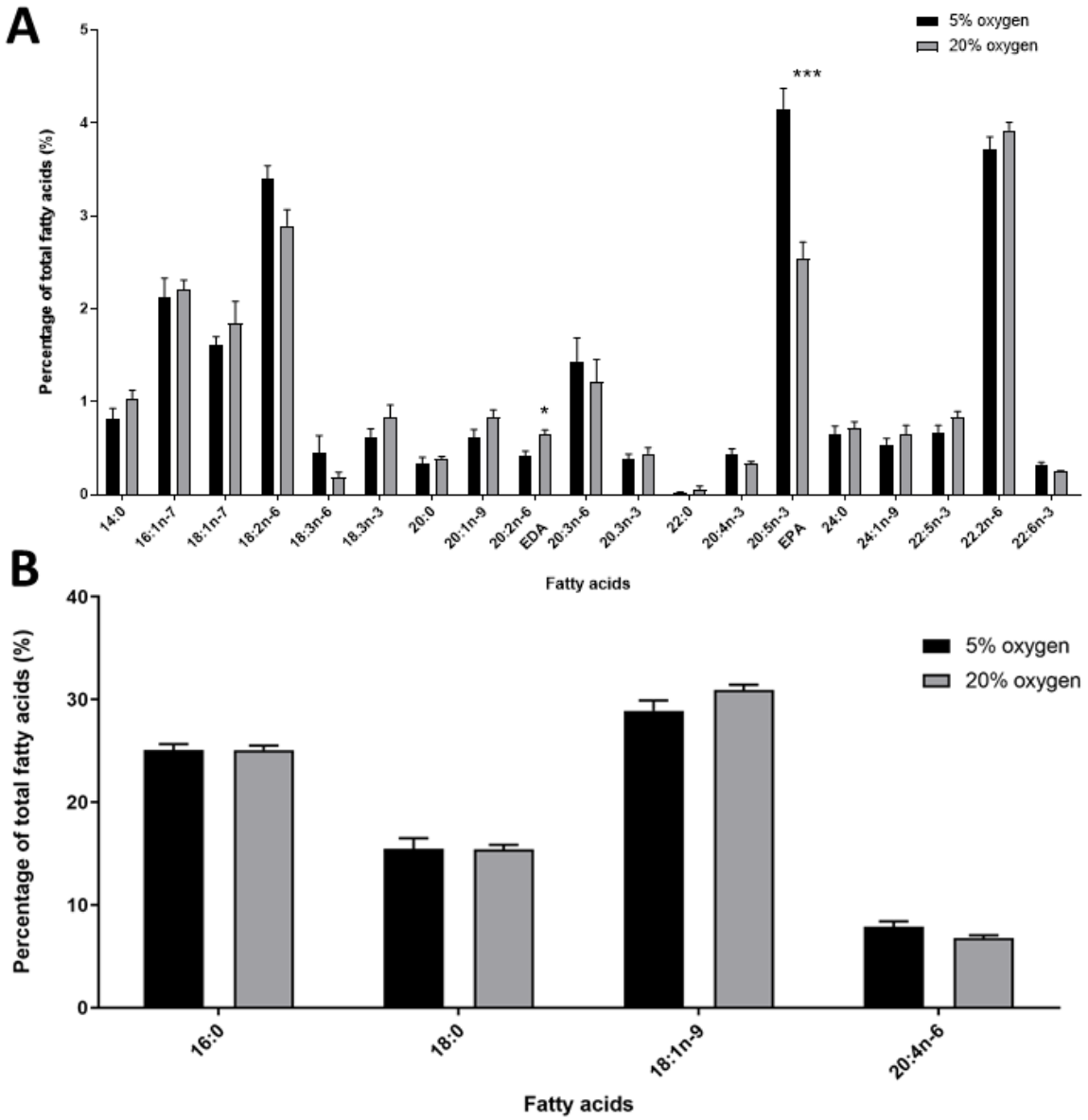

Figure 4.3 **Oxygen tension alters the fatty acids composition of hESCs.**

Individual fatty acids expressed as a percentage of total fatty acids that is (A) lower than 5% or (B) higher than 5%. EDA- eicosadienoic acid; EPA- eicosapentaenoic acid. Bars represent mean + SEM. *P<0.05, ***P<0.001 significantly different between 5% and 20% oxygen. n=5.

The fatty acid content was also expressed in absolute terms as μg/10^6 cells. The total amount of fatty acids was not significantly different between cells cultured at either 5% or 20% oxygen and was approximately 50 μg/10^6 cells for hESCs cultured in hypoxia and 41 μg/10^6 cells for hESCs maintained under atmospheric oxygen (Figure 4.5).

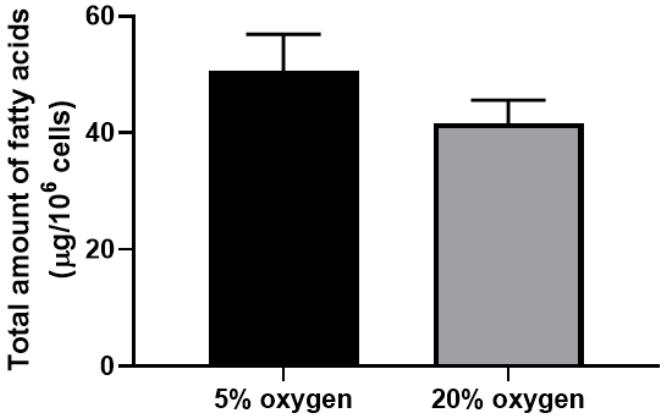

Figure 4.4 **Oxygen tension does not affect the total amount of fatty acids in hESCs.**

Bars represent mean + SEM. n=5.

Despite the similar total amount of fatty acids in cells cultured at either 5% or 20% oxygen, it was possible that absolute quantification could reveal differences in the amount of n-3 or n-6 fatty acids between hESCs cultured at either 5% or 20% oxygen. The analysis of results based on absolute quantification showed that the total amount of n-6 PUFAs was not altered by oxygen tension (Figure 4.5 A). The total amount of n-6 PUFAs was approximately 8.5 μg/10^6 cells for hESCs cultured at 5% oxygen and 6.5 μg/10^6 cells for hESCs maintained at 20% oxygen. The total amount of n-3 PUFAs was found to be significantly altered by environmental oxygen (Figure 4.5 B). Absolute quantification revealed that the total amount of n-3 PUFAs was significantly higher ($p=0.015$), approximately 3 μg/10^6 cells, in hESCs cultured at 5% oxygen, compared those maintained at 20% oxygen, where the level of n-3 PUFAs was around 2 μg/10^6 cells.

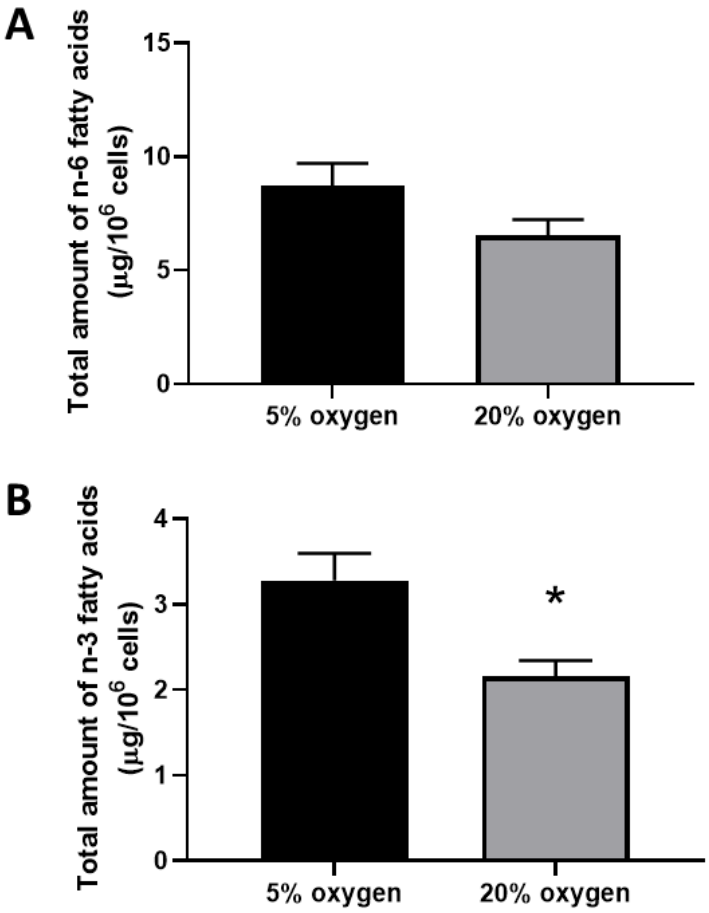

Figure 4.5 **Oxygen tension affects the total amount of n-3 fatty acids but not n-6 fatty acids in hESCs.**

Absolute quantification of (A) n-6 and (B) n-3 fatty acids in hESCs cultured at either 5% or 20% oxygen. Bars represent mean + SEM. *P<0.05 significantly different between 5% and 20% oxygen. n=5.

Absolute quantification of individual fatty acids showed that most of the analysed fatty acids had similar levels in hESCs cultured at either 5% or 20% oxygen. However, the total amount of EPA was significantly increased (p=0.005) by 100% in hESCs cultured at 5% oxygen compared to cells cultured at 20% oxygen (Figure 4.6 A). Interestingly, the analysis revealed that the total amount of 20:4n-6 (AA) was also significantly higher (p=0.020) and increased by nearly 36% in hESCs maintained in hypoxia compared to those maintained under atmospheric oxygen (Figure 4.6 B).

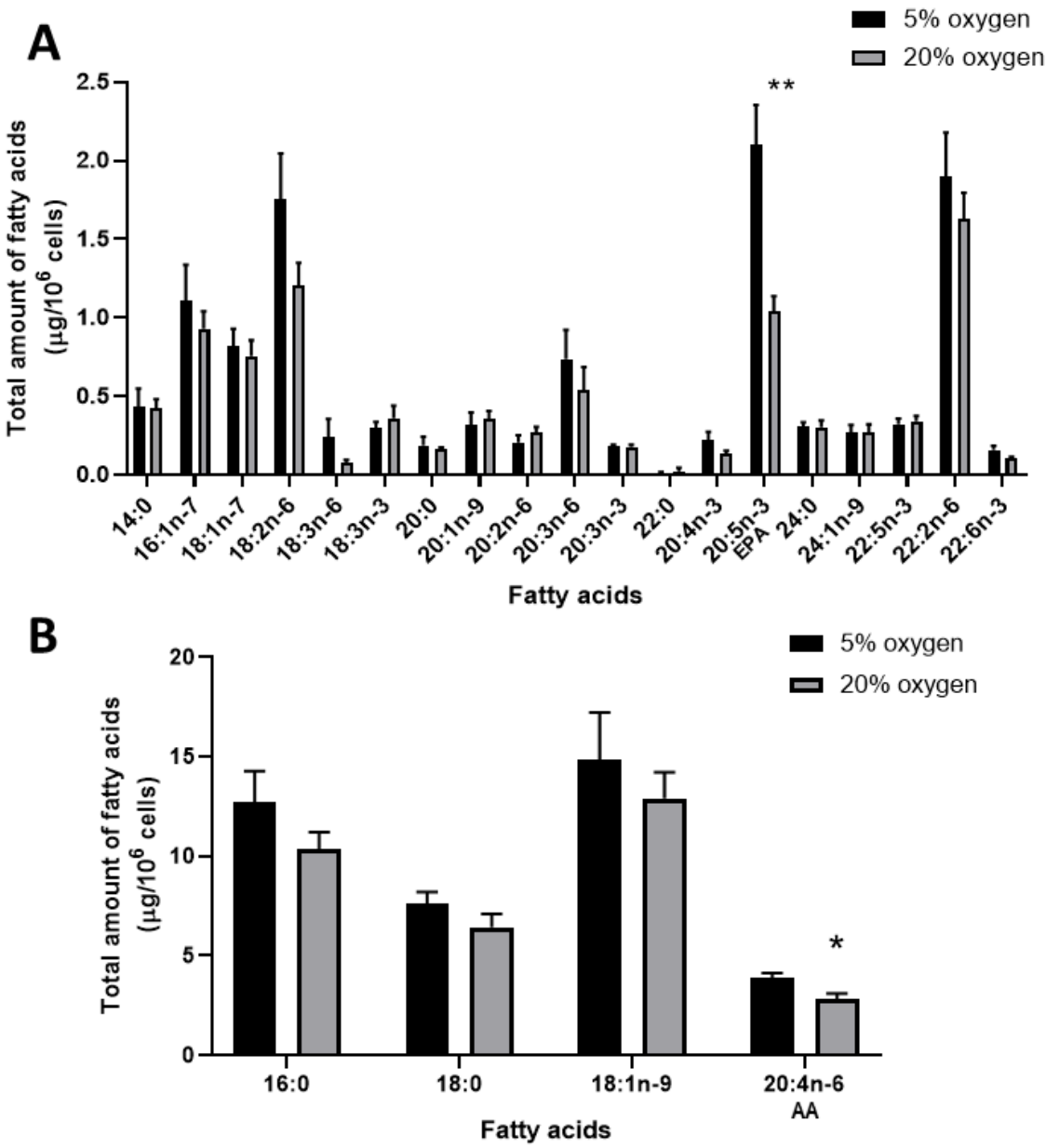

Figure 4.6 **Environmental oxygen affects the absolute fatty acid content of hESCs.**

Individual fatty acids with a total amount that is (A) lower than 2.5 µg/10^6 cells (B) higher than 2.5 µg/10^6 cells. EPA- eicosapentaenoic acid; AA- arachidonic acid. Bars represent mean + SEM. *P<0.05, **P<0.01 significantly different between 5% and 20% oxygen. n=5.

4.4.3 Effect of oxygen tension on the expression level of Δ5-desaturase in hESCs

The bioconversion of eicosatetraenoic acid (20:4n-3) to EPA (20:5n-3), which is the fatty acid most significantly altered in hESCs by oxygen tension, is catalysed by Δ5-desaturase (D5D). Bioconversion of 20:3n-6 to 20:4n-6 (AA), which was also found to be altered by the oxygen tension, is also mediated by D5D. Thus, the protein expression level of this enzyme was

determined in hESCs cultured at either 5% or 20% oxygen using Western blotting. HepG2 cell lysate was used as a positive control for D5D expression. Results from hESC lysate showed a double band, at a size of approximately 48 kDa and 52 kDa (Figure 4.7 A). Western blot of the HepG2 cell lysate positive control revealed a single band at a size of approximately 52 kDa that corresponds to D5D protein (Figure 4.7 A). Thus, the upper band was used to quantify the expression level of D5D in hESCs (Figure 4.7 B). The lower band might occur due to unspecific binding or possibly, it could be an alternative transcript, as multiple isoforms of FADS1 have been identified (Park *et al.*, 2012). Quantification of the Western blot results revealed that the expression of D5D was significantly reduced by almost 60% in hESCs cultured at 20% oxygen compared to hESCs cultured at 5% oxygen (p-value=0.007) (Figure 4.7 C). This suggests that D5D expression is regulated by environmental oxygen tension.

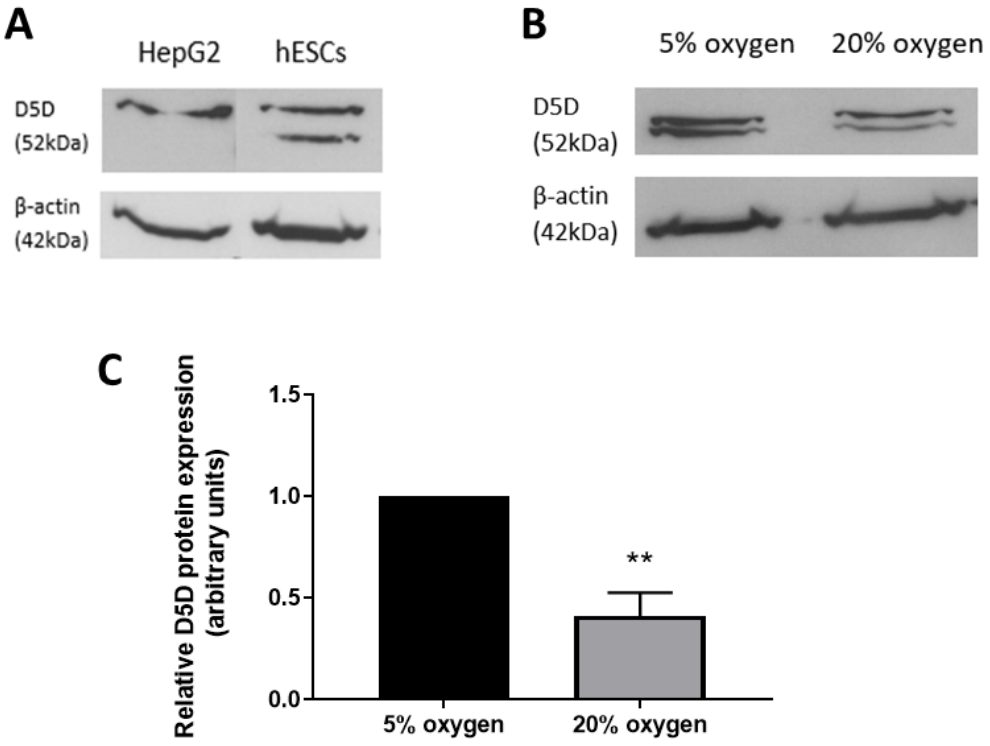

Figure 4.7 **Hypoxic culture promotes the expression of D5D in hESCs compared to atmospheric conditions.**

(A) Western blot of D5D and β-actin in HepG2 cells positive control and hESCs. (B) Representative Western blot of D5D and β-actin in hESCs cultured at either 5% or 20% oxygen. (C) Quantification of D5D expression in hESCs cultured at either 5% or 20% oxygen based on Western blot results. Data were normalized to β-actin and to 1 for 5% oxygen. Bars represent mean + SEM. **p<0.01 significantly different between 5% and 20% oxygen. n=3

4.4.4 Effect of silencing Δ5-desaturase on the expression of pluripotency markers in hESCs cultured at 5% oxygen

The expression of key pluripotency markers, OCT4, SOX2 and NANOG, was significantly increased in hESCs cultured at 5% oxygen compared to 20% oxygen (chapter 3.4.1.2), similarly to D5D expression. Thus, it was investigated whether D5D might play a role in the maintenance of hESC self-renewal under a low oxygen tension. Thus, *FADS1* (gene encoding D5D) was silenced using siRNA and the expression of OCT4, SOX2, NANOG quantified in hESCs cultured at hypoxic conditions. Silencing *FADS1* did not affect hESC cell morphology (Figure 4.8 A); however Western blotting results showed that expression of D5D was successfully silenced with an approximate 60% reduction in expression compared to AllStars negative control ($p<0.001$) (Figure 4.8 B and C). When *FADS1* was successfully silenced, expression of self-renewal markers in those cells was examined using Western blotting. Quantification of OCT4, SOX2 and NANOG protein expression showed that when *FADS1* was silenced, expression of key pluripotency markers was not affected compared to the AllStars negative control (Figure 4.9).

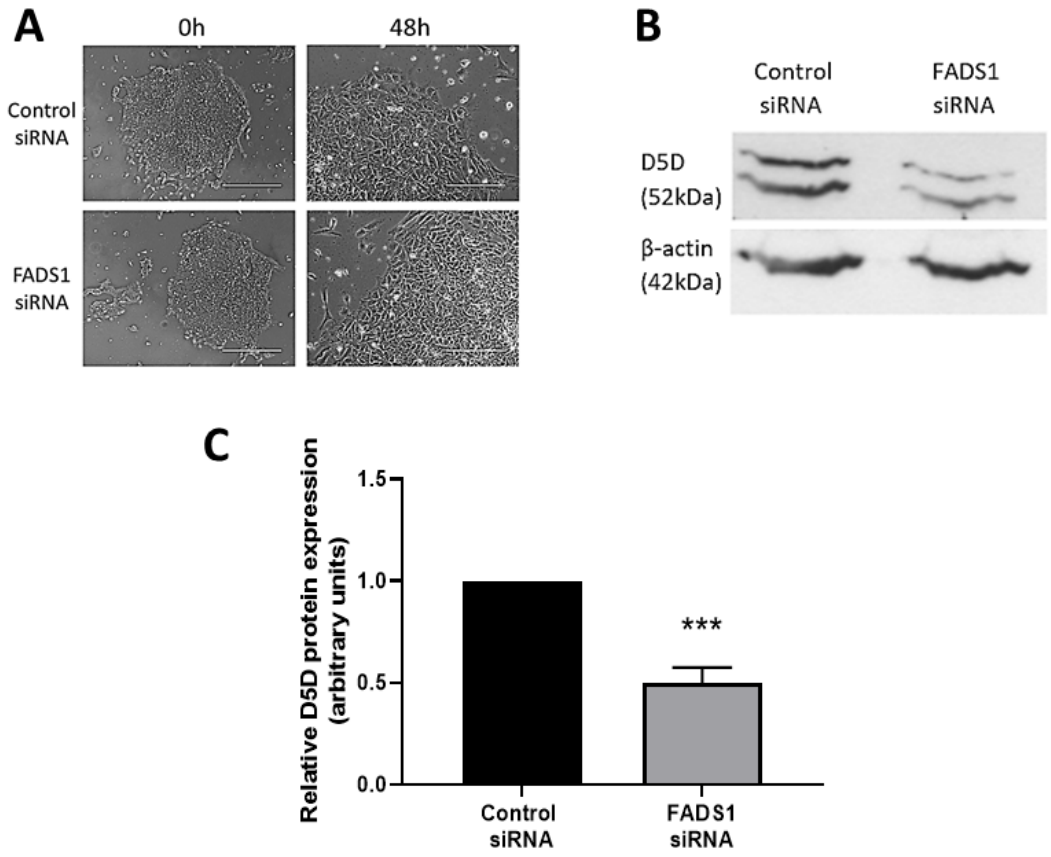

Figure 4.8 **D5D expression was decreased following transfection with *FADS1* siRNA.**

(A) Phase contrast images of hESCs morphology cultured at 5% oxygen before and after transfection for 48 hours with either AllStars negative control siRNA or FADS1 siRNA. Scale bar indicates 200 µm. (B) Representative Western blot of D5D and β-actin expression in hESCs cultured at 5% oxygen transfected with either FADS1 siRNA or AllStars negative control siRNA. (C) Quantification of D5D protein expression. Data were normalized to β-actin and to 1 for control siRNA. Bars represent mean + SEM. ***P<0.001 significantly different between FADS1 siRNA and AllStars negative control. n=5

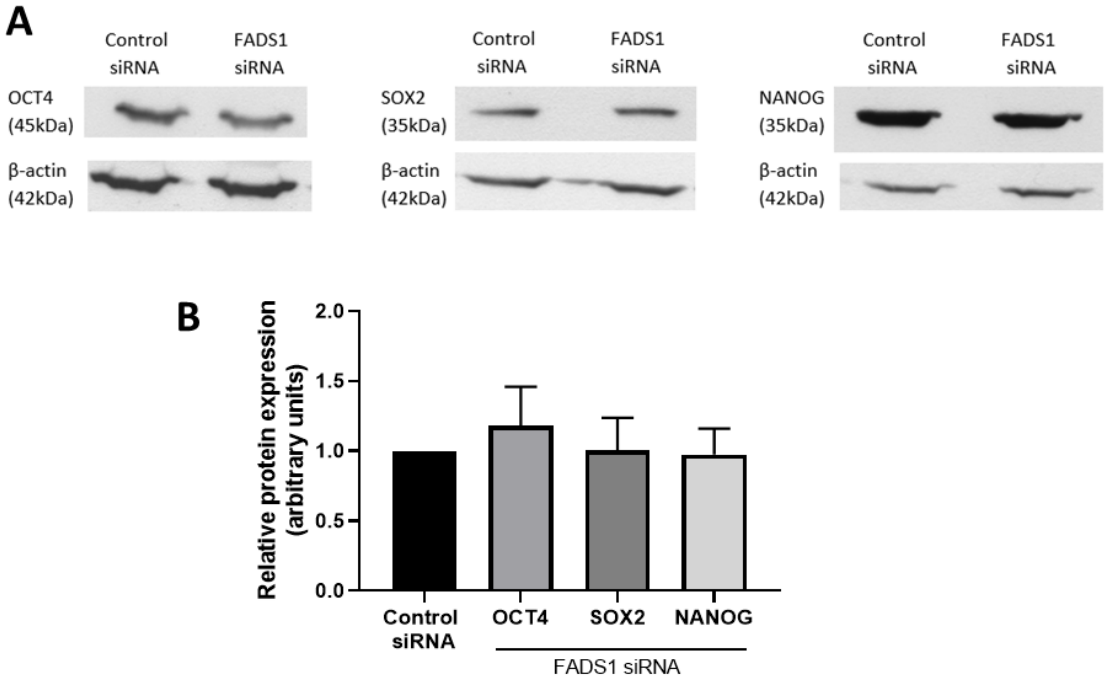

Figure 4.9 **Silencing of *FADS1* does not affect the expression of OCT4, SOX2 or NANOG in hESCs cultured at 5% oxygen.**

(A) Representative Western blot of OCT4, SOX2, NANOG and β-actin expression in hESCs cultured at 5% oxygen transfected with either FADS1 siRNA or AllStars siRNA negative control. (B) Quantification of OCT4, SOX2 and NANOG protein expression in hESCs where *FADS1* has been silenced compared to AllStars siRNA negative control. Data were normalized to β-actin and to 1 for control siRNA. Bars represent mean + SEM. n=3-5

4.4.5 Role of HIF2α in regulating the expression of D5D in hESCs cultured at 5% oxygen

Expression of D5D was found to be significantly increased in hESCs cultured at 5% oxygen compared to those maintained under atmospheric oxygen, therefore it was investigated whether this was due to HIF2α regulation. HIF2α is known to play an important role as a transcription factor in hESCs cultured in hypoxic conditions and is responsible for regulating the expression of several genes (Forristal *et al.*, 2010; Petruzzelli *et al.*, 2014). Thus, the expression of HIF2α was silenced using siRNA to investigate whether this might affect D5D levels. Silencing HIF2α did not affect hESC morphology (Figure 4.10 A) and the expression was quantified using Western blotting. HIF2α was identified as a single band at a size of approximately 118 kDa (Figure 4.10 B). Quantification confirmed a 40% reduction in HIF2α protein expression compared to AllStars siRNA

negative control (p=0.005) (Figure 4.10 C). The expression level of D5D was quantified in hESCs where HIF2α expression had been silenced and revealed a significantly decreased expression compared to AllStars negative control (Figure 4.11). This suggests that D5D is not only an oxygen sensitive gene but also that HIF2α is an upstream regulator of D5D.

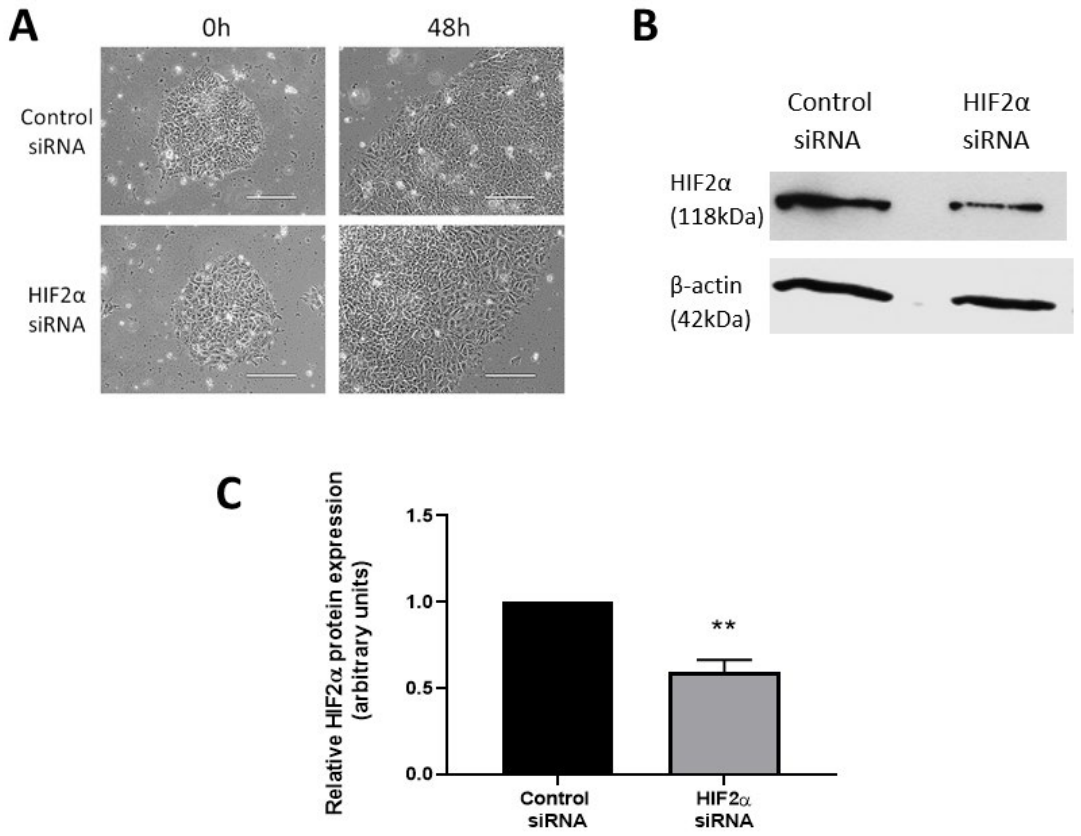

Figure 4.10 **Expression of HIF2α was successfully silenced in hESCs cultured at 5% oxygen.**

(A) Phase contrast images of hESCs morphology cultured at 5% oxygen before and after transfection for 48 hours with either AllStars negative control siRNA or HIF2α siRNA. Scale bar indicates 200 μm. (B) Representative Western blot of HIF2α and β-actin expression in hESCs cultured at 5% oxygen transfected with either HIF2α siRNA or AllStars siRNA negative control. (C) Quantification of HIF2α protein expression. Data were normalized to β-actin and to 1 for control siRNA. Bars represent mean + SEM. **P<0.01 significantly different between HIF2α siRNA and AllStars negative control. n=3

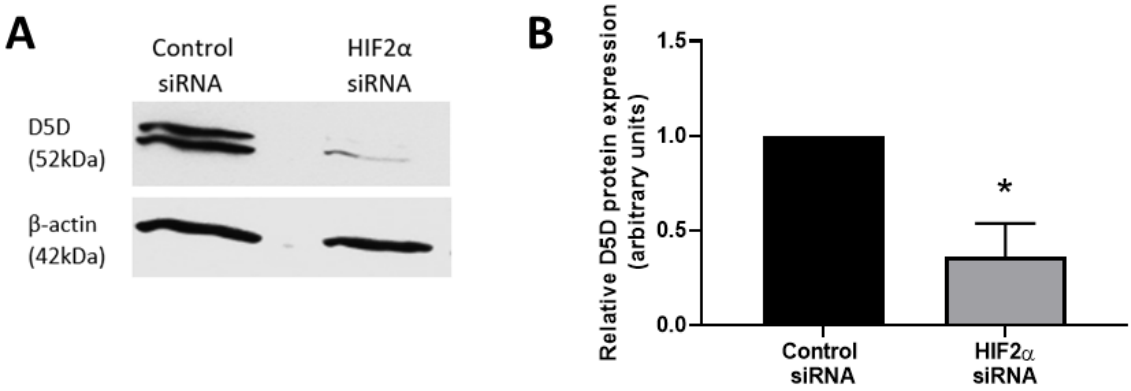

Figure 4.11 **Silencing HIF2α resulted in a significant decrease in the expression level of D5D in hESCs cultured at 5% oxygen.**

(A) Representative Western blot of D5D and β-actin expression in hESCs cultured at 5% oxygen transfected with either HIF2α siRNA or AllStars siRNA negative control. (B) Quantification of D5D protein expression. Data were normalized to β-actin and to 1 for control siRNA. Bars represent mean + SEM. *$p<0.05$ significantly different between HIF2α siRNA and AllStars negative control. n=3

To investigate whether HIF2a regulates D5D directly, it was first necessary to determine if the proximal promoter of the *FADS1* gene contains any putative HRE sites. Using bioinformatic analysis, two potential HREs within 1500bp upstream of the transcription start site (TSS) of the *FADS1* gene were identified (Figure 4.12). Two potential HREs were determined at -1075bp to -1070bp and -286bp to -281bp upstream of the TSS. The whole sequence containing promoter (1500bp upstream of the TSS), 5' UTR, exons and 3' UTR regions can be found in Appendix 3.

tattgtcaggactcgggtttatttccagtttttgctattaaattggctat
ttctgcatctttgcacagtctcccctactttaccaagagtgaaactgctt
gatcaaagaatagaaaatgttttgtagctcgcattagacactgccaagtt
gttgggcaaggtttttaaaaaaggaatattggctgtacagaggtgcagct
gtgtggaccatcattcctgagcagggtccaatagcctggcatcttacctg
gaagtcaggacatctaaacttccctatgggaacttggtaagccccttccc
catttcgaacctcaattttcttatctataaaatgaagaatttggatggaa
tgaattaatccttttctaccagaaatctagccatatttcacctagtctat
tctgtatcaccctctcctgactcctacgtgctcagaatctagctcagtgc
ttgggacagttatgtttccttttccctttgaagtgcccaaataccagtgta
atgagaaatatggcagagcctgagagttcagagcacaggccagggtcaaa
tctcagccctccacttacaagctgtgtgacaaaataacctcccccgggct
cagtttcttcactgtaaattaggttaattgttccaacctcatagggttgt
taggagaattaaatgagttaaggtttgcaaaacgctaagaacagtgcctg
gcacacagtaagtgctttataaagtgtttgttgaataaataaaattttgg
acctaaactctgggtctcttcaggactgcaacagctttgtaactggcaac
cccacttttaggtgcgttcccactcctctaaaacccagagatctaaatgc
caaatctctctgcttaaaaagtctcccagggctcctaggcgcctccaggc
tagaacagaaatgcctcagcttgaagacccaggcttttcaggtgaaacac
ctaagggtcaggagacgctaggatcatcactcaaggatcccagtgaattt
ttccaaaatacaataaaaataaaaacaaaaagaggcaaacagggttataa
aaattgtggggcattttaaatgtttcattgaacaaattaaagcattaaca
gccctcccccaaccaccaccaagcccaagagaccgtaaatatgctgttca
caagataactgcaactttcaagggctctcaggctgctacttcgggcagca
caattggcggcacgacgtggcaagcaggcagtagtttccaaccctggagg
gtcagcgtctggagaccccggccaaggcatccacagcctaaagatgatgt
ccgcgaccgcccgggcagcctcgtgcacggaaaaacctcaaccccggccc
cgcccacccttcctgcggccaccccgcagccctggcccctcagtccattc
actcctgcagcgcggccccgcacccagggcctgcactagaaccgctgttc
ctaccgcggcgcccccctgggagccaacgccgcgatgcccgcctgacgtca
GGAAGTCGAATCCGGCGGCGACGCCTTTAGGGAGCCCGCGAGGGGGCGCG
TGTTGGCAGCCCAGCTGTGAGTTGCCCAAGACCCACCGGGGGACGGGATC

Figure 4.12 **Part of the sequence of *FADS1* proximal promoter.**

The presented sequence is -1500bp to 100bp relative to TSS. Lower case letters indicate sequence upstream of TSS and upper case, blue letters sequence upstream of TSS. Potential HREs are highlighted (yellow and red colours); the HRE highlighted with red colour, located at -286bp to -281bp relative to TSS was selected for investigation using ChIP.

The HRE closest to the transcription start site (-286bp to -281bp) was selected for further investigation. Chromatin immunoprecipitation (ChIP) was performed on chromatin isolated from hESCs cultured at either 5% or 20% oxygen to investigate whether HIF2α directly binds to the HRE located at -286bp to -281bp relative to TSS in the proximal promoter of *FADS1* in hESCs cultured in hypoxia to regulate expression of D5D. ChIP results revealed a 7-fold (p=0.030) enrichment of HIF2a binding to the *FADS1* proximal promoter in chromatin obtained from hESCs cultured at 5% compared to chromatin isolated from hESCs maintained at 20% oxygen (Figure 4.13). These data show that HIF2α binds directly to the HRE of *FADS1* proximal promoter at -286bp to -281bp from the TSS in hESCs cultured in hypoxic conditions; the binding is significantly reduced in hESCs maintained under atmospheric oxygen.

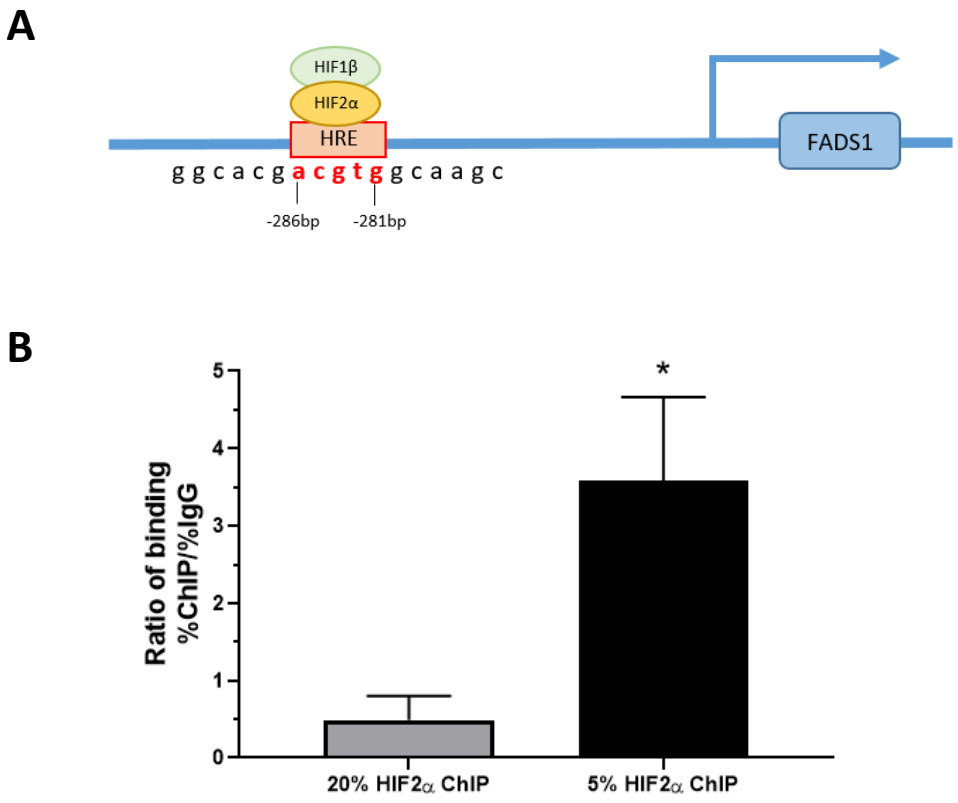

Figure 4.13 **HIF2α directly regulates *FADS1* expression by binding to an HRE located in the proximal promoter in hESCs cultured at 5% oxygen.**

(A) Schematic representation of HIF2α binding to HRE site located within the *FADS1* promoter. (B) ChIP quantification of HIF2α binding to the potential HRE in the proximal promoter of *FADS1*. ChIP was performed on chromatin isolated from hESCs cultured at either 5% or 20% oxygen. DNA enrichment is expressed as a ratio of binding %ChIP/%IgG. Bars represent mean + SEM. *p<0.05 significantly different between 20% HIF2α ChIP and 5% HIF2α ChIP. n=4

4.5 Discussion

Fatty acids are important metabolites: they are components of all cell membranes and are involved in cellular signalling and metabolism (Calder, 2016). However, little is known about how fatty acid content is regulated by environmental oxygen and whether it can affect the self-renewal properties of hESCs. This chapter aimed to investigate the effect of environmental oxygen on fatty acid biosynthesis and content.

The fatty acid content of NT2 cells was measured by gas chromatography to work up the technique. NT2 cells are malignant counterparts of hESCs and therefore it would be expected to obtain relatively similar fatty acid content between NT2 cells and hESCs. The analysis revealed that different fatty acids were altered by oxygen tension between these two cell types; however, only one fatty acid (EPA) was commonly altered. The gas chromatography results, when expressed as a percentage of total fatty acids, showed the low abundance of EPA in NT2 cells (<1%), while in hESCs the percentage of EPA was approximately 4.0% in cells cultured at 5% oxygen and approximately 2.5% for those maintained under atmospheric oxygen. The relatively low percentage of EPA was expected, as similar results were observed in other cells and tissues, such as red blood cells (<1%), platelets (~1.5%) (Risé *et al.*, 2007), sperm (1.2%) (Lenzi *et al.*, 2000) or adipose tissue (<1%) (Garaulet *et al.*, 2006). Interestingly, EPA level in hESCs was significantly higher in cells cultured at 5% oxygen while in NT2 cells EPA was higher in cells cultured at 20% oxygen. EPA was found to be involved in neuronal differentiation in rat neural stem cells (Katakura *et al.*, 2013). Since NT2 cells are known to resemble neuronal progenitors and when induced with retinoic acid they differentiate into neurons (Pleasure and Lee, 1993), the increased level of EPA in NT2 cells cultured at 20% oxygen might be involved in enhancing neuronal progenitor-like properties of these cells.

Research on serum and adrenal glands of neonatal rats revealed that fatty acid content could be altered by exposure to hypoxia (Bruder *et al.*, 2004). The mechanism behind such changes is not known; however, it is hypothesised that it might involve altered cellular signalling and mitochondrial functions that lead to slightly different membrane composition (Bruder *et al.*, 2004). In the current study, the fatty acid composition was found to be altered by oxygen tension. However, dependent on the method used (absolute quantification or percentage of total fatty acids) different fatty acids were found to be altered in hESCs. Yet, EPA level was found to significantly increased in hESCs cultured at 5% oxygen compared to those maintained under atmospheric oxygen, regardless of the quantification method used. When measuring fatty acids, the percentage of total fatty acids provides information about the composition, while absolute quantification determines the exact amount in µg per million cells. The abundance of fatty acids

can also affect quantification results. The overall, total amount of fatty acids (absolute quantification) in hESCs cultured at either 5% or 20% oxygen was not statistically different; however, the amount of n-3 PUFAs was significantly higher in cells maintained under hypoxic conditions. Since the abundance of n-3 PUFAs is relatively low (around 3 μg/10^6 cells in hESCs cultured at 5% oxygen compared to 2 μg/10^6 cells in cells maintained at 20% oxygen), this difference is too small to alter the total amount of fatty acids in the cell.

Percentage of EDA was significantly lower in hESCs cultured at 5% oxygen compared to 20% oxygen while linoleic acid (18:2n-6) exhibited a trend toward being significantly increased in cells cultured in hypoxia compared to normoxia. EDA is a product of the conversion of linoleic acid by elongase. These data suggest that in hypoxia, elongation of linoleic acid to EDA is decreased. Linoleic acid can also be converted to γ-linolenic acid through a desaturation process catalysed by Δ6-desaturase. This induces competition between Δ6-desaturase and elongase for the substrate, linoleic acid. These results indicate that cells maintained in low oxygen tension might prefer conversion of linoleic acid to γ-linolenic acid over biosynthesis of EDA or no conversion at all. Unfortunately, little is known about the biological role of EDA; however, in murine macrophages, EDA is involved in the regulation of pro-inflammatory mediators by promoting the production of prostaglandin E_2 (PGE_2) while reducing the production of nitric oxide (Huang *et al.*, 2011). It is not clear whether EDA might have an effect on nitric oxide or PGE_2 production in hESCs as demonstrated in murine macrophages, and why that would be dependent on oxygen tension.

EPA level was significantly higher in hESCs cultured in hypoxic conditions compared to those maintained under normoxia. While the role of EPA in hESCs is still not fully understood, in mESCs and mouse multipotent stem cells, EPA is involved in supporting the differentiation process. The mechanism is not well known; however, EPA might be a necessary component of the membrane recognised by n-3 receptors that can induce signalling cascades (Shabani *et al.*, 2015; Rossi *et al.*, 2017). mESCs and hESCs share some similarities, for example, up-regulation of OCT4 compared to differentiated cells, but obviously, some properties are characteristic only for a particular cell type and origin (Ginis *et al.*, 2004). It is an intriguing finding that cells maintained under low oxygen tension have a higher content of EPA, especially since hESCs cultured at 5% oxygen exhibit better properties, i.e. less spontaneous differentiation or upregulation of self-renewal markers, such as OCT4, SOX2 or NANOG (Ezashi *et al.*, 2005; Forristal *et al.*, 2010) compared to cells maintained under atmospheric oxygen. In the current study, there was an increased expression of D5D at 5% oxygen suggesting a higher capacity to synthesise EPA from its precursors when oxygen levels decline. The bioconversion to AA (arachidonic acid) is also catalysed by D5D and AA level was found to be significantly increased in hypoxic conditions based on absolute quantification results. A higher EPA level may also be a way to control the level of AA, suggesting a protective role of

EPA in hESCs maintained under hypoxic conditions. AA is a precursor for the synthesis of proinflammatory lipid mediators, such as PGE_2 and leukotriene B_4 (LTB_4). PGE_2 is necessary for hESC differentiation towards mesoderm (Zhang *et al.*, 2018a), and therefore a high level of this bioactive lipid is not desired for maintaining undifferentiated hESCs. AA was shown to stimulate vasculogenesis (Huang *et al.*, 2016) through PGE_2 production, which is recognised as a necessary compound in the activation of COX-2 activity that leads to vascular endothelial growth factor (VEGF) expression (Calviello *et al.*, 2004). EPA is an antagonist to AA and can inhibit the process of synthesis of PGE_2 and similar mediators (Caughey *et al.*, 1996). Moreover, EPA reduces the phosphorylation of ERK-1 and -2, both playing an important role in signalling pathways that cause VEGF overexpression (Calviello *et al.*, 2004). VEGF overexpression is not desired in a pluripotent population of stem cells as it may result in the differentiation of hESCs into endothelial cells (Nourse *et al.*, 2010). EPA might be an important inhibitor of the pro-differentiation activity of AA and thus helps to maintain stem cell pluripotency. AA is also responsible for an increase in the production of ROS in mESCs (Huang *et al.*, 2016). The significantly higher level of EPA in hESCs cultured at 5% oxygen compared to 20% oxygen might be connected to a mechanism reducing ROS production in hypoxic hESCs through inhibiting AA activity. Obtained results suggest a role of oxygen tension in the regulation of fatty acid biosynthesis in hESCs. However, it requires more investigation to understand why cells cultured at low oxygen tension prefer one conversion process to another and how such alterations could affect stem cell properties, such as the propensity for differentiation.

EPA is converted from eicosatetraenoic acid (20:4n-3) through a desaturation process catalysed by D5D. Thus, the availability of D5D might have an impact on the level of biosynthesised EPA. However, further investigation of its activity might be required. The higher expression level of D5D in hESCs cultured in hypoxia compared to normoxia might lead to an increased level of EPA, which could have a significant role in cell homeostasis in a low-level oxygen environment. D5D was found to be up-regulated in human colon cancer cells exposed to hypoxia (Lai *et al.*, 2016). In salmon hepatocytes exposed to hypoxia, D5D expression was also increased compared to control and was associated with changes in the fatty acid content, possibly as a response to maintain fatty acid and membrane homeostasis (Olufsen *et al.*, 2014). Increased expression of D5D in hESCs cultured at 5% oxygen might be also a mechanism supporting glycolysis. A recent study found that when aerobic respiration is impaired in mouse renal epithelial cells (therefore cells rely more on glycolysis) there is a novel mechanism for NAD^+ recycling through D5D and D6D activity (Kim *et al.*, 2019). Glycolysis continuously requires NAD^+, which is later reduced to NADH; the mitochondrial electron transport chain can regenerate NAD^+, however in hypoxic conditions this process is impaired. Nonetheless, the regeneration can be also facilitated through the reduction

of pyruvate to lactate. Desaturation catalysed by D5D and D6D requires NADH, which is regenerated into NAD^+ that can be used for glycolysis. The activity of desaturases also led to an increased content of PUFAs, including EPA (Kim *et al.*, 2019). The rate of flux through glycolysis in hESCs cultured at 5% oxygen is increased compared to hESCs cultured at 20% oxygen (Forristal *et al.*, 2013), as well as EPA level and D5D expression (chapter 4.4). Therefore, hESCs cultured in hypoxic conditions might promote higher expression of D5D to support NAD^+ requirements for highly glycolytic cells, which results in an increased level of EPA.

It was also hypothesised that increased expression of D5D in hESCs cultured at 5% oxygen might be connected to the self-renewal maintenance, as hypoxia is recognised to be beneficial for the maintenance of hESCs (Ezashi *et al.*, 2005; Forristal *et al.*, 2013). In the current study, when *FADS1* was silenced, expression of OCT4, SOX2 and NANOG was unaffected, suggesting that D5D is not directly involved in the maintenance of pluripotency in hESCs. It is an interesting result as it was shown that inhibition of D5D and D6D activity by curcumin and sesamin in mESCs promotes the pluripotent state. Oct4 and Nanog were up-regulated in mESCs compared to normal culture and neuronal differentiation was reduced when enzymatic activity was inhibited (Yanes *et al.*, 2010). In contrast, a study by Park *et al.* (2012) presented that D5D is significantly downregulated in neuroblastoma cells upon differentiation. This suggests that D5D might be important for the undifferentiated state, however, the specific role is not yet determined. Since the results of this thesis showed no regulation of self-renewal markers by D5D, the increased expression of this enzyme in hypoxic conditions might be directly or indirectly involved in reducing spontaneous differentiation in hESCs, observed in cells cultured at 5% oxygen (Ezashi *et al.*, 2005).

As D5D expression level was higher in hESCs cultured at 5% oxygen compared to 20%, it was investigated whether D5D expression is regulated by HIF2α, a known transcription factor stabilised during prolonged hypoxia (Forristal *et al.*, 2010; Petruzzelli *et al.*, 2014). It was shown that when HIF2α was silenced using siRNA, expression of the *FADS1* gene was repressed in human microvascular endothelial cells, suggesting regulation by HIF2α (Nauta *et al.*, 2017). This study provided similar results as Nauta *et al.* (2017), but also showed that HIF2α directly regulates the expression of *FADS1* by binding to a newly identified HRE site within the proximal promoter of *FADS1* in hypoxic hESCs. Ultimately, these results show that HIF2α is directly involved in regulating fatty acid metabolism.

Chapter 5 Effect of EPA on human embryonic stem cell self-renewal, proliferation and metabolic properties

5.1 Introduction

Fatty acids are mainly known as a source of energy (Lindsay, 2007) and a component of cell membranes (Nagy and Tiuca, 2017; de Carvalho and Caramujo, 2018). However, studies have shown that fatty acids are involved in various, complex cellular processes, such as cell signalling, regulation of gene expression and inflammatory responses (Calder, 2015; Fritsche, 2015; de Carvalho and Caramujo, 2018). At the whole-body level, altered intakes of certain fatty acids play a role in maintaining health and influencing disease risk (Nagakura *et al.*, 2000; Siscovick *et al.*, 2017; Sokola-Wysoczanska *et al.*, 2018). At a cellular level, polyunsaturated fatty acids (PUFAs) are known to alter membrane properties; for example, a higher content of n-3 and n-6 PUFAs in a membrane leads to increased fluidity (Frese *et al.*, 2016). As a consequence of this, increased membrane PUFA content can affect the permeability, effectiveness of transport processes as well as function of membrane-associated receptors and signalling proteins (Mead, 1984; Kogteva and Bezuglov, 1998). Moreover, some fatty acids are known to have a role in signalling through being a component of lipid rafts or by influencing formation and stability of rafts. Lipid rafts are structures within cell membranes that are responsible for initiating signal transduction (Simons and Toomre, 2000; Pike, 2003). N-3 PUFAs have been shown to alter raft function in several cell types including cancer cells (Schley *et al.*, 2007), neurones (Hashimoto *et al.*, 2005) and immune cells (Kim *et al.*, 2008; Hou *et al.*, 2016). Caveolae, a subdomain of lipid rafts, are flask-shaped structures within the cell membrane, highly enriched with caveolin-1 protein, responsible for lipid trafficking and regulating cell signalling (Galbiati *et al.*, 2000). Docosahexaenoic acid (DHA; 22:6n-3) was shown to have a role in regulating calcium influx in human endothelial cells that were subject to oxidative stress. One of the proteins forming the calcium ion channel, TRPC1, is associated with caveolar lipid rafts and upon DHA supplementation was displaced from caveolae leading to reduced calcium transport into the cell (Ye *et al.*, 2010). DHA was also responsible for the displacement of important inflammation signalling molecules, Src-family tyrosine kinases, such as Fyn and c-Yes, from caveolae in human retinal vascular endothelial cells (Chen *et al.*, 2007b). Supplementation of Jurkat T-cells with eicosapentaenoic acid (EPA; 20:5n-3), which is also a member of the n-3 PUFA family, caused changes in the unsaturation profile of lipid rafts which was associated with inhibited cell proliferation (Li *et al.*, 2006). Both EPA and DHA were also able

to affect the composition of lipid rafts in breast cancer cells causing signalling alterations in EGFR pathway leading to apoptosis (Field *et al.*, 2007).

Alterations in fatty acid composition can also regulate cell signalling through modulation of bioactive lipid mediators (Calviello *et al.*, 2013; Molfino *et al.*, 2017; So *et al.*, 2019). Lipid mediators are molecules derived from fatty acids (usually PUFAs) in response to external stimuli and have different properties depending on the type of PUFA they originate from (Bennett and Gilroy, 2016). As an example, lipid mediators derived from n-3 PUFAs, such as resolvins or protectins, are known to play a role in the resolution of inflammation. They act through various mechanisms, such as binding to regulatory proteins to modulate their activity or by indirectly regulating the transcription of enzymes involved in inflammation (Bazan, 2018; Serhan and Levy, 2018). Therefore, the availability of fatty acids is important to maintain homeostasis and fluctuations in such availability can alter cellular functions. Despite the focus on the role of PUFAs, saturated fatty acids have also been found to have a regulatory role in some cell types. A diet rich in saturated fatty acids leads to an increased expression of *PGC-1β* in mouse liver and mouse primary hepatocytes. *PGC-1β* coactivates sterol receptor element binding protein (SREBP) 1c and 1a, stimulating transcription of lipogenic genes, such as *FAS* or *SCD-1* (Lin *et al.*, 2005). Another study found that supplementation of mouse LM cells with saturated fatty acids causes inhibition of cell growth. Interestingly, when a mix of unsaturated fatty acids was added to the culture, this effect was abolished (Doi *et al.*, 1978). Various sources and studies claim that PUFAs either inhibit (Calviello *et al.*, 2000; Li *et al.*, 2006) or stimulate cell proliferation; for example linoleic acid positively regulates DNA synthesis and increases mESC number *in vitro* (Kim *et al.*, 2009). Other PUFAs, such as arachidonic acid (AA; 20:4n-6) and DHA were shown to increase the proliferation rate of rat neural stem/progenitor cells (Sakayori *et al.*, 2011).

There is increasing evidence that fatty acids might play a role in regulating the potency of stem cells. Supplementation of human pluripotent stem cell-derived cardiomyocytes with a mix of 105 µM palmitic acid, 81 µM oleic acid and 45 µM linoleic acid caused cell maturation that was characterised by a change in substrate utilisation from glucose to fatty acids (Yang *et al.*, 2019). Upon supplementation, β-oxidation-related genes were upregulated, and those responsible for fatty acid synthesis were downregulated (Yang *et al.*, 2019). In rat neuronal stem cells, supplementation of culture medium with DHA and EPA resulted in induction of cell differentiation (Katakura *et al.*, 2013). Supplementation of EPA and linoleic acid to mouse embryoid bodies was shown to induce vasculogenesis and ROS generation (Taha *et al.*, 2020). However, in mESCs with increased levels of n-3 PUFAs, the rate of cell proliferation was lower but pluripotency was not altered (Wei *et al.*, 2018). These contradictory observations suggest that the effect of individual PUFAs might be specific to a particular cell line or set of experimental conditions.

In addition to being a source of energy, some fatty acids can alter cell metabolism. Supplementation of EPA and DHA to a mouse myoblast cell line decreased metabolism, which was characterised by suppressed expression of genes related to mitochondrial function and biogenesis as well as reduced oxygen consumption rate compared to cells that were cultured without addition of exogenous PUFAs (Hsueh *et al.*, 2018). However, in human rhabdomyosarcoma cells, n-3 PUFA supplementation caused increased oxygen consumption as well as enhanced glycolytic capacity when compared to control (Vaughan *et al.*, 2012). Glucose utilisation is facilitated by glucose transporters. Glucose transporter 1 (GLUT1) protein expression, as well as the rate of glucose transport, was found to be increased in rat brain endothelial cells upon supplementation with DHA and EPA (Pifferi *et al.*, 2010). In contrast, another study found that the brains of rats fed a diet rich in n-3 PUFAs displayed an increased glucose uptake in the absence of any effect on GLUT1 and GLUT3 protein expression compared to control (Ximenes-Da-Silva *et al.*, 2002). These investigators speculated that n-3 PUFAs might alter the function and efficiency of glucose transporters but not regulate their expression (Ximenes-Da-Silva *et al.*, 2002).

The effect of EPA supplementation has been tested in various cancer cell types. In U937 leukaemia cells, 100 μM EPA was found to induce apoptosis, inhibit proliferation, but also, interestingly, to play a role in regulating gene expression (Ceccarelli *et al.*, 2011). EPA supplementation caused DNA demethylation resulting in re-expression of the tumour suppressor gene CCAAT/enhancer-binding protein δ (C/EBPδ), a transcription factor that regulates monocyte lineage-specific target genes (Ceccarelli *et al.*, 2011). EPA was also found to alter proliferation and apoptosis in other cancer cell lines (Finstad *et al.*, 1994; Finstad *et al.*, 1998; Finstad *et al.*, 2000) as well as to induce ROS generation (Fahrmann and Hardman, 2013; Fukui *et al.*, 2013). This evidence suggests that EPA is involved in various processes and has a role in regulating several physiological responses in the cell.

Despite the in-depth knowledge of the role of EPA and the consequences of EPA supplementation in cancer cells, little is known about its function in ESCs, particularly hESCs. In chapter 4 it has been shown that the level of EPA is significantly higher in hESCs cultured in hypoxic conditions, compared to those maintained under atmospheric oxygen. hESCs cultured at 5% oxygen display increased proliferation and expression of OCT4, SOX2 and NANOG (Forristal *et al.*, 2010; Forristal *et al.*, 2013) and the higher EPA content might have a role in regulating cellular responses to oxygen. Thus, it was hypothesised that the higher level of EPA increases the rate of flux through glycolysis, proliferation, ROS generation and the self-renewal in hESCs cultured at 20% oxygen.

5.2 Chapter aims

The aim of this chapter was to investigate the role of EPA on self-renewal, proliferation, ROS generation and regulation of metabolism in hESCs.

Specific aims were:

- To investigate whether the fatty acid composition of hESC medium is altered by conditioning on iMEFs using gas chromatography.
- To test a range of EPA concentrations that can be supplemented to hESCs cultured at 20% oxygen.
- To investigate the effect of EPA supplementation on the self-renewal of hESCs cultured at 20% oxygen using Western blotting.
- To examine the effect of EPA supplementation on the proliferation of hESCs cultured at 20% oxygen using Ki-67 labelling.
- To investigate the effect of EPA supplementation on the generation of ROS by hESCs cultured at 20% oxygen using immunocytochemistry analysis and flow cytometry.
- To investigate whether EPA is involved in regulating the expression of glucose transporters and flux through glycolysis in hESCs cultured at 20% oxygen using Western blotting and metabolic assays respectively.
- To examine the effect of EPA supplementation on Δ5-desaturase (D5D) and caveolin-1 protein expression in hESCs cultured at 20% oxygen using immunocytochemistry and Western blotting.

5.3 Materials and methods

5.3.1 Supplementation of medium with EPA

hESCs cultured at 20% oxygen were supplemented with EPA (eicosapentaenoic acid; Sigma) for 48 hours with medium changed each day. CM (conditioned medium) containing EPA in 0.1% ethanol was added to the cells; EPA was used at three different concentrations: 15 µM, 30 µM and 50 µM to establish an appropriate concentration for use with hESCs. On the third day post-passage, cells were collected for analysis by gas chromatography (chapter 2.6) to determine whether EPA was successfully incorporated.

5.3.2 Ki-67 cell proliferation assay

hESCs were cultured in 12-well plates at 20% oxygen and incubated in the presence or absence of 30 µM EPA. After 48 hours of incubation immunocytochemistry for Ki-67 was performed (chapter 2.3). Ki-67 (Abcam; ab15580) was used as a primary antibody, and the secondary antibody was goat anti-rabbit, Alexa 488 (Molecular Probes; A-11008). Ki-67 positive staining was counted in cells cultured with CM containing 30 µM EPA and in cells incubated with standard CM containing 0.1% ethanol (0 µM EPA).

5.3.3 Detection of reactive oxygen species

hESCs were cultured in 12-well plates at 20% oxygen and incubated in the presence or absence of 30 µM EPA. After 48 hours of incubation with EPA, cells were subject to reactive oxygen species assay, which was performed using a commercially available kit (Image- iT live green reactive oxygen species detection kit; Molecular Probes). Two wells per plate were used for positive control. ROS production was induced in positive control cells by applying 1 ml of 100 µM tert-butyl hydroperoxide (TBHP) solution in CM per well and incubated at 37ºC for 1 hour. Tested cells (0 µM EPA- control cells and cells supplemented with 30 µM EPA) and positive control cells were gently washed with warm Hank's balanced salt solution/Ca/Mg (HBSS/Ca/Mg, free of phenol red, Gibco) before adding, in the dark, 1 ml of 25 µM carboxy-H_2DCFDA solution in HBSS/Ca/Mg per well. Cells were then incubated for 30 minutes at 37ºC protected from light. During the last 5 minutes of the incubation, 1 µM of Hoechst 33342 stain was added to each well. Cells were gently washed three times in warm HBSS/Ca/Mg before viewing with a Zeiss fluorescence microscope and imaged using AxioVision software (Zeiss).

5.3.4 Flow cytometry

Reactive oxygen species assay was performed as described in section 5.3.3 on hESCs cultured at 20% oxygen supplemented with 30 µM or 0 µM EPA for 48 hours with medium changed every 24 hours. Unstained cells ('blank') were also collected and were used to monitor the autofluorescence of the cells. Cells were washed with PBS and 0.5 ml of trypsin-EDTA (0.05%) was added to each well. Cells were incubated for 4-5 minutes at 37ºC and 0.5 ml of CM medium was added. Cells were gently scraped, collected into a tube and centrifuged for 4 minutes at 450 x *g*. The cell pellet was resuspended in 1 ml of PBS. Samples were processed immediately. 100 µl of the sample was further resuspended in 100 µl PBS and vortexed before loading into a flow cytometer. The presence of ROS was determined using the oxidation product of carboxy-H_2DCFA that has excitation/emission maxima of approximately 495/529 nm. Data were acquired using a

FACSCalibur flow cytometer measuring fluorescence in the FL1 channel (FITC). Typically, data from 10,000 events/sample were recorded using CellQuest software. Cells of interest were gated on light scattering properties (forward-scattered light (FSC) vs side-scattered light (SSC)), excluding cell debris and analysis was based on a distinguished population of hESCs. Weasel software (Battye, 2015) was used for the analysis of flow cytometry data.

5.3.5 Glucose assay

hESCs cultured at 20% oxygen were cultured in 12-well plates and incubated in CM supplemented with 30 µM or 0 µM EPA for 48 hours with medium changed every 24 hours. The same batch of CM was used for all glucose assays. The medium was collected on the 3rd day post-passage; 0.5 ml of trypsin-EDTA (0.05%) was added to cells and incubated for 4-5 minutes at 37°C, causing cell dissociation. A haemocytometer was used to count the cell number. Collected media were stored at -80°C until assayed. EPPS buffer was prepared by dissolving EPPS in dH_2O to a concentration of 50 mM. The pH of the solution was adjusted to 8.0 with 1 M NaOH. 10 mg of penicillin and 10 mg of streptomycin was added and EPPS buffer was stored at 4°C. Glucose assay cocktail was prepared as shown in Table 5.1 aliquoted and stored at -20°C. Glucose standards were prepared by dissolving D-glucose in dH_2O to a concentration of 0.1 mM, 0.2 mM, 0.4 mM, 0.6 mM, 0.8 mM, 1 mM and 1.2 mM and used to produce a standard curve (Figure 5.1).

Table 5.1 **Composition of glucose assay cocktail.**

The concentration provided is for stock solution.

Component		**Volume**
EPPS buffer	Solution in dH_2O	15 ml
5 mM Dithiothreitol		2 ml
37 mM $MgSO_4$		2 ml
10 mM ATP		1 ml
10 mM NADP		3 ml
340 U/ml Hexokinase/ 170 U/ml G6PDH		1 ml

45 µl of glucose assay cocktail was added to wells of a flat-bottomed 96-well plate, before adding 5 µl of glucose standard and samples. After 10 minutes of incubation, fluorescence was measured

at 460 nm for each sample after excitation of NADPH at 340 nm using a FLUOstar Optima microplate reader (BMG Labtech) and Optima software. The glucose concentration of the medium samples was calculated from the glucose standard curve (Figure 5.1).

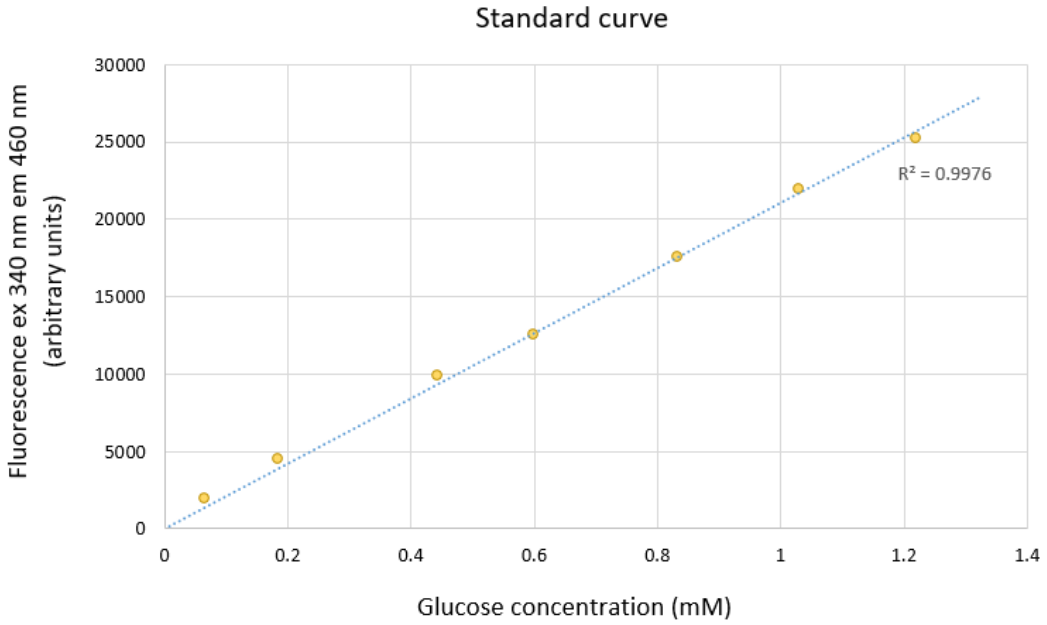

Figure 5.1 **Representative standard curve of glucose standards concentration determined using the glucose assay.**

5.3.6 Lactate assay

Media collected as described in 5.3.5 were also subject to lactate assay. Lactate standards were prepared out of commercially available lactate standard (concentration 8 mM) by diluting it with dH_2O to the concentration of 0.1 mM, 0.2 mM, 0.4 mM, 0.6 mM, 0.8 mM and 1 mM and used to produce a standard curve (Figure 5.2). Glycine buffer was prepared and consisted of 1 M glycine, 0.4 M hydrazine sulphate and 7 mM EDTA dissolved in 100 ml of dH_2O, pH adjusted to 9.4. 45 µl of lactate assay cocktail (Table 5.2) was added to sufficient wells of a flat-bottomed 96-well plate, before adding 5 µl of lactate standard and samples. After incubation for 25 minutes, fluorescence was measured at 460 nm for each sample after excitation of NADH at 340 nm using a FLUOstar Optima microplate reader (BMG Labtech) and Optima software. The lactate concentration of the medium samples was calculated from the glucose standard curve (Figure 5.2).

Table 5.2 **Composition of lactate assay cocktail.**

The concentration provided is for stock solution.

Component	**Volume**
Glycine buffer	9 ml
dH_2O	8 ml
15 mM NAD^+	1.5 ml
550 U/mg Lactate dehydrogenase	0.5 ml

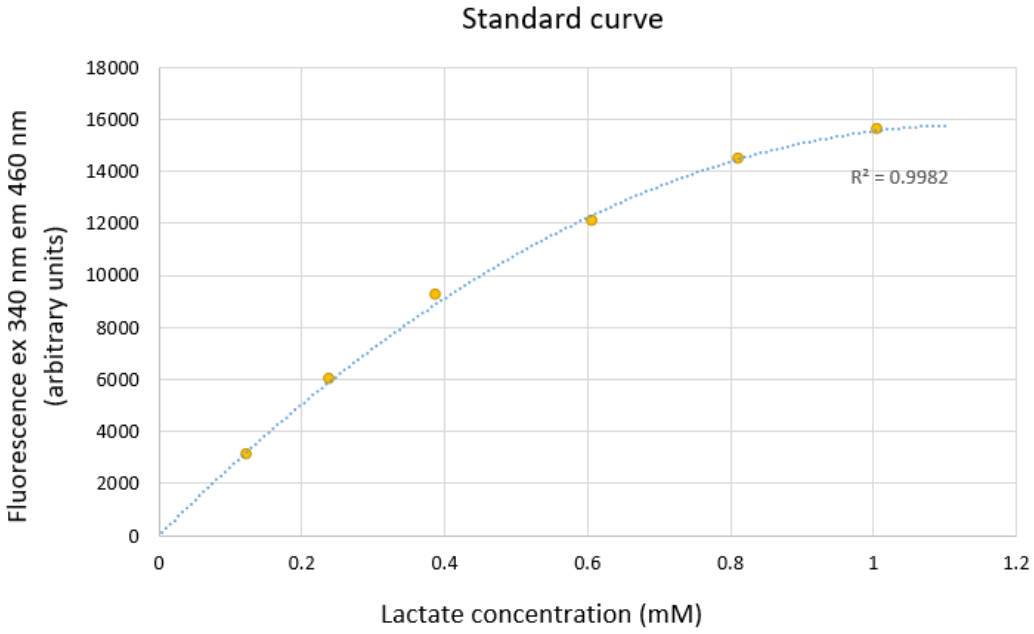

Figure 5.2 **Representative standard curve of lactate standards concentration determined using the lactate assay.**

5.3.7 Statistical analysis

Statistical analysis was performed using unpaired Student t-test or 2 way-ANOVA (section 5.5) in GraphPad Prism 7 software. Protein expression quantified based on Western blot results was normalised to β-actin and to a value of 1 for hESCs cultured at 20% oxygen without EPA supplementation. A value of $p<0.05$ was considered significant. All data represent at least 3 independent experiments and are presented as mean + SEM unless specified otherwise.

5.4 Results

5.4.1 The fatty acid composition of hESC medium and conditioned medium

Conditioning hESC medium on iMEFs for 24 hours prior to use was shown to enrich medium with nutrients, cytokines and growth factors necessary for maintaining an undifferentiated pluripotent culture of hESCs (Jozefczuk *et al.*, 2012; Villa-Diaz *et al.*, 2013). However, it was not known whether and how conditioning medium on iMEFs might impact the fatty acid composition of the medium. To investigate that, the fatty acid content of hESC medium and medium conditioned on iMEFs (CM) for 24 hours was measured using gas chromatography.

21 fatty acids were identified and quantified; results expressed as a percentage of total fatty acids revealed that hESC medium and CM were rich in 16:0, 18:0, 18:1n-9, 18:2n-6 and 18:3n-3, which together made up approximately 90%. There was a significant increase in the percentage of one of the abundant fatty acids, oleic acid 18:1n-9 ($p<0.05$) in CM compared to hESC medium (Figure 5.3 A). Percentages of arachidic acid 20:0 ($p=0.008$), gadoleic acid 20:1n-9 ($p=0.009$) and EPA 20:5n-3 ($p<0.001$) were also significantly increased in CM compared to hESC medium (Figure 5.3 B). In contrast, percentages of dihomo-γ-linolenic acid (DGLA) 20:3n-6 ($p<0.001$) and docosapentaenoic acid (DPA) 22:5n-3 ($p=0.005$) were decreased significantly in CM compared to hESC medium (Figure 5.3 B).

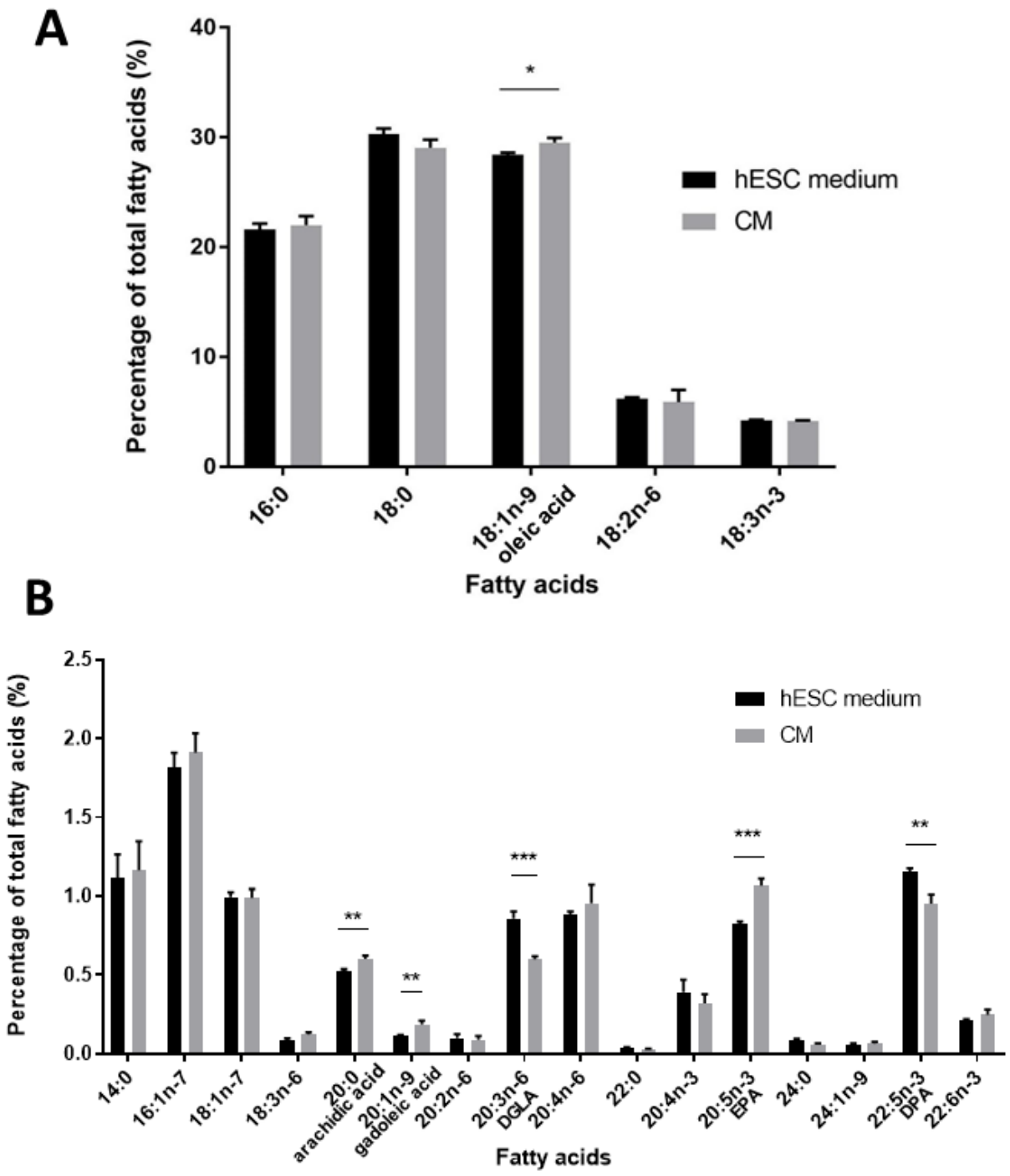

Figure 5.3 **Conditioning hESC medium on irradiated MEFs alters the fatty acid composition when expressed as a percentage of total fatty acids.**

Percentage of total fatty acids higher than 4% (A) and lower than 4% (B) in hESC medium compared to CM. hESC medium was conditioned on iMEFs for 24 hours. DGLA- dihomo-γ-linolenic acid; EPA- eicosapentaenoic acid; DPA- docosapentaenoic acid. Bars represent mean + SEM. *P<0.05, **P<0.01, ***P<0.001 significantly different between hESC medium and CM. n=7.

The gas chromatography results of fatty acid content in hESC medium compared to CM were also analysed based on the molar concentration of fatty acids (µM). Fatty acids 16:0, 18:0, 18:1n-9, 18:2n-6, 18:3n-3 had a high concentration (concentration higher than 30 µM) in hESC medium as well as in CM (Figure 5.4 A). Concentrations of all individual measured fatty acids were similar between hESC medium and CM; statistical tests revealed that there were no significant differences in the concentration of fatty acids between hESC medium and CM (Figure 5.4). EPA is present in both, hESC medium and CM, and concentration of this fatty acid was found to be approximately 6 µM in hESC medium and approximately 8 µM in CM (Figure 5.4 B).

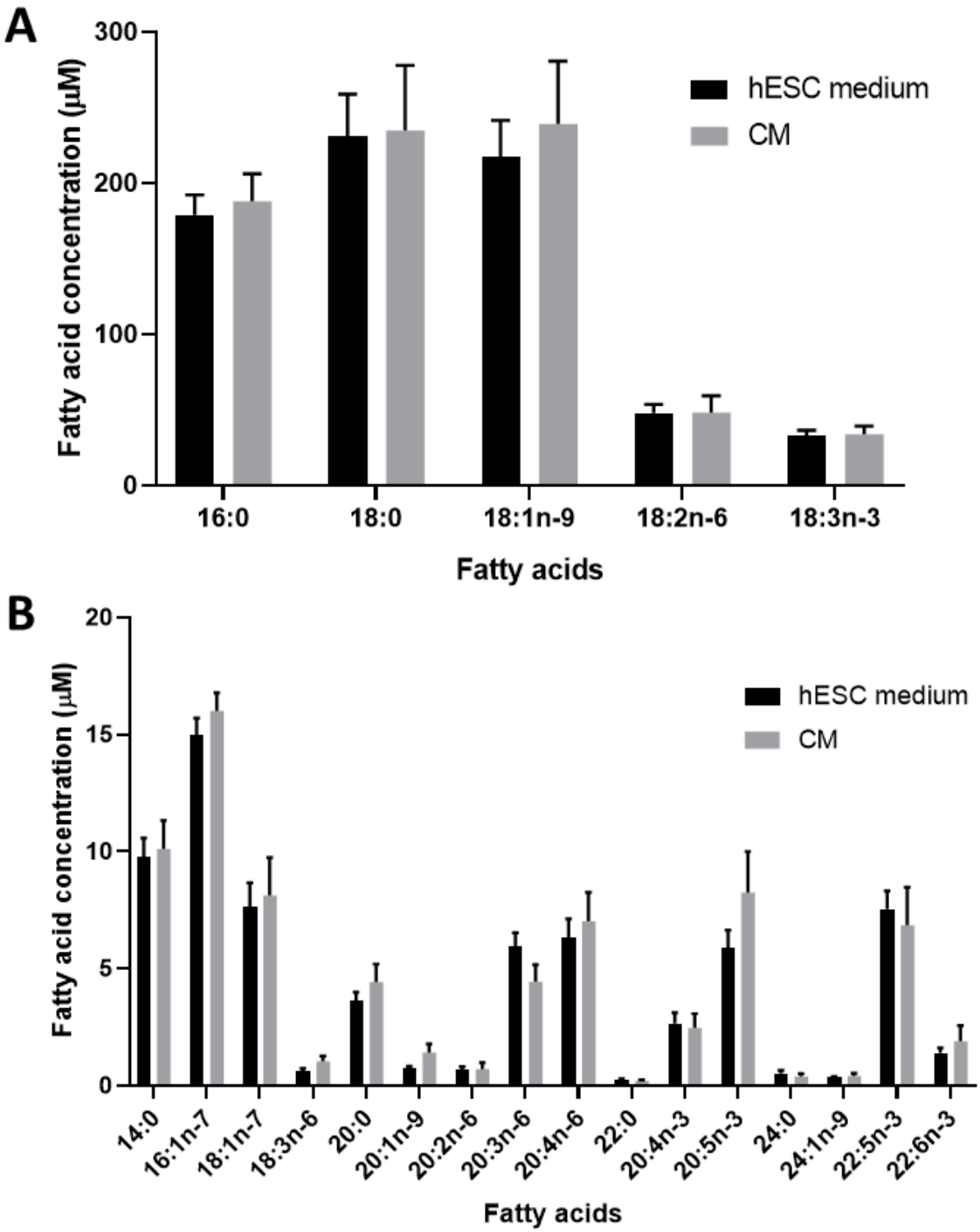

Figure 5.4 **Conditioning hESC medium with mitotically inactive MEFs does not affect the concentration of individual fatty acids.**

Individual fatty acids with a concentration that is higher than 30 µM (A) and lower than 30 µM (B) in hESC medium compared to CM. The medium was conditioned on iMEFs for 24 hours. Bars represent mean + SEM. n=7.

There was no statistical difference in fatty acid concentration of hESC medium or CM when concentration was expressed in µg/ml (Appendix 4).

5.4.2 Supplementation of hESC culture medium with EPA

EPA level was found to be significantly increased in hESCs cultured at 5% oxygen compared to those maintained at 20% oxygen (chapter 4.4.2). It was investigated whether beneficial properties of hESCs cultured in hypoxic conditions were related to the elevated level of EPA compared to hESCs cultured in normoxia. Thus, hESCs cultured at 20% oxygen were supplemented with EPA to investigate the role of this fatty acid on cell properties. Three different EPA concentrations, 15 µM, 30 µM and 50 µM, were supplemented to CM, which was changed every 24 hours. The total incubation time of cells in CM supplemented with EPA was 48 hours. The effect of each EPA concentration on hESC viability and potential cytotoxicity was investigated by monitoring cell morphology. Cells supplemented with 0 µM EPA, 15 µM EPA, 30 µM EPA and 50 µM EPA displayed good morphology and proliferation and no noticeable differences were observed between any of the groups. (Figure 5.5).

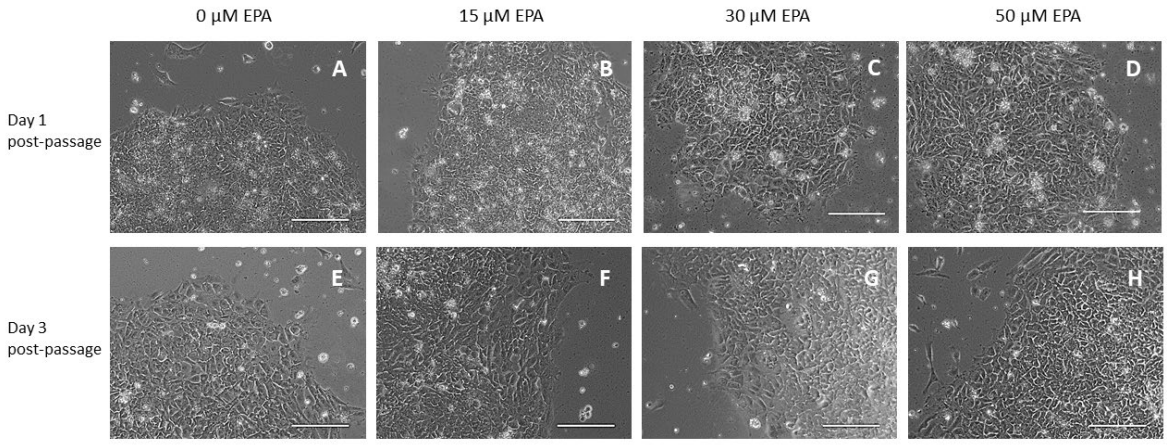

Figure 5.5 **Morphology of hESCs cultured at 20% oxygen and supplemented with EPA.**

Representative phase contrast images of hESC colonies before EPA supplementation (A, B, C, D) and after 48 hours incubation in CM enriched with 0 µM EPA (E), 15 µM (F), 30 µM (G) or 50 µM (H) EPA. Scale bars indicate 200 µm.

Gas chromatography was performed to test whether supplemented EPA was successfully incorporated into the hESCs. Results showed that the concentration of EPA (20:5n-3) increased in a dose-dependent manner (Figure 5.6 A), therefore confirming the cellular intake of EPA. Interestingly, the addition of EPA changed the global fatty acid composition of the hESCs. There was a significant increase in the concentrations of palmitic acid 16:0, stearic acid 18:0, oleic acid 18:1n-9, and docosapentaenoic acid (DPA) 22:5n-3 as well as a decrease in the level of linoleic acid 18:2n-6 in hESCs supplemented with 15 µM, 30 µM and 50 µM compared to those cultured

at 20% oxygen with no additional EPA. However, EPA supplementation did not affect the other 14 fatty acids measured (Figure 5.6 B). The concentration of AA 20:4n-6 was decreased only when cells were supplemented with 50 μM EPA compared to control cells. There was no significant difference in the concentration of 18:0, 18:1n-9, 22:5n-3 and 18:2n-6 in hESCs supplemented with 30 μM EPA compared to hESCs supplemented with 50 μM EPA (Table 5.3). The broad increase in fatty acid concentration was observed upon supplementation with 30 μM EPA, while the addition of 50 μM did not induce an overall big difference compared to 30 μM. Therefore, 30 μM EPA was used for further experiments.

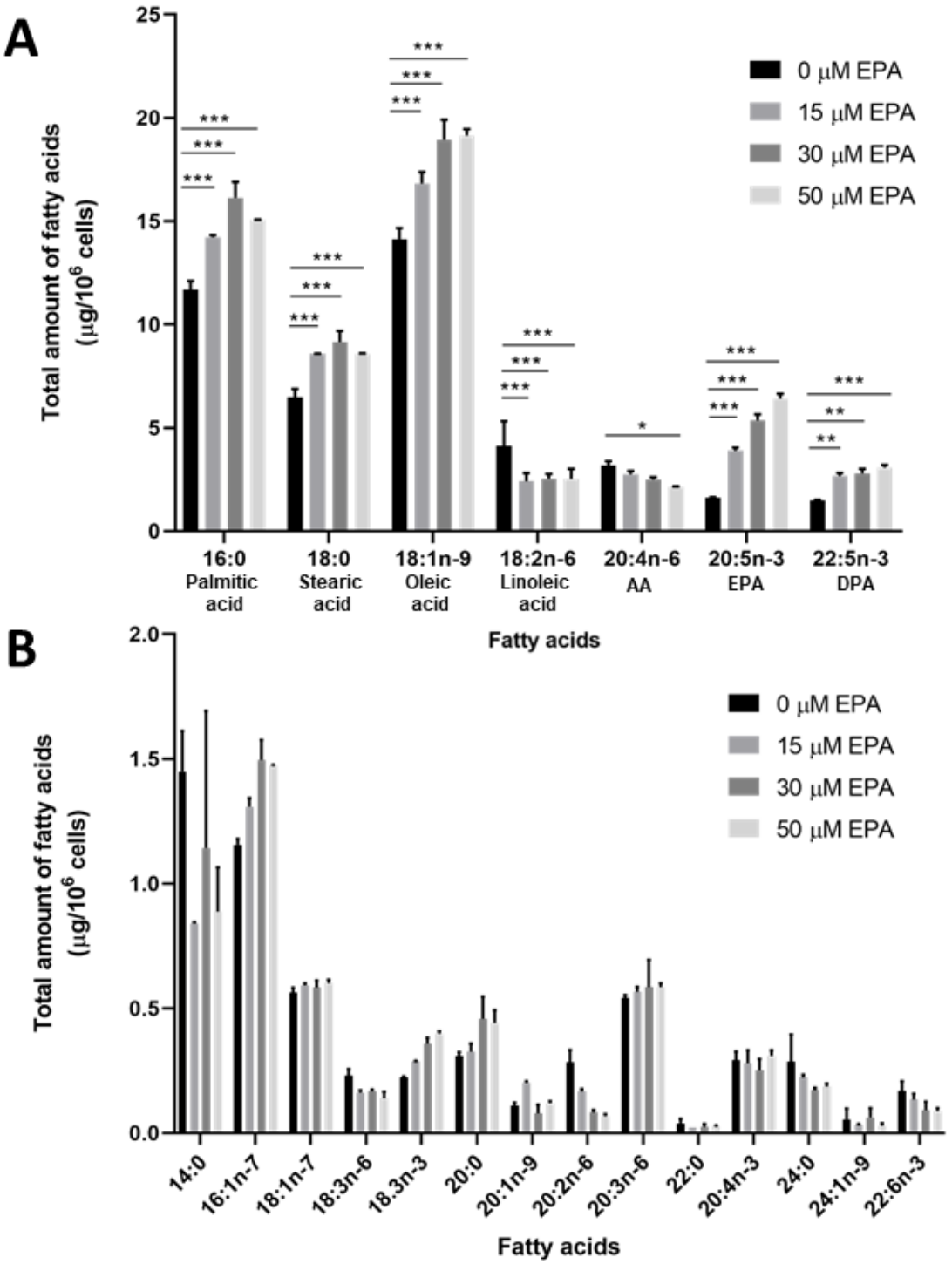

Figure 5.6 **hESCs cultured at 20% oxygen incorporated supplemented EPA.**

Individual fatty acids with a concentration higher than 1.5 µg/10^6 cells (A) and lower than 2 µg/10^6 cells (B) in hESCs cultured at 20% oxygen in CM supplemented with 0 µM EPA, 15 µM EPA, 30 µM EPA or 50 µM EPA for 48 hours. AA- arachidonic acid; EPA- eicosapentaenoic acid; DPA- docosapentaenoic acid. *P<0.05, **P<0.01, ***P<0.001 significantly different to 0 µM EPA. Bars represent mean + SEM. n=6 (2 replicates per condition).

Table 5.3 **Adjusted p-values for each comparison of supplemented EPA concentrations for previously identified significant fatty acids.**

Each row was used as a reference for increase/decrease comparisons. Grey colour indicates a significant increase (p-value <0.05) and yellow significant decrease between two supplemented EPA concentrations.

Fatty acid	EPA concentration	0 µM	15 µM	30 µM	50 µM
16:0	0 µM	-	<0.0001	<0.0001	<0.0001
	15 µM	<0.0001	-	<0.0001	0.0952
	30 µM	<0.0001	<0.0001	-	0.0229
	50 µM	<0.0001	0.0952	0.0229	-
18:0	0 µM	-	<0.0001	<0.0001	<0.0001
	15 µM	<0.0001	-	0.3869	>0.9999
	30 µM	<0.0001	0.3869	-	0.3678
	50 µM	<0.0001	>0.9999	0.3678	-
18:1n-9	0 µM	-	<0.0001	<0.0001	<0.0001
	15 µM	<0.0001	-	<0.0001	<0.0001
	30 µM	<0.0001	<0.0001	-	0.9332
	50 µM	<0.0001	<0.0001	0.9332	-
18:2n-6	0 µM	-	<0.0001	0.0002	0.0002
	15 µM	<0.0001	-	0.9828	0.9876
	30 µM	0.0002	0.9828	-	>0.9999
	50 µM	0.0002	0.9876	>0.9999	-
20:4n-6	0 µM	-	0.6206	0.2268	0.0237
	15 µM	0.6206	-	0.8932	0.3331
	30 µM	0.2268	0.8932	-	0.7582
	50 µM	0.0237	0.3331	0.7582	-
20:5n-3	0 µM	-	<0.0001	<0.0001	<0.0001
	15 µM	<0.0001	-	0.0006	<0.0001
	30 µM	<0.0001	0.0006	-	0.0244
	50 µM	<0.0001	<0.0001	0.0244	-
22:5n-3	0 µM	-	0.0074	0.0028	0.0002
	15 µM	0.0074	-	0.9898	0.7067
	30 µM	0.0028	0.9898	-	0.8697
	50 µM	0.0002	0.7067	0.8697	-

5.4.3 Effect of EPA on self-renewal abilities of hESCs

The expression of key pluripotency markers, OCT4, SOX2 and NANOG, was found to be significantly increased in hESCs cultured at 5% oxygen compared to those maintained at 20% oxygen (Forristal *et al.*, 2013). Environmental oxygen also altered the fatty acid composition of hESCs (Chapter 4.4.2). Since EPA level was also found to be increased in hESCs cultured at 5% oxygen compared to 20% oxygen (Chapter 4.4.2), it was investigated whether this change in fatty acid level might be involved in regulating the self-renewal. It was examined whether culturing hESCs at 20% oxygen but with a higher concentration of EPA might induce the increase in expression of pluripotency markers. Thus, the expression of OCT4, SOX2 and NANOG proteins were quantified in hESCs cultured at 20% oxygen in the presence or absence of supplemented 30 µM EPA. Using Western blotting, the addition of EPA was found to have no significant effect on the protein expression of OCT4, SOX2 and NANOG (Figure 5.7).

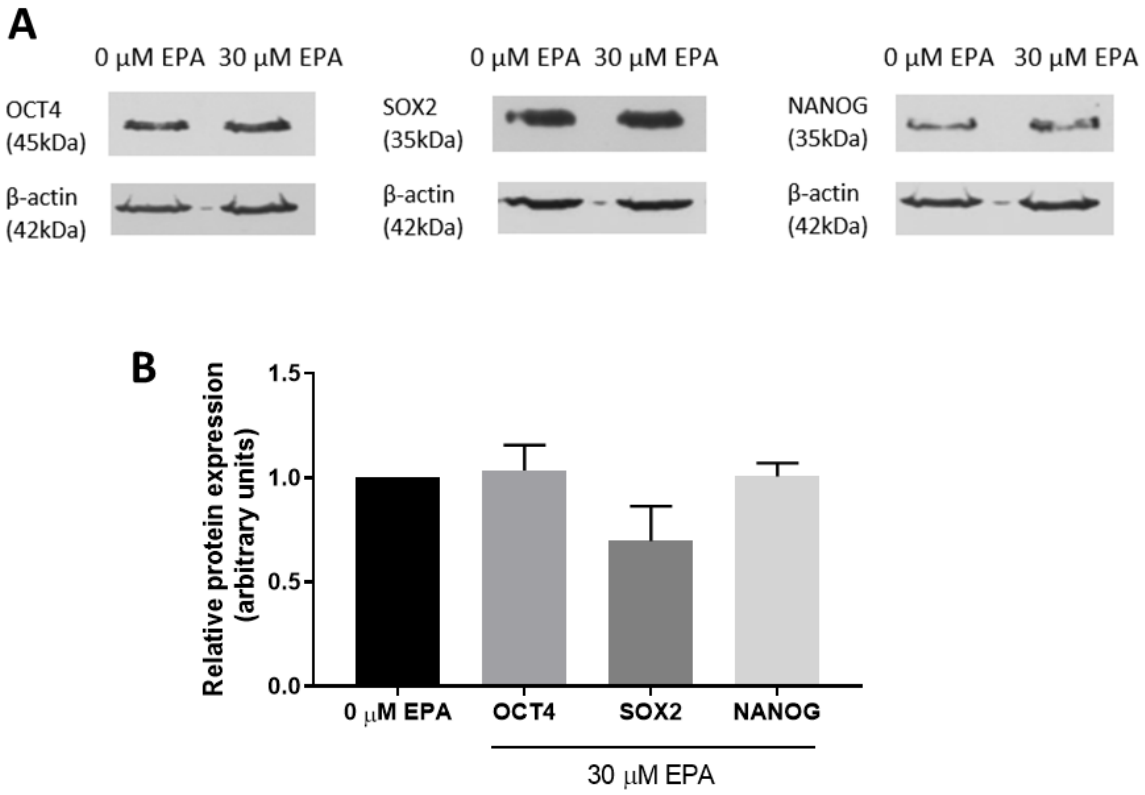

Figure 5.7 **EPA supplementation does not affect the expression of key proteins regulating self-renewal in hESCs cultured at 20% oxygen.**

Representative Western blot of OCT4, SOX2, NANOG and β-actin expression in hESCs cultured at 20% oxygen in the presence or absence of supplemented 30 µM EPA for 48 hours (A). Quantification of OCT4, SOX2 and NANOG protein expression (B). Data were normalized to β-actin and to 1 for 0 µM EPA. Bars represent mean + SEM. n=5

5.4.4 Effect of EPA on hESC proliferation

HESCs cultured at 5% oxygen were found to have a higher proliferation rate than those maintained at 20% oxygen (Forristal *et al.*, 2010). EPA level was also significantly increased in hESCs cultured at 5% oxygen compared to 20% oxygen. Thus, it was investigated whether EPA might play a role in cell proliferation.

Ki-67 protein was detected using immunocytochemistry in hESCs cultured at 20% oxygen and supplemented with either 0 µM or 30 µM EPA for 48 hours. Ki-67 is a protein expressed in phases of the active cell cycle (G1, S, G2 and M) and therefore it is used as a proliferation marker. More than 90% of cells per observation were positively stained for Ki-67 in hESCs cultured in the presence or absence of supplemented 30 µM EPA (Figure 5.8 A). Results showed that there was no significant difference in the percentage of cells stained positively for Ki-67 between hESCs cultured at 20% oxygen and supplemented with either 30 µM or 0 µM EPA (Figure 5.8 B).

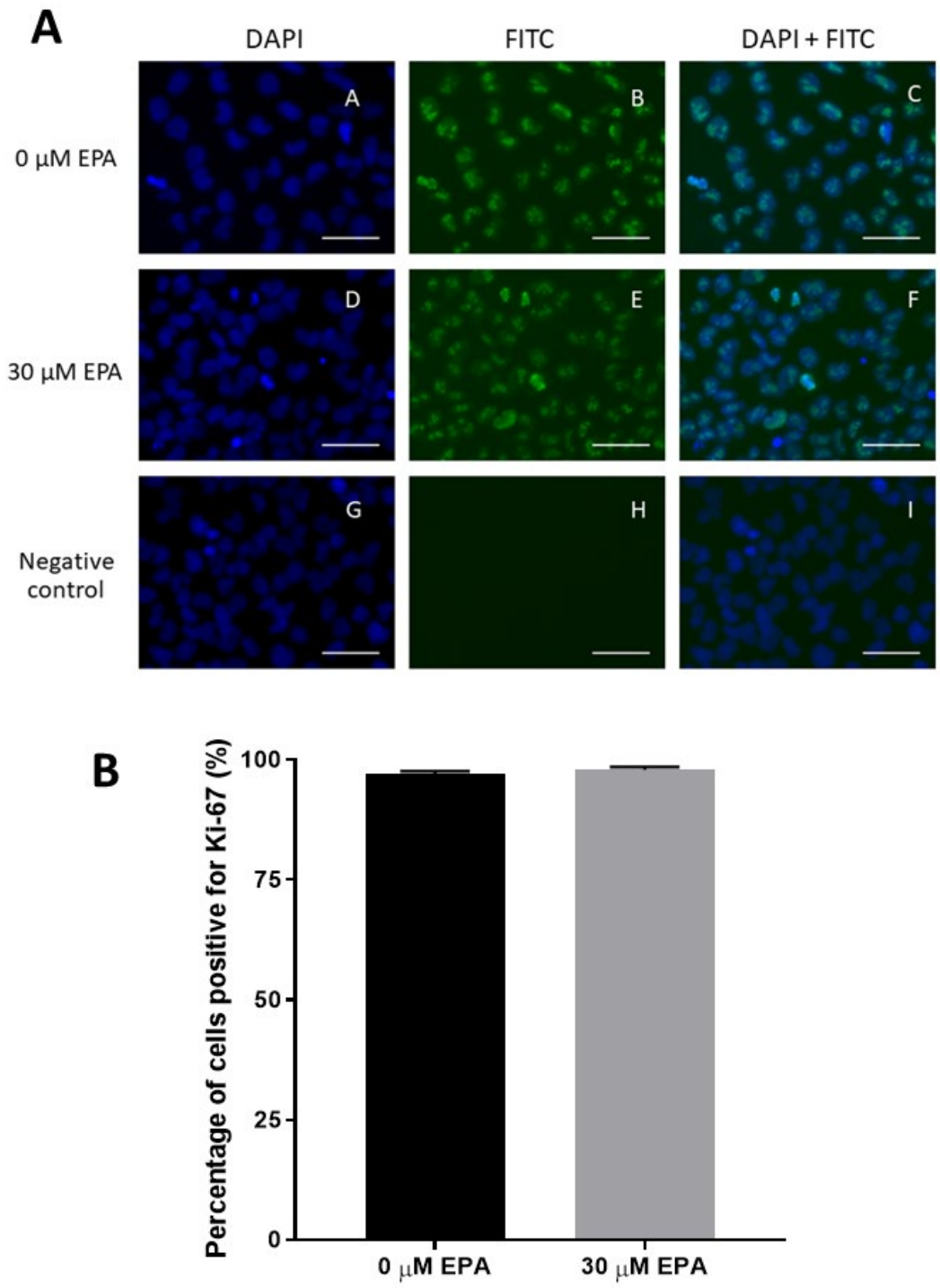

Figure 5.8 **EPA does not affect the proliferation rate of hESCs cultured at 20% oxygen.**

(A) Representative images of protein expression of Ki-67 in hESCs cultured at 20% oxygen (A-C) and supplemented with 30 µM EPA (D-F) for 48 hours. Images labelled with DAPI (blue; A, D, G) and FITC (green; B, E, H) were taken. Secondary antibody only, as a negative control, is shown in images G-I. Scale bars indicate 50 µm. (B) Quantification of Ki-67 positive cells of hESCs cultured at 20% oxygen and supplemented with either 0 µM or 30 µM EPA for 48 hours. Bars represent mean + SEM. n=3

5.4.5 Role of EPA on reactive oxygen species production by hESCs

Various studies found evidence that fatty acids, including EPA, are involved in positive regulation of ROS generation in cells (Fahrmann and Hardman, 2013; Fukui *et al.*, 2013). Therefore, it was examined whether EPA could play a similar role in hESCs.

The assay to detect ROS was performed on hESCs cultured at 20% oxygen in the presence and absence of supplemented 30 µM EPA for 48 hours. The technique was based on the use of 5-(and-6)-carboxy-2',7'-dichlorodihydrofluorescein diacetate (carboxy-H_2DCFDA), which produces a fluorescence signal when the acetate groups are removed by intracellular esterases and oxidation that is caused by ROS activity, hence it is known as a fluorogenic marker for ROS. Cells were analysed under a microscope to observe whether hESCs supplemented with EPA generated more ROS compared to cells cultured without additional EPA. hESCs supplemented with 30 µM EPA as well as with 0 µM EPA showed some fluorescence signal (Figure 5.9), however, it was not as bright as in cells treated with *tert*-butyl hydroperoxide (TBHP) to induce ROS production (positive control) (Figure 5.9 G-I). It was not possible to distinguish any overt difference in ROS generation between hESCs cultured at 20% oxygen in the presence or absence of additional EPA using immunocytochemistry.

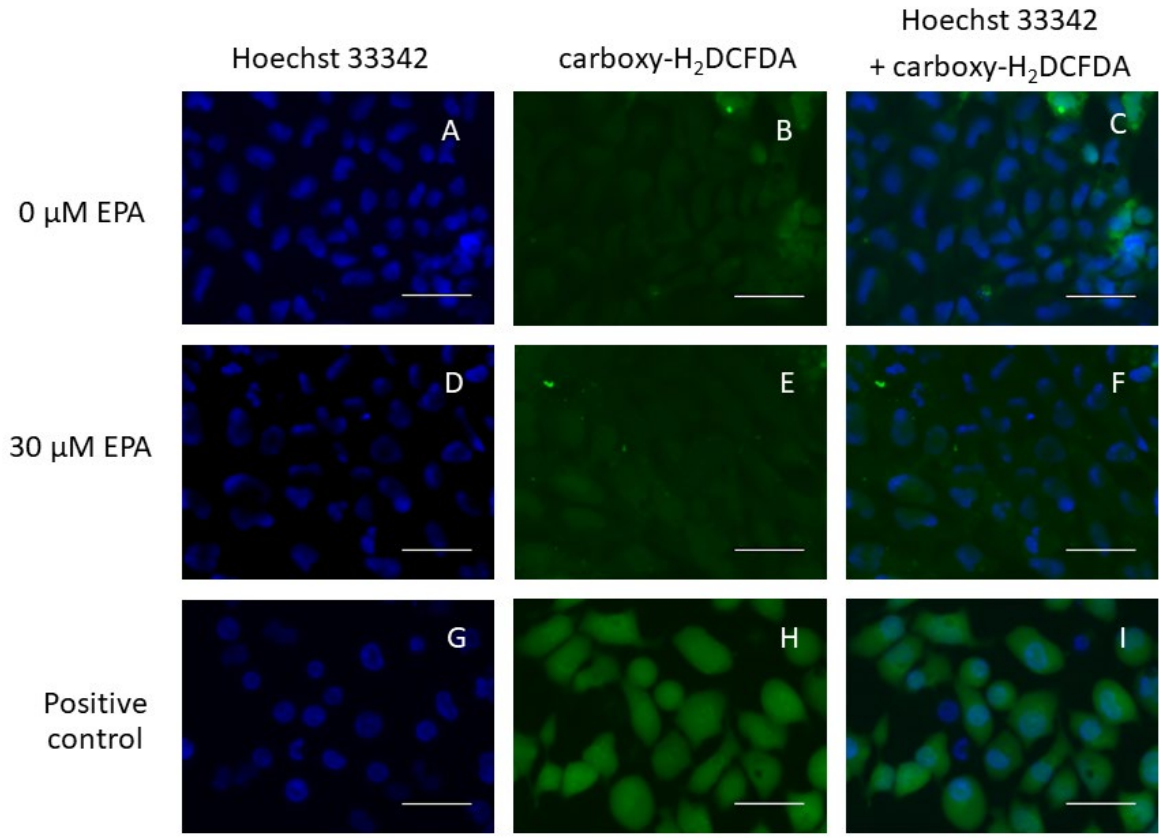

Figure 5.9 **hESCs cultured at 20% oxygen in the presence or absence of supplemented 30µM EPA generated low levels of ROS.**

Representative images of detected ROS in hESCs cultured at 20% oxygen (A-C) and supplemented with 30 µM EPA for 48 hours (D-F). Pictures of labelling with Hoechst 33342 (blue; A, D, G) and carboxy-H_2DCFDA (green; B, E, H) were taken. A positive control is shown in images G-I. Scale bars indicate 50 µm.

Flow cytometry was used to quantify ROS production. Samples used for flow cytometry were:

- 'blank' – unstained hESCs cultured in the presence or absence of supplemented 30 µM EPA; used to monitor the autofluorescence of the cells,
- 'carboxy-H_2DCFDA' – stained hESCs cultured in the presence or absence of supplemented 30 µM EPA that were subject to ROS assay based on carboxy-H_2DCFDA; used to detect ROS.

The population of interest was gated on cell morphology, based on light scattering properties (forward-scattered light (FSC) vs side-scattered light (SSC)), excluding cell debris (Figure 5.10). The gate was established semi-automatically using Weasel software and applied to all samples. The density plots, which were generated based on acquired data, revealed that samples were similar

between each other with reference to cell complexity/granularity and size as indicated by similar localisation of cells in the plot (Figure 5.10).

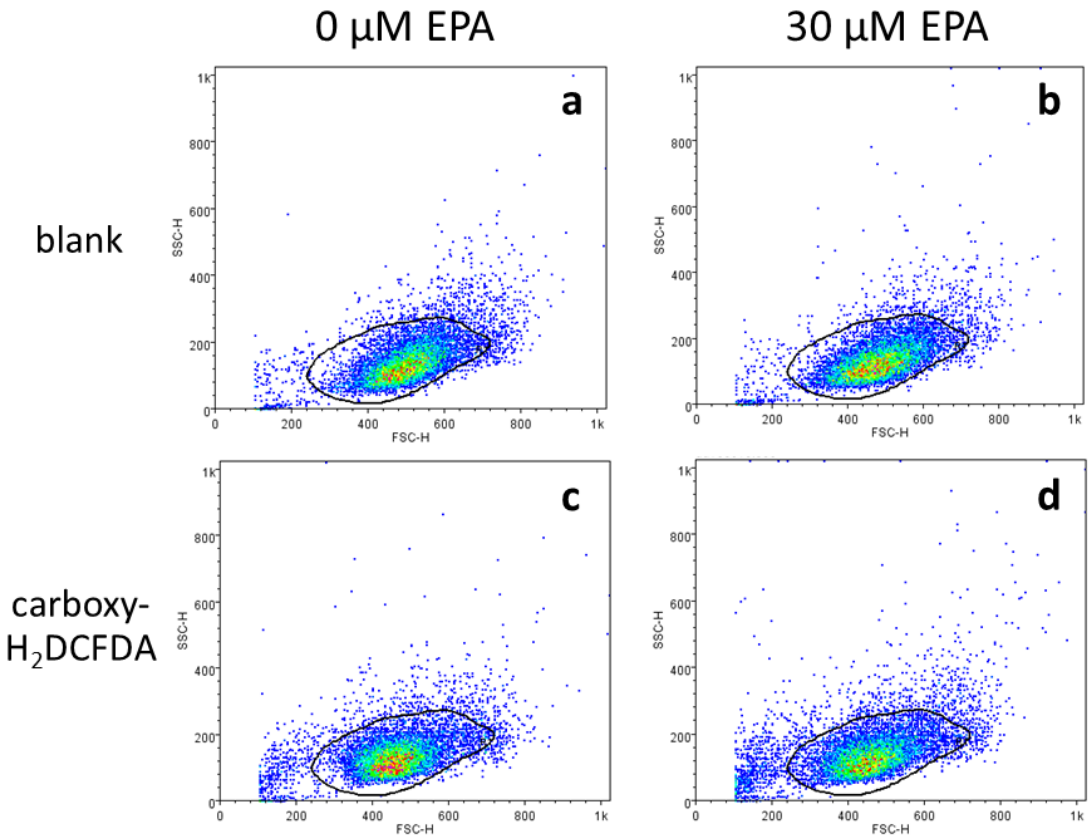

Figure 5.10 **Representative density plots of recorded events with gating of hESCs cultured at 20% oxygen in the presence or absence of supplemented 30 µM EPA.**

Representative FCS vs SSC density plots of events recorded by flow cytometry (10,000 events/sample) from samples of hESCs cultured at 20% oxygen in the presence (b, d) or absence (a, c) of 30 µM EPA supplemented for 48 hours. hESC samples cultured at 20% oxygen in the presence (b) or absence (a) of supplemented 30 µM EPA were used to monitor autofluorescence ('blank') or were subject to ROS assay ('carboxy-H_2DCFDA') (c, d). Cells of interest were gated on light scattering properties (FSC vs SSC), excluding cell debris, the gate was applied to all samples. SSC-H on y-axis represent side scatter- cell complexity/granularity; FSC-H on x-axis: forward scatter - cell size.

Analysis of flow cytometry results was based on the gated population. The flow cytometry results showed that the fluorescence intensity signal was similar between hESCs supplemented with 30 µM EPA compared to 0 µM EPA that were subject to ROS assay (carboxy-H_2DCFDA) (Figure 5.11

A). Flow cytometry analysis of 'blank' samples of hESCs cultured at 20% oxygen in the presence or absence of an additional 30 µM EPA in CM showed low fluorescence intensity (Figure 5.11 A). Results presented as percentage of cells producing ROS showed that nearly 80% of hESCs maintained at 20% oxygen in the absence of EPA were generating ROS, compared to approximately 83% of cells from samples of hESCs cultured in the presence of 30 µM EPA for 48 hours. Less than 1% of hESCs that were not dyed with carboxy-H_2DCFDA (blank) were found to produce ROS (Figure 5.11 B). This data suggest that EPA does not have any effect on ROS generation in hESCs cultured at 20% oxygen.

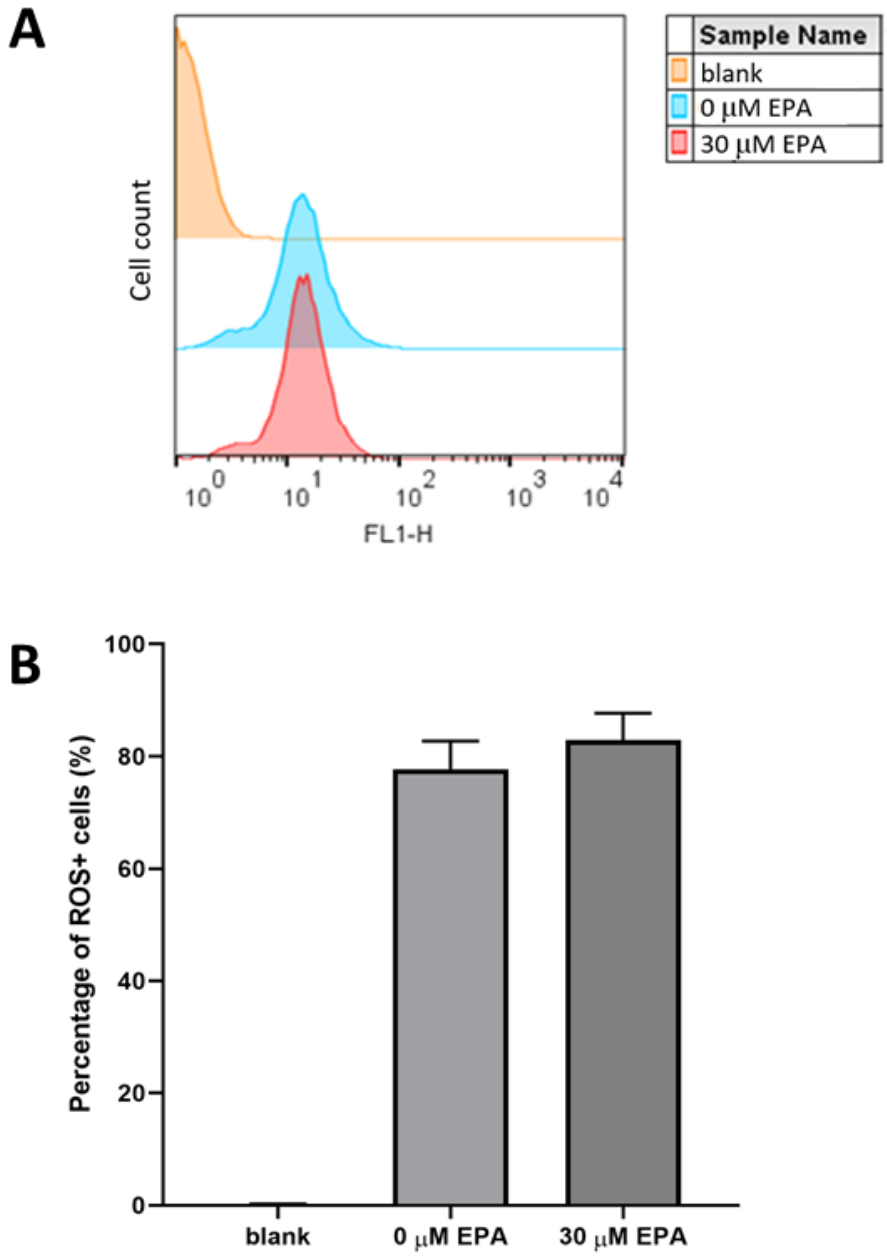

Figure 5.11 **EPA does not affect ROS generation in hESCs cultured at 20% oxygen.**

(A) Representative flow cytometric profiles of fluorescence intensity of hESCs cultured at 20% oxygen supplemented with 0 µM EPA (blue), 30 µM EPA for 48 hours (red) and blank (orange). Blank samples consisted of unstained cells (no ROS assay performed) to monitor the autofluorescence of cells. The x-axis FL1-H means the relative intensity of carboxy-H_2DCFDA fluorescence, which has excitation/emission maxima of approximately 495/529 nm. (B) Percentage of cells producing ROS was not significantly affected upon supplementation of hESCs cultured at 20% oxygen with 30 µM EPA for 48 hours. Bars represent mean + SEM. n=3

5.4.6 Effect of EPA on glucose transporter expression in hESCs cultured at 20% oxygen

There is emerging evidence (reviewed in section 5.1) that EPA might have an effect on glucose uptake and metabolism in cells (Ximenes-Da-Silva *et al.*, 2002; Pifferi *et al.*, 2010; Vaughan *et al.*, 2012). It was examined whether supplementation of hESCs cultured at 20% oxygen with 30 µM EPA alters expression of glucose transporters GLUT1 and GLUT3. GLUT3 is believed to be the main facilitator of the glucose uptake in hESCs (Christensen *et al.*, 2015) but also GLUT1 mRNA levels were found to be increased in hESCs cultured at 5% oxygen compared to 20% oxygen (Forristal *et al.*, 2013), therefore the effect of EPA supplementation on these two glucose transporters was investigated.

The protein expression level of GLUT1 in hESCs maintained under atmospheric oxygen and cultured in CM in the presence or absence of supplemented 30 µM EPA was investigated using Western blotting. The Western blotting result showed a single band at a size of approximately 55 kDa, which was identified as GLUT1 protein (Figure 5.12 A). The quantification of results revealed that there was no significant difference in the expression of GLUT1 in hESCs cultured at 20% oxygen in the presence or absence of supplemented 30 µM EPA (Figure 5.12 B).

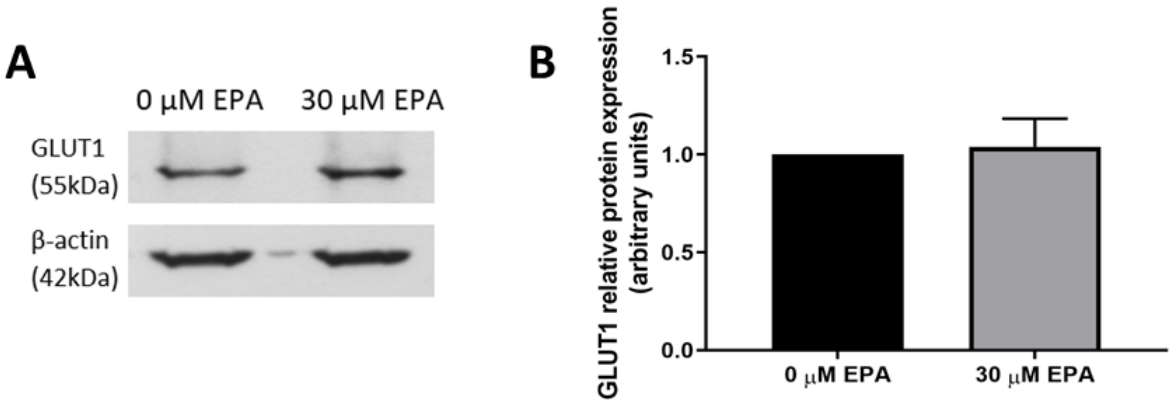

Figure 5.12 **EPA supplementation of hESCs cultured at 20% oxygen does not affect GLUT1 expression.**

(A) Representative Western blot of GLUT1 and β-actin in hESCs cultured at 20% oxygen and supplemented with ether 0 µM or 30 µM EPA for 48 hours. (B) Quantification of GLUT1 Western blotting results. Data were normalized to β-actin and to 1 for hESCs not supplemented with EPA. Bars represent mean + SEM. n=4

The expression of another glucose transporter, GLUT3, was analysed. Immunocytochemistry revealed that GLUT3 was expressed in the plasma membrane and intensity of fluorescence was higher in hESCs cultured in CM supplemented with 30 µM EPA compared to hESCs cultured in the absence of additional EPA (Figure 5.13).

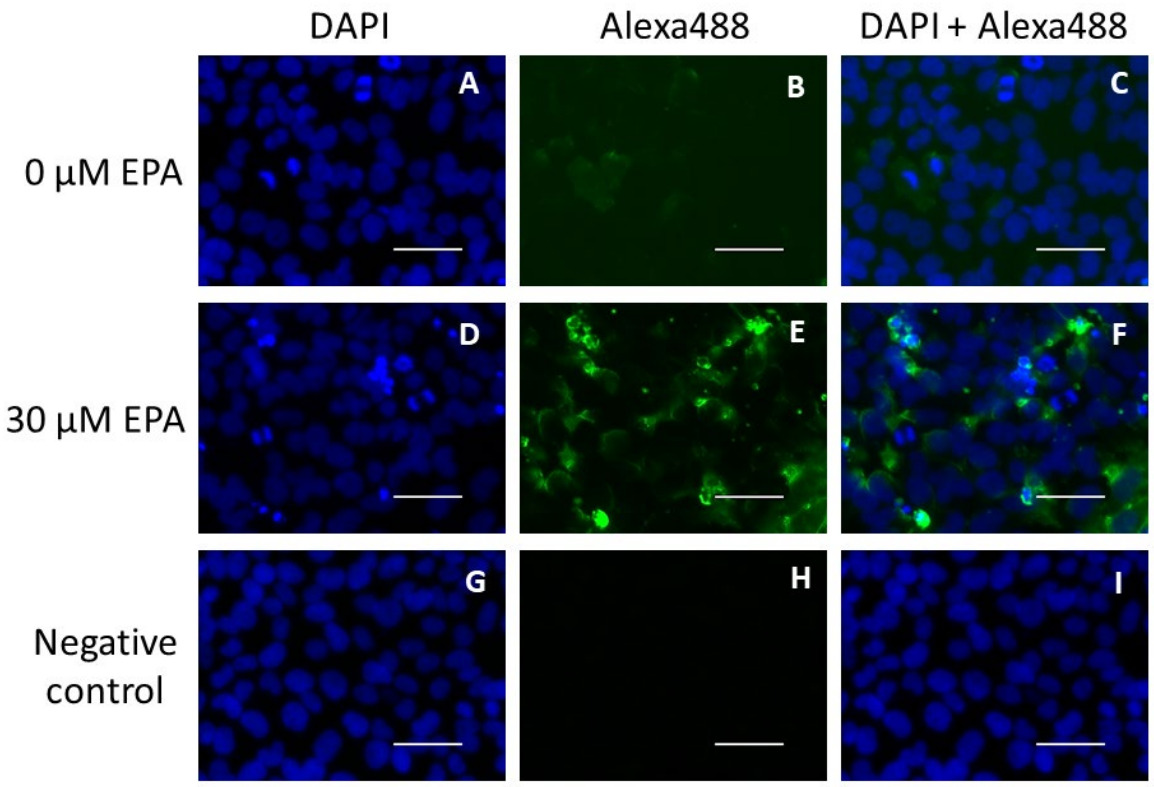

Figure 5.13 **hESCs cultured at 20% oxygen in the presence or absence of 30 µM EPA express GLUT3.**

Representative images of protein expression of GLUT3 in hESCs cultured at 20% oxygen (A-C) and supplemented with 30 µM EPA for 48 hours (D-F). Images of DAPI labelling (blue; A, D, G), Alexa 488 (green; B, E, H). A negative control is a secondary antibody only (goat anti-rabbit, Alexa 488) shown in images G-I. Scale bars indicate 50 µm.

Western blot was used to quantify the expression of GLUT3. The results showed a heavily glycosylated band as indicated by a broad range of migration (Boileau *et al.*, 1995) at a size of approximately 60 kDa. The expression of GLUT3 was increased in response to supplementation of 30 µM EPA to hESCs cultured at 20% oxygen. The expression of GLUT3 was significantly increased ($p=0.029$) being 2.5 times higher in cells incubated with 30 µM EPA compared to those cultured without the addition of this fatty acid (Figure 5.14).

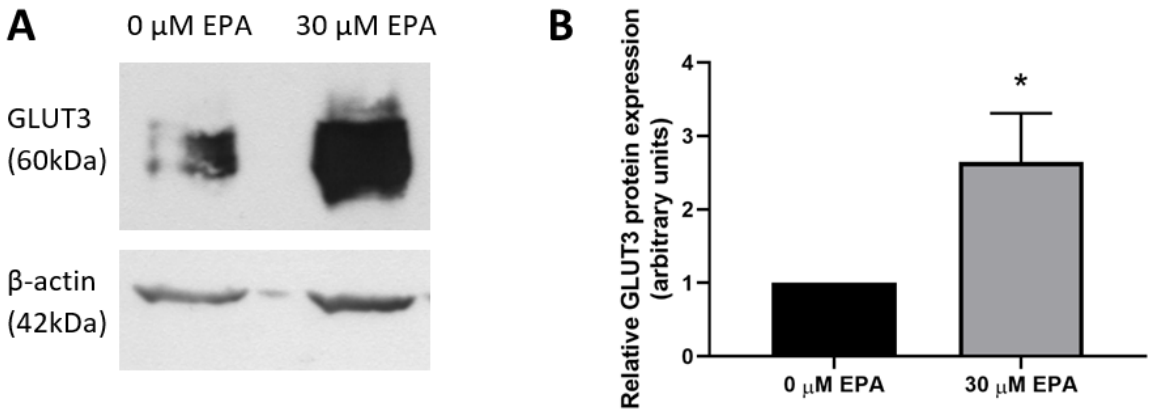

Figure 5.14 **Expression of GLUT3 in hESCs cultured at 20% oxygen is significantly increased in response to supplementation with 30 µM EPA.**

(A) Representative Western blot of GLUT3 and β-actin in hESCs cultured at 20% oxygen and cultured in presence or absence of supplemented 30 µM EPA for 48 hours. (B) Quantification of GLUT3 Western blot results. Data were normalized to β-actin and to 1 for hESCs not supplemented with EPA. *p<0.05 significantly different between 30 µM EPA and 0 µM EPA. Bars represent mean + SEM. n=7

5.4.7 Effect of EPA on glucose metabolism in hESCs cultured at 20% oxygen

GLUT3 is known to be the main transporter responsible for glucose uptake in hESCs cultured at 5% oxygen (Christensen *et al.*, 2015). It was investigated whether increased expression of GLUT3 caused by the higher concentration of EPA (chapter 5.4.6) might affect the glycolysis rate. Thus, the effect of EPA on glucose metabolism in hESCs cultured at 20% oxygen was investigated using glucose and lactate assays.

Glucose consumed by cells can be calculated based on a two-step reaction: first, a hexokinase facilitates the ATP phosphorylation of glucose, which yields glucose-6-phosphate (G6P) and ADP. The product, G6P, is then oxidized by glucose-6-phosphate dehydrogenase (G6PDH) to 6-phosphogluconate in the presence of NAD+. During this step, an equimolar amount of NAD^+ is reduced to NADH (Figure 5.15). The consequent increase in absorbance at 340 nm is proportional to the glucose concentration of the sample.

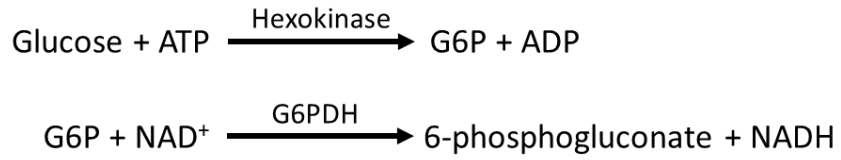

Figure 5.15 **Glucose consumed is calculated based on a two-step reaction.**

Similarly, the amount of lactate produced by cells can be calculated by measuring the amount of NADH produced during the oxidation reaction of lactate to pyruvate. This reaction is catalysed by lactate dehydrogenase (LDH) (Figure 5.16). The lactate assay reagent contains hydrazine sulphate, which removes pyruvate as it is formed, while the fluorescence of NADH, following excitation at 340 nm, is proportional to lactate produced.

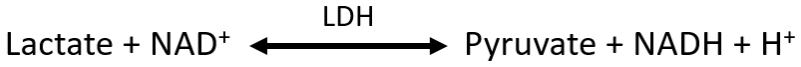

Figure 5.16 **Lactate produced is calculated based on reaction catalysed by LDH.**

Results of glucose and lactate assays revealed that there was no significant difference in glucose consumed or lactate produced between hESCs maintained at 20% oxygen in the presence or absence of supplemented 30 µM (Figure 5.17 A and B). Glucose flux to lactate was calculated relative to glycolysis, based on the assumption that 1 molecule of glucose is metabolised into 2 molecules of lactate. It was expected that glycolysis would be increased after EPA supplementation. However, results revealed that the flux through glycolysis was not altered in response to exogenous EPA; conversion rate of glucose to lactate was approximately 80% for hESCs cultured at 20% oxygen, and approximately 88% for hESCs cultured in the presence of 30 µM EPA (Figure 5.17 C).

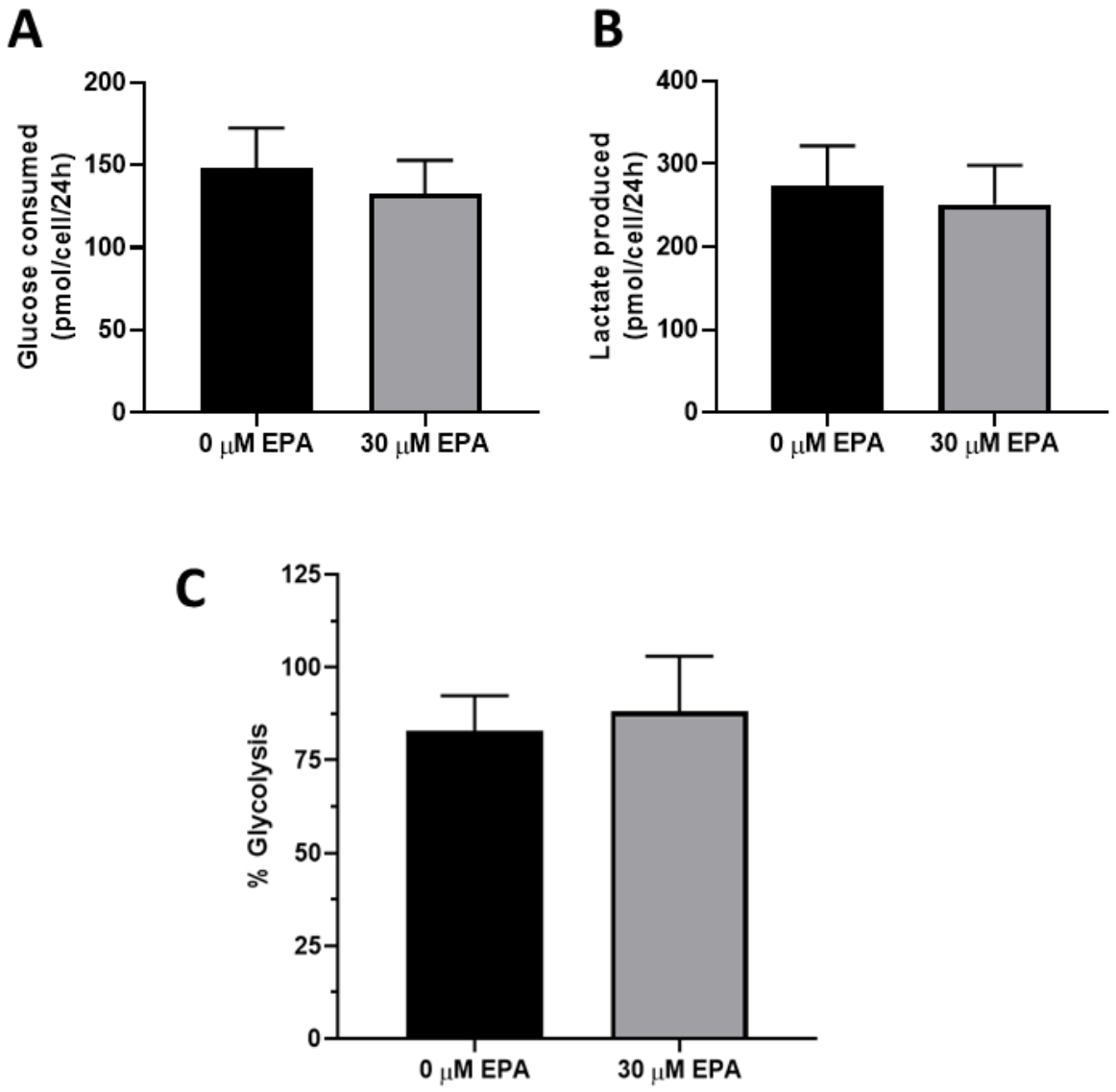

Figure 5.17 **EPA does not affect glucose metabolism in hESCs cultured at 20% oxygen.**

Glucose consumed (A) and lactate produced (B) by hESCs cultured at 20% oxygen in CM supplemented with either 0 μM or 30 μM EPA for 48 hours. Glucose consumption and lactate production were quantified on medium samples collected after 24 hours incubation on 3rd day post passage. Data were normalised to the cell number. The flux through glycolysis was calculated as % glycolysis based on the assumption that 1 molecule of glucose is metabolised to 2 molecules of lactate (C). Bars represent mean + SEM. n=9

5.4.8 Effect of EPA on D5D and caveolin-1 expression in hESCs cultured at 20% oxygen

Since the expression of GLUT3 was found to be altered by EPA supplementation in hESCs cultured at 20% oxygen (section 5.4.6), it was investigated whether EPA might affect expression of other proteins involved in fatty acid metabolism or binding, namely D5D and caveolin-1.

Bioconversion of eicosatetraenoic acid 20:4n-3 to EPA is catalysed by D5D. Thus, it was examined whether the increased concentration of product EPA might either positively or negatively alter the expression of the enzyme. hESCs cultured at 20% oxygen and cultured in CM in the presence or absence of supplemented 30 µM EPA were subject to immunocytochemistry analysis. The expression of D5D can be observed in the cytoplasm, as indicated by the presence of Alexa488 labelling that is not merged with DAPI (Figure 5.18). The signal corresponding to D5D expression is also noticeably brighter in hESCs cultured with 30 µM EPA compared to hESCs maintained without EPA supplementation (Figure 5.18).

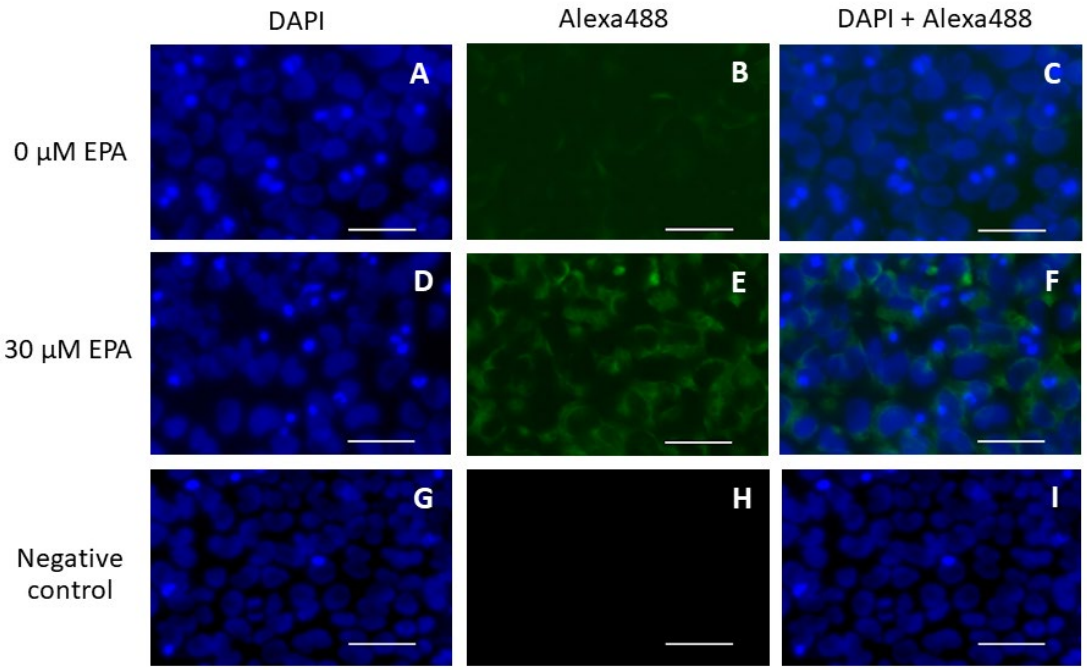

Figure 5.18 **D5D expression is increased in hESCs cultured at 20% oxygen and supplemented with 30 µM EPA.**

Representative images of protein expression of D5D in hESCs cultured at 20% oxygen (A-C) and supplemented with 30 µM EPA for 48 hours (D-F). Images of DAPI labelling (blue; A, D, G), Alexa 488 (green; B, E, H). A negative control is a secondary antibody only (goat anti-rabbit, Alexa 488) shown in images G-I. Scale bars indicate 50 µm.

Western blotting was used to quantify expression of D5D in hESCs cultured at 20% oxygen in the presence or absence of supplemented 30 µM EPA. Results showed a double band; however, it

was established in Chapter 2.4.3 that only the upper band corresponds to D5D protein. Quantification showed that expression of D5D was significantly (p=0.004) increased, by almost 50% in cells that were cultured in CM supplemented with 30 µM EPA compared to those maintained without the addition of EPA (Figure 5.19).

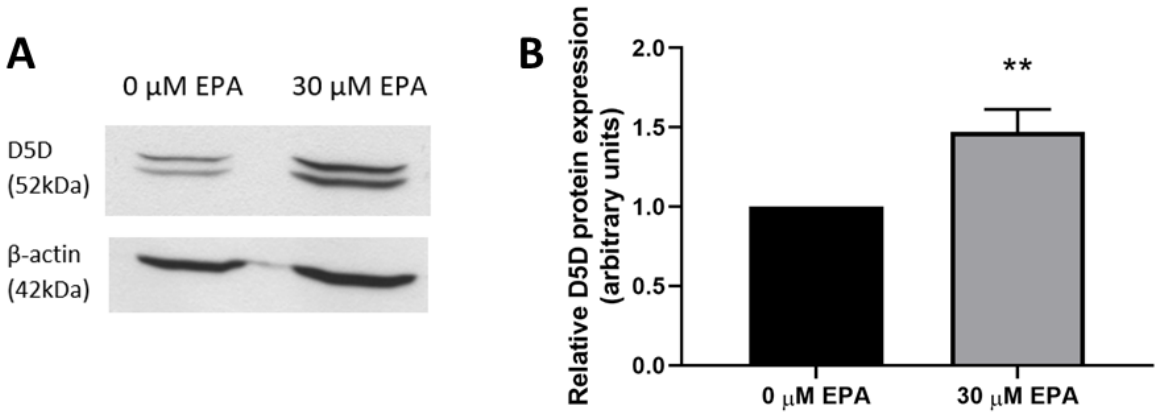

Figure 5.19 **Supplementation of hESCs cultured at 20% oxygen with 30 µM increased the protein expression of D5D.**

(A) Representative Western blot of D5D and β-actin in hESCs cultured at 20% oxygen in the presence or absence of supplemented 30 µM EPA for 48 hours. (B) Quantification of D5D Western blot results. Data were normalized to β-actin and to 1 for hESCs cultured in the absence of EPA. **p<0.01 significantly different between 30 µM EPA and 0 µM EPA. Bars represent mean + SEM. n=7

Previous studies showed that cell supplementation with PUFA had a significant impact on caveolae, which was shown to cause, for example, reduced proliferation or altered signalling events in a cell (reviewed in chapter 5.1). Since caveolin-1 is highly enriched within caveolae, the expression of this protein was examined to investigate a possible effect of EPA supplementation in hESCs cultured at 20% oxygen.

The expression of caveolin-1 in hESCs cultured at 20% oxygen in the presence or absence of 30 µM EPA was evaluated using immunocytochemistry analysis. Images showed that caveolin-1 was located in the cytoplasm and the expression was indicated by a bright signal in hESCs cultured at 20% oxygen. In hESCs supplemented with 30 µM the fluorescence signal was much weaker, indicating a reduction in expression of caveolin-1 (Figure 5.20).

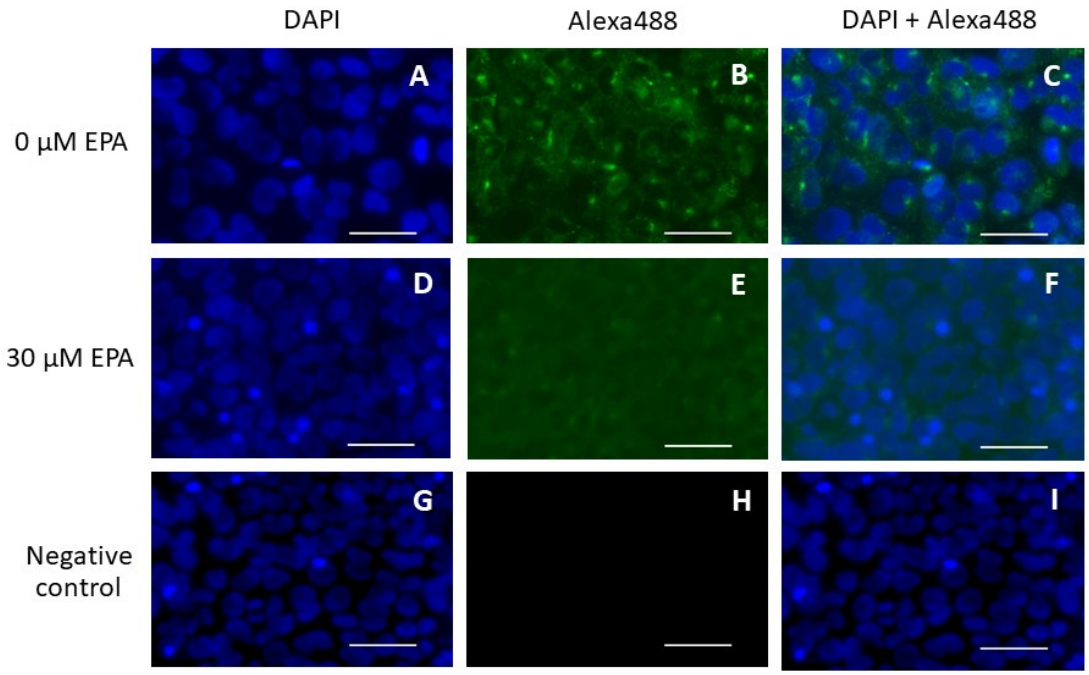

Figure 5.20 **Expression of caveolin-1 is reduced in hESCs cultured at 20% oxygen and supplemented with 30 µM EPA.**

Representative images of protein expression of caveolin-1 in hESCs cultured at 20% oxygen (A-C) and supplemented with 30 µM EPA for 48 hours (D-F). Images of DAPI labelling (blue; A, D, G), Alexa 488 (green; B, E, H). A negative control is a secondary antibody only (goat anti-rabbit, Alexa 488) shown in images G-I. Scale bars indicate 50 µm.

The expression level of caveolin-1 was quantified using Western blotting. The results showed a single band at an approximate size of 22 kDa, which corresponds to caveolin-1 (Figure 5.21 A). Quantification revealed that protein expression of caveolin-1 was altered upon EPA supplementation. The level of protein was significantly decreased by more than 30% ($p=0.007$) in hESCs cultured at 20% oxygen and supplemented with 30 µM EPA, compared to cells cultured without the addition of EPA (Figure 5.21 B).

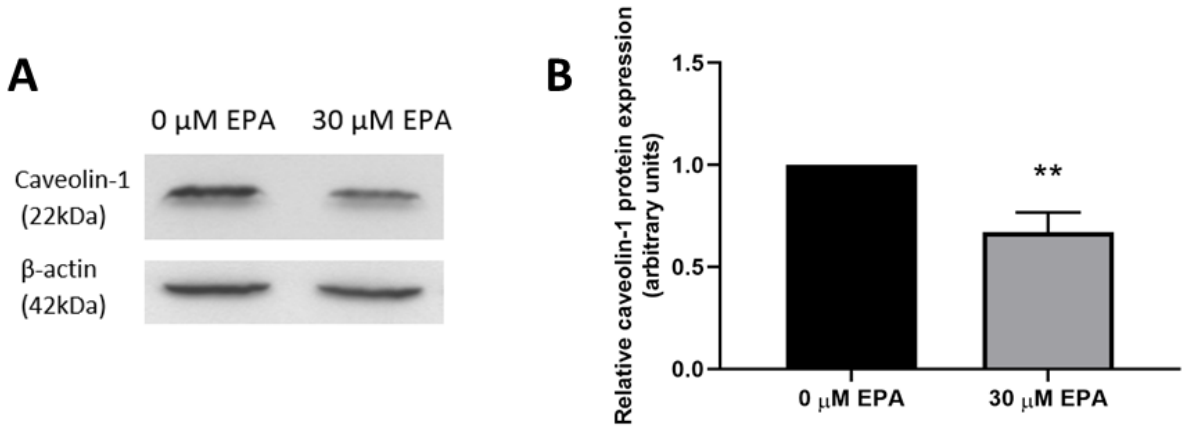

Figure 5.21 **EPA supplementation decreases caveolin-1 protein expression in hESCs cultured at 20% oxygen.**

(A) Representative Western blot of caveolin-1 and β-actin in hESCs cultured at 20% oxygen and cultured in the presence or absence of supplemented 30 μM EPA for 48 hours. (B) Quantification of caveolin-1 Western blot results. Data were normalized to β-actin and to 1 for hESCs not supplemented with EPA. **p<0.01 significantly different between 30 μM EPA and 0 μM EPA. Bars represent mean + SEM. n=6

5.5 Discussion

The availability of nutrients in the culture medium is important for sustaining the undifferentiated state of hESCs and self-renewal abilities. Fatty acids are important components of a cell but to date, the effect of conditioning medium on iMEFs on fatty acid levels was not previously investigated. This study found that conditioning does not alter the fatty acid concentrations of CM, however, the proportion of particular fatty acids changed significantly. Such a difference is a direct consequence of the specific method here presented. The concentration provides details about the absolute quantity of fatty acid (μM), while relative abundance (expressed in percentage) helps to calculate the overall composition profile, where the sum of all fatty acids is equal to 100%. Therefore, even small differences in concentration that are not statistically significant might affect this proportion. When fatty acid content was presented as percentage of total fatty acids, four fatty acids, oleic acid 18:1n-9, 20:0, 20:1n-9 and EPA 20:5n-3, were found to be significantly increased while 20:3n-6 (DGLA) and 22:5n-3 decreased in CM compared to hESC medium. Since CM is known to support pluripotent hESC culture, contrary to unconditioned hESC medium, fatty acids secreted by iMEFs might play a role in sustaining pluripotency. hESCs maintained in CM can possibly uptake more PUFA from the medium to utilise them for

synthesizing phospholipids necessary to build cell membranes of those highly proliferative cells. The composition of phospholipids is an important factor for cell growth; PUFA were found to support proliferation while saturated fatty acids limit that process (Doi *et al.*, 1978). One of the PUFAs, oleic acid, was found to have a beneficial effect, showing increased proliferation rate in breast cancer lines or reducing oxidative stress induced by H_2O_2 in porcine pulmonary artery endothelial cells (Hart *et al.*, 1993; Soto-Guzman *et al.*, 2008). The increased availability of oleic acid in CM compared to hESC medium might lead to enhanced uptake of this fatty acid by hESCs, which in turn could positively regulate proliferation. The decreased level of DGLA in CM compared to hESC medium suggests protective mechanism. The lipid mediators derived from DGLA were found to be involved in inhibiting proliferation (Fan and Chapkin, 1998; Wang *et al.*, 2012a; Gallagher *et al.*, 2019), therefore lower level of this fatty acid in CM might be involved in promoting the proliferation of hESCs cultured in CM.

In the current study, three different EPA concentrations were tested, 15 µM, 30 µM and 50 µM to assess the most appropriate concentration for hESC supplementation. While neither of EPA concentration affected cell viability, supplementation of 30 µM EPA caused the broadest effect on the fatty acid composition of hESCs. In addition, EPA concentration in human serum was found to be approximately 40 µM (Abdelmagid *et al.*, 2015), while in follicular fluid of pregnant women is approximately 20 µM (Valckx *et al.*, 2014), therefore suggesting that 30 µM is the most representative physiological concentration. The alteration in the fatty acid composition can have major effects on cell fate and properties; for example, supplementation of rat neural stem cells with EPA and DHA was shown to induce neuronal differentiation (Katakura *et al.*, 2013). However, EPA was increased in hESCs cultured at 5% oxygen compared to 20% oxygen (Chapter 4.4.2). hESCs cultured in hypoxic conditions exhibit increased proliferation and expression of pluripotency markers (Forristal *et al.*, 2010), and therefore it was hypothesised that the increased level of EPA at 5% oxygen might be involved in the regulation of self-renewal and cell growth. The expression of OCT4, SOX2 and NANOG was not altered upon EPA supplementation, suggesting that EPA is not involved in regulating self-renewal. However, since the expression of key pluripotency markers was not altered, it also indicates that EPA is not inducing differentiation in hESCs. Previous studies found a diverse effect of EPA supplementation on cell proliferation: in B-lymphocytes, cell growth was increased upon addition of this fatty acid, while in pancreatic cancer SW1990 cells it caused the opposite effect (Verlengia *et al.*, 2004; Zhang *et al.*, 2007). In hESCs, EPA was found to have no effect on proliferation, neither inducing cell growth nor inhibiting. This suggests that EPA might be involved in different processes in hESCs. The literature provides several examples of EPA being responsible for inhibiting ROS production in cancer cells, with supplementation concentration varying from 55 µM to 500 µM (Fahrmann and Hardman, 2013;

Fukui *et al.*, 2013; Oono *et al.*, 2020). In hESCs, EPA was found to not affect ROS generation. A plausible explanation could be that the concentration of EPA used in this study (30 μM) was too low to induce any changes to ROS generation, compared to the studies that used much higher dosage of this fatty acid. Whilst 50 μM of EPA was found to not alter hESCs morphology, higher concentrations, for example, 100 μM were not tested.

PUFAs are known to be involved in glucose or fatty acid metabolism, yet, the molecular mechanisms behind this are not well understood. Some studies suggest an ability of PUFAs to regulate the expression of metabolic genes, such as pyruvate kinase or fatty acid synthase (Dentin et al., 2005; Manzi et al., 2015). hESCs cultured at 5% oxygen rely more on glycolysis than oxidative phosphorylation for energy requirements compared to cells maintained under atmospheric oxygen and this switch in metabolism is believed to be associated with pluripotency maintenance through increased expression of key pluripotency markers (Forristal *et al.*, 2013; Christensen *et al.*, 2015). The enhanced glucose consumption requires increased cellular uptake, which is facilitated by glucose transporters. GLUT3 was found to be the major glucose transporter mediating this uptake since the expression of GLUT1 was only increased on mRNA level in hypoxia compared to hESCs cultured at 20% oxygen (Forristal *et al.*, 2013; Christensen *et al.*, 2015). EPA level was found to be increased by culture in hypoxic conditions and therefore it was investigated whether EPA might be involved in glucose metabolism in hESCs cultured at 20% oxygen. There is evidence showing that EPA is responsible for regulating expression and functions of GLUT1 and GLUT3 that consequently caused an increased glycolytic rate in rat brain cells (Ximenes-Da-Silva *et al.*, 2002; Pifferi *et al.*, 2010). In this study, EPA was found to be involved in regulating the expression of GLUT3, which was found to have increased protein expression upon EPA supplementation. However, GLUT1 level was not altered. One explanation for this could be that glucose uptake in hESCs has been shown to be facilitated by GLUT3 and not GLUT1 (Christensen *et al.*, 2015). The increased expression of GLUT3 suggests a higher rate of glucose uptake that could lead to enhanced glycolysis. However, glucose metabolism was not affected by EPA in hESCs; neither glucose consumption nor lactate production was altered. Such a surprising result leads to the question: why GLUT3 expression is increased but glycolysis is not affected? The glucose assay used in this project quantifies the glucose consumed, therefore reflecting the amount of glucose utilised during glycolysis. However, the increased GLUT3 expression might mean that there is an enhanced glucose uptake but this carbohydrate might be used for different purposes than glycolysis. Increased glucose concentration in rat muscle satellite cells was found to induce *de novo* lipogenesis, a metabolic process that results in fatty acid and lipid synthesis (Guillet-Deniau *et al.*, 2004). Synthesised lipids are usually stored in a form of neutral lipid droplets in a cell. In rat muscle satellite cells, increased availability of glucose resulted in the higher expression of genes

involved in lipogenesis, such as fatty acid synthase and acetyl-CoA carboxylase 2, as well as lipid accumulation (Guillet-Deniau *et al.*, 2004). Increased expression of GLUT3 in human macrophages was shown to lead to higher uptake of glucose and the carbohydrate substrate was found to be utilised for lipogenesis, characterised by increased lipid droplets accumulation (Li *et al.*, 2012). Similar effects might be induced in hESCs upon EPA supplementation, where increased glucose is utilised for lipogenesis instead of glycolysis.

The EPA supplementation to hESC culture caused alteration in the fatty acid composition of cells (Figure 5.6). The change in fatty acid composition after addition of EPA might be also inducing the decreased expression of caveolin-1 in hESCs cultured at 20% oxygen in the presence of 30 µM EPA compared to cells maintained in culture without supplementation. It was shown that when human umbilical vein endothelial cells were treated with 50 µM EPA, caveolae microenvironment was altered. The lipid composition of isolated caveolae changed with increased levels of palmitic acid (16:0), EPA and 22:5n-3. Similar results can be observed in the work presented in this chapter, even though fatty acid composition was examined on the whole cell not only caveolae fraction. Interestingly, Li *et al.* (2007b) also showed that EPA supplementation caused the displacement of caveolin-1 out of the caveolae. As mentioned, the current study showed that supplementation of hESCs with EPA changed not only EPA concentration but also other fatty acids, that probably resulted in the disruption of caveolae. The decreased expression of caveolin-1 was also found to be associated with increased lipogenesis (Li *et al.*, 2017), which would support the hypothesis that increased concentration of EPA enhances this metabolic process in hESCs. During lipogenesis, fatty acids can be synthesised from carbohydrates or proteins by a cascade of molecular reactions. Firstly, acetyl-CoA is carboxylated by acetyl-CoA carboxylase 1 to malonyl-CoA. During repeated cycles, malonyl-CoA serves as a donor of two carbons that are attached to acetyl-CoA by fatty acid synthase that results in the generation of palmitic acid 16:0. The synthesised fatty acids can be later extended by elongases, resulting in saturated long-chain fatty acids (Calder, 2016; Liu *et al.*, 2017). Results showed that the levels of saturated fatty acids, palmitic acid 16:0 and stearic acid 18:0, were increased in hESCs supplemented with 30 µM EPA compared to cells cultured without exogenous EPA, suggesting that *de novo* synthesis is enhanced. A recent study found that D5D is involved in the fatty acid synthesis, proving decreased lipogenesis in *FADS1* knock-out mice (Gromovsky *et al.*, 2018). Increased expression of D5D in hESCs cultured with 30 µM EPA might represent a response to enhanced lipogenesis in cells, hence higher concentration of synthesised fatty acids. Possibly, not only D5D expression is increased but also other enzymes involved in fatty acid bioconversion pathway as a result of a higher concentration of EPA and synthesised fatty acids.

This chapter investigated the role of EPA and for the first time showed its effect on hESC properties. Even though some of the aspects that were expected to be altered were not changed, such as proliferation or ROS generation, EPA was found to be involved in regulating the expression of proteins that are involved in glucose transport, EPA biosynthesis and cell signalling/fatty acid-binding. These data points at the broad regulatory role of EPA within hESCs. These results, together with altered fatty acid composition upon EPA supplementation, suggests that increased concentration of EPA in hESCs might cause enhanced lipogenesis. However, more evidence would be required to prove this hypothesis.

Chapter 6 Conclusions and future work

This thesis provides evidence that environmental oxygen regulates the proteome of hESCs as well as both fatty acid composition and biosynthesis in these cells. In addition, one of the fatty acids, EPA, was found to be responsible for altering the expression level of proteins involved in glucose transport, fatty acid biosynthesis and stability of caveolae in hESCs cultured at 20% oxygen. This shows a fatty acid-mediated link between oxygen tension and metabolism in hESCs.

Successful establishment of pluripotent, self-renewing hESCs in 1998 brought a promise for advances in regenerative medicine and developmental studies (Thomson *et al.*, 1998). However, hESC culture proved to be challenging due to spontaneous differentiation (Amit and Itskovitz-Eldor, 2002). Environmental oxygen is an important factor proven to impact the properties of hESCs; low oxygen (5%) was found to be beneficial for hESCs that exhibit a lower level of spontaneous differentiation and chromosomal aberrations, increased proliferation and expression of pluripotency markers, OCT4, SOX2 and NANOG (Ezashi *et al.*, 2005; Forsyth *et al.*, 2006; Forristal *et al.*, 2010; Petruzzelli *et al.*, 2014). Previous studies also showed that hypoxic conditions could induce changes in the transcriptome of hESCs (Westfall *et al.*, 2008). However, to date, little was known about how environmental oxygen alters the global proteome of hESCs.

The current study presented for the first time that the overall proteomic profile of hESCs differs in cells cultured at 5% oxygen compared to those maintained at 20% oxygen. IPA analysis of the hESC proteome showed that pathways connected to metabolism, such as ‘glycolysis’, ‘oxidative phosphorylation’ and ‘mitochondrial dysfunction’ were among the most significantly affected by oxygen tension (chapter 3.4.5.1). This is in agreement with the work of Forristal *et al.* (2013) that presented a switch in metabolism from oxidative phosphorylation to glycolysis upon prolonged exposure to hypoxia in hESCs. Moreover, a study on glioblastoma cells cultured in hypoxic conditions presented similar results; proteomics results revealed upregulation of glycolytic enzymes, such as phosphoglycerate kinase 1 (PGK1) or phosphoglucomutase-2 (PGM2) (Zhang *et al.*, 2017). Interestingly, Zhang *et al.* (2017) were unable to detect HIF1α, the main regulator of hypoxia response, in glioblastoma cells cultured at 1% oxygen using mass spectrometry. HIF2α is the main hypoxia response facilitator in hESCs but the expression of HIF2α was also not identified by mass spectrometry in work undertaken in this thesis. Moreover, the mentioned study of Zhang *et al.* (2017) was unable to identify SOX2 using mass spectrometry, which expression proved to be increased in hypoxic cancer cells but was only detectable by Western blotting. Similarly, the expression of SOX2, but also OCT4 and NANOG, was not identified by mass spectrometry and only measured based on Western blotting results (chapter 3.4.1.2). The most probable explanation

includes the sensitivity of the mass spectrometry technique and the abundance of transcription factors, which are known to be localised in the nucleus. The majority of proteins detected in this project was found to be localised within the cytosol (44% of all proteins), and only a small percentage (4%) was associated with 'nuclear part' term, based on GO analysis (chapter 3.4.3). Mass spectrometry performed on the isolated nuclear fraction could address this problem and provide more information on expression profiles of transcription factors present in hESCs. Despite the lack of detection of OCT4, SOX2 or NANOG, several other proteins were identified.

Among the proteins detected by mass spectrometry as significantly altered in expression by environmental oxygen were PARP-1 and caveolin-1. The expression of these proteins was validated using Western blotting and they proved to be significantly increased in hESCs cultured in 5% oxygen compared to 20% oxygen (chapter 3.4.7). PARP-1 was not involved in pluripotency maintenance in hESCs and increased expression at 5% oxygen was not due to HIF2α regulation. It has been shown that PARP-1 is a coactivator of HIF1α in leukaemia cells and directly regulates expression of HIF2α in MEFs and human embryonic kidney cells HEK 293T (Elser *et al.*, 2008; Gonzalez-Flores *et al.*, 2014). Moreover, PARP-1 forms a protein complex with HIF2α in MEFs and HEK 293T cells, which regulates the expression of HIF target genes. When PARP-1 was silenced or inhibited, Gonzalez-Flores *et al.* (2014) observed reduced mRNA expression of HIF2α target genes, such as angiopoietin-like 4 (ANGPTL4). However, it remains to be investigated whether PARP-1 might play a role as a HIF2α coactivator/regulator in hESCs cultured at 5% oxygen. Since silencing PARP-1 did not affect the expression of OCT4, SOX2 and NANOG in hESCs (chapter 3.4.9), it could be investigated whether the PARP-1-HIF2α complex might be involved in the regulation of other HIF2α target genes or HIF2α itself. It could be tested by silencing the expression of PARP-1, HIF2α and both while examining the consequences on expression of HIF2α/PARP-1 target genes. The increased expression of PARP-1 in hESCs cultured at 5% oxygen might also be connected to enhanced DNA repair system. hESCs are known to have superior DNA damage response compared to somatic cells (Maynard *et al.*, 2008; Mani *et al.*, 2020), thus it could be hypothesised that hypoxia, together with increased levels of PARP-1, is involved in the improved repair of DNA in the cell. As the STRING analysis showed (chapter 3.4.6), PARP-1 was found to interact with two other proteins connected to DNA damage control and repair- PCNA and RPA1. Interestingly, both of these proteins were significantly increased in expression in hESCs cultured at 5% oxygen compared to 20% oxygen (Appendix 2). PARP-1 is known to interact with PCNA in HeLa cells, where both proteins regulate each others activity: PARP-1 negatively regulates the PCNA-mediated DNA replication and repair under damage conditions while PCNA negatively regulates the PARP-1 activity (Frouin *et al.*, 2003). The latter regulation is speculated to be a mechanism to possibly decrease NAD^+ consumption, which is a consequence of PARP-1 activity (Frouin *et al.*,

2003). Since hESCs cultured at 5% oxygen rely more on glycolysis than oxidative phosphorylation (Forristal *et al.*, 2013), the interaction of PCNA with PARP-1 could be a mechanism that limits NAD^+ use by PARP-1 to sustain glucose metabolism. PARP-1 also interacts with RPA1, which is poly(ADP-ribosyl)ated when DNA damage occurs (Jungmichel *et al.*, 2013). In turn, RPA1 regulates PARP-1 poly(ADP-ribosyl)ation activity; RPA1 inhibits PARP-1 activity in the presence of single stranded DNA while double-stranded DNA promotes it (Maltseva *et al.*, 2018). However, to investigate whether PCNA and RPA1 interact with PARP-1 in hESCs, it would be necessary to perform a pull-down assay, which allows identifying physical interactions between proteins. The expression of other genes/proteins involved in DNA repair mechanisms could be quantified to investigate whether hypoxia enhances this process in hESCs. The comet assay, which helps to evaluate DNA damage, could be performed on hESCs cultured at 5% oxygen and compared to results obtained from cells maintained under atmospheric oxygen to evaluate whether oxygen tension can affect DNA strand breaks occurrence.

Another protein identified by mass spectrometry and validated to be significantly increased in hESCs cultured at 5% oxygen is caveolin-1 (chapter 3.4.10). This plasma membrane protein is found within caveolae and is involved in fatty acid binding (Trigatti *et al.*, 1999) but also pluripotency maintenance in mESCs (Lee *et al.*, 2010b). Lee *et al.* (2010b) presented that disruption of caveolae by methyl-β-cyclodextrin or silencing of caveolin-1 in mESCs led to decreased expression of Oct4 and Sox2 as well as caused lower proliferation. It remains to be elucidated whether caveolin-1 might play a similar role in regulating the expression of OCT4, SOX2 and NANOG in hESCs. This could be performed by silencing caveolin-1 in hESCs and examining the expression of self-renewal markers by Western blotting, while proliferation could be assessed using the Ki-67 assay. Caveolin-1 was also shown to facilitate long-chain fatty acid uptake in HepG2 cells (Pohl *et al.*, 2002). Since the expression of caveolin-1 was increased in hESCs cultured at 5% oxygen, it would suggest that long-chain fatty acid uptake might be more efficient in these cells. The gas chromatography results showed a different fatty acid profile in hESCs cultured at 5% oxygen compared to those maintained at 20% oxygen. However, the major alteration to the composition of fatty acids was an increased level of EPA and AA. The bioconversion to EPA and AA is mediated by the same enzyme, D5D. The level of D5D was found to be significantly increased in hESCs cultured at 5% oxygen compared to 20%, suggesting that elevated level of EPA is due to higher affinity and availability of this enzyme rather than uptake facilitated by caveolae. Silencing of D5D showed no effect on the expression of OCT4, SOX2 and NANOG, therefore indicating that this enzyme is not involved in hESC self-renewal. However, it could be investigated whether increased expression of D5D in hESCs cultured at 5% oxygen is linked to the higher proliferation rate observed during hypoxia (Forristal *et al.*, 2010). A study on T-cells showed that 'proliferating'

cells upregulate D5D, compared to 'resting' cells (Robichaud *et al.*, 2018). The overexpression of D5D in melanocytes led to higher proliferation while silencing of *FADS1*, the gene that encodes D5D, had the opposite effect (Tang *et al.*, 2019). The effect of D5D on cell growth in hESCs could be examined by silencing *FADS1* and using Ki-67 proliferation assay. Increased expression of D5D in hESCs cultured at 5% oxygen might be also a mechanism regulating glycolysis as this desaturase enzyme recycles NAD+ (Kim *et al.*, 2019), which is required for glucose metabolism. The role of D5D in regulating glycolysis could be investigated by measuring NAD^+ and NADH redox states using SoNar sensor (Zhao *et al.*, 2015b) and glucose consumption/lactate production in hESCs where *FADS1* was silenced compared to cells with unaffected expression. So far, this thesis was able to show that bioconversion of fatty acids in hESCs is regulated by the environmental oxygen tension through direct regulation of D5D by HIF2α. It remains to be elucidated whether silencing of PARP-1 expression might decrease HIF2α binding to D5D.

Since the level of EPA was elevated in hESCs cultured at 5% oxygen compared to those maintained at 20% oxygen, it was hypothesised that this fatty acid might be connected to the beneficial properties observed in hypoxia (Ezashi *et al.*, 2005; Forristal *et al.*, 2010). Therefore, hESCs cultured at 20% were supplemented with 30μM EPA and it was examined whether this might affect cell properties, such as cell growth or metabolism. The results showed that EPA is not involved in regulating proliferation or ROS generation in hESCs. The latter finding was surprising since EPA supplementation was shown to induce ROS production in cancer cells (Fahrmann and Hardman, 2013; Fukui *et al.*, 2013) and mouse models (Hsu and Yin, 2016). However, several studies present contradictory results indicating that cell supplementation with EPA and/or DHA led to decreased levels of ROS (Kang *et al.*, 2010; Moloudizargari *et al.*, 2018; Zhang *et al.*, 2018b; Farooq *et al.*, 2020). It can only be speculated whether it would be necessary to additionally supplement DHA to hESCs to observe any effect on ROS generation. However, levels of DHA in hESCs were not significantly altered by environmental oxygen (chapter 4.4.2) or by increasing concentration of EPA (chapter 5.4.2). Therefore, there was no rationale for the addition of DHA. Proliferation and apoptosis are other processes widely reported to be regulated by n-3 PUFA such as EPA (Chiu and Wan, 1999; Finstad *et al.*, 2000; Arita *et al.*, 2001; Kang *et al.*, 2010; Abdi *et al.*, 2014). Proliferation rate was not significantly altered in hESCs upon EPA supplementation. Around 97% of hESCs cultured in the presence or absence of supplemented 30 μM EPA were stained positive for Ki-67, the marker used for determining proliferation rate. Such an expression level of the Ki-67 marker was expected, as a previous study from Forristal *et al.* (2010) reported that hESCs are highly (almost 100%) proliferative. High expression of Ki-67 is known to be negatively correlated with apoptosis in cancer cells (Tan *et al.*, 2005; Li *et al.*, 2015). Thus, the results of this thesis showing an unaltered level of proliferation, regardless of the presence or absence of 30 μM

EPA, might suggest that apoptosis is not increased in hESCs supplemented with this fatty acid. However, to be certain, it would be necessary to conduct the TUNEL assay to assess the level of apoptosis. Another interesting approach would be investigating possible changes in the expression of PARP-1. The full-length form of PARP-1 (116 kDa) is involved in DNA repair; however, following cleavage by caspases, PARP-1 is trimmed into the 89 kDa and 24 kDa forms, a hallmark of apoptosis (Gobeil *et al.*, 2001). The cleavage of PARP-1 was found to be induced by supplementation of human pancreatic cancer cells with 100 µM EPA (Fukui *et al.*, 2013). It would be interesting to examine whether a similar effect could be observed upon EPA supplementation in hESCs or whether the full-size PARP-1 protein would be the most prevalent form, as observed in cells cultured at either 5% or 20% oxygen (chapter 3.4.7).

EPA supplementation of hESCs did not alter those same cell properties observed changing when supplementing other cell types. However, EPA was found to be involved in regulating the expression of GLUT3, D5D and caveolin-1 (chapter 5.4.6 and 5.4.8). The expression of GLUT3 and D5D was significantly increased in hESCs cultured at 20% oxygen and supplemented with 30 µM EPA. Interestingly, GLUT3 was found to be regulated by environmental oxygen in hESCs, with higher expression in hypoxia than normoxia (Christensen *et al.*, 2015). Similarly, D5D was shown to be regulated by environmental oxygen through HIF2α transcriptional activity (chapter 4.4.5). The results of this thesis show that EPA can regulate the expression of GLUT3 and D5D, despite the atmospheric oxygen conditions. This suggests that alteration in fatty acid composition induced through EPA supplementation is enough to increase the expression of GLUT3 and D5D despite the normoxic conditions. Fatty acids and their metabolites are known to directly regulate the activity of transcription factors, for example, sterol regulatory element-binding protein-1c (SREBP-1c) or Peroxisome Proliferator Activated Receptors (PPARs) (Duplus *et al.*, 2000; Ou *et al.*, 2001; Jump, 2004). However, fatty acids can also indirectly regulate transcription. The hypothesised mechanism of *GLUT3* expression includes the cAMP signalling pathway. EPA was found to induce cAMP generation in colonic epithelial cells (Roy *et al.*, 2010). In turn, cAMP regulates *GLUT3* expression, but not *GLUT1*, through the activation of its promoter in breast cancer cells (Meneses *et al.*, 2008). It could be investigated whether the GLUT3 expression increase in hESCs cultured in the presence of EPA is due to increased cAMP levels. This could be examined by adding 8-br-cAMP (8-bromoadenosine 3, 5, cyclic monophosphate), the synthetic analogue of cAMP, to hESC culture and measuring whether GLUT3 expression is increased. To establish whether the increase in expression is due to cAMP regulation on the transcriptional level, it would be necessary to design promoter-reporter vectors containing *GLUT3* promoter region, which could be transfected to hESCs. The increased signal of reporter upon addition of stimulus, in this case 8-br-cAMP, would suggest the activation of the promoter and therefore would prove the regulation by cAMP.

The increase in the level of D5D in hESCs supplemented with 30 µM EPA is an unexpected result. A study on adipocytes conducted by Ralston *et al.* (2015) found that EPA negatively regulates expression of *FADS1* at both the mRNA and protein levels. The results of this thesis show a contradictory effect. This could be due to cell type specificity but also a possible effect of EPA in hESCs that involves a positive feedback loop of this fatty acid and D5D, whereas higher levels of EPA increase expression or activity of this enzyme.

Caveolin-1 expression was downregulated in hESCs upon EPA supplementation. The decrease of caveolin-1 mRNA levels was also observed in human epithelial colorectal adenocarcinoma cells supplemented with EPA (Yang *et al.*, 2018) and is probably a consequence of disruption of the caveolae microenvironment (Li *et al.*, 2007b; Lian *et al.*, 2019). EPA treatment was also found to translocate endothelial nitric oxide synthase (eNOS) out of caveolae and stimulate the activity of this enzyme, leading to increased levels of nitric oxide (Li *et al.*, 2007b). Future work should investigate whether nitric oxide production is altered by EPA supplementation in hESCs using nitric oxide colorimetric assay.

In conclusion, this thesis described overall proteomic changes of hESCs cultured in varying oxygen tension conditions (Figure 6.1). Several proteins were found to be upregulated in hypoxic conditions that are involved in glycolysis, DNA repair as well as fatty acid metabolism. While it was possible to describe a novel oxygen-dependent mechanism regulating fatty acid biosynthesis in hESCs, it still remains to be elucidated how the altered composition of fatty acids might affect hESC properties.

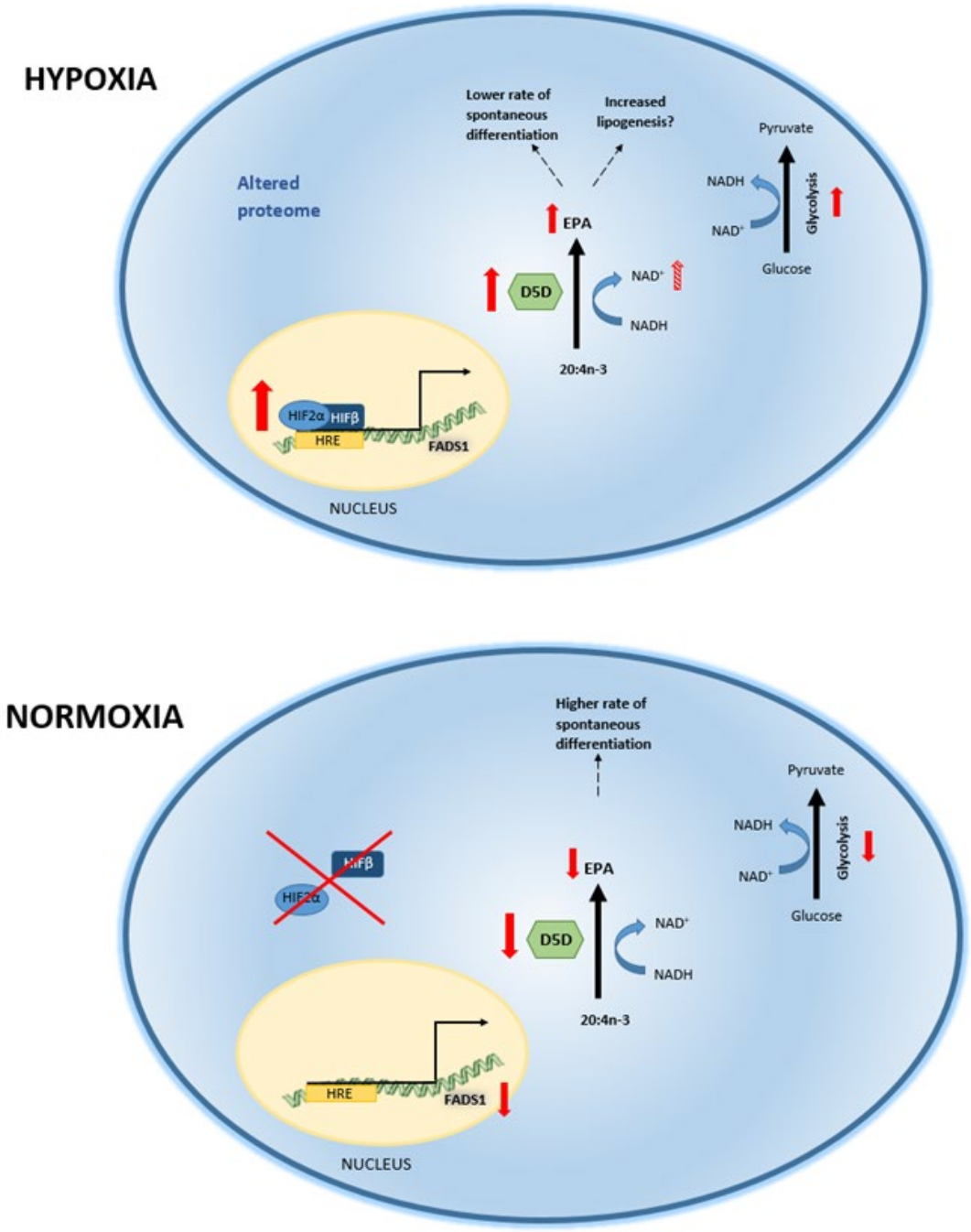

Figure 6.1 **Proposed mechanisms and the effect of environmental oxygen on hESCs.**

The proteome of hESCs was found to be affected by environmental oxygen as well as fatty acid composition and biosynthesis. In hypoxia, the expression of D5D is increased and directly regulated by HIF2α, which might lead to higher levels of EPA. The higher activity of D5D, which utilises NADH as a substrate, can be connected to increased glycolysis that requires NAD^+. EPA might be involved in reducing the rate of spontaneous differentiation of hESCs cultured at 5% oxygen, compared to those maintained at 20% oxygen. The increase in EPA level might be also leading to increased lipogenesis in cells.

Appendix

A.1 Principal component analysis of hESC sample data

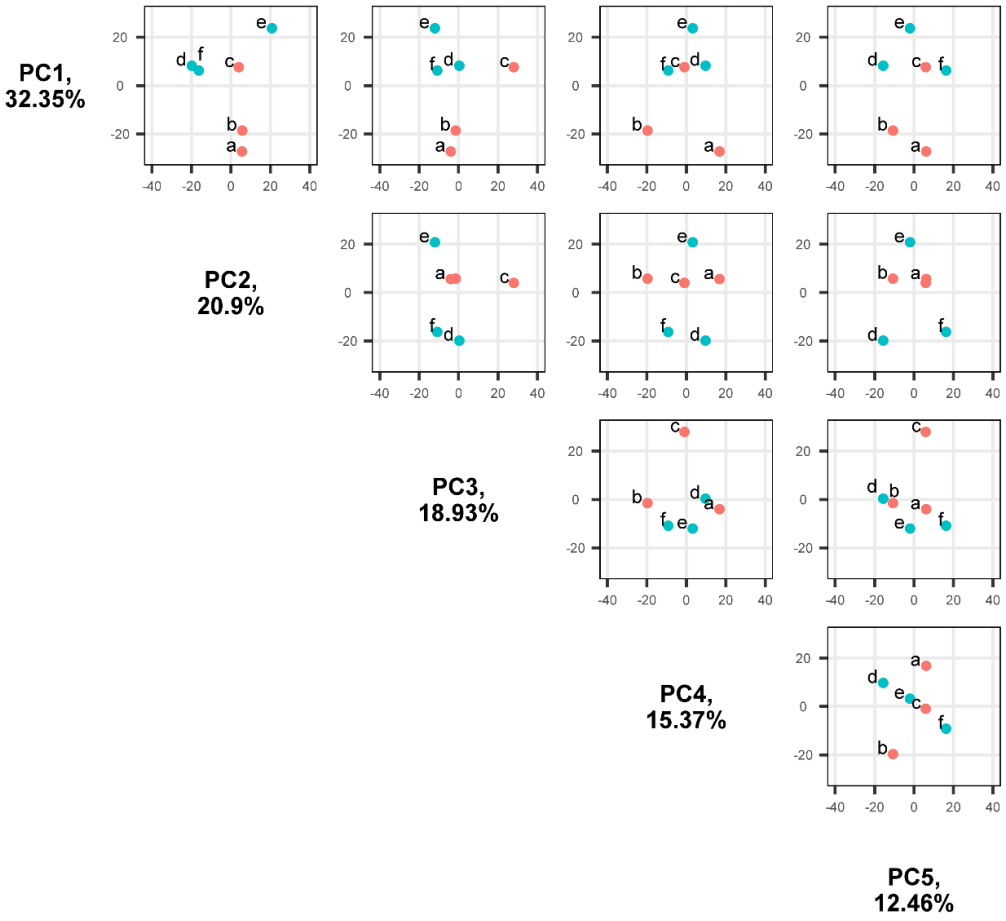

Figure A.1 Principal component analysis of hESC sample data.

Samples a, b, c- hESCs cultured at 20% oxygen; samples d, e, f- hESCs cultured at 5% oxygen.

A.2 List of proteins which expression was significantly different between hESCs cultured at either 5% or 20% oxygen.

UniProt ID	Protein name	p-value	log_2FC
P43307	Translocon-associated protein subunit alpha	0.001351	-2.03728
Q71U36	Tubulin alpha-1A chain	0.000317	-1.83036
Q96CT7	Coiled-coil domain-containing protein 124	0.031819	-1.79676
Q9UBE0	SUMO-activating enzyme subunit 1	0.000925	-1.6045
Q9BWD1	Acetyl-CoA acetyltransferase cytosolic	0.007053	-1.51302
O95865	N(G) N(G)-dimethylarginine dimethylaminohydrolase 2	0.002447	-1.39459
Q9H3K6	BolA-like protein 2	0.028288	-1.37683
O14579	Coatomer subunit epsilon	0.041792	-1.34293
Q96AY3	Peptidyl-prolyl cis-trans isomerase FKBP10	0.003233	-1.33383
P32322	Pyrroline-5-carboxylate reductase 1 mitochondrial	0.013691	-1.31058
P16422	Epithelial cell adhesion molecule	0.009717	-1.25565
P21399	Cytoplasmic aconitate hydratase	0.023682	-1.20385
P07951	Tropomyosin beta chain	0.025174	-1.18349
P61020	Ras-related protein Rab-5B	0.000544	-1.16712
P45973	Chromobox protein homolog 5	0.00298	-1.12661
Q01581	Hydroxymethylglutaryl-CoA synthase cytoplasmic	0.008781	-1.08734
Q96IZ0	PRKC apoptosis WT1 regulator protein	0.012599	-1.01845
Q8NBS9	Thioredoxin domain-containing protein 5	0.02659	-0.95334
P08243	Asparagine synthetase [glutamine-hydrolyzing]	0.02573	-0.94196
P36405	ADP-ribosylation factor-like protein 3	0.031123	-0.8821
P18085	ADP-ribosylation factor 4	0.045093	-0.8461
P15559	NAD(P)H dehydrogenase [quinone] 1	0.004394	-0.82231

UniProt ID	Protein name	p-value	log_2FC
O00273	DNA fragmentation factor subunit alpha	0.015242	-0.78491
P08133	Annexin A6	0.020152	-0.69772
Q92598	Heat shock protein 105 kDa	0.011378	-0.69031
P31689	DnaJ homolog subfamily A member 1	0.011629	-0.67609
Q01995	Transgelin	0.015012	-0.67221
Q9NY33	Dipeptidyl peptidase 3	0.030351	-0.64606
Q15758	Neutral amino acid transporter B(0)	0.009915	-0.61731
Q02790	Peptidyl-prolyl cis-trans isomerase FKBP4	0.004676	-0.58165
P08107	Heat shock 70 kDa protein 1A/1B	0.034181	-0.56842
P33176	Kinesin-1 heavy chain	0.003086	-0.49428
Q9GZL7	Ribosome biogenesis protein WDR12	0.031359	-0.48646
P27348	14-3-3 protein theta	0.015378	-0.46506
P63241	Eukaryotic translation initiation factor 5A-1	0.025057	-0.43652
P42224	Signal transducer and activator of transcription 1-alpha/beta	0.014336	-0.41499
Q9NR28	Diablo homolog mitochondrial	0.006813	-0.41484
P49368	T-complex protein 1 subunit gamma	0.010796	-0.41073
P15374	Ubiquitin carboxyl-terminal hydrolase isozyme L3	0.007125	-0.39253
Q9Y2Z0	Suppressor of G2 allele of SKP1 homolog	0.010256	-0.39133
P14550	Alcohol dehydrogenase [NADP(+)]	0.007434	-0.38597
P43490	Nicotinamide phosphoribosyltransferase	0.025387	-0.38517
P67870	Casein kinase II subunit beta	0.024492	-0.37348
P78371	T-complex protein 1 subunit beta	0.044176	-0.36768
P09211	Glutathione S-transferase P	0.043921	-0.35105
P50454	Serpin H1	0.036448	-0.35105

UniProt ID	Protein name	p-value	log_2FC
P06748	Nucleophosmin	0.042809	-0.34412
Q8NE71	ATP-binding cassette sub-family F member 1	0.023571	-0.31917
P09622	Dihydrolipoyl dehydrogenase mitochondrial	0.043909	-0.30043
P60842	Eukaryotic initiation factor 4A-I	0.040058	-0.28321
P61163	Alpha-centractin	0.015433	-0.26653
P56747	Claudin-6	0.04147	-0.25776
Q6NXE6	Armadillo repeat-containing protein 6	0.038794	-0.24148
P50502	Hsc70-interacting protein	0.041328	-0.20383
P05783	Keratin type I cytoskeletal 18	0.005221	-0.20058
Q9NQ29	Putative RNA-binding protein Luc7-like 1	0.04076	-0.1991
Q15393	Splicing factor 3B subunit 3	0.036739	-0.14907
Q99848	Probable rRNA-processing protein EBP2	0.01264	0.034622
Q6IAA8	Ragulator complex protein LAMTOR1	0.046576	0.068805
P10809	60 kDa heat shock protein mitochondrial	0.011387	0.120315
Q9UBS4	DnaJ homolog subfamily B member 11	0.03396	0.131635
Q15691	Microtubule-associated protein RP/EB family member 1	0.016918	0.172764
P50453	Serpin B9	0.049934	0.219608
P09651	Heterogeneous nuclear ribonucleoprotein A1	0.023623	0.266611
Q03135	Caveolin-1	0.041296	0.268354
Q6FI81	Anamorsin	0.038627	0.274518
P18669	Phosphoglycerate mutase 1	0.004431	0.275737
P25705	ATP synthase subunit alpha mitochondrial	0.012843	0.282984
O43390	Heterogeneous nuclear ribonucleoprotein R	0.028606	0.303167

UniProt ID	Protein name	p-value	log_2FC
O75643	U5 small nuclear ribonucleoprotein 200 kDa helicase	0.008149	0.312299
P35998	26S protease regulatory subunit 7	0.033727	0.326723
P26368	Splicing factor U2AF 65 kDa subunit	0.04177	0.33091
P14868	Aspartate--tRNA ligase cytoplasmic	0.04751	0.331388
Q9Y3U8	60S ribosomal protein L36	0.028389	0.33282
Q12904	Aminoacyl tRNA synthase complex-interacting multifunctional protein 1	0.019469	0.341778
P37802	Transgelin-2	0.038468	0.361689
P12004	Proliferating cell nuclear antigen	0.039886	0.369901
Q4VC31	Coiled-coil domain-containing protein 58	0.032406	0.408049
Q13547	Histone deacetylase 1	0.048671	0.416232
O75534	Cold shock domain-containing protein E1	0.026697	0.423187
Q96EK6	Glucosamine 6-phosphate N-acetyltransferase	0.005022	0.439938
Q14694	Ubiquitin carboxyl-terminal hydrolase 10	0.029715	0.443877
Q15365	Poly(rC)-binding protein 1	0.028098	0.453189
P20042	Eukaryotic translation initiation factor 2 subunit 2	0.013268	0.455161
P47755	F-actin-capping protein subunit alpha-2	0.017904	0.471611
P62873	Guanine nucleotide-binding protein G(I)/G(S)/G(T) subunit beta-1	0.008401	0.477719
Q9UKA9	Polypyrimidine tract-binding protein 2	0.026967	0.479983
Q9Y5L4	Mitochondrial import inner membrane translocase subunit Tim13	0.028885	0.484873
P49189	4-trimethylaminobutyraldehyde dehydrogenase	0.027773	0.48737
Q9P258	Protein RCC2	0.011275	0.490022
P17844	Probable ATP-dependent RNA helicase DDX5	0.013947	0.497562

UniProt ID	Protein name	p-value	log_2FC
Q92973	Transportin-1	0.014659	0.505064
P08621	U1 small nuclear ribonucleoprotein 70 kDa	0.009627	0.552682
O14744	Protein arginine N-methyltransferase 5	0.027147	0.552869
Q9BY44	Eukaryotic translation initiation factor 2A	0.001731	0.588643
P52907	F-actin-capping protein subunit alpha-1	0.032508	0.592592
P27694	Replication protein A 70 kDa DNA-binding subunit	0.008523	0.596414
P13797	Plastin-3	0.045045	0.603809
Q99497	Protein DJ-1	0.026282	0.620378
O75348	V-type proton ATPase subunit G 1	0.02722	0.632052
Q9Y2T2	AP-3 complex subunit mu-1	0.002676	0.654594
Q16401	26S proteasome non-ATPase regulatory subunit 5	0.042312	0.666697
Q9BSD7	Cancer-related nucleoside-triphosphatase	0.035784	0.685816
Q99714	3-hydroxyacyl-CoA dehydrogenase type-2	0.02252	0.687901
O60888	Protein CutA	0.02239	0.695726
P00558	Phosphoglycerate kinase 1	0.004528	0.704138
O95747	Serine/threonine-protein kinase OSR1	0.016493	0.719944
O75396	Vesicle-trafficking protein SEC22b	0.006454	0.735874
P08754	Guanine nucleotide-binding protein G(k) subunit alpha	0.006281	0.74208
P09874	Poly [ADP-ribose] polymerase 1	0.006168	0.788315
P18754	Regulator of chromosome condensation	6.73E-05	0.81838
Q9H0W9	Ester hydrolase C11orf54	0.004713	0.91519
P09382	Galectin-1	0.021346	0.931815
Q53GS9	U4/U6.U5 tri-snRNP-associated protein 2	0.001933	0.958779

UniProt ID	Protein name	p-value	log_2FC
P11166	Solute carrier family 2 facilitated glucose transporter member 1	0.005728	1.029667
Q96I24	Far upstream element-binding protein 3	0.029112	1.065205
Q9P0L0	Vesicle-associated membrane protein-associated protein A	0.04238	1.115086
Q9C0C9	E2/E3 hybrid ubiquitin-protein ligase UBE2O	0.004263	1.125632
Q5BKZ1	DBIRD complex subunit ZNF326	0.010582	1.151163
Q9UBU9	Nuclear RNA export factor 1	0.02943	1.189995
Q08170	Serine/arginine-rich splicing factor 4	0.047882	1.190882
Q9NRR5	Ubiquilin-4	0.027304	1.493982
P51003	Poly(A) polymerase alpha	0.046096	1.498614
Q92785	Zinc finger protein ubi-d4	0.006393	1.602427
P11233	Ras-related protein Ral-A	0.03202	2.047507
Q6TFL3	Coiled-coil domain-containing protein 171	0.000395	2.092077
Q96IR7	4-hydroxyphenylpyruvate dioxygenase-like protein	0.015992	2.498115
Q86TU7	Histone-lysine N-methyltransferase setd3	0.000617	2.633625
P20338	Ras-related protein Rab-4A	0.040436	3.670681

A.3 *FADS1* sequence containing 1500bp upstream of transcription start site, 5' UTR, exons and 3' UTR

```
>hg19_knownGene_uc010rlm.2_0 range=chr11:61584530-
61586029 5'pad=0 3'pad=0 strand=- repeatMasking=none
#PROMOTER1500bp
tattgtcaggactcgggtttatttccagttttgctattaaattggctat
ttctgcatctttgcacagtctcccctactttaccaagagtgaaactgctt
gatcaaagaatagaaaatgttttgtagctcgcattagacactgccaagtt
gttgggcaaggtttttaaaaaaggaatattggctgtacagaggtgcagct
gtgtggaccatcattcctgagcagggtccaatagcctggcatcttacctg
gaagtcaggacatctaaacttccctatgggaacttggtaagccccttccc
catttcgaacctcaattttcttatctataaaatgaagaatttggatggaa
tgaattaatccttttctaccagaaatctagccatatttcacctagtctat
tctgtatcaccctctcctgactcctacgtgctcagaatctagctcagtgc
ttgggacagttatgtttcctttccctttgaagtgcccaaataccagtgta
atgagaaatatggcagagcctgagagttcagagcacaggccagggtcaaa
tctcagccctccacttacaagctgtgtgacaaaataacctcccccgggct
cagtttcttcactgtaaattaggttaattgttccaacctcatagggttgt
taggagaattaaatgagttaaggtttgcaaaacgctaagaacagtgcctg
gcacacagtaagtgctttataaagtgtttgttgaataaataaaattttgg
acctaaactctgggtctcttcaggactgcaacagctttgtaactggcaac
cccacttttaggtgcgttcccactcctctaaaacccagagatctaaatgc
caaatctctctgcttaaaaagtctcccagggctcctaggcgcctccaggc
tagaacagaaatgcctcagcttgaagacccaggcttttcaggtgaaacac
ctaagggtcaggagacgctaggatcatcactcaaggatcccagtgaattt
ttccaaaatacaataaaaataaaaacaaaaagaggcaaacagggttataa
aaattgtggggcattttaaatgtttcattgaacaaattaaagcattaaca
gccctcccccaaccaccaccaagcccaagagaccgtaaatatgctgttca
caagataactgcaactttcaagggctctcaggctgctacttcgggcagca
caattggcggcacgacgtggcaagcaggcagtagtttccaaccctggagg
gtcagcgtctggagaccccggccaaggcatccacagcctaaagatgatgt
ccgcgaccgcccgggcagcctcgtgcacggaaaaacctcaaccccggccc
cgcccacccttcctgcggccaccccgcagccctggcccctcagtccattc
actcctgcagcgcggccccgcacccagggcctgcactagaaccgctgttc
ctaccgcggcgcccccctgggagccaacgccgcgatgcccgcctgacgtca
>hg19_knownGene_uc010rlm.2_1 range=chr11:61584402-
61584529 5'pad=0 3'pad=0 strand=- repeatMasking=none
#5UTR - TSS
GGAAGTCGAATCCGGCGGCGACGCCTTTAGGGAGCCCGCGAGGGGGCGCG
TGTTGGCAGCCCAGCTGTGAGTTGCCCAAGACCCACCGGGGGGACGGGATC
TCGCTCCCCGCGCCACGAGGCTCGGCCA
>hg19_knownGene_uc010rlm.2_2 range=chr11:61584027-
61584401 5'pad=0 3'pad=0 strand=- repeatMasking=none
#EXON1/12
ATGGGAACGCGCGCTGCGAGGCCCGCCGGTCTGCCCTGCGGTGCTGAAAA
```

CCCGGCGCGCAGGCGGCTGGCTCTGGGCGCGCGCCAGCAAATCCACTCCT
GGAGCCCGCGGACCCCGAGCACGCGCCTGACAGCCCCTGCTGGCCCGGCG
CGCGGCGTCGCCAGGCCAGCTATGGCCCCCGACCCGGTGGCCGCCGAGAC
CGCGGCTCAGGGACCTACCCCGCGCTACTTCACCTGGGACGAGGTGGCCC
AGCGCTCAGGGTGCGAGGAGCGGTGGCTAGTGATCGACCGTAAGGTGTAC
AACATCAGCGAGTTCACCCGCCGGCATCCAGGGGGCTCCCGGGTCATCAG
CCACTACGCCGGGCAGGATGCCACG
>hg19_knownGene_uc010rlm.2_3 range=chr11:61580715-
61580825 5'pad=0 3'pad=0 strand=- repeatMasking=none
#EXON2/12
GATCCCTTTGTGGCCTTCCACATCAACAAGGGCCTTGTGAAGAAGTATAT
GAACTCTCTCCTGATTGGAGAACTGTCTCCAGAGCAGCCCAGCTTTGAGC
CCACCAAGAAT
>hg19_knownGene_uc010rlm.2_4 range=chr11:61579943-
61580140 5'pad=0 3'pad=0 strand=- repeatMasking=none
#EXON3/12
AAAGAGCTGACAGATGAGTTCCGGGAGCTGCGGGCCACAGTGGAGCGGAT
GGGGCTCATGAAGGCCAACCATGTCTTCTTCCTGCTGTACCTGCTGCACA
TCTTGCTGCTGGATGGTGCAGCCTGGCTCACCCTTTGGGTCTTTGGGACG
TCCTTTTTGCCCTTCCTCCTCTGTGCGGTGCTGCTCAGTGCAGTTCAG
>hg19_knownGene_uc010rlm.2_5 range=chr11:61578446-
61578547 5'pad=0 3'pad=0 strand=- repeatMasking=none
#EXON4/12
GCCCAGGCTGGCTGGCTGCAGCATGACTTTGGGCACCTGTCGGTCTTCAG
CACCTCAAAGTGGAACCATCTGCTACATCATTTTGTGATTGGCCACCTGA
AG
>hg19_knownGene_uc010rlm.2_6 range=chr11:61578223-
61578351 5'pad=0 3'pad=0 strand=- repeatMasking=none
#EXON5/12
GGGGCCCCCGCCAGTTGGTGGAACCACATGCACTTCCAGCACCATGCCAA
GCCCAACTGCTTCCGCAAAGACCCAGACATCAACATGCATCCCTTCTTCT
TTGCCTTGGGGAAGATCCTCTCTGTGGAG
>hg19_knownGene_uc010rlm.2_7 range=chr11:61574136-
61574196 5'pad=0 3'pad=0 strand=- repeatMasking=none
#EXON6/12
CTTGGGAAACAGAAGAAAAAATATATGCCGTACAACCACCAGCACAAATA
CTTCTTCCTAA
>hg19_knownGene_uc010rlm.2_8 range=chr11:61572157-
61572233 5'pad=0 3'pad=0 strand=- repeatMasking=none
#EXON7/12
TTGGGCCCCCAGCCTTGCTGCCTCTCTACTTCCAGTGGTATATTTTCTAT
TTTGTTATCCAGCGAAAGAAGTGGGTG
>hg19_knownGene_uc010rlm.2_9 range=chr11:61571142-
61571239 5'pad=0 3'pad=0 strand=- repeatMasking=none
#EXON8/12
GACTTGGCCTGGATGATTACCTTCTACGTCCGCTTCTTCCTCACTTATGT
GCCACTATTGGGGCTGAAAGCCTTCCTGGGCCTTTTCTTCATAGTCAG
>hg19_knownGene_uc010rlm.2_10 range=chr11:61570835-
61570931 5'pad=0 3'pad=0 strand=- repeatMasking=none

#EXON9/12
GTTCCTGGAAAGCAACTGGTTTGTGTGGGTGACACAGATGAACCATATTC
CCATGCACATTGATCATGACCGGAACATGGACTGGGTTTCCACCCAG
>hg19_knownGene_uc010rlm.2_11 range=chr11:61570504-
61570583 5'pad=0 3'pad=0 strand=- repeatMasking=none
#EXON10/12
CTCCAGGCCACATGCAATGTCCACAAGTCTGCCTTCAATGACTGGTTCAG
TGGACACCTCAACTTCCAGATTGAGCACCA
>hg19_knownGene_uc010rlm.2_12 range=chr11:61570273-
61570398 5'pad=0 3'pad=0 strand=- repeatMasking=none
#EXON11/12
TCTTTTTCCCACGATGCCTCGACACAATTACCACAAAGTGGCTCCCCTGG
TGCAGTCCTTGTGTGCCAAGCATGGCATAGAGTACCAGTCCAAGCCCCTG
CTGTCAGCCTTCGCCGACATCATCCA
>hg19_knownGene_uc010rlm.2_13 range=chr11:61569883-
61569934 5'pad=0 3'pad=0 strand=- repeatMasking=none
#EXON12/12
CTCACTAAAGGAGTCAGGGCAGCTCTGGCTAGATGCCTATCTTCACCAAT
AA
>hg19_knownGene_uc010rlm.2_14 range=chr11:61567097-
61569882 5'pad=0 3'pad=0 strand=- repeatMasking=none
#3UTR
CAACAGCCACCCTGCCCAGTCTGGAAGAAGAGGAGGAAGACTCTGGAGCC
AAGGCAGAGGGGAGCTTGAGGGACAATGCCACTATAGTTTAATACTCAGA
GGGGGTTGGGTTTGGGGACATAAAGCCTCTGACTCAAACTCCTCCCTTTT
ATCTTCTAGCCACAGTTCTAAGACCCAAAGTGGGGGGTGGACACAGAAGT
CCCTAGGAGGGAAGGAGCTGTTGGGGCAGGGGTGTAAATTATTTCCTTTT
TCTAGTTTGGCACATGCAGGTAGTTGGTGAACAGAGAGAACCAGGAGGGT
AACAGAAGAGGAGGGACCTACTGAACCCAGAGTCAGGAAGAGATTTAACA
CTAAAATTCCACTCATGCCGGGCGTGGTGGCACGCGCCTGTAATCCCAGC
TACCCAGGAGGCTGAGGCAGGAGAATCGCTTGAACCGGGGAGGTGGAGGT
TGCAGTGAGCTGAGATCACGCCATTGTACTCCAGCCTGGGCGACAGAGCA
AGACTCCATTTCAAAAAAAAAAAAAAAATCCACTCATATAAAAGGTGAGC
TCAGCTCACTGGTCCATTTCTCAGTGGCTTCTCCATCCTCATTTGCAAAC
CTCAGAGGGATAAGGCAGTTGAACCTGATGAGCAAGAATTATAACAGCAA
GGAAACATTAATGCTTAGAATTCTGAGATCCAGCACAACTCAGTCTGTGG
GAGCTCAGCTCGCTGCCCAGGGATAGGTATGACCTATGTCTGCCTTAGGC
TGCTGGGAGATGCCATTCTCCAGTTTCAGAAGCAGGCAGGGCAAAGGTCA
AGACTGTGGTATTGGGGTCTTTTGGCTCTGAAGGATCCTGGAACCACTGA
TTTTGGTTTATTCCCTCCAGGGTCTAAAGAGAACAAGAGGTGCTAGCTCT
TACCAAAACAGATGGTAGAGAGAGTTGCTGGCTATTTAAAAAGCTCTTTC
ATCTTTTAATTCACCTCTTCTTTTCACCTCTTTAACCACTCCTCAGGAAC
AGAACACTTCTAGGACTGGGGGTCTTTTAGCTCCATAAGCAAGTGAGCAG
ATGGGACAAGTTAGTCTTTTCTCCCTAGAAACAAAGGGGATGCCCAGTGG
TTTCCCTTTGCTTCCCAACCTAAAATTTCAAGTTTAATAAAATAGCAATT
AGCAGAAGTGACCAAATTGGGAGATAATTATCAGTCATGAGGAAAGACAC
AGATTTCGGTCATAAAGAATGTAAGGGCTATAAGTAGAAACTTTCTATAA
CCTAAATGATGTTATAGAATTATTTTTGAGCAGGAGCAGAAAGATTAAAT
ATGATCACTTCATACTTCTAAATCAGAAATAGGAAGATTAAAACCACAGA

ACAGTTTGTGATTTCTATTGCTGTAGCTAGGTATCTTACTCTGTCCACTC
TTGTTCAAGTATCTAACTCTTCTGGAAACCAAATAGGCTTTAGAAGAGAT
TATCCTATATTCCTATCAGTATAATACTAAAATGTAACTTTTTAATCATC
TGGTTTTTAAAAGATAAACAGTTTAGCCCATCTCTCCAGAGAGCAAACAT
AGGAATATGACTCAGGAGCCTCCTAGGGCTTATCATCAGCCCTCACACCC
GCTTCCCCCTCCAACCCACAGCCTTTGCTTCCAGGTGGCAGGATTACTAC
TTTGCCTCTTCAGCAGCATCTACTCTAGGCATATTGATCATTTTAGACAC
TGGGAGAAGAGAACCTCAAACTAGGAGGAAAAGACAGAGCCTCCACTTAG
TTTTGGGAGGGGATGGCAGACAGTCAAGGAGATGAGCGTCCTAAGGCATG
TTGGGATAGGGTCAGATGCACCACCCATGGAGAGGTTTGTCAACACAAAG
ACATGGAAGGTTAGAGGTTTGTCAACAAAAAGACATGGAAGGTTAGGTTT
GTCAACACAAAGACATGGAAGATTAGAGGTTTGTCAACACAAAGACACAG
GAAGAATGGGCTGCAGAAGATTTAGATGTTTTCCATTTGGGCACATTTTA
CTTAGCTGGAGAACTAGGTTTAAAACAGCCTGGGTAGGAAAATTAGAAGC
AAGCTGGATGCAGTGGCTCATGCCTGTAATCCCAACACTTTTGGGAGGTC
CAGGCAGGAGGATCACTTGGGCCCAGGAGGTCAAGCCTGCAGCGAGCTGA
GATCACACCACTGCACTCCAGCCTGGGGTGATAGAACAAGACCCTGTCTC
AAAAAAAAAAAAAACAACAAAAACTTAGAATTGAGGAGTTGTACCTCCAT
TGGCTTCCTCACTCCAAAATAGGTGCTGATCCTTCCTATTCCTATTCTTT
GCCACCTTTTGGGTGTGGTGTCACCAGCCTGTTTAGCCAAGTAGCTTTGG
GCATAGGCTGCCCAATCTGAGCAAACACCAGTGAGGCTCTATTGAGCCAA
GACCAAGTCCTCAAAGCACCTGAACCACTGTGGCCTTCTCAGCCTACAGC
AGTGTGGTCTCTTACATGGCCACAAAGGGACACACAGTGACAAAAGGCTC
GGAATGTTACAATGGTAAAATGAGTGATCTCAAATCCACTGACAGATATA
AAATAGGCTTAGAGAGGAAAAGCTGCCTCTGGTCAAGTAGATCATGGCAG
CATGAATTCCAACTCACTTTTTTACAACTCCAACTTCTATGTTTATCTTT
GTTACTTTCACTTTTTTACAACCTGGCCAGAGGCATTTTTTAAATCAGGC
CCAATATCAGTATTCTTTTTGTGTGTGCCAATTTTGTTATCACATCCCTA
TGAAGTTGAAAAATAAAGTTAATTTTGACCAAAAGA

A.4 Concentration of individual fatty acids in hESC medium and CM

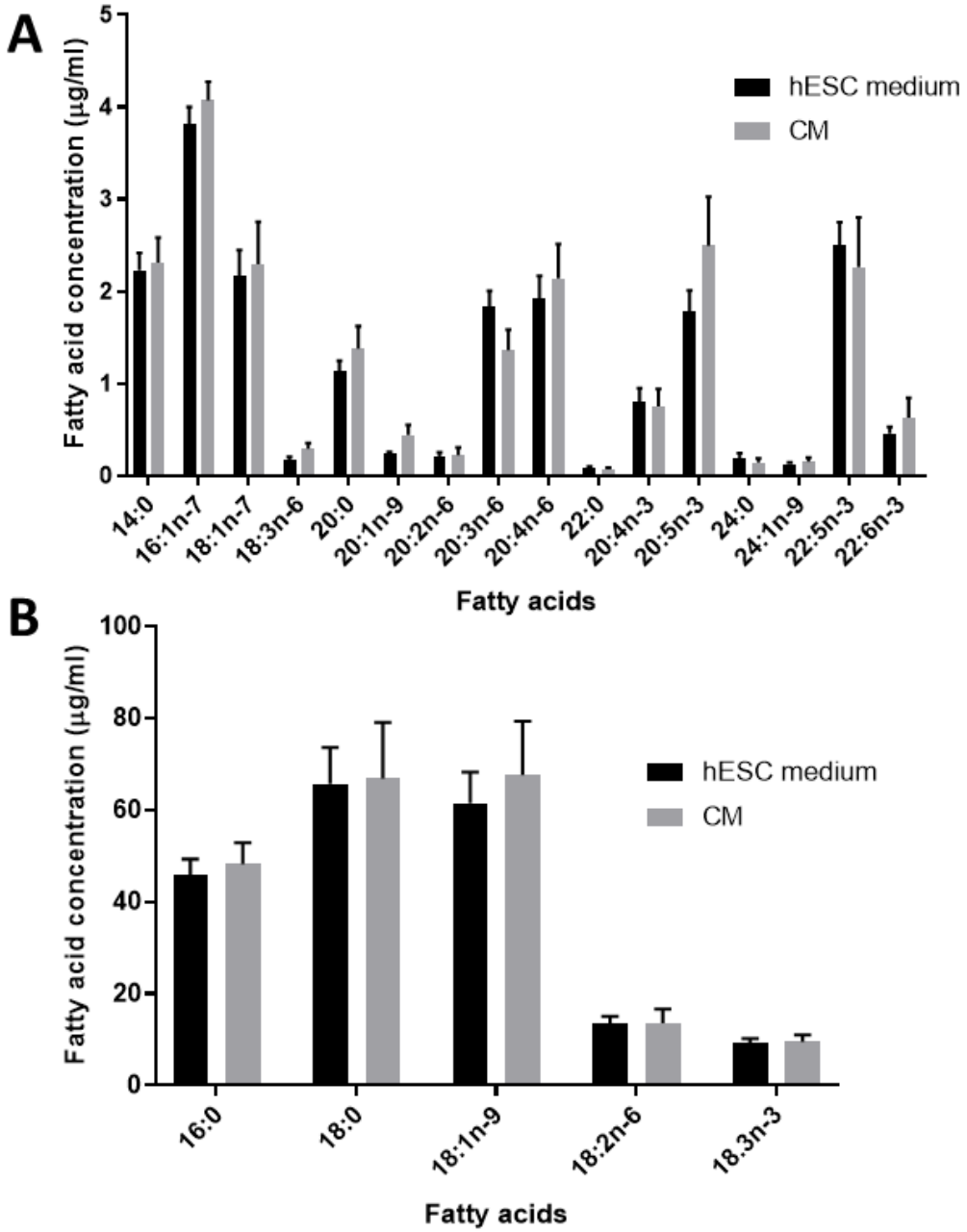

Figure A.4 Conditioning hESC medium with mitotically inactive MEFs does not affect the concentration of individual fatty acids.

Individual fatty acids with a concentration that is higher than 9 µg/ml (A) and lower than 9 µg/ml (B) in hESC medium compared to CM. The medium was conditioned on iMEFs for 24 hours. Bars represent mean + SEM. n=7.

Bibliography

Abdelmagid, S.A., Clarke, S.E., Nielsen, D.E., Badawi, A., El-Sohemy, A., Mutch, D.M. and Ma, D.W.L. (2015) Comprehensive Profiling of Plasma Fatty Acid Concentrations in Young Healthy Canadian Adults. *PLOS ONE,* 10 (2), e0116195.

Abdi, J., Garssen, J., Faber, J. and Redegeld, F.A. (2014) Omega-3 fatty acids, EPA and DHA induce apoptosis and enhance drug sensitivity in multiple myeloma cells but not in normal peripheral mononuclear cells. *Journal of Nutritional Biochemistry,* 25 (12), 1254-1262.

Abolpour Mofrad, S., Kuenzel, K., Friedrich, O. and Gilbert, D.F. (2016) Optimizing neuronal differentiation of human pluripotent NT2 stem cells in monolayer cultures. *Development, Growth & Differentiation,* 58 (8), 664-676.

Abulrob, A., Giuseppin, S., Andrade, M.F., Mcdermid, A., Moreno, M. and Stanimirovic, D. (2004) Interactions of EGFR and caveolin-1 in human glioblastoma cells: evidence that tyrosine phosphorylation regulates EGFR association with caveolae. *Oncogene,* 23 (41), 6967-6979.

Ali, A.a.E., Timinszky, G., Arribas-Bosacoma, R., Kozlowski, M., Hassa, P.O., Hassler, M., Ladurner, A.G., Pearl, L.H. and Oliver, A.W. (2012) The zinc-finger domains of PARP1 cooperate to recognize DNA strand breaks. *Nature Structural & Molecular Biology,* 19 (7), 685-692.

Allegrucci, C. and Young, L.E. (2007) Differences between human embryonic stem cell lines. *Human Reproduction Update,* 13 (2), 103-120.

Amit, M. and Itskovitz-Eldor, J. (2002) Derivation and spontaneous differentiation of human embryonic stem cells. *Journal of anatomy,* 200 (Pt 3), 225-232.

Amit, M., Margulets, V., Segev, H., Shariki, K., Laevsky, I., Coleman, R. and Itskovitz-Eldor, J. (2003) Human Feeder Layers for Human Embryonic Stem Cells. *Biology of Reproduction,* 68 (6), 2150-2156.

Aponte, P.M. (2015) Spermatogonial stem cells: Current biotechnological advances in reproduction and regenerative medicine. *World journal of stem cells,* 7 (4), 669-680.

Appelhoff, R.J., Tian, Y.-M., Raval, R.R., Turley, H., Harris, A.L., Pugh, C.W., Ratcliffe, P.J. and Gleadle, J.M. (2004) Differential Function of the Prolyl Hydroxylases PHD1, PHD2, and PHD3 in the Regulation of Hypoxia-inducible Factor. *Journal of Biological Chemistry,* 279 (37), 38458-38465.

Araki, R., Hoki, Y., Uda, M., Nakamura, M., Jincho, Y., Tamura, C., Sunayama, M., Ando, S., Sugiura, M., Yoshida, M.A., Kasama, Y. and Abe, M. (2011) Crucial role of c-Myc in the generation of induced pluripotent stem cells. *Stem Cells,* 29 (9), 1362-1370.

Arany, Z., Huang, L.E., Eckner, R., Bhattacharya, S., Jiang, C., Goldberg, M.A., Bunn, H.F. and Livingston, D.M. (1996) An essential role for p300/CBP in the cellular response to hypoxia. *Proceedings of the National Academy of Sciences,* 93 (23), 12969-12973.

Arita, K., Kobuchi, H., Utsumi, T., Takehara, Y., Akiyama, J., Horton, A.A. and Utsumi, K. (2001) Mechanism of apoptosis in HL-60 cells induced by n-3 and n-6 polyunsaturated fatty acids. *Biochemical Pharmacology,* 62 (7), 821-828.

Augstein, A., Poitz, D.M., Braun-Dullaeus, R.C., Strasser, R.H. and Schmeisser, A. (2011) Cell-specific and hypoxia-dependent regulation of human HIF-3alpha: inhibition of the expression of HIF target genes in vascular cells. *Cellular and Molecular Life Sciences,* 68 (15), 2627-2642.

Avilion, A.A., Nicolis, S.K., Pevny, L.H., Perez, L., Vivian, N. and Lovell-Badge, R. (2003) Multipotent cell lineages in early mouse development depend on SOX2 function. *Genes & Development,* 17 (1), 126-140.

Azimi, I., Petersen, R.M., Thompson, E.W., Roberts-Thomson, S.J. and Monteith, G.R. (2017) Hypoxia-induced reactive oxygen species mediate N-cadherin and SERPINE1 expression,

EGFR signalling and motility in MDA-MB-468 breast cancer cells. *Scientific Reports,* 7 (1), 15140.

Babaie, Y., Herwig, R., Greber, B., Brink, T.C., Wruck, W., Groth, D., Lehrach, H., Burdon, T. and Adjaye, J. (2007) Analysis of Oct4-dependent transcriptional networks regulating self-renewal and pluripotency in human embryonic stem cells. *Stem Cells,* 25 (2), 500-510.

Bar-Nur, O., Russ, H.A., Efrat, S. and Benvenisty, N. (2011) Epigenetic memory and preferential lineage-specific differentiation in induced pluripotent stem cells derived from human pancreatic islet beta cells. *Cell Stem Cell,* 9 (1), 17-23.

Barthelery, M., Jaishankar, A., Salli, U., Freeman, W.M. and Vrana, K.E. (2009) 2-D DIGE identification of differentially expressed heterogeneous nuclear ribonucleoproteins and transcription factors during neural differentiation of human embryonic stem cells. *Proteomics - Clinical Applications,* 3 (4), 505-514.

Bartova, E., Galiova, G., Krejci, J., Harnicarova, A., Strasak, L. and Kozubek, S. (2008) Epigenome and chromatin structure in human embryonic stem cells undergoing differentiation. *Developmental Dynamics,* 237 (12), 3690-3702.

Battye, F. (2015) *Weasel for Display and Analysis of Flow Cytometry Data*. Available from: https://frankbattye.com.au/Weasel/index.html.

Bazan, N.G. (2018) Docosanoids and elovanoids from omega-3 fatty acids are pro-homeostatic modulators of inflammatory responses, cell damage and neuroprotection. *Molecular Aspects of Medicine,* 64, 18-33.

Beitner-Johnson, D. and Millhorn, D.E. (1998) Hypoxia induces phosphorylation of the cyclic AMP response element-binding protein by a novel signaling mechanism. *Journal of Biological Chemistry,* 273 (31), 19834-19839.

Bell, A.W., Deutsch, E.W., Au, C.E., Kearney, R.E., Beavis, R., Sechi, S., Nilsson, T., Bergeron, J.J.M. and Group, H.T.S.W. (2009) A HUPO test sample study reveals common problems in mass spectrometry-based proteomics. *Nature methods,* 6 (6), 423-430.

Bennett, M. and Gilroy, D.W. (2016) Lipid Mediators in Inflammation. *Microbiology Spectrum,* 4 (6).

Bensaad, K., Favaro, E., Lewis, C.A., Peck, B., Lord, S., Collins, J.M., Pinnick, K.E., Wigfield, S., Buffa, F.M., Li, J.L., Zhang, Q., Wakelam, M.J.O., Karpe, F., Schulze, A. and Harris, A.L. (2014) Fatty acid uptake and lipid storage induced by HIF-1alpha contribute to cell growth and survival after hypoxia-reoxygenation. *Cell Reports,* 9 (1), 349-365.

Berra, E., Benizri, E., Ginouves, A., Volmat, V., Roux, D. and Pouyssegur, J. (2003) HIF prolyl-hydroxylase 2 is the key oxygen sensor setting low steady-state levels of HIF-1alpha in normoxia. *The EMBO journal,* 22 (16), 4082-4090.

Bharathan, S.P., Manian, K.V., Aalam, S.M.M., Palani, D., Deshpande, P.A., Pratheesh, M.D., Srivastava, A. and Velayudhan, S.R. (2017) Systematic evaluation of markers used for the identification of human induced pluripotent stem cells. *Biology open,* 6 (1), 100-108.

Bibikova, M., Chudin, E., Wu, B., Zhou, L., Garcia, E.W., Liu, Y., Shin, S., Plaia, T.W., Auerbach, J.M., Arking, D.E., Gonzalez, R., Crook, J., Davidson, B., Schulz, T.C., Robins, A., Khanna, A., Sartipy, P., Hyllner, J., Vanguri, P., Savant-Bhonsale, S., Smith, A.K., Chakravarti, A., Maitra, A., Rao, M., Barker, D.L., Loring, J.F. and Fan, J.B. (2006) Human embryonic stem cells have a unique epigenetic signature. *Genome Research,* 16 (9), 1075-1083.

Boer, B., Kopp, J., Mallanna, S., Desler, M., Chakravarthy, H., Wilder, P.J., Bernadt, C. and Rizzino, A. (2007) Elevating the levels of Sox2 in embryonal carcinoma cells and embryonic stem cells inhibits the expression of Sox2:Oct-3/4 target genes†. *Nucleic Acids Research,* 35 (6), 1773-1786.

Boileau, P., Mrejen, C., Girard, J. and Hauguel-De Mouzon, S. (1995) Overexpression of GLUT3 placental glucose transporter in diabetic rats. *The journal of Clinical Investigation,* 96 (1), 309-317.

Bongso, A. and Lee, E.H. (2005) Stem Cells: Their Definition, Classification and Sources *Stem Cells - From Bench to Bedside*. World Scientific Publishing Co. Pte. Ltd., 1-13.

Bontekoe, S., Mantikou, E., Van Wely, M., Seshadri, S., Repping, S. and Mastenbroek, S. (2012) Low oxygen concentrations for embryo culture in assisted reproductive technologies. *Cochrane Database of Systematic Reviews,* (7), Cd008950.

Boyer, L.A., Lee, T.I., Cole, M.F., Johnstone, S.E., Levine, S.S., Zucker, J.P., Guenther, M.G., Kumar, R.M., Murray, H.L., Jenner, R.G., Gifford, D.K., Melton, D.A., Jaenisch, R. and Young, R.A. (2005) Core transcriptional regulatory circuitry in human embryonic stem cells. *Cell,* 122 (6), 947-956.

Brivanlou, A.H., Gage, F.H., Jaenisch, R., Jessell, T., Melton, D. and Rossant, J. (2003) Stem cells. Setting standards for human embryonic stem cells. *Science,* 300 (5621), 913-916.

Bruder, E.D., Lee, P.C. and Raff, H. (2004) Metabolomic analysis of adrenal lipids during hypoxia in the neonatal rat: implications in steroidogenesis. *American Journal of Physiology: Endocrinology and Metabolism,* 286 (5), E697-703.

Calder, P.C. (2015) Functional Roles of Fatty Acids and Their Effects on Human Health. *Parenteral and Enteral Nutrition,* 39 (1 Suppl), 18s-32s.

Calder, P.C. (2016) Fatty Acids: Metabolism IN: Caballero, B., Finglas, P. and Toldra, F. (eds) *The Encyclopedia of Food and Health*. Oxford: Academic Press: Elsevier Ltd., 632-644.

Calviello, G., Di Nicuolo, F., Gragnoli, S., Piccioni, E., Serini, S., Maggiano, N., Tringali, G., Navarra, P., Ranelletti, F.O. and Palozza, P. (2004) n-3 PUFAs reduce VEGF expression in human colon cancer cells modulating the COX-2/PGE 2 induced ERK-1 and -2 and HIF-1α induction pathway. *Carcinogenesis,* 25 (12), 2303-2310.

Calviello, G., Palozza, P., Di Nicuolo, F., Maggiano, N. and Bartoli, G.M. (2000) n-3 PUFA dietary supplementation inhibits proliferation and store-operated calcium influx in thymoma cells growing in Balb/c mice. *Journal of Lipid Research,* 41 (2), 182-189.

Calviello, G., Su, H.M., Weylandt, K.H., Fasano, E., Serini, S. and Cittadini, A. (2013) Experimental evidence of omega-3 polyunsaturated fatty acid modulation of inflammatory cytokines and bioactive lipid mediators: their potential role in inflammatory, neurodegenerative, and neoplastic diseases. *BioMed Research International,* 2013, 743171.

Carrero, P., Okamoto, K., Coumailleau, P., O'brien, S., Tanaka, H. and Poellinger, L. (2000) Redox-regulated recruitment of the transcriptional coactivators CREB-binding protein and SRC-1 to hypoxia-inducible factor 1alpha. *Mol Cell Biol,* 20 (1), 402-415.

Castillo Bennett, J., Silva, P., Martinez, S., Torres, V.A. and Quest, A.F.G. (2018) Hypoxia-Induced Caveolin-1 Expression Promotes Migration and Invasion of Tumor Cells. *Current Molecular Medicine,* 18 (4), 199-206.

Caughey, G.E., Mantzioris, E., Gibson, R.A., Cleland, L.G. and James, M.J. (1996) The effect on human tumor necrosis factor alpha and interleukin 1 beta production of diets enriched in n-3 fatty acids from vegetable oil or fish oil. *The American Journal of Clinical Nutrition,* 63 (1), 116-122.

Ceccarelli, V., Racanicchi, S., Martelli, M.P., Nocentini, G., Fettucciari, K., Riccardi, C., Marconi, P., Di Nardo, P., Grignani, F., Binaglia, L. and Vecchini, A. (2011) Eicosapentaenoic acid demethylates a single CpG that mediates expression of tumor suppressor CCAAT/enhancer-binding protein delta in U937 leukemia cells. *Journal of Biological Chemistry,* 286 (31), 27092-27102.

Cerychova, R. and Pavlinkova, G. (2018) HIF-1, Metabolism, and Diabetes in the Embryonic and Adult Heart. *Frontiers in Endocrinology,* 9 (460).

Chaerkady, R., Kerr, C.L., Marimuthu, A., Kelkar, D.S., Kashyap, M.K., Gucek, M., Gearhart, J.D. and Pandey, A. (2009) Temporal analysis of neural differentiation using quantitative proteomics. *Journal of Proteome Research,* 8 (3), 1315-1326.

Chaitanya, G.V., Steven, A.J. and Babu, P.P. (2010) PARP-1 cleavage fragments: signatures of cell-death proteases in neurodegeneration. *Cell communication and signaling,* 8, 31-31.

Chambers, I., Colby, D., Robertson, M., Nichols, J., Lee, S., Tweedie, S. and Smith, A. (2003) Functional expression cloning of Nanog, a pluripotency sustaining factor in embryonic stem cells. *Cell,* 113 (5), 643-655.

Chambers, I., Silva, J., Colby, D., Nichols, J., Nijmeijer, B., Robertson, M., Vrana, J., Jones, K., Grotewold, L. and Smith, A. (2007) Nanog safeguards pluripotency and mediates germline development. *Nature,* 450, 1230.

Chan, K.K., Zhang, J., Chia, N.Y., Chan, Y.S., Sim, H.S., Tan, K.S., Oh, S.K., Ng, H.H. and Choo, A.B. (2009) KLF4 and PBX1 directly regulate NANOG expression in human embryonic stem cells. *Stem Cells,* 27 (9), 2114-2125.

Chandel, N.S., Maltepe, E., Goldwasser, E., Mathieu, C.E., Simon, M.C. and Schumacker, P.T. (1998) Mitochondrial reactive oxygen species trigger hypoxia-induced transcription. *Proceedings of the National Academy of Sciences of the United States of America,* 95 (20), 11715-11720.

Chang, D.F., Tsai, S.C., Wang, X.C., Xia, P., Senadheera, D. and Lutzko, C. (2009) Molecular Characterization of the Human NANOG Protein. *Stem Cells,* 27 (4), 812-821.

Chatgilialoglu, A., Rossi, M., Alviano, F., Poggi, P., Zannini, C., Marchionni, C., Ricci, F., Tazzari, P.L., Taglioli, V., Calder, P.C. and Bonsi, L. (2017) Restored in vivo-like membrane lipidomics positively influence in vitro features of cultured mesenchymal stromal/stem cells derived from human placenta. *Stem Cell Research & Therapy,* 8, 31.

Chen, A.E. and Melton, D.A. (2007) Derivation of human embryonic stem cells by immunosurgery. *Journal of visualized experiments : JoVE,* (10), 574-574.

Chen, C.-Y., Su, C.-W. and Kang, J.X. (2020) Endogenous Omega-3 Polyunsaturated Fatty Acids Reduce the Number and Differentiation of White Adipocyte Progenitors in Mice. *Obesity,* 28 (2), 235-240.

Chen, H.F., Kuo, H.C., Chien, C.L., Shun, C.T., Yao, Y.L., Ip, P.L., Chuang, C.Y., Wang, C.C., Yang, Y.S. and Ho, H.N. (2007a) Derivation, characterization and differentiation of human embryonic stem cells: comparing serum-containing versus serum-free media and evidence of germ cell differentiation. *Human Reproduction,* 22 (2), 567-577.

Chen, W., Jump, D.B., Esselman, W.J. and Busik, J.V. (2007b) Inhibition of cytokine signaling in human retinal endothelial cells through modification of caveolae/lipid rafts by docosahexaenoic acid. *Investigative Ophthalmology & Visual Science,* 48 (1), 18-26.

Chew, J.-L., Loh, Y.-H., Zhang, W., Chen, X., Tam, W.-L., Yeap, L.-S., Li, P., Ang, Y.-S., Lim, B., Robson, P. and Ng, H.-H. (2005) Reciprocal Transcriptional Regulation of Pou5f1 and Sox2 via the Oct4/Sox2 Complex in Embryonic Stem Cells. *Molecular and Cellular Biology,* 25 (14), 6031-6046.

Chiu, L.C. and Wan, J.M. (1999) Induction of apoptosis in HL-60 cells by eicosapentaenoic acid (EPA) is associated with downregulation of bcl-2 expression. *Cancer Letters,* 145 (1-2), 17-27.

Cho, Y.H., Han, K.M., Kim, D., Lee, J., Lee, S.H., Choi, K.W., Kim, J. and Han, Y.M. (2014) Autophagy regulates homeostasis of pluripotency-associated proteins in hESCs. *Stem Cells,* 32 (2), 424-435.

Cho, Y.M., Kwon, S., Pak, Y.K., Seol, H.W., Choi, Y.M., Park, D.J., Park, K.S. and Lee, H.K. (2006) Dynamic changes in mitochondrial biogenesis and antioxidant enzymes during the spontaneous differentiation of human embryonic stem cells. *Biochemical and Biophysical Research Communications,* 348 (4), 1472-1478.

Christensen, D.R., Calder, P.C. and Houghton, F.D. (2015) GLUT3 and PKM2 regulate OCT4 expression and support the hypoxic culture of human embryonic stem cells. *Scientific Reports,* 5, 17500.

Cianci, E., Recchiuti, A., Trubiani, O., Diomede, F., Marchisio, M., Miscia, S., Colas, R.A., Dalli, J., Serhan, C.N. and Romano, M. (2016) Human Periodontal Stem Cells Release Specialized Proresolving Mediators and Carry Immunomodulatory and Prohealing Properties Regulated by Lipoxins. *Stem Cells Translational Medicine,* 5 (1), 20-32.

Clark, D.P. and Pazdernik, N.J. (2013) Chapter e15 - Proteomics: The Global Analysis of Proteins IN: Clark, D.P. and Pazdernik, N.J. (eds.) *Molecular Biology (Second Edition)*. Boston: Academic Press, e309-e314.

Cockman, M.E., Masson, N., Mole, D.R., Jaakkola, P., Chang, G.-W., Clifford, S.C., Maher, E.R., Pugh, C.W., Ratcliffe, P.J. and Maxwell, P.H. (2000) Hypoxia Inducible Factor-α Binding and

Ubiquitylation by the von Hippel-Lindau Tumor Suppressor Protein. *Journal of Biological Chemistry,* 275 (33), 25733-25741.

Condic, M.L. (2014) Totipotency: what it is and what it is not. *Stem cells and development,* 23 (8), 796-812.

Cook, H.W. and Mcmaster, C.R. (2002) Fatty acid desaturation and chain elongation in eukaryotes *New Comprehensive Biochemistry*. Elsevier, 181-204.

Crespo, F.L., Sobrado, V.R., Gomez, L., Cervera, A.M. and Mccreath, K.J. (2010) Mitochondrial reactive oxygen species mediate cardiomyocyte formation from embryonic stem cells in high glucose. *Stem Cells,* 28 (7), 1132-1142.

D'amours, D., Sallmann, F.R., Dixit, V.M. and Poirier, G.G. (2001) Gain-of-function of poly(ADP-ribose) polymerase-1 upon cleavage by apoptotic proteases: implications for apoptosis. *Journal of Cell Science,* 114 (Pt 20), 3771-3778.

Da Cruz, L., Fynes, K., Georgiadis, O., Kerby, J., Luo, Y.H., Ahmado, A., Vernon, A., Daniels, J.T., Nommiste, B., Hasan, S.M., Gooljar, S.B., Carr, A.-J.F., Vugler, A., Ramsden, C.M., Bictash, M., Fenster, M., Steer, J., Harbinson, T., Wilbrey, A., Tufail, A., Feng, G., Whitlock, M., Robson, A.G., Holder, G.E., Sagoo, M.S., Loudon, P.T., Whiting, P. and Coffey, P.J. (2018) Phase 1 clinical study of an embryonic stem cell–derived retinal pigment epithelium patch in age-related macular degeneration. *Nature Biotechnology,* 36 (4), 328-337.

Daskalaki, I., Gkikas, I. and Tavernarakis, N. (2018) Hypoxia and Selective Autophagy in Cancer Development and Therapy. *Frontiers in Cell and Developmental Biology,* 6 (104).

Dayan, F., Roux, D., Brahimi-Horn, M.C., Pouyssegur, J. and Mazure, N.M. (2006) The oxygen sensor factor-inhibiting hypoxia-inducible factor-1 controls expression of distinct genes through the bifunctional transcriptional character of hypoxia-inducible factor-1alpha. *Cancer Research,* 66 (7), 3688-3698.

De Carvalho, C.C.C.R. and Caramujo, M.J. (2018) The Various Roles of Fatty Acids. *Molecules (Basel, Switzerland),* 23 (10), 2583.

De Rooij, D.G. (2017) The nature and dynamics of spermatogonial stem cells. *Development,* 144 (17), 3022-3030.

Deng, P., Zhou, C., Alvarez, R., Hong, C. and Wang, C.-Y. (2016) Inhibition of IKK/NF-κB Signaling Enhances Differentiation of Mesenchymal Stromal Cells from Human Embryonic Stem Cells. *Stem cell reports,* 6 (4), 456-465.

Di Vizio, D., Adam, R.M., Kim, J., Kim, R., Sotgia, F., Williams, T., Demichelis, F., Solomon, K.R., Loda, M., Rubin, M.A., Lisanti, M.P. and Freeman, M.R. (2008) Caveolin-1 interacts with a lipid raft-associated population of fatty acid synthase. *Cell Cycle,* 7 (14), 2257-2267.

Doi, O., Doi, F., Schroeder, F., Alberts, A.W. and Vagelos, P.R. (1978) Manipulation of fatty acid composition of membrane phospholipid and its effects on cell growth in mouse LM cells. *Biochimica et Biophysica Acta,* 509 (2), 239-250.

Dormeyer, W., Van Hoof, D., Braam, S.R., Heck, A.J.R., Mummery, C.L. and Krijgsveld, J. (2008) Plasma Membrane Proteomics of Human Embryonic Stem Cells and Human Embryonal Carcinoma Cells. *Journal of Proteome Research,* 7 (7), 2936-2951.

Drakulic, D., Vicentic, J.M., Schwirtlich, M., Tosic, J., Krstic, A., Klajn, A. and Stevanovic, M. (2015) The overexpression of SOX2 affects the migration of human teratocarcinoma cell line NT2/D1. *Annals of the Brazilian Academy of Sciences,* 87 (1), 389-404.

Drukker, M., Katchman, H., Katz, G., Even-Tov Friedman, S., Shezen, E., Hornstein, E., Mandelboim, O., Reisner, Y. and Benvenisty, N. (2006) Human Embryonic Stem Cells and Their Differentiated Derivatives Are Less Susceptible to Immune Rejection Than Adult Cells. *Stem Cells,* 24 (2), 221-229.

Duan, C. (2016) Hypoxia-inducible factor 3 biology: complexities and emerging themes. *American Journal of Physiology-Cell Physiology,* 310 (4), C260-C269.

Duan, L.-J., Takeda, K. and Fong, G.-H. (2014) Hypoxia Inducible Factor-2α Regulates the Development of Retinal Astrocytic Network by Maintaining Adequate Supply of Astrocyte Progenitors. *PLOS ONE,* 9 (1), e84736.

Duplus, E., Glorian, M. and Forest, C. (2000) Fatty acid regulation of gene transcription. *The Journal of Biological Chemistry,* 275 (40), 30749-30752.

Eden, E., Navon, R., Steinfeld, I., Lipson, D. and Yakhini, Z. (2009) GOrilla: a tool for discovery and visualization of enriched GO terms in ranked gene lists. *BMC Bioinformatics,* 10 (1), 48.

Elser, M., Borsig, L., Hassa, P.O., Erener, S., Messner, S., Valovka, T., Keller, S., Gassmann, M. and Hottiger, M.O. (2008) Poly(ADP-ribose) polymerase 1 promotes tumor cell survival by coactivating hypoxia-inducible factor-1-dependent gene expression. *Molecular Cancer Research,* 6 (2), 282-290.

Ezashi, T., Das, P. and Roberts, R.M. (2005) Low O2 tensions and the prevention of differentiation of hES cells. *Proceedings of the National Academy of Sciences of the United States of America,* 102 (13), 4783-4788.

Ezzeddini, R., Taghikhani, M., Somi, M.H., Samadi, N. and Rasaee, M.J. (2019) Clinical importance of FASN in relation to HIF-1alpha and SREBP-1c in gastric adenocarcinoma. *Life Sciences,* 224, 169-176.

Fahrmann, J.F. and Hardman, W.E. (2013) Omega 3 fatty acids increase the chemo-sensitivity of B-CLL-derived cell lines EHEB and MEC-2 and of B-PLL-derived cell line JVM-2 to anti-cancer drugs doxorubicin, vincristine and fludarabine. *Lipids in Health and Disease,* 12, 36.

Fan, Y.-Y. and Chapkin, R.S. (1998) Importance of Dietary γ-Linolenic Acid in Human Health and Nutrition. *The Journal of Nutrition,* 128 (9), 1411-1414.

Fan, Y.-Y., Monk, J.M., Hou, T.Y., Callway, E., Vincent, L., Weeks, B., Yang, P. and Chapkin, R.S. (2012) Characterization of an arachidonic acid-deficient (Fads1 knockout) mouse model. *Journal of lipid research,* 53 (7), 1287-1295.

Fan, Y.Y., Ly, L.H., Barhoumi, R., Mcmurray, D.N. and Chapkin, R.S. (2004) Dietary docosahexaenoic acid suppresses T cell protein kinase C theta lipid raft recruitment and IL-2 production. *Journal of Immunology,* 173 (10), 6151-6160.

Farooq, M.A., Gaertner, S., Amoura, L., Niazi, Z.R., Park, S.-H., Qureshi, A.W., Oak, M.-H., Toti, F., Schini-Kerth, V.B. and Auger, C. (2020) Intake of omega-3 formulation EPA:DHA 6:1 by old rats for 2 weeks improved endothelium-dependent relaxations and normalized the expression level of ACE/AT1R/NADPH oxidase and the formation of ROS in the mesenteric artery. *Biochemical Pharmacology,* 173, 113749.

Fernandez-Torres, J., Zamudio-Cuevas, Y., Martinez-Nava, G.A. and Lopez-Reyes, A.G. (2017) Hypoxia-Inducible Factors (HIFs) in the articular cartilage: a systematic review. *European review for medical and pharmacological sciences,* 21 (12), 2800-2810.

Fernández, M.A., Albor, C., Ingelmo-Torres, M., Nixon, S.J., Ferguson, C., Kurzchalia, T., Tebar, F., Enrich, C., Parton, R.G. and Pol, A. (2006) Caveolin-1 Is Essential for Liver Regeneration. *Science,* 313 (5793), 1628-1632.

Field, C.J., Schley, P.D. and Brindley, D.N. (2007) Omega-3 polyunsaturated fatty acids alter raft lipid composition and decrease epidermal growth factor receptor levels in lipid rafts of human breast cancer cells. *The FASEB Journal,* 21 (5), A165-A165.

Finstad, H.S., Dyrendal, H., Myhrstad, M.C., Heimli, H. and Drevon, C.A. (2000) Uptake and activation of eicosapentaenoic acid are related to accumulation of triacylglycerol in Ramos cells dying from apoptosis. *Journal of Lipid Research,* 41 (4), 554-563.

Finstad, H.S., Kolset, S.O., Holme, J.A., Wiger, R., Farrants, A.K., Blomhoff, R. and Drevon, C.A. (1994) Effect of n-3 and n-6 fatty acids on proliferation and differentiation of promyelocytic leukemic HL-60 cells. *Blood,* 84 (11), 3799-3809.

Finstad, H.S., Myhrstad, M.C., Heimli, H., Lomo, J., Blomhoff, H.K., Kolset, S.O. and Drevon, C.A. (1998) Multiplication and death-type of leukemia cell lines exposed to very long-chain polyunsaturated fatty acids. *Leukemia,* 12 (6), 921-929.

Fischer, B. and Bavister, B.D. (1993) Oxygen tension in the oviduct and uterus of rhesus monkeys, hamsters and rabbits. *Journal of reproduction and fertility,* 99 (2), 673-679.

Fisher, A.E., Hochegger, H., Takeda, S. and Caldecott, K.W. (2007) Poly(ADP-ribose) polymerase 1 accelerates single-strand break repair in concert with poly(ADP-ribose) glycohydrolase. *Molecular and Cellular Biology,* 27 (15), 5597-5605.

Fogarty, N.M.E., Mccarthy, A., Snijders, K.E., Powell, B.E., Kubikova, N., Blakeley, P., Lea, R., Elder, K., Wamaitha, S.E., Kim, D., Maciulyte, V., Kleinjung, J., Kim, J.-S., Wells, D., Vallier, L.,

Bertero, A., Turner, J.M.A. and Niakan, K.K. (2017) Genome editing reveals a role for OCT4 in human embryogenesis. *Nature,* 550 (7674), 67-73.

Forristal, C.E., Christensen, D.R., Chinnery, F.E., Petruzzelli, R., Parry, K.L., Sanchez-Elsner, T. and Houghton, F.D. (2013) Environmental oxygen tension regulates the energy metabolism and self-renewal of human embryonic stem cells. *PLoS One,* 8 (5), e62507.

Forristal, C.E., Wright, K.L., Hanley, N.A., Oreffo, R.O. and Houghton, F.D. (2010) Hypoxia inducible factors regulate pluripotency and proliferation in human embryonic stem cells cultured at reduced oxygen tensions. *Reproduction,* 139 (1), 85-97.

Forsyth, N.R., Musio, A., Vezzoni, P., Simpson, A.H., Noble, B.S. and Mcwhir, J. (2006) Physiologic oxygen enhances human embryonic stem cell clonal recovery and reduces chromosomal abnormalities. *Cloning Stem Cells,* 8 (1), 16-23.

Frese, L., Dijkman, P.E. and Hoerstrup, S.P. (2016) Adipose Tissue-Derived Stem Cells in Regenerative Medicine. *Transfusion Medicine and Hemotherapy,* 43 (4), 268-274.

Fritsche, K.L. (2015) The science of fatty acids and inflammation. *Advances in nutrition (Bethesda, Md.),* 6 (3), 293S-301S.

Frouin, I., Maga, G., Denegri, M., Riva, F., Savio, M., Spadari, S., Prosperi, E. and Scovassi, A.I. (2003) Human proliferating cell nuclear antigen, poly(ADP-ribose) polymerase-1, and p21waf1/cip1. A dynamic exchange of partners. *Journal of Biological Chemistry,* 278 (41), 39265-39268.

Fukui, M., Kang, K.S., Okada, K. and Zhu, B.T. (2013) EPA, an omega-3 fatty acid, induces apoptosis in human pancreatic cancer cells: Role of ROS accumulation, caspase-8 activation, and autophagy induction. *Journal of Cellular Biochemistry,* 114 (1), 192-203.

Furuta, E., Pai, S.K., Zhan, R., Bandyopadhyay, S., Watabe, M., Mo, Y.Y., Hirota, S., Hosobe, S., Tsukada, T., Miura, K., Kamada, S., Saito, K., Iiizumi, M., Liu, W., Ericsson, J. and Watabe, K. (2008) Fatty acid synthase gene is up-regulated by hypoxia via activation of Akt and sterol regulatory element binding protein-1. *Cancer Research,* 68 (4), 1003-1011.

Gafni, O., Weinberger, L., Mansour, A.A., Manor, Y.S., Chomsky, E., Ben-Yosef, D., Kalma, Y., Viukov, S., Maza, I., Zviran, A., Rais, Y., Shipony, Z., Mukamel, Z., Krupalnik, V., Zerbib, M., Geula, S., Caspi, I., Schneir, D., Shwartz, T., Gilad, S., Amann-Zalcenstein, D., Benjamin, S., Amit, I., Tanay, A., Massarwa, R., Novershtern, N. and Hanna, J.H. (2013) Derivation of novel human ground state naive pluripotent stem cells. *Nature,* 504 (7479), 282-286.

Galbiati, F., Volonte, D., Brown, A.M., Weinstein, D.E., Ben-Ze'ev, A., Pestell, R.G. and Lisanti, M.P. (2000) Caveolin-1 expression inhibits Wnt/beta-catenin/Lef-1 signaling by recruiting beta-catenin to caveolae membrane domains. *Journal of Biological Chemistry,* 275 (30), 23368-23377.

Gallagher, H., Williams, J.O., Ferekidis, N., Ismail, A., Chan, Y.-H., Michael, D.R., Guschina, I.A., Tyrrell, V.J., O'donnell, V.B., Harwood, J.L., Khozin-Goldberg, I., Boussiba, S. and Ramji, D.P. (2019) Dihomo-γ-linolenic acid inhibits several key cellular processes associated with atherosclerosis. *Biochimica et Biophysica Acta (BBA) - Molecular Basis of Disease,* 1865 (9), 2538-2550.

Gameiro, P.A., Yang, J., Metelo, A.M., Perez-Carro, R., Baker, R., Wang, Z., Arreola, A., Rathmell, W.K., Olumi, A., Lopez-Larrubia, P., Stephanopoulos, G. and Iliopoulos, O. (2013) In vivo HIF-mediated reductive carboxylation is regulated by citrate levels and sensitizes VHL-deficient cells to glutamine deprivation. *Cell Metabolism,* 17 (3), 372-385.

Gao, F., Kwon, S.W., Zhao, Y. and Jin, Y. (2009) PARP1 poly(ADP-ribosyl)ates Sox2 to control Sox2 protein levels and FGF4 expression during embryonic stem cell differentiation. *Journal of Biological Chemistry,* 284 (33), 22263-22273.

Garaulet, M., Hernandez-Morante, J.J., Lujan, J., Tebar, F.J. and Zamora, S. (2006) Relationship between fat cell size and number and fatty acid composition in adipose tissue from different fat depots in overweight/obese humans. *International Journal of Obesity,* 30 (6), 899-905.

García-Cardeña, G., Fan, R., Stern, D.F., Liu, J. and Sessa, W.C. (1996) Endothelial Nitric Oxide Synthase Is Regulated by Tyrosine Phosphorylation and Interacts with Caveolin-1. *Journal of Biological Chemistry,* 271 (44), 27237-27240.

Ge, L., Gordon, J.S., Hsuan, C., Stenn, K. and Prouty, S.M. (2003) Identification of the delta-6 desaturase of human sebaceous glands: expression and enzyme activity. *Journal of Investigative Dermatology,* 120 (5), 707-714.

Gilbert, S. (2000) Early Mammalian Development IN: *Developmental Biology*, 6th ed. Sunderland (MA): Sinauer Associates. Available from: https://www.ncbi.nlm.nih.gov/books/NBK10052/.

Ginis, I., Luo, Y., Miura, T., Thies, S., Brandenberger, R., Gerecht-Nir, S., Amit, M., Hoke, A., Carpenter, M.K., Itskovitz-Eldor, J. and Rao, M.S. (2004) Differences between human and mouse embryonic stem cells. *Developmental Biology,* 269 (2), 360-380.

Gobeil, S., Boucher, C.C., Nadeau, D. and Poirier, G.G. (2001) Characterization of the necrotic cleavage of poly(ADP-ribose) polymerase (PARP-1): implication of lysosomal proteases. *Cell Death & Differentiation,* 8 (6), 588-594.

Gong, C.X., Liu, F., Grundke-Iqbal, I. and Iqbal, K. (2005) Post-translational modifications of tau protein in Alzheimer's disease. *Journal of Neural Transmission,* 112 (6), 813-838.

Gonzalez-Flores, A., Aguilar-Quesada, R., Siles, E., Pozo, S., Rodriguez-Lara, M.I., Lopez-Jimenez, L., Lopez-Rodriguez, M., Peralta-Leal, A., Villar, D., Martin-Oliva, D., Del Peso, L., Berra, E. and Oliver, F.J. (2014) Interaction between PARP-1 and HIF-2alpha in the hypoxic response. *Oncogene,* 33 (7), 891-898.

Gonzalez, F., Boue, S. and Izpisua Belmonte, J.C. (2011) Methods for making induced pluripotent stem cells: reprogramming a la carte. *Nature Reviews Genetics,* 12 (4), 231-242.

Gromovsky, A.D., Schugar, R.C., Brown, A.L., Helsley, R.N., Burrows, A.C., Ferguson, D., Zhang, R., Sansbury, B.E., Lee, R.G., Morton, R.E., Allende, D.S., Parks, J.S., Spite, M. and Brown, J.M. (2018) Delta-5 Fatty Acid Desaturase FADS1 Impacts Metabolic Disease by Balancing Proinflammatory and Proresolving Lipid Mediators. *Arteriosclerosis, Thrombosis, and Vascular Biology,* 38 (1), 218-231.

Gu, W., Gaeta, X., Sahakyan, A., Chan, Alanna b., Hong, Candice s., Kim, R., Braas, D., Plath, K., Lowry, William e. and Christofk, Heather r. (2016) Glycolytic Metabolism Plays a Functional Role in Regulating Human Pluripotent Stem Cell State. *Cell Stem Cell,* 19 (4), 476-490.

Guan, J.-L., Simon, A.K., Prescott, M., Menendez, J.A., Liu, F., Wang, F., Wang, C., Wolvetang, E., Vazquez-Martin, A. and Zhang, J. (2013) Autophagy in stem cells. *Autophagy,* 9 (6), 830-849.

Guillet-Deniau, I., Pichard, A.-L., Koné, A., Esnous, C., Nieruchalski, M., Girard, J. and Prip-Buus, C. (2004) Glucose induces de novo lipogenesis in rat muscle satellite cells through a sterol-regulatory-element-binding-protein-1c-dependent pathway. *Journal of Cell Science,* 117 (10), 1937-1944.

Guo, G., Huss, M., Tong, G.Q., Wang, C., Li Sun, L., Clarke, N.D. and Robson, P. (2010) Resolution of cell fate decisions revealed by single-cell gene expression analysis from zygote to blastocyst. *Developmental Cell,* 18 (4), 675-685.

Guo, G., Yang, J., Nichols, J., Hall, J.S., Eyres, I., Mansfield, W. and Smith, A. (2009) Klf4 reverts developmentally programmed restriction of ground state pluripotency. *Development,* 136 (7), 1063-1069.

Gupte, R., Liu, Z. and Kraus, W.L. (2017) PARPs and ADP-ribosylation: recent advances linking molecular functions to biological outcomes. *Genes & Development,* 31 (2), 101-126.

Gustafsson, M.V., Zheng, X., Pereira, T., Gradin, K., Jin, S., Lundkvist, J., Ruas, J.L., Poellinger, L., Lendahl, U. and Bondesson, M. (2005) Hypoxia requires notch signaling to maintain the undifferentiated cell state. *Developmental Cell,* 9 (5), 617-628.

Gutierrez-Aranda, I., Ramos-Mejia, V., Bueno, C., Munoz-Lopez, M., Real, P.J., Mácia, A., Sanchez, L., Ligero, G., Garcia-Parez, J.L. and Menendez, P. (2010) Human induced pluripotent stem cells develop teratoma more efficiently and faster than human embryonic stem cells regardless the site of injection. *Stem cells (Dayton, Ohio),* 28 (9), 1568-1570.

Hambiliki, F., Ström, S., Zhang, P. and Stavreus-Evers, A. (2012) Co-localization of NANOG and OCT4 in human pre-implantation embryos and in human embryonic stem cells. *Journal of assisted reproduction and genetics,* 29 (10), 1021-1028.

Hansis, C., Grifo, J.A. and Krey, L.C. (2000) Oct-4 expression in inner cell mass and trophectoderm of human blastocysts. *Molecular Human Reproduction,* 6 (11), 999-1004.

Hart, A.H., Hartley, L., Ibrahim, M. and Robb, L. (2004) Identification, cloning and expression analysis of the pluripotency promoting Nanog genes in mouse and human. *Developmental Dynamics,* 230 (1), 187-198.

Hart, C.M., Andreoli, S.P., Patterson, C.E. and Garcia, J.G.N. (1993) Oleic acid supplementation reduces oxidant-mediated dysfunction of cultured porcine pulmonary artery endothelial cells. *Journal of Cellular Physiology,* 156 (1), 24-34.

Harvey, R.D. and Calaghan, S.C. (2012) Caveolae create local signalling domains through their distinct protein content, lipid profile and morphology. *Journal of molecular and cellular cardiology,* 52 (2), 366-375.

Hashimoto, M. and Hossain, S. (2018) Fatty Acids: From Membrane Ingredients to Signaling Molecules *Biochemistry and Health Benefits of Fatty Acids*.

Hashimoto, M., Hossain, S., Agdul, H. and Shido, O. (2005) Docosahexaenoic acid-induced amelioration on impairment of memory learning in amyloid beta-infused rats relates to the decreases of amyloid beta and cholesterol levels in detergent-insoluble membrane fractions. *Biochimica et Biophysica Acta,* 1738 (1-3), 91-98.

Hay, D.C., Sutherland, L., Clark, J. and Burdon, T. (2004) Oct-4 knockdown induces similar patterns of endoderm and trophoblast differentiation markers in human and mouse embryonic stem cells. *Stem Cells,* 22 (2), 225-235.

Hayashi, M., Sakata, M., Takeda, T., Yamamoto, T., Okamoto, Y., Sawada, K., Kimura, A., Minekawa, R., Tahara, M., Tasaka, K. and Murata, Y. (2004) Induction of glucose transporter 1 expression through hypoxia-inducible factor 1alpha under hypoxic conditions in trophoblast-derived cells. *Journal of Endocrinology,* 183 (1), 145-154.

He, S., Nakada, D. and Morrison, S.J. (2009) Mechanisms of stem cell self-renewal. *Annual Review of Cell and Developmental Biology,* 25, 377-406.

Heard, E. (2004) Recent advances in X-chromosome inactivation. *Current Opinion in Cell Biology,* 16 (3), 247-255.

Heimerl, S., Liebisch, G., Le Lay, S., Bottcher, A., Wiesner, P., Lindtner, S., Kurzchalia, T.V., Simons, K. and Schmitz, G. (2008) Caveolin-1 deficiency alters plasma lipid and lipoprotein profiles in mice. *Biochemical and Biophysical Research Communications,* 367 (4), 826-833.

Henderson, J.K., Draper, J.S., Baillie, H.S., Fishel, S., Thomson, J.A., Moore, H. and Andrews, P.W. (2002) Preimplantation human embryos and embryonic stem cells show comparable expression of stage-specific embryonic antigens. *Stem Cells,* 20 (4), 329-337.

Herceg, Z. and Wang, Z.Q. (1999) Failure of poly(ADP-ribose) polymerase cleavage by caspases leads to induction of necrosis and enhanced apoptosis. *Molecular and Cellular Biology,* 19 (7), 5124-5133.

Hou, T.Y., Mcmurray, D.N. and Chapkin, R.S. (2016) Omega-3 fatty acids, lipid rafts, and T cell signaling. *European journal of pharmacology,* 785, 2-9.

Houten, S.M. and Wanders, R.J. (2010) A general introduction to the biochemistry of mitochondrial fatty acid beta-oxidation. *Journal of Inherited Metabolic Disease,* 33 (5), 469-477.

Hsieh, M.-H., Chen, Y.-T., Chen, Y.-T., Lee, Y.-H., Lu, J., Chien, C.-L., Chen, H.-F., Ho, H.-N., Yu, C.-J., Wang, Z.-Q. and Teng, S.-C. (2017) PARP1 controls KLF4-mediated telomerase expression in stem cells and cancer cells. *Nucleic Acids Research,* 45 (18), 10492-10503.

Hsu, Y.-M. and Yin, M.-C. (2016) EPA or DHA enhanced oxidative stress and aging protein expression in brain of d-galactose treated mice. *BioMedicine,* 6 (3), 17-17.

Hsueh, T.-Y., Baum, J.I. and Huang, Y. (2018) Effect of Eicosapentaenoic Acid and Docosahexaenoic Acid on Myogenesis and Mitochondrial Biosynthesis during Murine Skeletal Muscle Cell Differentiation. *Frontiers in Nutrition,* 5 (15).

Hu, B., Guo, Y., Garbacz, W.G., Jiang, M., Xu, M., Huang, H., Tsung, A., Billiar, T.R., Ramakrishnan, S.K., Shah, Y.M., Lam, K.S., Huang, M. and Xie, W. (2015) Fatty acid binding protein-4 (FABP4) is a hypoxia inducible gene that sensitizes mice to liver ischemia/reperfusion injury. *Journal of Hepatology,* 63 (4), 855-862.

Hu, C.J., Sataur, A., Wang, L., Chen, H. and Simon, M.C. (2007) The N-terminal transactivation domain confers target gene specificity of hypoxia-inducible factors HIF-1alpha and HIF-2alpha. *Molecular Biology of the Cell,* 18 (11), 4528-4542.

Huang, D., Li, C. and Zhang, H. (2014a) Hypoxia and cancer cell metabolism. *Acta biochimica et biophysica Sinica,* 46.

Huang, D., Li, T., Li, X., Zhang, L., Sun, L., He, X., Zhong, X., Jia, D., Song, L., Semenza, Gregg l., Gao, P. and Zhang, H. (2014b) HIF-1-Mediated Suppression of Acyl-CoA Dehydrogenases and Fatty Acid Oxidation Is Critical for Cancer Progression. *Cell Reports,* 8 (6), 1930-1942.

Huang, L.E., Gu, J., Schau, M. and Bunn, H.F. (1998) Regulation of hypoxia-inducible factor 1α is mediated by an O2-dependent degradation domain via the ubiquitin-proteasome pathway. *Proceedings of the National Academy of Sciences,* 95 (14), 7987-7992.

Huang, Y.-S., Huang, W.-C., Li, C.-W. and Chuang, L.-T. (2011) Eicosadienoic acid differentially modulates production of pro-inflammatory modulators in murine macrophages. *Molecular and Cellular Biochemistry,* 358 (1), 85-94.

Huang, Y., Kempen, M.B., Munck, A.B., Swagemakers, S., Driegen, S., Mahavadi, P., Meijer, D., Van Ijcken, W., Van Der Spek, P., Grosveld, F., Gunther, A., Tibboel, D. and Rottier, R.J. (2012) Hypoxia-inducible factor 2alpha plays a critical role in the formation of alveoli and surfactant. *American Journal of Respiratory Cell and Molecular Biology,* 46 (2), 224-232.

Huang, Y.H., Sharifpanah, F., Becker, S., Wartenberg, M. and Sauer, H. (2016) Impact of Arachidonic Acid and the Leukotriene Signaling Pathway on Vasculogenesis of Mouse Embryonic Stem Cells. *Cells Tissues Organs,* 201 (5), 319-332.

Hyslop, L., Stojkovic, M., Armstrong, L., Walter, T., Stojkovic, P., Przyborski, S., Herbert, M., Murdoch, A., Strachan, T. and Lako, M. (2005) Downregulation of NANOG induces differentiation of human embryonic stem cells to extraembryonic lineages. *Stem Cells,* 23 (8), 1035-1043.

Inc., P.T. Collaborative data science. Montréal, QC: Plotly Technologies Inc. Available from: https://plot.ly.

Ivan, M., Kondo, K., Yang, H., Kim, W., Valiando, J., Ohh, M., Salic, A., Asara, J.M., Lane, W.S. and Kaelin, W.G., Jr. (2001) HIFalpha targeted for VHL-mediated destruction by proline hydroxylation: implications for O2 sensing. *Science,* 292 (5516), 464-468.

Iyer, N.V., Kotch, L.E., Agani, F., Leung, S.W., Laughner, E., Wenger, R.H., Gassmann, M., Gearhart, J.D., Lawler, A.M., Yu, A.Y. and Semenza, G.L. (1998) Cellular and developmental control of O2 homeostasis by hypoxia-inducible factor 1 alpha. *Genes & Development,* 12 (2), 149-162.

Jaakkola, P., Mole, D.R., Tian, Y.M., Wilson, M.I., Gielbert, J., Gaskell, S.J., Von Kriegsheim, A., Hebestreit, H.F., Mukherji, M., Schofield, C.J., Maxwell, P.H., Pugh, C.W. and Ratcliffe, P.J. (2001) Targeting of HIF-alpha to the von Hippel-Lindau ubiquitylation complex by O2-regulated prolyl hydroxylation. *Science,* 292 (5516), 468-472.

Jack-Hays, M.G., Xie, Z., Wang, Y., Huang, W. and Askari, A. (1995) Activation of na+/ k+- ATPase by fatty acids, acylglycerols, and related amphiphiles: structure-activity relationship. *Biochimica et Biophysica Acta,* (1279), 43-48.

Jacobs, K., Zambelli, F., Mertzanidou, A., Smolders, I., Geens, M., Nguyen, H.T., Barbé, L., Sermon, K. and Spits, C. (2016) Higher-Density Culture in Human Embryonic Stem Cells Results in DNA Damage and Genome Instability. *Stem cell reports,* 6 (3), 330-341.

Jarc, E. and Petan, T. (2020) A twist of FATe: Lipid droplets and inflammatory lipid mediators. *Biochimie,* 169, 69-87.

Ji, A.-R., Ku, S.-Y., Cho, M.S., Kim, Y.Y., Kim, Y.J., Oh, S.K., Kim, S.H., Moon, S.Y. and Choi, Y.M. (2010) Reactive oxygen species enhance differentiation of human embryonic stem cells into mesendodermal lineage. *Experimental & Molecular Medicine,* 42 (3), 175-186.

Jiang, B.H., Zheng, J.Z., Leung, S.W., Roe, R. and Semenza, G.L. (1997) Transactivation and inhibitory domains of hypoxia-inducible factor 1alpha. Modulation of transcriptional activity by oxygen tension. *Journal of Biological Chemistry,* 272 (31), 19253-19260.

Jozefczuk, J., Drews, K. and Adjaye, J. (2012) Preparation of mouse embryonic fibroblast cells suitable for culturing human embryonic and induced pluripotent stem cells. *Journal of visualized experiments : JoVE,* (64), 3854.

Jump, D.B. (2004) Fatty acid regulation of gene transcription. *Critical Reviews in Clinical Laboratory Sciences,* 41 (1), 41-78.

Jump, D.B. (2009) Mammalian Fatty Acid Elongases. *Methods in molecular biology (Clifton, N.J.),* 579, 375-389.

Jungmichel, S., Rosenthal, F., Altmeyer, M., Lukas, J., Hottiger, Michael o. and Nielsen, Michael l. (2013) Proteome-wide Identification of Poly(ADP-Ribosyl)ation Targets in Different Genotoxic Stress Responses. *Molecular Cell,* 52 (2), 272-285.

Kagawa, Y., Yasumoto, Y., Sharifi, K., Ebrahimi, M., Islam, A., Miyazaki, H., Yamamoto, Y., Sawada, T., Kishi, H., Kobayashi, S., Maekawa, M., Yoshikawa, T., Takaki, E., Nakai, A., Kogo, H., Fujimoto, T. and Owada, Y. (2015) Fatty acid-binding protein 7 regulates function of caveolae in astrocytes through expression of caveolin-1. *Glia,* 63 (5), 780-794.

Kamachi, Y. and Kondoh, H. (2013) Sox proteins: regulators of cell fate specification and differentiation. *Development,* 140 (20), 4129-4144.

Kameshita, I., Matsuda, Z., Taniguchi, T. and Shizuta, Y. (1984) Poly (ADP-Ribose) synthetase. Separation and identification of three proteolytic fragments as the substrate-binding domain, the DNA-binding domain, and the automodification domain. *Journal of Biological Chemistry,* 259 (8), 4770-4776.

Kang, J.X., Wan, J.-B. and He, C. (2014) Concise Review: Regulation of Stem Cell Proliferation and Differentiation by Essential Fatty Acids and Their Metabolites. *Stem Cells,* 32 (5), 1092-1098.

Kang, K.S., Wang, P., Yamabe, N., Fukui, M., Jay, T. and Zhu, B.T. (2010) Docosahexaenoic acid induces apoptosis in MCF-7 cells in vitro and in vivo via reactive oxygen species formation and caspase 8 activation. *PLoS One,* 5 (4), e10296.

Katakura, M., Hashimoto, M., Okui, T., Shahdat, H.M., Matsuzaki, K. and Shido, O. (2013) Omega-3 polyunsaturated Fatty acids enhance neuronal differentiation in cultured rat neural stem cells. *Stem cells international,* 2013, 490476-490476.

Keirstead, H.S., Nistor, G., Bernal, G., Totoiu, M., Cloutier, F., Sharp, K. and Steward, O. (2005) Human embryonic stem cell-derived oligodendrocyte progenitor cell transplants remyelinate and restore locomotion after spinal cord injury. *The Journal of Neuroscience,* 25 (19), 4694-4705.

Keller, A., Dziedzicka, D., Zambelli, F., Markouli, C., Sermon, K., Spits, C. and Geens, M. (2018) Genetic and epigenetic factors which modulate differentiation propensity in human pluripotent stem cells. *Human Reproduction Update,* 24 (2), 162-175.

Kelly, B.D., Hackett, S.F., Hirota, K., Oshima, Y., Cai, Z., Berg-Dixon, S., Rowan, A., Yan, Z., Campochiaro, P.A. and Semenza, G.L. (2003) Cell type-specific regulation of angiogenic growth factor gene expression and induction of angiogenesis in nonischemic tissue by a constitutively active form of hypoxia-inducible factor 1. *Circulation Research,* 93 (11), 1074-1081.

Keramari, M., Razavi, J., Ingman, K.A., Patsch, C., Edenhofer, F., Ward, C.M. and Kimber, S.J. (2010) Sox2 Is Essential for Formation of Trophectoderm in the Preimplantation Embryo. *PLoS ONE,* 5 (11), e13952.

Kim, H.S., Oh, S.K., Park, Y.B., Ahn, H.J., Sung, K.C., Kang, M.J., Lee, L.A., Suh, C.S., Kim, S.H., Kim, D.W. and Moon, S.Y. (2005) Methods for derivation of human embryonic stem cells. *Stem Cells,* 23 (9), 1228-1233.

Kim, J.W., Tchernyshyov, I., Semenza, G.L. and Dang, C.V. (2006) HIF-1-mediated expression of pyruvate dehydrogenase kinase: a metabolic switch required for cellular adaptation to hypoxia. *Cell Metabolism,* 3 (3), 177-185.

Kim, K., Doi, A., Wen, B., Ng, K., Zhao, R., Cahan, P., Kim, J., Aryee, M.J., Ji, H., Ehrlich, L.I.R., Yabuuchi, A., Takeuchi, A., Cunniff, K.C., Hongguang, H., Mckinney-Freeman, S., Naveiras, O., Yoon, T.J., Irizarry, R.A., Jung, N., Seita, J., Hanna, J., Murakami, P., Jaenisch, R.,

Weissleder, R., Orkin, S.H., Weissman, I.L., Feinberg, A.P. and Daley, G.Q. (2010) Epigenetic memory in induced pluripotent stem cells. *Nature,* 467 (7313), 285-290.

Kim, M.H., Kim, M.O., Kim, Y.H., Kim, J.S. and Han, H.J. (2009) Linoleic acid induces mouse embryonic stem cell proliferation via Ca2+/PKC, PI3K/Akt, and MAPKs. *Cellular Physiology and Biochemistry,* 23 (1-3), 53-64.

Kim, W., Deik, A., Gonzalez, C., Gonzalez, M.E., Fu, F., Ferrari, M., Churchhouse, C.L., Florez, J.C., Jacobs, S.B.R., Clish, C.B. and Rhee, E.P. (2019) Polyunsaturated Fatty Acid Desaturation Is a Mechanism for Glycolytic NAD(+) Recycling. *Cell Metabolism,* 29 (4), 856-870.e857.

Kim, W., Fan, Y.Y., Barhoumi, R., Smith, R., Mcmurray, D.N. and Chapkin, R.S. (2008) n-3 polyunsaturated fatty acids suppress the localization and activation of signaling proteins at the immunological synapse in murine CD4+ T cells by affecting lipid raft formation. *The Journal of Immunology,* 181 (9), 6236-6243.

Klinger, P., Schietke, R.E., Warnecke, C., Swoboda, B., Wiesener, M., Hennig, F.F. and Gelse, K. (2011) Deletion of the oxygen-dependent degradation domain results in impaired transcriptional activity of hypoxia-inducible factors. *Transcription,* 2 (6), 269-275.

Kogteva, G. and Bezuglov, V. (1998) Unsaturated fatty acids as endogenous bioregulators. *Biochemistry. Biokhimiia,* 63, 4-12.

Koizume, S. and Miyagi, Y. (2015) Diverse Mechanisms of Sp1-Dependent Transcriptional Regulation Potentially Involved in the Adaptive Response of Cancer Cells to Oxygen-Deficient Conditions. *Cancers,* 8 (1), 2.

Komatsu, K. and Fujimori, T. (2015) Multiple phases in regulation of Nanog expression during pre-implantation development. *Development, Growth & Differentiation,* 57 (9), 648-656.

Kondo, M., Weissman, I.L. and Akashi, K. (1997) Identification of Clonogenic Common Lymphoid Progenitors in Mouse Bone Marrow. *Cell,* 91 (5), 661-672.

Kondoh, H. and Kamachi, Y. (2010) SOX-partner code for cell specification: Regulatory target selection and underlying molecular mechanisms. *The International Journal of Biochemistry & Cell Biology,* 42 (3), 391-399.

Kozera, L., White, E. and Calaghan, S. (2009) Caveolae act as membrane reserves which limit mechanosensitive I(Cl,swell) channel activation during swelling in the rat ventricular myocyte. *PloS one,* 4 (12), e8312-e8312.

Krietsch, J., Rouleau, M., Pic, E., Ethier, C., Dawson, T.M., Dawson, V.L., Masson, J.Y., Poirier, G.G. and Gagne, J.P. (2013) Reprogramming cellular events by poly(ADP-ribose)-binding proteins. *Molecular Aspects of Medicine,* 34 (6), 1066-1087.

Krishnan, J., Suter, M., Windak, R., Krebs, T., Felley, A., Montessuit, C., Tokarska-Schlattner, M., Aasum, E., Bogdanova, A., Perriard, E., Perriard, J.C., Larsen, T., Pedrazzini, T. and Krek, W. (2009) Activation of a HIF1alpha-PPARgamma axis underlies the integration of glycolytic and lipid anabolic pathways in pathologic cardiac hypertrophy. *Cell Metabolism,* 9 (6), 512-524.

Kumari, D. (2016) States of Pluripotency: Naïve and Primed Pluripotent Stem Cells IN: Tomizawa, M. (ed.) *Pluripotent Stem Cells - From the Bench to the Clinic*. Rijeka: InTech, Ch. 03.

Kunarso, G., Chia, N.Y., Jeyakani, J., Hwang, C., Lu, X., Chan, Y.S., Ng, H.H. and Bourque, G. (2010) Transposable elements have rewired the core regulatory network of human embryonic stem cells. *Nature Genetics,* 42 (7), 631-634.

Kyttälä, A., Moraghebi, R., Valensisi, C., Kettunen, J., Andrus, C., Pasumarthy, Kalyan k., Nakanishi, M., Nishimura, K., Ohtaka, M., Weltner, J., Van handel, B., Parkkonen, O., Sinisalo, J., Jalanko, A., Hawkins, R.D., Woods, N.-B., Otonkoski, T. and Trokovic, R. (2016) Genetic Variability Overrides the Impact of Parental Cell Type and Determines iPSC Differentiation Potential. *Stem Cell Reports,* 6 (2), 200-212.

Lai, M.-C., Chang, C.-M. and Sun, H.S. (2016) Hypoxia Induces Autophagy through Translational Up-Regulation of Lysosomal Proteins in Human Colon Cancer Cells. *PLoS ONE,* 11 (4), e0153627.

Lai, Y.S., Chang, C.W., Pawlik, K.M., Zhou, D., Renfrow, M.B. and Townes, T.M. (2012) SRY (sex determining region Y)-box2 (Sox2)/poly ADP-ribose polymerase 1 (Parp1) complexes

regulate pluripotency. *Proceedings of the National Academy of Sciences of the United States of America,* 109 (10), 3772-3777.

Lando, D., Peet, D.J., Gorman, J.J., Whelan, D.A., Whitelaw, M.L. and Bruick, R.K. (2002) FIH-1 is an asparaginyl hydroxylase enzyme that regulates the transcriptional activity of hypoxia-inducible factor. *Genes & Development,* 16 (12), 1466-1471.

Langelier, M.F., Planck, J.L., Roy, S. and Pascal, J.M. (2012) Structural basis for DNA damage-dependent poly(ADP-ribosyl)ation by human PARP-1. *Science,* 336 (6082), 728-732.

Lee, J., Cho, Y.S., Jung, H. and Choi, I. (2018) Pharmacological Regulation of Oxidative Stress in Stem Cells. *Oxidative medicine and cellular longevity,* 2018, 4081890-4081890.

Lee, J.E., Kang, M.S., Park, M.H., Shim, S.H., Yoon, T.K., Chung, H.M. and Lee, D.R. (2010a) Evaluation of 28 human embryonic stem cell lines for use as unrelated donors in stem cell therapy: implications of HLA and ABO genotypes. *Cell Transplantation,* 19 (11), 1383-1395.

Lee, J.E. and Lee, D.R. (2011) Human embryonic stem cells: derivation, maintenance and cryopreservation. *International journal of stem cells,* 4 (1), 9-17.

Lee, J.M., Lee, H., Kang, S. and Park, W.J. (2016) Fatty Acid Desaturases, Polyunsaturated Fatty Acid Regulation, and Biotechnological Advances. *Nutrients,* 8 (1), 23.

Lee, M.Y., Ryu, J.M., Lee, S.H., Park, J.H. and Han, H.J. (2010b) Lipid rafts play an important role for maintenance of embryonic stem cell self-renewal. *Journal of lipid research,* 51 (8), 2082-2089.

Lee, Y., Jung, J., Cho, K.J., Lee, S.K., Park, J.W., Oh, I.H. and Kim, G.J. (2013) Increased SCF/c-kit by hypoxia promotes autophagy of human placental chorionic plate-derived mesenchymal stem cells via regulating the phosphorylation of mTOR. *Journal of Cellular Biochemistry,* 114 (1), 79-88.

Lees, J.G., Rathjen, J., Sheedy, J.R., Gardner, D.K. and Harvey, A.J. (2015) Distinct profiles of human embryonic stem cell metabolism and mitochondria identified by oxygen. *Reproduction,* 150 (4), 367-382.

Lehrke, M. and Lazar, M.A. (2005) The many faces of PPARgamma. *Cell,* 123 (6), 993-999.

Lenzi, A., Gandini, L., Maresca, V., Rago, R., Sgrò, P., Dondero, F. and Picardo, M. (2000) Fatty acid composition of spermatozoa and immature germ cells. *Molecular Human Reproduction,* 6 (3), 226-231.

Leonard, A.E., Kelder, B., Bobik, E.G., Chuang, L.T., Parker-Barnes, J.M., Thurmond, J.M., Kroeger, P.E., Kopchick, J.J., Huang, Y.S. and Mukerji, P. (2000) cDNA cloning and characterization of human Delta5-desaturase involved in the biosynthesis of arachidonic acid. *Biochemical Journal,* 347 Pt 3, 719-724.

Li, J., Wang, G., Wang, C., Zhao, Y., Zhang, H., Tan, Z., Song, Z., Ding, M. and Deng, H. (2007a) MEK/ERK signaling contributes to the maintenance of human embryonic stem cell self-renewal. *Differentiation,* 75 (4), 299-307.

Li, L., Baroja, M., Sen Majumdar, A., Chadwick, K., Rouleau, A., Gallacher, L., Ferber, I., Lebkowski, J., Martin, T., Madrenas, J. and Bhatia, M. (2004) Human Embryonic Stem Cells Possess Immune-Privileged Properties. *Stem cells (Dayton, Ohio),* 22, 448-456.

Li, L., Chen, Z., Zhang, L., Liu, G., Hua, J., Jia, L. and Liao, M. (2016) Genome-wide targets identification of "core" pluripotency transcription factors with integrated features in human embryonic stem cells. *Mol Biosyst,* 12 (4), 1324-1332.

Li, L., Liu, B., Haversen, L., Lu, E., Magnusson, L.U., Stahlman, M., Boren, J., Bergstrom, G., Levin, M.C. and Hulten, L.M. (2012) The importance of GLUT3 for de novo lipogenesis in hypoxia-induced lipid loading of human macrophages. *PLoS One,* 7 (8), e42360.

Li, L.T., Jiang, G., Chen, Q. and Zheng, J.N. (2015) Ki67 is a promising molecular target in the diagnosis of cancer. *Molecular Medicine Reports,* 11 (3), 1566-1572.

Li, M., Chen, D., Huang, H., Wang, J., Wan, X., Xu, C., Li, C., Ma, H., Yu, C. and Li, Y. (2017) Caveolin1 protects against diet induced hepatic lipid accumulation in mice. *PLOS ONE,* 12 (6), e0178748.

Li, Q., Tan, L., Wang, C., Li, N., Li, Y., Xu, G. and Li, J. (2006) Polyunsaturated eicosapentaenoic acid changes lipid composition in lipid rafts. *European Journal of Nutrition,* 45 (3), 144-151.

Li, Q., Zhang, Q., Wang, M., Zhao, S., Ma, J., Luo, N., Li, N., Li, Y., Xu, G. and Li, J. (2007b) Eicosapentaenoic acid modifies lipid composition in caveolae and induces translocation of endothelial nitric oxide synthase. *Biochimie,* 89 (1), 169-177.

Li, S., Zheng, E.B., Zhao, L. and Liu, S. (2019) Nonreciprocal and Conditional Cooperativity Directs the Pioneer Activity of Pluripotency Transcription Factors. *Cell Reports,* 28 (10), 2689-2703.e2684.

Li, X., Fang, P., Mai, J., Choi, E.T., Wang, H. and Yang, X.-F. (2013) Targeting mitochondrial reactive oxygen species as novel therapy for inflammatory diseases and cancers. *Journal of hematology & oncology,* 6, 19-19.

Li, Y., Lau, W.M., So, K.F., Tong, Y. and Shen, J. (2011a) Caveolin-1 inhibits oligodendroglial differentiation of neural stem/progenitor cells through modulating beta-catenin expression. *Neurochemistry International,* 59 (2), 114-121.

Li, Y., Luo, J., Lau, W.M., Zheng, G., Fu, S., Wang, T.T., Zeng, H.P., So, K.F., Chung, S.K., Tong, Y., Liu, K. and Shen, J. (2011b) Caveolin-1 plays a crucial role in inhibiting neuronal differentiation of neural stem/progenitor cells via VEGF signaling-dependent pathway. *PLoS One,* 6 (8), e22901.

Lian, X., Matthaeus, C., Kaßmann, M., Daumke, O. and Gollasch, M. (2019) Pathophysiological Role of Caveolae in Hypertension. *Frontiers in Medicine,* 6 (153).

Lin, J., Yang, R., Tarr, P.T., Wu, P.H., Handschin, C., Li, S., Yang, W., Pei, L., Uldry, M., Tontonoz, P., Newgard, C.B. and Spiegelman, B.M. (2005) Hyperlipidemic effects of dietary saturated fats mediated through PGC-1beta coactivation of SREBP. *Cell,* 120 (2), 261-273.

Lindahl, T., Satoh, M.S., Poirier, G.G. and Klungland, A. (1995) Post-translational modification of poly(ADP-ribose) polymerase induced by DNA strand breaks. *Trends in Biochemical Sciences,* 20 (10), 405-411.

Lindsay, D.B. (2007) Fatty acids as energy sources. *Proceedings of the Nutrition Society,* 34 (3), 241-248.

Liou, J.Y., Ellent, D.P., Lee, S., Goldsby, J., Ko, B.S., Matijevic, N., Huang, J.C. and Wu, K.K. (2007) Cyclooxygenase-2-derived prostaglandin e2 protects mouse embryonic stem cells from apoptosis. *Stem Cells,* 25 (5), 1096-1103.

Lisy, K. and Peet, D.J. (2008) Turn me on: regulating HIF transcriptional activity. *Cell Death and Differentiation,* 15 (4), 642-649.

Liu, S., Mahairaki, V., Bai, H., Ding, Z., Li, J., Witwer, K.W. and Cheng, L. (2019) Highly Purified Human Extracellular Vesicles Produced by Stem Cells Alleviate Aging Cellular Phenotypes of Senescent Human Cells. *STEM CELLS,* 37 (6), 779-790.

Liu, X., Wang, H., Liang, X. and Roberts, M.S. (2017) Chapter 30 - Hepatic Metabolism in Liver Health and Disease IN: Muriel, P. (ed.) *Liver Pathophysiology*. Boston: Academic Press, 391-400.

Liu, Y., Ma, Z., Zhao, C., Wang, Y., Wu, G., Xiao, J., Mcclain, C.J., Li, X. and Feng, W. (2014) HIF-1alpha and HIF-2alpha are critically involved in hypoxia-induced lipid accumulation in hepatocytes through reducing PGC-1alpha-mediated fatty acid beta-oxidation. *Toxicology Letters,* 226 (2), 117-123.

Liu, Y., Xu, H.W., Wang, L., Li, S.Y., Zhao, C.J., Hao, J., Li, Q.Y., Zhao, T.T., Wu, W., Wang, Y., Zhou, Q., Qian, C., Wang, L. and Yin, Z.Q. (2018) Human embryonic stem cell-derived retinal pigment epithelium transplants as a potential treatment for wet age-related macular degeneration. *Cell Discovery,* 4 (1), 50.

Loh, Y.H., Wu, Q., Chew, J.L., Vega, V.B., Zhang, W., Chen, X., Bourque, G., George, J., Leong, B., Liu, J., Wong, K.Y., Sung, K.W., Lee, C.W., Zhao, X.D., Chiu, K.P., Lipovich, L., Kuznetsov, V.A., Robson, P., Stanton, L.W., Wei, C.L., Ruan, Y., Lim, B. and Ng, H.H. (2006) The Oct4 and Nanog transcription network regulates pluripotency in mouse embryonic stem cells. *Nature Genetics,* 38 (4), 431-440.

Los, M., Mozoluk, M., Ferrari, D., Stepczynska, A., Stroh, C., Renz, A., Herceg, Z., Wang, Z.Q. and Schulze-Osthoff, K. (2002) Activation and caspase-mediated inhibition of PARP: a molecular switch between fibroblast necrosis and apoptosis in death receptor signaling. *Molecular Biology of the Cell,* 13 (3), 978-988.

Ludwig, T. and Thomson, J. (2007) Defined, Feeder-Independent Medium for Human Embryonic Stem Cell Culture. *Current Protocols in Stem Cell Biology,* 2 (1), 1C.2.1-1C.2.16.

Ma, D.W., Seo, J., Davidson, L.A., Callaway, E.S., Fan, Y.Y., Lupton, J.R. and Chapkin, R.S. (2004) n-3 PUFA alter caveolae lipid composition and resident protein localization in mouse colon. *The FASEB Journal,* 18 (9), 1040-1042.

Malanga, M., Pleschke, J.M., Kleczkowska, H.E. and Althaus, F.R. (1998) Poly(ADP-ribose) binds to specific domains of p53 and alters its DNA binding functions. *Journal of Biological Chemistry,* 273 (19), 11839-11843.

Maltseva, E.A., Krasikova, Y.S., Sukhanova, M.V., Rechkunova, N.I. and Lavrik, O.I. (2018) Replication protein A as a modulator of the poly(ADP-ribose)polymerase 1 activity. *DNA Repair,* 72, 28-38.

Mani, C., Reddy, P.H. and Palle, K. (2020) DNA repair fidelity in stem cell maintenance, health, and disease. *Biochimica et Biophysica Acta (BBA) - Molecular Basis of Disease,* 1866 (4), 165444.

Mao, X., Wong, S.Y., Tse, E.Y., Ko, F.C., Tey, S.K., Yeung, Y.S., Man, K., Lo, R.C., Ng, I.O. and Yam, J.W. (2016) Mechanisms through Which Hypoxia-Induced Caveolin-1 Drives Tumorigenesis and Metastasis in Hepatocellular Carcinoma. *Cancer Research,* 76 (24), 7242-7253.

Marquardt, A., Stöhr, H., White, K. and Weber, B.H.F. (2000) cDNA Cloning, Genomic Structure, and Chromosomal Localization of Three Members of the Human Fatty Acid Desaturase Family. *Genomics,* 66 (2), 175-183.

Martin-Oliva, D., Aguilar-Quesada, R., O'valle, F., Munoz-Gamez, J.A., Martinez-Romero, R., Garcia Del Moral, R., Ruiz De Almodovar, J.M., Villuendas, R., Piris, M.A. and Oliver, F.J. (2006) Inhibition of poly(ADP-ribose) polymerase modulates tumor-related gene expression, including hypoxia-inducible factor-1 activation, during skin carcinogenesis. *Cancer Research,* 66 (11), 5744-5756.

Martinez-Outschoorn, U.E., Sotgia, F. and Lisanti, M.P. (2015) Caveolae and signalling in cancer. *Nature Reviews Cancer,* 15 (4), 225-237.

Masui, S., Nakatake, Y., Toyooka, Y., Shimosato, D., Yagi, R., Takahashi, K., Okochi, H., Okuda, A., Matoba, R., Sharov, A.A., Ko, M.S. and Niwa, H. (2007) Pluripotency governed by Sox2 via regulation of Oct3/4 expression in mouse embryonic stem cells. *Nature Cell Biology,* 9 (6), 625-635.

Mathew, S.A. and Bhonde, R.R. (2018) Omega-3 polyunsaturated fatty acids promote angiogenesis in placenta derived mesenchymal stromal cells. *Pharmacological Research,* 132, 90-98.

Matin, M.M., Walsh, J.R., Gokhale, P.J., Draper, J.S., Bahrami, A.R., Morton, I., Moore, H.D. and Andrews, P.W. (2004) Specific knockdown of Oct4 and beta2-microglobulin expression by RNA interference in human embryonic stem cells and embryonic carcinoma cells. *Stem Cells,* 22 (5), 659-668.

Maynard, M.A., Evans, A.J., Hosomi, T., Hara, S., Jewett, M.A. and Ohh, M. (2005) Human HIF-3alpha4 is a dominant-negative regulator of HIF-1 and is down-regulated in renal cell carcinoma. *The FASEB Journal,* 19 (11), 1396-1406.

Maynard, M.A., Qi, H., Chung, J., Lee, E.H., Kondo, Y., Hara, S., Conaway, R.C., Conaway, J.W. and Ohh, M. (2003) Multiple splice variants of the human HIF-3 alpha locus are targets of the von Hippel-Lindau E3 ubiquitin ligase complex. *Journal of Biological Chemistry,* 278 (13), 11032-11040.

Maynard, S., Swistowska, A.M., Lee, J.W., Liu, Y., Liu, S.-T., Da Cruz, A.B., Rao, M., De Souza-Pinto, N.C., Zeng, X. and Bohr, V.A. (2008) Human embryonic stem cells have enhanced repair of multiple forms of DNA damage. *Stem cells (Dayton, Ohio),* 26 (9), 2266-2274.

Mead, J.F. (1984) The non-eicosanoid functions of the essential fatty acids. *Journal of Lipid Research,* 25 (13), 1517-1521.

Mehat, M.S., Sundaram, V., Ripamonti, C., Robson, A.G., Smith, A.J., Borooah, S., Robinson, M., Rosenthal, A.N., Innes, W., Weleber, R.G., Lee, R.W.J., Crossland, M., Rubin, G.S., Dhillon, B., Steel, D.H.W., Anglade, E., Lanza, R.P., Ali, R.R., Michaelides, M. and Bainbridge, J.W.B.

(2018) Transplantation of Human Embryonic Stem Cell-Derived Retinal Pigment Epithelial Cells in Macular Degeneration. *Ophthalmology,* 125 (11), 1765-1775.

Meneses, A.M., Medina, R.A., Kato, S., Pinto, M., Jaque, M.P., Lizama, I., Garcia Mde, L., Nualart, F. and Owen, G.I. (2008) Regulation of GLUT3 and glucose uptake by the cAMP signalling pathway in the breast cancer cell line ZR-75. *Journal of Cellular Physiology,* 214 (1), 110-116.

Merino, F., Ng, Calista keow l., Veerapandian, V., Schöler, Hans r., Jauch, R. and Cojocaru, V. (2014) Structural Basis for the SOX-Dependent Genomic Redistribution of OCT4 in Stem Cell Differentiation. *Structure,* 22 (9), 1274-1286.

Meshulam, T., Simard, J.R., Wharton, J., Hamilton, J.A. and Pilch, P.F. (2006) Role of caveolin-1 and cholesterol in transmembrane fatty acid movement. *Biochemistry,* 45 (9), 2882-2893.

Messmer, T., Von Meyenn, F., Savino, A., Santos, F., Mohammed, H., Lun, A.T.L., Marioni, J.C. and Reik, W. (2019) Transcriptional Heterogeneity in Naive and Primed Human Pluripotent Stem Cells at Single-Cell Resolution. *Cell reports,* 26 (4), 815-824.e814.

Mi, H., Muruganujan, A., Ebert, D., Huang, X. and Thomas, P.D. (2018) PANTHER version 14: more genomes, a new PANTHER GO-slim and improvements in enrichment analysis tools. *Nucleic Acids Research,* 47 (D1), D419-D426.

Mitalipov, S. and Wolf, D. (2009) Totipotency, Pluripotency and Nuclear Reprogramming. *Advances in biochemical engineering/biotechnology,* 114, 185-199.

Mitsui, K., Tokuzawa, Y., Itoh, H., Segawa, K., Murakami, M., Takahashi, K., Maruyama, M., Maeda, M. and Yamanaka, S. (2003) The Homeoprotein Nanog Is Required for Maintenance of Pluripotency in Mouse Epiblast and ES Cells. *Cell,* 113 (5), 631-642.

Mobasheri, A., Richardson, S., Mobasheri, R., Shakibaei, M. and Hoyland, J.A. (2005) Hypoxia inducible factor-1 and facilitative glucose transporters GLUT1 and GLUT3: putative molecular components of the oxygen and glucose sensing apparatus in articular chondrocytes. *Histology & Histopathology,* 20 (4), 1327-1338.

Mohyeldin, A., Garzon-Muvdi, T. and Quinones-Hinojosa, A. (2010) Oxygen in stem cell biology: a critical component of the stem cell niche. *Cell Stem Cell,* 7 (2), 150-161.

Mojsin, M., Topalovic, V., Marjanovic Vicentic, J. and Stevanovic, M. (2015) Transcription factor NF-Y inhibits cell growth and decreases SOX2 expression in human embryonal carcinoma cell line NT2/D1. *Biochemistry,* 80 (2), 202-207.

Molfino, A., Amabile, M.I., Monti, M. and Muscaritoli, M. (2017) Omega-3 Polyunsaturated Fatty Acids in Critical Illness: Anti-Inflammatory, Proresolving, or Both? *Oxidative Medicine and Cellular Longevity,* 2017, 5987082.

Moloudizargari, M., Mortaz, E., Hossein Asghari, M., Adcock, I.M., Redegeld, F.A. and Garssen, J. (2018) Effects of the polyunsaturated fatty acids, EPA and DHA, on hematological malignancies: a systematic review. *Oncotarget,* 9 (14).

Muiras, M.L., Müller, M., Schächter, F. and Bürkle, A. (1998) Increased poly(ADP-ribose) polymerase activity in lymphoblastoid cell lines from centenarians. *Journal of molecular medicine (Berlin, Germany),* 76 (5), 346-354.

Mylonis, I., Sembongi, H., Befani, C., Liakos, P., Siniossoglou, S. and Simos, G. (2012) Hypoxia causes triglyceride accumulation by HIF-1-mediated stimulation of lipin 1 expression. *Journal of Cell Science,* 125 (Pt 14), 3485-3493.

Mylonis, I., Simos, G. and Paraskeva, E. (2019) Hypoxia-Inducible Factors and the Regulation of Lipid Metabolism. *Cells,* 8 (3).

Nagakura, T., Matsuda, S., Shichijyo, K., Sugimoto, H. and Hata, K. (2000) Dietary supplementation with fish oil rich in omega-3 polyunsaturated fatty acids in children with bronchial asthma. *European Respiratory Journal,* 16 (5), 861-865.

Nagy, K. and Tiuca, I.-D. (2017) Importance of Fatty Acids in Physiopathology of Human Body *Fatty Acids*.

Närvä, E., Pursiheimo, J.-P., Laiho, A., Rahkonen, N., Emani, M.R., Viitala, M., Laurila, K., Sahla, R., Lund, R., Lähdesmäki, H., Jaakkola, P. and Lahesmaa, R. (2013) Continuous Hypoxic Culturing of Human Embryonic Stem Cells Enhances SSEA-3 and MYC Levels. *PLOS ONE,* 8 (11), e78847.

Nauta, T.D., Van Den Broek, M., Gibbs, S., Van Der Pouw-Kraan, T.C.T.M., Oudejans, C.B., Van Hinsbergh, V.W.M. and Koolwijk, P. (2017) Identification of HIF-2α-regulated genes that play a role in human microvascular endothelial sprouting during prolonged hypoxia in vitro. *Angiogenesis,* 20 (1), 39-54.

Niakan, K.K. and Eggan, K. (2013) Analysis of human embryos from zygote to blastocyst reveals distinct gene expression patterns relative to the mouse. *Developmental Biology,* 375 (1), 54-64.

Nichols, J. and Smith, A. (2009) Naive and primed pluripotent states. *Cell Stem Cell,* 4 (6), 487-492.

Nikitenko, L.L., Smith, D.M., Bicknell, R. and Rees, M.C. (2003) Transcriptional regulation of the CRLR gene in human microvascular endothelial cells by hypoxia. *The FASEB Journal,* 17 (11), 1499-1501.

Niwa, H., Burdon, T., Chambers, I. and Smith, A. (1998) Self-renewal of pluripotent embryonic stem cells is mediated via activation of STAT3. *Genes & development,* 12 (13), 2048-2060.

Niwa, H., Miyazaki, J. and Smith, A.G. (2000) Quantitative expression of Oct-3/4 defines differentiation, dedifferentiation or self-renewal of ES cells. *Nature Genetics,* 24 (4), 372-376.

Niwa, H., Toyooka, Y., Shimosato, D., Strumpf, D., Takahashi, K., Yagi, R. and Rossant, J. (2005) Interaction between Oct3/4 and Cdx2 determines trophectoderm differentiation. *Cell,* 123 (5), 917-929.

Noguchi, H., Miyagi-Shiohira, C. and Nakashima, Y. (2018) Induced Tissue-Specific Stem Cells and Epigenetic Memory in Induced Pluripotent Stem Cells. *International journal of molecular sciences,* 19 (4), 930.

Nourse, M.B., Halpin, D.E., Scatena, M., Mortisen, D.J., Tulloch, N.L., Hauch, K.D., Torok-Storb, B., Ratner, B.D., Pabon, L. and Murry, C.E. (2010) VEGF induces differentiation of functional endothelium from human embryonic stem cells: implications for tissue engineering. *Arteriosclerosis, thrombosis, and vascular biology,* 30 (1), 80.

Nugud, A., Sandeep, D. and El-Serafi, A.T. (2018) Two faces of the coin: Minireview for dissecting the role of reactive oxygen species in stem cell potency and lineage commitment. *Journal of Advanced Research,* 14, 73-79.

Obach, M., Navarro-Sabate, A., Caro, J., Kong, X., Duran, J., Gomez, M., Perales, J.C., Ventura, F., Rosa, J.L. and Bartrons, R. (2004) 6-Phosphofructo-2-kinase (pfkfb3) gene promoter contains hypoxia-inducible factor-1 binding sites necessary for transactivation in response to hypoxia. *Journal of Biological Chemistry,* 279 (51), 53562-53570.

Ohh, M., Park, C.W., Ivan, M., Hoffman, M.A., Kim, T.-Y., Huang, L.E., Pavletich, N., Chau, V. and Kaelin, W.G. (2000) Ubiquitination of hypoxia-inducible factor requires direct binding to the β-domain of the von Hippel–Lindau protein. *Nature Cell Biology,* 2, 423.

Okumura-Nakanishi, S., Saito, M., Niwa, H. and Ishikawa, F. (2005) Oct-3/4 and Sox2 regulate Oct-3/4 gene in embryonic stem cells. *Journal of Biological Chemistry,* 280 (7), 5307-5317.

Olufsen, M., Cangialosi, M.V. and Arukwe, A. (2014) Modulation of Membrane Lipid Composition and Homeostasis in Salmon Hepatocytes Exposed to Hypoxia and Perfluorooctane Sulfonamide, Given Singly or in Combination. *PLOS ONE,* 9 (7), e102485.

Oono, K., Ohtake, K., Watanabe, C., Shiba, S., Sekiya, T. and Kasono, K. (2020) Contribution of Pyk2 pathway and reactive oxygen species (ROS) to the anti-cancer effects of eicosapentaenoic acid (EPA) in PC3 prostate cancer cells. *Lipids in Health and Disease,* 19 (1), 15.

Ortmann, B., Druker, J. and Rocha, S. (2014) Cell cycle progression in response to oxygen levels. *Cellular and Molecular Life Sciences,* 71 (18), 3569-3582.

Ou, J., Tu, H., Shan, B., Luk, A., Debose-Boyd, R.A., Bashmakov, Y., Goldstein, J.L. and Brown, M.S. (2001) Unsaturated fatty acids inhibit transcription of the sterol regulatory element-binding protein-1c (SREBP-1c) gene by antagonizing ligand-dependent activation of the LXR. *Proceedings of the National Academy of Sciences of the United States of America,* 98 (11), 6027-6032.

Ozolek, J. and Castro, C. (2011) Teratomas Derived from Embryonic Stem Cells as Models for Embryonic Development, Disease, and Tumorigenesis *Embryonic Stem Cells - Basic Biology to Bioengineering*.

Pansky, B. (1982a) Germ Layers and Their Derivatives *Review of Medical Embryology*. New York: Macmillan.

Pansky, B. (1982b) Week 1 of Embryonic Development: Ovulation to Implantation *Review of Medical Embryology*. New York: Macmillan.

Papandreou, I., Cairns, R.A., Fontana, L., Lim, A.L. and Denko, N.C. (2006) HIF-1 mediates adaptation to hypoxia by actively downregulating mitochondrial oxygen consumption. *Cell Metabolism,* 3 (3), 187-197.

Pardo, M., Lang, B., Yu, L., Prosser, H., Bradley, A., Babu, M.M. and Choudhary, J. (2010) An expanded Oct4 interaction network: implications for stem cell biology, development, and disease. *Cell stem cell,* 6 (4), 382-395.

Park, H., Haynes, C.A., Nairn, A.V., Kulik, M., Dalton, S., Moremen, K. and Merrill, A.H. (2010) Transcript profiling and lipidomic analysis of ceramide subspecies in mouse embryonic stem cells and embryoid bodies. *Journal of Lipid Research,* 51 (3), 480-489.

Park, W.J., Kothapalli, K.S.D., Reardon, H.T., Lawrence, P., Qian, S.-B. and Brenna, J.T. (2012) A novel FADS1 isoform potentiates FADS2-mediated production of eicosanoid precursor fatty acids. *Journal of Lipid Research,* 53 (8), 1502-1512.

Park, Y.B., Kim, Y.Y., Oh, S.K., Chung, S.G., Ku, S.-Y., Kim, S.H., Choi, Y.M. and Moon, S.Y. (2008) Alterations of proliferative and differentiation potentials of human embryonic stem cells during long-term culture. *Experimental & Molecular Medicine,* 40 (1), 98-108.

Pasanen, A., Heikkila, M., Rautavuoma, K., Hirsila, M., Kivirikko, K.I. and Myllyharju, J. (2010) Hypoxia-inducible factor (HIF)-3alpha is subject to extensive alternative splicing in human tissues and cancer cells and is regulated by HIF-1 but not HIF-2. *The International Journal of Biochemistry & Cell Biology,* 42 (7), 1189-1200.

Pascal, J.M. (2018) The comings and goings of PARP-1 in response to DNA damage. *DNA Repair (Amst),* 71, 177-182.

Patterson, S.D. and Aebersold, R.H. (2003) Proteomics: the first decade and beyond. *Nature Genetics,* 33, 311.

Pearl, J.I., Kean, L.S., Davis, M.M. and Wu, J.C. (2012) Pluripotent Stem Cells: Immune to the Immune System? *Science Translational Medicine,* 4 (164), 164ps125-164ps125.

Petan, T., Jarc, E. and Jusovic, M. (2018) Lipid Droplets in Cancer: Guardians of Fat in a Stressful World. *Molecules,* 23 (8).

Petersen, S., Saretzki, G. and Von Zglinicki, T. (1998) Preferential accumulation of single-stranded regions in telomeres of human fibroblasts. *Experimental Cell Research,* 239 (1), 152-160.

Petrucco, S. and Percudani, R. (2008) Structural recognition of DNA by poly(ADP-ribose)polymerase-like zinc finger families. *The FASEB Journal,* 275 (5), 883-893.

Petruzzelli, R., Christensen, D.R., Parry, K.L., Sanchez-Elsner, T. and Houghton, F.D. (2014) HIF-2α Regulates NANOG Expression in Human Embryonic Stem Cells following Hypoxia and Reoxygenation through the Interaction with an Oct-Sox Cis Regulatory Element. *PLOS ONE,* 9 (10), e108309.

Pevny, L.H. and Nicolis, S.K. (2010) Sox2 roles in neural stem cells. *The International Journal of Biochemistry & Cell Biology,* 42 (3), 421-424.

Pifferi, F., Jouin, M., Alessandri, J.M., Roux, F., Perriere, N., Langelier, B., Lavialle, M., Cunnane, S. and Guesnet, P. (2010) n-3 long-chain fatty acids and regulation of glucose transport in two models of rat brain endothelial cells. *Neurochemistry International,* 56 (5), 703-710.

Pike, L.J. (2003) Lipid rafts: bringing order to chaos. *Journal of Lipid Research,* 44 (4), 655-667.

Pike, L.J. (2006) Rafts defined: a report on the Keystone symposium on lipid rafts and cell function. *Journal of Lipid Research,* 47 (7), 1597-1598.

Pilch, P.F., Souto, R.P., Liu, L., Jedrychowski, M.P., Berg, E.A., Costello, C.E. and Gygi, S.P. (2007) Cellular spelunking: exploring adipocyte caveolae. *Journal of Lipid Research,* 48 (10), 2103-2111.

Pleasure, S.J. and Lee, V.M. (1993) NTera 2 cells: a human cell line which displays characteristics expected of a human committed neuronal progenitor cell. *Journal of Neuroscience Research,* 35 (6), 585-602.

Pohl, J., Ring, A. and Stremmel, W. (2002) Uptake of long-chain fatty acids in HepG2 cells involves caveolae: analysis of a novel pathway. *Journal of Lipid Research,* 43 (9), 1390-1399.

Qiu, B., Ackerman, D., Sanchez, D.J., Li, B., Ochocki, J.D., Grazioli, A., Bobrovnikova-Marjon, E., Diehl, J.A., Keith, B. and Simon, M.C. (2015) HIF2alpha-Dependent Lipid Storage Promotes Endoplasmic Reticulum Homeostasis in Clear-Cell Renal Cell Carcinoma. *Cancer Discovery,* 5 (6), 652-667.

R Development Core Team (2020) R: A Language and Environment for Statistical Computing. Vienna, Austria: R Foundation for Statistical Computing. Available from: https://www.R-project.org.

Rafiee, M.-R., Girardot, C., Sigismondo, G. and Krijgsveld, J. (2016) Expanding the Circuitry of Pluripotency by Selective Isolation of Chromatin-Associated Proteins. *Molecular cell,* 64 (3), 624-635.

Rajasingh, J. and Bright, J.J. (2006) 15-Deoxy-delta12,14-prostaglandin J2 regulates leukemia inhibitory factor signaling through JAK-STAT pathway in mouse embryonic stem cells. *Experimental Cell Research,* 312 (13), 2538-2546.

Ralston, J.C., Matravadia, S., Gaudio, N., Holloway, G.P. and Mutch, D.M. (2015) Polyunsaturated fatty acid regulation of adipocyte FADS1 and FADS2 expression and function. *Obesity (Silver Spring, Md.),* 23 (4), 725-728.

Rashid, M.A., Haque, M. and Akbar, M. (2016) Role of Polyunsaturated Fatty Acids and Their Metabolites on Stem Cell Proliferation and Differentiation. *Advances in Neurobiology,* 12, 367-380.

Ray Chaudhuri, A. and Nussenzweig, A. (2017) The multifaceted roles of PARP1 in DNA repair and chromatin remodelling. *Nature Reviews Molecular Cell Biology,* 18 (10), 610-621.

Ray, P.D., Huang, B.-W. and Tsuji, Y. (2012) Reactive oxygen species (ROS) homeostasis and redox regulation in cellular signaling. *Cellular signalling,* 24 (5), 981-990.

Richards, M., Fong, C.-Y., Chan, W.-K., Wong, P.-C. and Bongso, A. (2002) Human feeders support prolonged undifferentiated growth of human inner cell masses and embryonic stem cells. *Nature Biotechnology,* 20 (9), 933-936.

Risé, P., Eligini, S., Ghezzi, S., Colli, S. and Galli, C. (2007) Fatty acid composition of plasma, blood cells and whole blood: Relevance for the assessment of the fatty acid status in humans. *Prostaglandins, Leukotrienes and Essential Fatty Acids,* 76 (6), 363-369.

Robichaud, P.-P., Munganyiki, J.E., Boilard, E. and Surette, M.E. (2018) Polyunsaturated fatty acid elongation and desaturation in activated human T-cells: ELOVL5 is the key elongase. *Journal of Lipid Research,* 59 (12), 2383-2396.

Rodda, D.J., Chew, J.L., Lim, L.H., Loh, Y.H., Wang, B., Ng, H.H. and Robson, P. (2005) Transcriptional regulation of nanog by OCT4 and SOX2. *Journal of Biological Chemistry,* 280 (26), 24731-24737.

Rodin, S., Antonsson, L., Niaudet, C., Simonson, O.E., Salmela, E., Hansson, E.M., Domogatskaya, A., Xiao, Z., Damdimopoulou, P., Sheikhi, M., Inzunza, J., Nilsson, A.S., Baker, D., Kuiper, R., Sun, Y., Blennow, E., Nordenskjold, M., Grinnemo, K.H., Kere, J., Betsholtz, C., Hovatta, O. and Tryggvason, K. (2014) Clonal culturing of human embryonic stem cells on laminin-521/E-cadherin matrix in defined and xeno-free environment. *Nature Communications,* 5, 3195.

Rodríguez-Vargas, J.M., Oliver-Pozo, F.J. and Dantzer, F. (2019) PARP1 and Poly(ADP-ribosyl)ation Signaling during Autophagy in Response to Nutrient Deprivation. *Oxidative medicine and cellular longevity,* 2019, 2641712-2641712.

Roper, S.J., Chrysanthou, S., Senner, C.E., Sienerth, A., Gnan, S., Murray, A., Masutani, M., Latos, P. and Hemberger, M. (2014) ADP-ribosyltransferases Parp1 and Parp7 safeguard pluripotency of ES cells. *Nucleic Acids Research,* 42 (14), 8914-8927.

Rossi, M., Spichty, M., Attorri, L., Distante, C., Nervi, C., Salvati, S. and Vitelli, L. (2017) Eicosapentaenoic acid modulates the synergistic action of CREB1 and ID/E2A family members in the rat pup brain and mouse embryonic stem cells. *Biochimica et Biophysica Acta,* 1860 (8), 870-884.

Rothberg, K.G., Heuser, J.E., Donzell, W.C., Ying, Y.S., Glenney, J.R. and Anderson, R.G. (1992) Caveolin, a protein component of caveolae membrane coats. *Cell,* 68 (4), 673-682.

Rouault-Pierre, K., Lopez-Onieva, L., Foster, K., Anjos-Afonso, F., Lamrissi-Garcia, I., Serrano-Sanchez, M., Mitter, R., Ivanovic, Z., De Verneuil, H., Gribben, J., Taussig, D., Rezvani, H.R., Mazurier, F. and Bonnet, D. (2013) HIF-2alpha protects human hematopoietic stem/progenitors and acute myeloid leukemic cells from apoptosis induced by endoplasmic reticulum stress. *Cell Stem Cell,* 13 (5), 549-563.

Roy, J., Lefkimmiatis, K., Moyer, M.P., Curci, S. and Hofer, A.M. (2010) The omega-3 fatty acid eicosapentaenoic acid elicits cAMP generation in colonic epithelial cells via a "store-operated" mechanism. *American journal of physiology. Gastrointestinal and liver physiology,* 299 (3), G715-G722.

Roy, S., Luetterforst, R., Harding, A., Apolloni, A., Etheridge, M., Stang, E., Rolls, B., Hancock, J.F. and Parton, R.G. (1999) Dominant-negative caveolin inhibits H-Ras function by disrupting cholesterol-rich plasma membrane domains. *Nature Cell Biology,* 1 (2), 98-105.

Ruas, J.L., Berchner-Pfannschmidt, U., Malik, S., Gradin, K., Fandrey, J., Roeder, R.G., Pereira, T. and Poellinger, L. (2010) Complex regulation of the transactivation function of hypoxia-inducible factor-1 alpha by direct interaction with two distinct domains of the CREB-binding protein/p300. *Journal of Biological Chemistry,* 285 (4), 2601-2609.

Sakayori, N., Maekawa, M., Numayama-Tsuruta, K., Katura, T., Moriya, T. and Osumi, N. (2011) Distinctive effects of arachidonic acid and docosahexaenoic acid on neural stem/progenitor cells. *Genes to Cells,* 16 (7), 778-790.

Saretzki, G., Walter, T., Atkinson, S., Passos, J.F., Bareth, B., Keith, W.N., Stewart, R., Hoare, S., Stojkovic, M., Armstrong, L., Von Zglinicki, T. and Lako, M. (2008) Downregulation of multiple stress defense mechanisms during differentiation of human embryonic stem cells. *Stem Cells,* 26 (2), 455-464.

Sato, N., Meijer, L., Skaltsounis, L., Greengard, P. and Brivanlou, A.H. (2004) Maintenance of pluripotency in human and mouse embryonic stem cells through activation of Wnt signaling by a pharmacological GSK-3-specific inhibitor. *Nature Medicine,* 10 (1), 55-63.

Scheuermann, T.H., Tomchick, D.R., Machius, M., Guo, Y., Bruick, R.K. and Gardner, K.H. (2009) Artificial ligand binding within the HIF2alpha PAS-B domain of the HIF2 transcription factor. *Proceedings of the National Academy of Sciences of the United States of America,* 106 (2), 450-455.

Schley, P.D., Brindley, D.N. and Field, C.J. (2007) (n-3) PUFA alter raft lipid composition and decrease epidermal growth factor receptor levels in lipid rafts of human breast cancer cells. *Journal of Nutrition,* 137 (3), 548-553.

Schlicker, A., Domingues, F.S., Rahnenführer, J. and Lengauer, T. (2006) A new measure for functional similarity of gene products based on Gene Ontology. *BMC Bioinformatics,* 7 (1), 302.

Schöler, H.R., Hatzopoulos, A.K., Balling, R., Suzuki, N. and Gruss, P. (1989) A family of octamer-specific proteins present during mouse embryogenesis: evidence for germline-specific expression of an Oct factor. *The EMBO Journal,* 8 (9), 2543-2550.

Schopperle, W.M. and Dewolf, W.C. (2007) The TRA-1-60 and TRA-1-81 human pluripotent stem cell markers are expressed on podocalyxin in embryonal carcinoma. *Stem Cells,* 25 (3), 723-730.

Schreck, R., Rieber, P. and Baeuerle, P.A. (1991) Reactive oxygen intermediates as apparently widely used messengers in the activation of the NF-kappa B transcription factor and HIV-1. *The EMBO journal,* 10 (8), 2247-2258.

Schwartz, S.D., Regillo, C.D., Lam, B.L., Eliott, D., Rosenfeld, P.J., Gregori, N.Z., Hubschman, J.P., Davis, J.L., Heilwell, G., Spirn, M., Maguire, J., Gay, R., Bateman, J., Ostrick, R.M., Morris, D., Vincent, M., Anglade, E., Del Priore, L.V. and Lanza, R. (2015) Human embryonic stem cell-derived retinal pigment epithelium in patients with age-related macular degeneration and Stargardt's macular dystrophy: follow-up of two open-label phase 1/2 studies. *Lancet,* 385 (9967), 509-516.

Semenza, Gregg l. (2012) Hypoxia-Inducible Factors in Physiology and Medicine. *Cell,* 148 (3), 399-408.

Semenza, G.L. (2013) HIF-1 mediates metabolic responses to intratumoral hypoxia and oncogenic mutations. *The Journal of Clinical Investigation,* 123 (9), 3664-3671.

Semenza, G.L., Jiang, B.H., Leung, S.W., Passantino, R., Concordet, J.P., Maire, P. and Giallongo, A. (1996) Hypoxia response elements in the aldolase A, enolase 1, and lactate dehydrogenase A gene promoters contain essential binding sites for hypoxia-inducible factor 1. *Journal of Biological Chemistry,* 271 (51), 32529-32537.

Semenza, G.L. and Wang, G.L. (1992) A nuclear factor induced by hypoxia via de novo protein synthesis binds to the human erythropoietin gene enhancer at a site required for transcriptional activation. *Molecular and Cellular Biology,* 12 (12), 5447-5454.

Seo, J., Barhoumi, R., Johnson, A.E., Lupton, J.R. and Chapkin, R.S. (2006) Docosahexaenoic acid selectively inhibits plasma membrane targeting of lipidated proteins. *The FASEB Journal,* 20 (6), 770-772.

Serhan, C.N. and Levy, B.D. (2018) Resolvins in inflammation: emergence of the pro-resolving superfamily of mediators. *The Journal of Clinical Investigation,* 128 (7), 2657-2669.

Shabani, P., Ghazizadeh, Z., Pahlavan, S., Hashemizadeh, S., Baharvand, H., Aghdami, N. and Doosti, M. (2015) Exogenous treatment with eicosapentaenoic acid supports maturation of cardiomyocytes derived from embryonic stem cells. *Biochemical and Biophysical Research Communications,* 461 (2), 281-286.

Shahriyari, L. and Komarova, N.L. (2013) Symmetric vs. Asymmetric Stem Cell Divisions: An Adaptation against Cancer? *PLOS ONE,* 8 (10), e76195.

Shammas, M.A. (2011) Telomeres, lifestyle, cancer, and aging. *Current opinion in clinical nutrition and metabolic care,* 14 (1), 28-34.

Shekari, F., Nezari, H., Larijani, M.R., Han, C.-L., Baharvand, H., Chen, Y.-J. and Salekdeh, G.H. (2017) Proteome analysis of human embryonic stem cells organelles. *Journal of Proteomics,* 162, 108-118.

Shroff, G. (2016) Human Embryonic Stem Cell Therapy in Chronic Spinal Cord Injury: A Retrospective Study. *Clinical and Translational Science,* 9 (3), 168-175.

Silva, J.C., Gorenstein, M.V., Li, G.Z., Vissers, J.P. and Geromanos, S.J. (2006) Absolute quantification of proteins by LCMSE: a virtue of parallel MS acquisition. *Molecular & Cellular Proteomics,* 5 (1), 144-156.

Silvan, U., Diez-Torre, A., Arluzea, J., Andrade, R., Silio, M. and Arechaga, J. (2009) Hypoxia and pluripotency in embryonic and embryonal carcinoma stem cell biology. *Differentiation,* 78 (2-3), 159-168.

Simons, K. and Toomre, D. (2000) Lipid rafts and signal transduction. *Nature Reviews Molecular Cell Biology,* 1 (1), 31-39.

Siscovick, D.S., Barringer, T.A., Fretts, A.M., Wu, J.H.Y., Lichtenstein, A.H., Costello, R.B., Kris-Etherton, P.M., Jacobson, T.A., Engler, M.B., Alger, H.M., Appel, L.J. and Mozaffarian, D. (2017) Omega-3 Polyunsaturated Fatty Acid (Fish Oil) Supplementation and the Prevention of Clinical Cardiovascular Disease. *Circulation,* 135 (15), e867-e884.

Smith, Z.D., Chan, M.M., Humm, K.C., Karnik, R., Mekhoubad, S., Regev, A., Eggan, K. and Meissner, A. (2014) DNA methylation dynamics of the human preimplantation embryo. *Nature,* 511 (7511), 611-615.

So, J., Matthan, N., Maddipati, K., Lichtenstein, A., Wu, D. and Lamon-Fava, S. (2019) Effects of EPA and DHA Supplementation on Plasma Specialized Pro-resolving Lipid Mediators and Blood Monocyte Inflammatory Response in Subjects with Chronic Inflammation (OR29-01-19). *Current Developments in Nutrition,* 3.

Sohn, J., Brick, R.M. and Tuan, R.S. (2016) From embryonic development to human diseases: The functional role of caveolae/caveolin. *Birth Defects Research Part C: Embryo Today,* 108 (1), 45-64.

Sokola-Wysoczanska, E., Wysoczanski, T., Wagner, J., Czyz, K., Bodkowski, R., Lochynski, S. and Patkowska-Sokola, B. (2018) Polyunsaturated Fatty Acids and Their Potential Therapeutic Role in Cardiovascular System Disorders-A Review. *Nutrients,* 10 (10).

Solari, C., Petrone, M.V., Vazquez Echegaray, C., Cosentino, M.S., Waisman, A., Francia, M., Barañao, L., Miriuka, S. and Guberman, A. (2018) Superoxide dismutase 1 expression is modulated by the core pluripotency transcription factors Oct4, Sox2 and Nanog in embryonic stem cells. *Mechanisms of Development,* 154, 116-121.

Soldani, C., Lazze, M.C., Bottone, M.G., Tognon, G., Biggiogera, M., Pellicciari, C.E. and Scovassi, A.I. (2001) Poly(ADP-ribose) polymerase cleavage during apoptosis: when and where? *Experimental Cell Research,* 269 (2), 193-201.

Soto-Guzman, A., Robledo, T., Lopez-Perez, M. and Salazar, E.P. (2008) Oleic acid induces ERK1/2 activation and AP-1 DNA binding activity through a mechanism involving Src kinase and EGFR transactivation in breast cancer cells. *Molecular and Cellular Endocrinology,* 294 (1-2), 81-91.

Sotthibundhu, A., Promjuntuek, W., Liu, M., Shen, S. and Noisa, P. (2018) Roles of autophagy in controlling stem cell identity: a perspective of self-renewal and differentiation. *Cell and Tissue Research,* 374 (2), 205-216.

Stefanovic, S., Abboud, N., Désilets, S., Nury, D., Cowan, C. and Pucéat, M. (2009) Interplay of Oct4 with Sox2 and Sox17: a molecular switch from stem cell pluripotency to specifying a cardiac fate. *The Journal of Cell Biology,* 186 (5), 665-673.

Stevens, L.C. (1967) Origin of Testicular Teratomas From Primordial Germ Cells in Mice. *Journal of the National Cancer Institute,* 38 (4), 549-552.

Sun, W., Kato, H., Kitajima, S., Lee, K.L., Gradin, K., Okamoto, T. and Poellinger, L. (2017) Interaction between von Hippel-Lindau Protein and Fatty Acid Synthase Modulates Hypoxia Target Gene Expression. *Scientific reports,* 7 (1), 7190-7190.

Supek, F., Bošnjak, M., Škunca, N. and Šmuc, T. (2011) REVIGO Summarizes and Visualizes Long Lists of Gene Ontology Terms. *PLOS ONE,* 6 (7), e21800.

Swijnenburg, R.J., Schrepfer, S., Govaert, J.A., Cao, F., Ransohoff, K., Sheikh, A.Y., Haddad, M., Connolly, A.J., Davis, M.M., Robbins, R.C. and Wu, J.C. (2008) Immunosuppressive therapy mitigates immunological rejection of human embryonic stem cell xenografts. *Proceedings of the National Academy of Sciences of the United States of America,* 105 (35), 12991-12996.

Swindall, A.F., Stanley, J.A. and Yang, E.S. (2013) PARP-1: Friend or Foe of DNA Damage and Repair in Tumorigenesis? *Cancers,* 5 (3), 943-958.

Szklarczyk, D., Gable, A.L., Lyon, D., Junge, A., Wyder, S., Huerta-Cepas, J., Simonovic, M., Doncheva, N.T., Morris, J.H., Bork, P., Jensen, L.J. and Mering, C.V. (2019) STRING v11: protein-protein association networks with increased coverage, supporting functional discovery in genome-wide experimental datasets. *Nucleic Acids Research,* 47 (D1), D607-d613.

Taabazuing, C., Hangasky Iii, J. and Knapp, M. (2014) Oxygen Sensing Strategies in Mammals and Bacteria. *Journal of inorganic biochemistry,* 133.

Tafani, M., Sansone, L., Limana, F., Arcangeli, T., De Santis, E., Polese, M., Fini, M. and Russo, M.A. (2016) The Interplay of Reactive Oxygen Species, Hypoxia, Inflammation, and Sirtuins in Cancer Initiation and Progression. *Oxidative Medicine and Cellular Longevity,* 2016, 3907147.

Taha, A., Sharifpanah, F., Wartenberg, M. and Sauer, H. (2020) Omega-3 and Omega-6 polyunsaturated fatty acids stimulate vascular differentiation of mouse embryonic stem cells. *Journal of Cellular Physiology*.

Takagahara, S., Shinohara, H., Itokawa, S., Satomi, Y., Ando, A., Yamamoto, T., Suzuki, H., Fujimoto, T., Kubo, K. and Ikeda, S. (2019) A novel orally available delta-5 desaturase inhibitor prevents atherosclerotic lesions accompanied with changes of fatty acid composition and eicosanoid production in ApoE knockout mice. *Journal of Pharmacology and Experimental Therapeutics*, jpet.119.259846.

Takahashi, K. and Yamanaka, S. (2006) Induction of Pluripotent Stem Cells from Mouse Embryonic and Adult Fibroblast Cultures by Defined Factors. *Cell,* 126 (4), 663-676.

Takashima, Y., Guo, G., Loos, R., Nichols, J., Ficz, G., Krueger, F., Oxley, D., Santos, F., Clarke, J., Mansfield, W., Reik, W., Bertone, P. and Smith, A. (2014) Resetting transcription factor control circuitry toward ground-state pluripotency in human. *Cell,* 158 (6), 1254-1269.

Takubo, K., Goda, N., Yamada, W., Iriuchishima, H., Ikeda, E., Kubota, Y., Shima, H., Johnson, R.S., Hirao, A., Suematsu, M. and Suda, T. (2010) Regulation of the HIF-1alpha level is essential for hematopoietic stem cells. *Cell Stem Cell,* 7 (3), 391-402.

Tan, P.-H., Bay, B.-H., Yip, G., Selvarajan, S., Tan, P., Wu, J., Lee, C.-H. and Li, K.-B. (2005) Immunohistochemical detection of Ki67 in breast cancer correlates with transcriptional regulation of genes related to apoptosis and cell death. *Modern Pathology,* 18 (3), 374-381.

Tan, Q., Wang, M., Yu, M., Zhang, J., Bristow, R.G., Hill, R.P. and Tannock, I.F. (2016) Role of Autophagy as a Survival Mechanism for Hypoxic Cells in Tumors. *Neoplasia (New York, N.Y.),* 18 (6), 347-355.

Tanaka, T., Wiesener, M., Bernhardt, W., Eckardt, K.U. and Warnecke, C. (2009) The human HIF (hypoxia-inducible factor)-3alpha gene is a HIF-1 target gene and may modulate hypoxic gene induction. *Biochemical Journal,* 424 (1), 143-151.

Tang, L., Li, J., Fu, W., Wu, W. and Xu, J. (2019) Suppression of FADS1 induces ROS generation, cell cycle arrest, and apoptosis in melanocytes: implications for vitiligo. *Aging,* 11 (24), 11829-11843.

Tesar, P.J., Chenoweth, J.G., Brook, F.A., Davies, T.J., Evans, E.P., Mack, D.L., Gardner, R.L. and Mckay, R.D. (2007) New cell lines from mouse epiblast share defining features with human embryonic stem cells. *Nature,* 448 (7150), 196-199.

Teslaa, T. and Teitell, M.A. (2015) Pluripotent stem cell energy metabolism: an update. *The EMBO Journal,* 34 (2), 138-153.

Thomson, J.A., Itskovitz-Eldor, J., Shapiro, S.S., Waknitz, M.A., Swiergiel, J.J., Marshall, V.S. and Jones, J.M. (1998) Embryonic Stem Cell Lines Derived from Human Blastocysts. *Science,* 282 (5391), 1145-1147.

Tomanek, L. (2011) Environmental proteomics: changes in the proteome of marine organisms in response to environmental stress, pollutants, infection, symbiosis, and development. *The Annual Review of Marine Science,* 3, 373-399.

Tomioka, M., Nishimoto, M., Miyagi, S., Katayanagi, T., Fukui, N., Niwa, H., Muramatsu, M. and Okuda, A. (2002) Identification of Sox-2 regulatory region which is under the control of Oct-3/4-Sox-2 complex. *Nucleic Acids Research,* 30 (14), 3202-3213.

Tompkins, J.D., Hall, C., Chen, V.C.-Y., Li, A.X., Wu, X., Hsu, D., Couture, L.A. and Riggs, A.D. (2012) Epigenetic stability, adaptability, and reversibility in human embryonic stem cells. *Proceedings of the National Academy of Sciences,* 109 (31), 12544-12549.

Trigatti, B.L., Anderson, R.G.W. and Gerber, G.E. (1999) Identification of Caveolin-1 as a Fatty Acid Binding Protein. *Biochemical and Biophysical Research Communications,* 255 (1), 34-39.

Tsuzuki, Y., Fukumura, D., Oosthuyse, B., Koike, C., Carmeliet, P. and Jain, R.K. (2000) Vascular endothelial growth factor (VEGF) modulation by targeting hypoxia-inducible factor-1alpha--> hypoxia response element--> VEGF cascade differentially regulates vascular response and growth rate in tumors. *Cancer Research,* 60 (22), 6248-6252.

Turetsky, T., Aizenman, E., Gil, Y., Weinberg, N., Shufaro, Y., Revel, A., Laufer, N., Simon, A., Abeliovich, D. and Reubinoff, B.E. (2008) Laser-assisted derivation of human embryonic stem cell lines from IVF embryos after preimplantation genetic diagnosis. *Human Reproduction,* 23 (1), 46-53.

Turk, H.F. and Chapkin, R.S. (2013) Membrane lipid raft organization is uniquely modified by n-3 polyunsaturated fatty acids. *Prostaglandins, leukotrienes, and essential fatty acids,* 88 (1), 43-47.

Turksen, K. and Troy, T.C. (2006) Human embryonic stem cells: isolation, maintenance, and differentiation. *Methods in Molecular Biology,* 331, 1-12.

Valadi, H., Ekström, K., Bossios, A., Sjöstrand, M., Lee, J.J. and Lötvall, J.O. (2007) Exosome-mediated transfer of mRNAs and microRNAs is a novel mechanism of genetic exchange between cells. *Nature Cell Biology,* 9 (6), 654-659.

Valckx, S.D., Arias-Alvarez, M., De Pauw, I., Fievez, V., Vlaeminck, B., Fransen, E., Bols, P.E. and Leroy, J.L. (2014) Fatty acid composition of the follicular fluid of normal weight, overweight and obese women undergoing assisted reproductive treatment: a descriptive cross-sectional study. *Reproductive Biology and Endocrinology,* 12, 13.

Valli, A., Rodriguez, M., Moutsianas, L., Fischer, R., Fedele, V., Huang, H.L., Van Stiphout, R., Jones, D., Mccarthy, M., Vinaxia, M., Igarashi, K., Sato, M., Soga, T., Buffa, F., Mccullagh, J., Yanes, O., Harris, A. and Kessler, B. (2015) Hypoxia induces a lipogenic cancer cell phenotype via HIF1alpha-dependent and -independent pathways. *Oncotarget,* 6 (4), 1920-1941.

Van Der Torren, C.R., Zaldumbide, A., Duinkerken, G., Brand-Schaaf, S.H., Peakman, M., Stangé, G., Martinson, L., Kroon, E., Brandon, E.P., Pipeleers, D. and Roep, B.O. (2017) Immunogenicity of human embryonic stem cell-derived beta cells. *Diabetologia,* 60 (1), 126-133.

Vaňhara, P., Kučera, L., Prokeš, L., Jurečková, L., Peña-Méndez, E.M., Havel, J. and Hampl, A. (2018) Intact Cell Mass Spectrometry as a Quality Control Tool for Revealing Minute Phenotypic Changes of Cultured Human Embryonic Stem Cells. *Stem cells translational medicine,* 7 (1), 109-114.

Varlakhanova, N., Cotterman, R., Bradnam, K., Korf, I. and Knoepfler, P.S. (2011) Myc and Miz-1 have coordinate genomic functions including targeting Hox genes in human embryonic stem cells. *Epigenetics & Chromatin,* 4 (1), 20.

Vaskova, E.A., Stekleneva, A.E., Medvedev, S.P. and Zakian, S.M. (2013) "Epigenetic memory" phenomenon in induced pluripotent stem cells. *Acta naturae,* 5 (4), 15-21.

Vaughan, R.A., Garcia-Smith, R., Bisoffi, M., Conn, C.A. and Trujillo, K.A. (2012) Conjugated linoleic acid or omega 3 fatty acids increase mitochondrial biosynthesis and metabolism in skeletal muscle cells. *Lipids in Health and Disease,* 11 (1), 142.

Verlengia, R., Gorjão, R., Kanunfre, C.C., Bordin, S., De Lima, T.M., Martins, E.F., Newsholme, P. and Curi, R. (2004) Effects of EPA and DHA on proliferation, cytokine production, and gene expression in Raji cells. *Lipids,* 39 (9), 857-864.

Villa-Diaz, L.G., Ross, A.M., Lahann, J. and Krebsbach, P.H. (2013) Concise review: The evolution of human pluripotent stem cell culture: from feeder cells to synthetic coatings. *Stem Cells,* 31 (1), 1-7.

Von Zglinicki, T. (2000) Role of Oxidative Stress in Telomere Length Regulation and Replicative Senescence. *Annals of the New York Academy of Sciences,* 908 (1), 99-110.

Wang, G.L., Jiang, B.H., Rue, E.A. and Semenza, G.L. (1995) Hypoxia-inducible factor 1 is a basic-helix-loop-helix-PAS heterodimer regulated by cellular O2 tension. *Proceedings of the National Academy of Sciences of the United States of America,* 92 (12), 5510-5514.

Wang, K., Guzman, A.K., Yan, Z., Zhang, S., Hu, M.Y., Hamaneh, M.B., Yu, Y.K., Tolu, S., Zhang, J., Kanavy, H.E., Ye, K., Bartholdy, B. and Bouhassira, E.E. (2019) Ultra-High-Frequency Reprogramming of Individual Long-Term Hematopoietic Stem Cells Yields Low Somatic Variant Induced Pluripotent Stem Cells. *Cell Reports,* 26 (10), 2580-2592.e2587.

Wang, L., Zhang, T., Wang, L., Cai, Y., Zhong, X., He, X., Hu, L., Tian, S., Wu, M., Hui, L., Zhang, H. and Gao, P. (2017) Fatty acid synthesis is critical for stem cell pluripotency via promoting mitochondrial fission. *The EMBO Journal,* 36 (10), 1330-1347.

Wang, S., Kan, Q., Sun, Y., Han, R., Zhang, G., Peng, T. and Jia, Y. (2013) Caveolin-1 regulates neural differentiation of rat bone mesenchymal stem cells into neurons by modulating Notch signaling. *International Journal of Developmental Neuroscience,* 31 (1), 30-35.

Wang, X., Lin, H. and Gu, Y. (2012a) Multiple roles of dihomo-γ-linolenic acid against proliferation diseases. *Lipids in health and disease,* 11, 25-25.

Wang, Y., Roche, O., Xu, C., Moriyama, E.H., Heir, P., Chung, J., Roos, F.C., Chen, Y., Finak, G., Milosevic, M., Wilson, B.C., Teh, B.T., Park, M., Irwin, M.S. and Ohh, M. (2012b) Hypoxia promotes ligand-independent EGF receptor signaling via hypoxia-inducible factor–mediated upregulation of caveolin-1. *Proceedings of the National Academy of Sciences,* 109 (13), 4892-4897.

Wang, Z., Oron, E., Nelson, B., Razis, S. and Ivanova, N. (2012c) Distinct lineage specification roles for NANOG, OCT4, and SOX2 in human embryonic stem cells. *Cell Stem Cell,* 10 (4), 440-454.

Warren, L., Manos, P.D., Ahfeldt, T., Loh, Y.-H., Li, H., Lau, F., Ebina, W., Mandal, P.K., Smith, Z.D., Meissner, A., Daley, G.Q., Brack, A.S., Collins, J.J., Cowan, C., Schlaeger, T.M. and Rossi, D.J. (2010) Highly efficient reprogramming to pluripotency and directed differentiation of human cells with synthetic modified mRNA. *Cell stem cell,* 7 (5), 618-630.

Wei, X., Yang, X., Han, Z.-P., Qu, F.-F., Shao, L. and Shi, Y.-F. (2013) Mesenchymal stem cells: a new trend for cell therapy. *Acta Pharmacologica Sinica,* 34 (6), 747-754.

Wei, Z., Li, D., Zhu, L., Yang, L., Chen, C., Bai, C. and Li, G. (2018) Omega 3 polyunsaturated fatty acids inhibit cell proliferation by regulating cell cycle in fad3b transgenic mouse embryonic stem cells. *Lipids in health and disease,* 17 (1), 210-210.

Weinberger, L., Ayyash, M., Novershtern, N. and Hanna, J.H. (2016) Dynamic stem cell states: naive to primed pluripotency in rodents and humans. *Nature Reviews Molecular Cell Biology,* 17 (3), 155-169.

Westfall, S., Sachdev, S., Das, P., Hearne, L., Hannink, M., Roberts, R. and Ezashi, T. (2008) Identification of Oxygen-Sensitive Transcriptional Programs in Human Embryonic Stem Cells. *Stem cells and development,* 17, 869-881.

Weylandt, K.H., Chiu, C.-Y., Gomolka, B., Waechter, S.F. and Wiedenmann, B. (2012) Omega-3 fatty acids and their lipid mediators: Towards an understanding of resolvin and protectin formation. *Prostaglandins & Other Lipid Mediators,* 97 (3), 73-82.

Wise, D.R., Ward, P.S., Shay, J.E., Cross, J.R., Gruber, J.J., Sachdeva, U.M., Platt, J.M., Dematteo, R.G., Simon, M.C. and Thompson, C.B. (2011) Hypoxia promotes isocitrate dehydrogenase-dependent carboxylation of alpha-ketoglutarate to citrate to support cell growth and viability. *Proceedings of the National Academy of Sciences of the United States of America,* 108 (49), 19611-19616.

Wobma, H.M., Tamargo, M.A., Goeta, S., Brown, L.M., Duran-Struuck, R. and Vunjak-Novakovic, G. (2018) The influence of hypoxia and IFN-γ on the proteome and metabolome of therapeutic mesenchymal stem cells. *Biomaterials,* 167, 226-234.

Wright, A.J. and Andrews, P.W. (2009) Surface marker antigens in the characterization of human embryonic stem cells. *Stem Cell Research,* 3 (1), 3-11.

Wu, D., Potluri, N., Lu, J., Kim, Y. and Rastinejad, F. (2015) Structural integration in hypoxia-inducible factors. *Nature,* 524 (7565), 303-308.

Wu, D. and Rastinejad, F. (2017) Structural characterization of mammalian bHLH-PAS transcription factors. *Current opinion in structural biology,* 43, 1-9.

Wu, L.Y., Wang, Y., Jin, B., Zhao, T., Wu, H.T., Wu, Y., Fan, M., Wang, X.M. and Zhu, L.L. (2008) The role of hypoxia in the differentiation of P19 embryonal carcinoma cells into dopaminergic neurons. *Neurochemical Research,* 33 (10), 2118-2125.

Xie, L., Xue, X., Taylor, M., Ramakrishnan, S.K., Nagaoka, K., Hao, C., Gonzalez, F.J. and Shah, Y.M. (2014) Hypoxia-inducible factor/MAZ-dependent induction of caveolin-1 regulates colon permeability through suppression of occludin, leading to hypoxia-induced inflammation. *Molecular and cellular biology,* 34 (16), 3013-3023.

Ximenes-Da-Silva, A., Lavialle, F., Gendrot, G., Guesnet, P., Alessandri, J.-M. and Lavialle, M. (2002) Glucose transport and utilization are altered in the brain of rats deficient in n-3 polyunsaturated fatty acids. *Journal of neurochemistry,* 81, 1328-1337.

Xu, R.H., Chen, X., Li, D.S., Li, R., Addicks, G.C., Glennon, C., Zwaka, T.P. and Thomson, J.A. (2002) BMP4 initiates human embryonic stem cell differentiation to trophoblast. *Nat Biotechnol,* 20 (12), 1261-1264.

Xu, Y., Yang, X., Wang, T., Yang, L., He, Y.-Y., Miskimins, K. and Qian, S.Y. (2018) Knockdown delta-5-desaturase in breast cancer cells that overexpress COX-2 results in inhibition of growth, migration and invasion via a dihomo-γ-linolenic acid peroxidation dependent mechanism. *BMC Cancer,* 18 (1), 330.

Yan, Q., Bartz, S., Mao, M., Li, L. and Kaelin, W.G., Jr. (2007) The hypoxia-inducible factor 2alpha N-terminal and C-terminal transactivation domains cooperate to promote renal tumorigenesis in vivo. *Molecular and Cellular Biology,* 27 (6), 2092-2102.

Yanes, O., Clark, J., Wong, D.M., Patti, G.J., Sánchez-Ruiz, A., Benton, H.P., Trauger, S.A., Desponts, C., Ding, S. and Siuzdak, G. (2010) Metabolic oxidation regulates embryonic stem cell differentiation. *Nature chemical biology,* 6 (6), 411-417.

Yang, F., Chen, G., Ma, M., Qiu, N., Zhu, L. and Li, J. (2018) Fatty acids modulate the expression levels of key proteins for cholesterol absorption in Caco-2 monolayer. *Lipids in Health and Disease,* 17 (1), 32.

Yang, J., Zhang, L., Erbel, P.J., Gardner, K.H., Ding, K., Garcia, J.A. and Bruick, R.K. (2005) Functions of the Per/ARNT/Sim domains of the hypoxia-inducible factor. *Journal of Biological Chemistry,* 280 (43), 36047-36054.

Yang, X., Rodriguez, M.L., Leonard, A., Sun, L., Fischer, K.A., Wang, Y., Ritterhoff, J., Zhao, L., Kolwicz, S.C., Pabon, L., Reinecke, H., Sniadecki, N.J., Tian, R., Ruohola-Baker, H., Xu, H. and Murry, C.E. (2019) Fatty Acids Enhance the Maturation of Cardiomyocytes Derived from Human Pluripotent Stem Cells. *Stem Cell Reports,* 13 (4), 657-668.

Yang, X., Xu, Y., Miskimins, K.W. and Qian, S.Y. (2016) Knocking Down Delta-5 Desaturase and Exploiting High Expression Level of COX-2 to Inhibit Cancer Migration and Invasion. *Free Radical Biology and Medicine,* 100, S133.

Yao, S., Chen, S., Clark, J., Hao, E., Beattie, G.M., Hayek, A. and Ding, S. (2006) Long-term self-renewal and directed differentiation of human embryonic stem cells in chemically defined conditions. *Proceedings of the National Academy of Sciences of the United States of America,* 103 (18), 6907-6912.

Ye, S., Tan, L., Ma, J., Shi, Q. and Li, J. (2010) Polyunsaturated docosahexaenoic acid suppresses oxidative stress induced endothelial cell calcium influx by altering lipid composition in membrane caveolar rafts. *Prostaglandins, Leukotrienes and Essential Fatty Acids,* 83 (1), 37-43.

Yocum, A.K., Gratsch, T.E., Leff, N., Strahler, J.R., Hunter, C.L., Walker, A.K., Michailidis, G., Omenn, G.S., Shea, K.S. and Andrews, P.C. (2008) Coupled Global and Targeted Proteomics of Human Embryonic Stem Cells during Induced Differentiation. *Molecular & Cellular Proteomics,* 7 (4), 750.

Yuan, H., Corbi, N., Basilico, C. and Dailey, L. (1995) Developmental-specific activity of the FGF-4 enhancer requires the synergistic action of Sox2 and Oct-3. *Genes & Development,* 9 (21), 2635-2645.

Yusuf, B., Gopurappilly, R., Dadheech, N., Gupta, S., Bhonde, R. and Pal, R. (2013) Embryonic fibroblasts represent a connecting link between mesenchymal and embryonic stem cells. *Development, Growth & Differentiation,* 55 (3), 330-340.

Zafarana, G., Avery, S.R., Avery, K., Moore, H.D. and Andrews, P.W. (2009) Specific Knockdown of OCT4 in Human Embryonic Stem Cells by Inducible Short Hairpin RNA Interference. *Stem Cells (Dayton, Ohio),* 27 (4), 776-782.

Zakrzewski, W., Dobrzyński, M., Szymonowicz, M. and Rybak, Z. (2019) Stem cells: past, present, and future. *Stem Cell Research & Therapy,* 10 (1), 68.

Zaniolo, K., Desnoyers, S., Leclerc, S. and Guérin, S.L. (2007) Regulation of poly(ADP-ribose) polymerase-1 (PARP-1) gene expression through the post-translational modification of Sp1: a nuclear target protein of PARP-1. *BMC Molecular Biology,* 8 (1), 96.

Zeineddine, D., Hammoud, A.A., Mortada, M. and Boeuf, H. (2014) The Oct4 protein: more than a magic stemness marker. *American Journal of Stem Cells,* 3 (2), 74-82.

Zhang, B., He, L., Liu, Y., Zhang, J., Zeng, Q., Wang, S., Fan, Z., Fang, F., Chen, L., Lv, Y., Xi, J., Yue, W., Li, Y. and Pei, X. (2018a) Prostaglandin E2 Is Required for BMP4-Induced Mesoderm Differentiation of Human Embryonic Stem Cells. *Stem Cell Reports,* 10 (3), 905-919.

Zhang, J., Song, L.P., Huang, Y., Zhao, Q., Zhao, K.W. and Chen, G.Q. (2008) Accumulation of hypoxia-inducible factor-1 alpha protein and its role in the differentiation of myeloid leukemic cells induced by all-trans retinoic acid. *Haematologica,* 93 (10), 1480-1487.

Zhang, K., Xu, P., Sowers, J.L., Machuca, D.F., Mirfattah, B., Herring, J., Tang, H., Chen, Y., Tian, B., Brasier, A.R. and Sowers, L.C. (2017) Proteome Analysis of Hypoxic Glioblastoma Cells Reveals Sequential Metabolic Adaptation of One-Carbon Metabolic Pathways. *Molecular & cellular proteomics : MCP,* 16 (11), 1906-1921.

Zhang, S., Bell, E., Zhi, H., Brown, S., Imran, S.a.M., Azuara, V. and Cui, W. (2019) OCT4 and PAX6 determine the dual function of SOX2 in human ESCs as a key pluripotent or neural factor. *Stem Cell Research & Therapy,* 10 (1), 122.

Zhang, W., Long, Y., Zhang, J. and Wang, C. (2007) Modulatory effects of EPA and DHA on proliferation and apoptosis of pancreatic cancer cells. *Journal of Huazhong University of Science and Technology,* 27 (5), 547-550.

Zhang, Y.-P., Brown, R.E., Zhang, P.-C., Zhao, Y.-T., Ju, X.-H. and Song, C. (2018b) DHA, EPA and their combination at various ratios differently modulated Aβ25-35-induced neurotoxicity in SH-SY5Y cells. *Prostaglandins, Leukotrienes and Essential Fatty Acids,* 136, 85-94.

Zhao, P., Schulz, T.C., Sherrer, E.S., Weatherly, D.B., Robins, A.J. and Wells, L. (2015a) The human embryonic stem cell proteome revealed by multidimensional fractionation followed by tandem mass spectrometry. *Proteomics,* 15 (2-3), 554-566.

Zhao, W., Ji, X., Zhang, F., Li, L. and Ma, L. (2012) Embryonic stem cell markers. *Molecules (Basel, Switzerland),* 17 (6), 6196-6236.

Zhao, Y., Hu, Q., Cheng, F., Su, N., Wang, A., Zou, Y., Hu, H., Chen, X., Zhou, H.-M., Huang, X., Yang, K., Zhu, Q., Wang, X., Yi, J., Zhu, L., Qian, X., Chen, L., Tang, Y., Loscalzo, J. and Yang, Y. (2015b) SoNar, a Highly Responsive NAD+/NADH Sensor, Allows High-Throughput Metabolic Screening of Anti-tumor Agents. *Cell metabolism,* 21 (5), 777-789.

Zhou, W., Choi, M., Margineantu, D., Margaretha, L., Hesson, J., Cavanaugh, C., Blau, C.A., Horwitz, M.S., Hockenbery, D., Ware, C. and Ruohola-Baker, H. (2012) HIF1α induced switch from bivalent to exclusively glycolytic metabolism during ESC-to-EpiSC/hESC transition. *The EMBO journal,* 31 (9), 2103-2116.

Ziegler, M. and Oei, S.L. (2001) A cellular survival switch: poly(ADP-ribosyl)ation stimulates DNA repair and silences transcription. *Bioessays,* 23 (6), 543-548.